LONG RANGE ATMOSPHERIC TRANSPORT OF PERSISTENT ORGANIC POLLUTANTS TO IZMIR

A Thesis Submitted to
The Graduate School of
İzmir Institute of Technology
in Partial Fulfillment of the Requirements for the Degree of

MASTER OF SCIENCE

in Environmental Engineering

by
İlknur AYRİ

July 2021
İZMİR

ACKNOWLEDGMENTS

Firstly, I would like to express my deepest appreciation my supervisor Prof. Dr. Sait C. SOFUOĞLU for his supervision throughout this study. I would also like to thank my co-supervisor Prof. Dr. Aysun SOFUOĞLU for her academic support. I would like to express special thanks to Prof. Dr. Perihan Binnur KURT KARAKUŞ and Assist. Prof. Dr. Aşkın BİRGÜL for their help instrumental analysis of the study.

My special thanks go to my family for supporting me during all my educational life. This study would never have been concluded without their support, encouragement, patience and love. I would like to extend my endless thanks to my dear math teacher, the decedent L. Kürşad Üçok, who has been the greatest contributor to my achievement to this point, who has supported me throughout my all-education life.

My thanks and appreciation go to my colleague and people who have willingly helped me out with their abilities.

This thesis was supported by a grant number 118Y254 from the Scientific and Technological Research Council of Turkey (TUBITAK).

ABSTRACT

LONG RANGE ATMOSPHERIC TRANSPORT OF PERSISTENT ORGANIC POLLUTANTS TO IZMIR

In this study, passive samplers were placed in 10 provinces and an active sampler in Izmir in order to examine the long-range transport of POPs that are released into the environment due to the effects of the war in countries next to our southeast border. The ten cities were classified into three proximity groups: close, middle, and far. According to correlation analysis, central tendency statistics for various congeners showed an increasing trend with proximity to the war zone. However, support by hypothesis testing with Kruskal-Wallis or ANOVA tests were limited: PBDE-183, Σ_{45}PCB and dieldrin in winter, PBDE-28, PBDE-99, PBDE-154, *p,p′*-DDE, Σ_{14}PBDE and Σ_{25}OCP in the transition period, and PBDE-28, PBDE-99, PBDE-85, PBDE-154, PBDE-190, PCB-52, Σ_{45}PCB, *p,p′*-DDE and Σ_{25}OCP in the whole sampling period. Back-trajectory frequency analysis of passive sampling indicated that air masses were transported from the war zone to the close region, but it was limited for middle and far regions deeming support by back-trajectory analysis of active sampling not possible, which show that the main route of air masses were Europe, Russia, and the former Soviet Union countries, and North Africa. Concentrations measured by passive air sampling being relatively higher both in the close-group and far-group especially in winter than in the middle-group. The result of passive sampling indicates that the southwest border of Turkey was impacted by POPs which were transported from the war zone while the west of the country was impacted by those from areas in north and northeast.

ÖZET

KALICI ORGANİK KİRLETİCİLERİN İZMİR'E UZUN MESAFELİ ATMOSFERİK TAŞINIMI

Bu çalışmada, güneydoğu sınırımızda devam eden savaşın etkileri nedeniyle çevreye salınan KOK'ların uzun mesafeli taşınmasını incelemek amacıyla 10 ile pasif örnekleyici ve İzmir'e bir aktif örnekleyici yerleştirilmiştir. On örnekleme noktası savaş bölgesine olan mesafeye göre yakın, orta ve uzak olarak üç gruba ayrılmıştır. Spearman rank korelasyonunda, çeşitli türdeşlerin merkezi eğilim istatistik değerlerinin savaş bölgesine yakınlık ile artan bir eğilim gösterdiği görülmüştür. Ancak, Kruskal-Wallis veya ANOVA testleri ile hipotez testi desteği sınırlıdır; PBDE-183, Σ_{45}PCB ve Dieldrin kışın, PBDE-28, PBDE-99, PBDE-154, *p,p'*-DDE, Σ_{14}PBDE ve Σ_{25}OCP geçiş döneminde, tüm örnekleme döneminde değerlendirildiğinde ise PBDE-28, PBDE-99, PBDE-85, PBDE-154, PBDE-190, PCB-52, Σ_{45}PCB, *p,p'*-DDE ve Σ_{25}OCP için anlamlı sonuç elde edilmiştir. Pasif örneklemenin geri yörünge frekans analizi, hava kütlelerinin savaş bölgesinden yakın bölgeye taşındığını, ancak orta ve uzak bölgeler için sınırlı olduğunu ve aktif örnekleme sonuçlarıyla uyumlu olmadığını göstermiştir. Sonuçlar, hava kütlelerinin ana rotasının Avrupa, Rusya ve eski Sovyetler Birliği ülkeleri ve Kuzey Afrika olduğunu göstermektedir. Pasif hava örneklemesi ile ölçülen konsantrasyonlar, özellikle kış aylarında hem yakın grupta hem de uzak grupta orta gruba göre nispeten daha yüksektir. Pasif örnekleme sonuçları, Türkiye'nin güneybatı sınırına yakın alanların savaş bölgesinden taşınan KOK'lardan etkilendiğini gösterirken, ülkenin batısının kuzey, kuzeydoğu ülkeleri tarafından KOK'lardan etkilendiğini göstermektedir.

TABLE OF CONTENTS

LIST OF FIGURES vii

LIST OF TABLES x

CHAPTER 1. INTRODUCTION 1

CHAPTER 2. LITERATURE REVIEW 6

2.1. Persistent Organic Pollutants 6

2.2. Chemical Structures and Properties 7

2.2.1. PBDEs 7

2.2.2. PCBs 9

2.2.3. OCPs 11

2.3. POPs Sampling 12

2.4. Active Sampling 14

2.5. Environmental Sources 15

2.6. Health Effects of POPs 17

2.7. Ambient Air POP Concentrations Around The World 19

2.8. Ambient Air POP Concentrations in Turkey 30

2.9. LRAT of POPs 54

2.10. Back-Trajectory Analysis 55

2.11. Motivation and Objectives 56

CHAPTER 3. MATERIAL AND METHODS 57

3.1. Sampling Sites 57

3.2. Sampler Preparation and Deployment 59

3.3. Calculation of Air Volume Passed Through PAS 60

3.4. Sample Collection 61

3.5. Sample Extraction and Analysis 65

3.5.1. PUF Extraction 65

3.5.2. Quartz Filter Extraction 66

3.5.3. Instrumental Analysis 66
3.6. Quality Assurance Quality Control 70
3.6.1. Field Blanks 70
3.6.2. Calibration Linearity 70
3.6.3. Procedural Recovery 70
3.6.4. Detection Limits 71
3.7. Trajectory Analysis 72
3.7.1. Back Trajectory Computational Calculation 72
3.7.2. Computational Calculation of Trajectory Cluster Analysis 73
3.7.3. Computational Calculation of Cluster Frequency 74
3.8. Statistical Analyses 75

CHAPTER 4. RESULTS AND DISCUSSION 76
4.1. Central Tendency of Proximity Groups 76
4.2. Proximity Concentration Relation 87
4.2.1. Correlation Analysis 88
4.2.1.1. Winter 88
4.2.1.2. Transition Period 90
4.2.1.3. The Whole Sampling Period 92
4.3. Back-Trajectory 94
4.3.1. Back Trajectory Frequency Analysis of the Passive Sampling Period 103
4.3.2. Cluster Analysis 114

CHAPTER 5. CONCLUSION 125

REFERENCES 127

APPENDIX 142

LIST OF FIGURES

Figure **Page**

Figure 2.1. Structure of polybrominated flame retardants…….7
Figure 2.2. The general structure of a polychlorinated biphenyl……9
Figure 2.3. Chemical structure of γ-hexachlorocyclohexane as an example……...11
Figure 2.4. Uptake phases of airborne chemicals by passive air samplers ……..…….14
Figure 2.5. Polyurethane foam based passive air sampler..……..14
Figure 2.6 Active air sampler……..…….15
Figure 2.7. Multiple cycles of evaporation, transport by air, and condensation of POPs (Grasshopper effect)……..…….55
Figure 3.1. Samplings sites…….…….….58
Figure 3.2. Photographs of sampling points (from top-left to bottom-right: Isparta, Mugla, Denizli, Izmir) as examples…….....……..62
Figure 3.3. Schematic illustration of procedures from sampling to instrumental analysis……..……..…...…..67
Figure 4.1. The mean POPs concentrations (pg/m^3) and percent contribution…….....80
Figure 4.2. The winter period mean POPs concentrations (pg/m^3) and percent contribution……...81
Figure 4.3. The transition period mean POPs concentrations (pg/m^3) and percent contribution……...84
Figure 4.4. Active sampling Σ_{14}PBDEs concentrations and percent contribution sampling periods Winter-Transition-Other…….……...…85
Figure 4.5. Active Sampling Σ_{45}PCBs concentrations percent contribution sampling periods Winter- Transition-Other……..……86
Figure 4.6. Active Sampling Σ_{25}OCPs concentrations and percent contributions sampling periods Winter-Transition-Other……87
Figure 4.7. Back trajectory analysis of winter period …….……96
Figure 4.8. Back trajectory analysis of transition period…..…….……..98
Figure 4.9. Other back trajectories……..……...……101
Figure 4.10. Passive sampling period monthly back trajectory frequency analysis-Adana…….……104

Figure **Page**

Figure 4.11. Passive sampling period monthly back trajectory frequency analysis-Gaziantep…..……..……..…….105
Figure 4.12. Passive sampling period monthly back trajectory frequency analysis-Osmaniye……..…….106
Figure 4.13. Passive sampling period monthly back trajectory frequency analysis-Karaman……..…..…….……...……..107
Figure 4.14. Passive sampling period monthly back trajectory frequency analysis-Malatya…….……...……...……..……108
Figure 4.15. Passive sampling period monthly back trajectory frequency analysis-Denizli……109
Figure 4.16. Passive sampling period monthly back trajectory frequency analysis-Isparta……..…….……110
Figure 4.17. Passive sampling period monthly back trajectory frequency analysis-Mugla……..111
Figure 4.18. Passive sampling period monthly back trajectory frequency analysis-Bursa……..112
Figure 4.19. Passive sampling period monthly back trajectory frequency analysis-Izmir…….……...……...113
Figure 4.20. Passive sampling period monthly back trajectory cluster analysis-Adana……...……..115
Figure 4.21. Passive sampling period monthly back trajectory cluster analysis Gaziantep…….…….…….116
Figure 4.22. Passive sampling period monthly back trajectory cluster analysis-Osmaniye…..……...……...117
Figure 4.23. Passive sampling period monthly back trajectory cluster analysis-Karaman…….…….……...118
Figure 4.24. Passive sampling period monthly back trajectory cluster analysis-Malatya…….……...…….……..…119
Figure 4.25. Passive sampling period monthly back trajectory cluster analysis-Denizli……..…….120
Figure 4.26 Passive sampling period monthly back trajectory cluster analysis-Isparta..……..……121

Figure **Page**

Figure 4.27. Passive sampling period monthly back trajectory cluster analysis-Mugla……..…….....122
Figure 4.28. Passive sampling period monthly back trajectory cluster analysis-Bursa……...…….……...……..……123
Figure 4.29. Passive sampling period monthly back trajectory cluster analysis-Izmir……...……..……124

LIST OF TABLES

Table **Page**

Table 1.1. POPs recognized in Stockholm Convention revised in 2019. …….2
Table 2.1. Global percentage contribution of PBDE emissions from production, use, and waste management phases to total PBDE emissions (%) based on year 2016……..8
Table 2.2. Physical and chemical properties of PCBs, PBDEs ……9
Table 2.3. Total PCB production (in tons) reported in literature ……..10
Table 2.4. Physiochemical properties of some OCPs ……..12
Table 2.5. Environmental Sources…….16
Table 2.6. Various diseases and health problems associated with POPs…….18
Table 2.7. PBDE, PCB, and OCP, concentrations reported from selected locations of the world……..22
Table 2.8. Passive sampling PCBs concentration reported in Turkey Ambient air…..33
Table 2.9 Active sampling PCBs concentration reported in Turkey Ambient air…..38
Table 2.10. OCP concentrations measured by passive sampling in Turkey……44
Table 2.11. OCP concentrations measured by active sampling in Turkey……46
Table 2.12. PBDE concentrations measured by passive sampling in Turkey…..52
Table 2.13. PBDE concentrations measured by active sampling in Turkey……53
Table 3.1. Depuration compounds spiked on passive PUFs……59
Table 3.2 Passive sampling information……63
Table 3.3. Active sampling information……64
Table 3.4. Target Analytes……68
Table 3.5. Operating conditions of GC-MS……69
Table 3.6. Recovery of Surrogate Compounds……71
Table 4.1. Central Tendency of Concentration (pg/m^3)……76
Table 4.2. Seasonal central tendency statistics for total PBDE, PCB and OCP concentrations (pg/m^3)……78
Table 4.3. Winter season Kruskal Wallis and ANOVA results……90
Table 4.4. Transition season Kruskal Wallis and ANOVA results……91
Table 4.5. All sampling months Kruskal Wallis and ANOVA results……91
Table 4.6 G+P (pg/m^3) concentration of the winter samples……102
Table 4.7. G+P (pg/m^3) concentration of transition samples……102

Table **Page**

Table 4.8. G+P (pg/m^3) concentration of other samples……..……..….102

CHAPTER 1

INTRODUCTION

Persistent Organic Pollutants (POPs) are semi-volatile organic compounds that over the recent decades have become chemicals of concern due to their significant resistance to degradation, their ability to be transported by air over long distances from sources, known as Long Range Atmospheric Transport (LRAT) (Nadal et al. 2015, Pozo et al. 2017). They have capacity to bioaccumulate through terrestrial and aquatic food chains to the levels that may cause adverse animal and human health effects such as immunotoxicity, neurotoxicity, developmental toxicity, cancer, mutagenicity, and endocrine disruption (Nadal et al. 2015). POPs are toxic organic compounds that are resistant to most of the degradation processes in the environment. Therefore, they tend to persist in the environment, bioaccumulating in organisms and biomagnifying along with the food chains and in ecosystems, which make them pose a risk of causing adverse effects to human and wildlife health in particular, and the environment in general (Zacharia 2019).

POPs are ubiquitous, even in remote areas (Qiu et al. 2020). In order to manage POPs, international efforts included the global treaty of the Stockholm Convention (SC) on POPs that was signed in 2001 and came into force in 2004 with the aim of reducing and eliminating the release of POPs into the environment (Stockholm Convention). Stockholm Convention includes 12 POPs compounds which are commonly referred to as dirty dozen in first priority. (SC, 2005).

Over the last decade, the priority list of POPs has been updated. Brominated flame retardants (BFRs), such as polybrominated diphenyl ethers (PBDEs), perfluorinated alkyl substances, perfluorooctane sulfonate (PFOS), its salts, and perfluorooctane sulfonyl fluoride were added to the Stockholm list in 2017. Additionally, new list includes endosulfan, lindane, pentachlorobenzene, chlordecone, and hexabromocyclododecane (HBCD) (Stockholm Convention). Table 1.1 lists the POPs and restrictions included in the Stockholm convention. The Stockholm Convention is divided into three groups, Annex A, Annex B, and Annex C. Each Annex contains elimination restriction, unintentional productions, respectively.

Table 1.1. POPs recognized in Stockholm Convention revised in 2019 (Source: SC, 2019)

Class	Compounds
Annex A (Elimination)	Aldrin[a], Chlordane[a], Chlordecone[a], Decabromodiphenyl ether[b] (commercial mixture, c-decaBDE), Dicofol[a], Dieldrin[a], Endrin[a], Heptachlor[a], Hexabromobiphenyl[b], Hexabromocyclododecane (HBCDD)[b], Hexabromodiphenyl ether[b] and heptabromodiphenyl ether[b] (commercial octabromodiphenyl ether), Hexachlorobenzene[b] (HCB), Hexachlorobutadiene[b] (HCBD), Alpha hexachlorocyclohexane[a], Beta hexachlorocyclohexane[a], Lindane[a], Mirex[a], Pentachlorobenzene[a,b] (PeCB), Pentachlorophenol and its salts and esters[a] (PCP), Polychlorinated biphenyls[b] (PCB), Polychlorinated naphthalenes[b] (PCNs), Perfluorooctanoic acid[b] (PFOA), its salts and PFOA-related compounds[b], Short-chained chlorinated paraffins[b], Technical endosulfan and its related isomers[a], Tetrabromodiphenyl ether and pentabromodiphenyl ether[b] (commercial pentabromodiphenyl ether), Toxaphene[a].
Annex B (Restriction)	DDT[a], Perfluorooctane sulfonic acid (PFOS), its salts and perfluorooctane sulfonyl fluoride [a, b] (PFOS-F)
Annex C (Unintentional production)	Hexachlorobenzene[c] (HCB), Hexachlorobutadiene[c] (HCBD), Pentachlorobenzene[c] (PeCB), Polychlorinated biphenyls[c] (PCB), Polychlorinated dibenzo-p-dioxins[c] (PCDD), Polychlorinated dibenzofurans[c] (PCDF), Polychlorinated naphthalene's[c] (PCNs)

[a]: Pesticides
[b]: Industrial Chemical
[c]: Unintentional Production

POPs can be released into the environment in a variety of ways. As a result of spills and volatilization, polychlorinated biphenyls (PCBs) that were used as oil, dielectrics, and cooling fluids in capacitors and transformers are discharged into the environment. Many industrial operations, mostly thermal (fuel combustion and waste incineration, ferrous industry, coke and aluminum manufacturing, road transport, chemical synthesis of chlorinated chemicals, etc.), generate dioxins/furans, PAHs, and HCB, which are discharged directly into the air (Zacharia 2019).

Organochlorine Pesticides (OCPs) have been used for food crops widely throughout the globe, particularly in developed countries; rice (Oryza sativa L.) being a staple food is also under strong pesticide pressure in developing countries (Mumtaz et al. 2015). Polybrominated diphenyl ethers (PBDEs) were used as additives in numerous electrical and computer devices, textiles, paints, construction materials and furniture to mitigate flammability. PBDEs degrade in polymers that make their release easier from these materials during their manufacturing, usage, and disposal (Li et al. 2016).

LRAT is today considered to be the primary path of transport for many POPs. Selected POPs enter even the Arctic where they are accumulated in soil, ice, and

sediments, and may even persist in the Arctic food web (Corsolini and Sarà 2017). POPs may be transported in the atmosphere in the gas phase and by association with particulate matter. The transport of large quantities of fine sandy particles from the Sahara Desert to the Middle Europe visually demonstrates a clear potential for atmospheric transport of pollutants over vast distances (Kallenborn, Hung, and Brorström-Lundén 2015). Long-term air monitoring is considered to be the backbone of international research into the atmospheric distribution of POPs. As the temperature gradient is one the driving factors of the LRAT, climate change is likely to strongly influence global and polar distribution of contaminants in the near future. Although POPs were detected in Antarctica decades ago, there are still large knowledge gaps, and a comprehensive understanding of their fundamental patterns is lacking (Vecchiato et al. 2015).

People are exposed to POPs mostly in foods, workplaces, and while they are growing in the womb. Because of bioaccumulation in fat tissues and bioaccumulation through the food chain, approximately 90% of humans who are not exposed to POPs by accidental or occupational sources get their exposure from animal food products. POP serum levels rise with age in general, and females have higher amounts than males. (Zacharia 2019). Soils play an important role in supplying and receiving POPs from the atmosphere. Agricultural soils are clearly the source or reservoirs of agrochemical POPs acting as the primary emissions or the reemissions (secondary sources) to atmosphere. The distribution of POPs in background surface soils is a complex function of proximity to source regions, the LRAT of the POP in question, soil properties, degradation, climatic conditions and processes of air–soil exchange. Due to its high storage capacity, soil organic matter (SOM) may act as a sink and has been a focus for the global POPs distribution and budget evaluation (Wang et al. 2012). POPs deposited into the soils are released back when temperature increases seasonally, as well as through fires, and possibly during war. POPs partition to solid and gas phases based on their physicochemical properties such as the octanol-air partitioning coefficient (K_{OA}) and soil properties such as its organic matter (OM) content. Depending on the soil OM content, the higher-molecular-weight POPs, particularly with high K_{OA} values, deposit to a larger extent and accumulate in the soil. K_{OA} is also a temperature-dependent variable. If the temperature increases, POPs are transported to the gas phase at higher rates; thus, they become available for LRAT. War zones may be a special case because there are war vehicles and weapons that may be POP sources, and explosions result in a sudden disruption in soil and rise in temperature that may lead to massive shift of accumulated

POPs from soil to air. Destruction of military and industrial facilities during the Balkan conflicts (1991–1999) resulted in the escape of large amounts of various chemicals into the environment. United Nations Environment Programme (UNEP) identified that 2,500 kg of PCBs escaped into the Morava river in Kragujevac, Serbia (UNEP, 1999). There are two studies addressing the POP and war relationship. Turk et al. (2007) reported that several industrial and military targets were burnt and damaged during the war, resulting in a significant release of POPs. During the massive destruction of industrial complex in Kragujevac, a huge amount of PCB congeners was generated and released into environment. The relatively high concentration of PCBs was detected on locality in proximity of the main production building and two large transformers. Concentration levels of DDT and its metabolites at the same location were increased in comparison to the levels at two other investigated locations (Turk et al. 2007). Later Radonic et al. (2009) reported that since the sampling sites varied from backgrounds to heavily contaminated sites (Bosnia and Herzegovina, Croatia, Serbia), PCB concentrations ranged over three orders of magnitude. Similarly, PAH levels varied over three orders of magnitude, while there was less variability in the pesticide data (Radonic et al. 2009). The literature show that Saharan dust outbreaks occur more frequently in the Mediterranean Basin during the transition seasons of spring and fall (Kabatas et al. 2018). It is well known that in the spring months, Saharan dust outbreaks are often transported to western Turkey (Baltaci 2017). The first study on the Sahara dust storm in Turkey was conducted by Kubilay et al. (2005) in Erdemli, Mersin. Dust storms have been reported in the region originating mostly from the central Sahara in the spring, the eastern Sahara in the summer, and the Middle East/Arabian Peninsula in the autumn. Later, Griffin et al. (2007) worked at the same location showing that the site was affected by the dust generated from North Africa. Kocak et al. (2007), collected $PM_{2.5}$ and PM_{10} samples in the same area. PM_{10} levels were highest during the transition season (March, April, and May) as a result of mineral dust transported from North Africa, and during the winter as a result of sea spray formation. Kuzu et al. (2016) reported that periodically, different air mass transportation route from the Saharan Region of North Africa to Istanbul is formed. Mostly in the winter and in spring, dust outbreaks were observed in Istanbul, and showed that our country is under the influence of desert dust from time to time. Recently, Rastgeldi-Dogan et al. (2020) found that southeastern city of Sanliurfa receives dust from the Sahara Desert, the Syrian desert and even the Arabian desert. Dust transport is may be important because the air masses that pass over the Middle East conflict/war zones

may be transporting POPs to Turkey. In fact, one of the possible LRAT source regions of POPs was identified as the Middle East in a previous research project conducted by our group (TÜBİTAK,112Y315).

CHAPTER 2

LITERATURE REVIEW

POPs in ambient air have been observed extensively across the globe. So, there are many reports from all over the world showing LRAT of POPs. The following sections include general information such as their chemical structures and properties, environmental sources, transportation, and fate, and sampling methods, and a review of the literature on atmospheric concentrations and back-trajectory analysis.

2.1. Persistent Organic Pollutants

POPs are chemicals of global significance due to their ability for long-range transport, environmental persistence, tendency to bio-magnify and bio-accumulate in soils, and their major adverse effects on human health and the environment. People are exposed to these contaminants in a number of ways: especially through the food we consume, but also through the air we breathe, indoors, outside, and at work. Many items that are used in our everyday lives may include POPs that have been added to enhance product properties, such as flame retardants or surfactants. OCPs, PCBs, and PBDEs are the most frequently identified POPs. The POPs bio-magnify and bio-accumulate in organisms throughout the food chain. Thus, the highest levels of POPs are identified at the top of the food chain of organisms. The current levels of POPs can also be found within the human body. Human exposure -for certain chemicals and conditions, even at low levels- will contribute to increased risk of cancer, developmental disturbances, immune system changes, neurobehavioral dysfunction, endocrine disturbance, genotoxicity and increased birth defects (EPA).

2.2. Chemical Structures and Properties

2.2.1. PBDEs

PBDEs are a group of aromatic brominated compounds as shown in Figure 2.1 which were used in abundance as additive flame-retardants in polymers found in textiles and electrical appliances such as computers and televisions. They have emerged as a significant class of environmental contaminants, being detected in a wide range of environmental and human biomonitoring, i.e. milk, blood plasma, and adipose tissue (Wong et al. 2001).

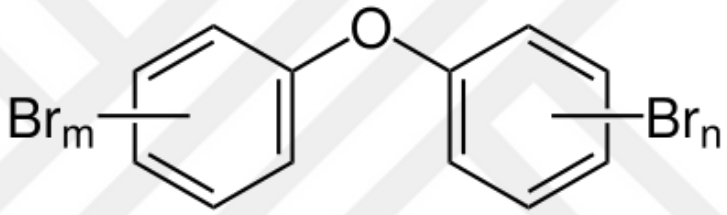

Figure 2.1. Structure of polybrominated flame retardants.

In principle there are 209 congeners of PBDE, which can be divided into 10 classes, identified by bromine substitution (mono- to deca-BDE). PBDEs are produced commercially at three high bromination levels pentaBDE, octaBDE, and decaBDE, representing the mean bromine content (Chen et al. 2012).

Under the Stockholm Convention, Commercial PentaBDE (c-PentaBDE), the homologues' tetrabromodiphenyl ether and pentabromodiphenyl ether and c-OctaBDE,' hexabromodiphenyl ether, and heptabromodiphenyl ether are mentioned. TetraBDE, pentaBDE, hexaBDE, and heptaBDE are mentioned in Annex A to the Convention and their production and use, subject to the exemptions authorized by the Convention, must be removed by the parties involved where the amendment has entered into force. In the latest version (Stockholm Convection, 2017), these mentioned POPs are referred to as POP-PBDEs. In Annex A of the Convention, hexabromobiphenyl (HBB) is mentioned. For its production or uses, there is no specific exemption (Stockholm Convection, 2017). They were used in paints, plastics, foam furniture padding, textiles, rugs, curtains,

televisions, building materials, aircraft, and automobiles. PBDEs account for 5% to 30% of some of these products by weight (Siddiqi et al. 2003). PBDEs are environmental concern because of their high lipophilicity and high resistance to degradation processes. They are expected to readily bioaccumulate (Rahman et al. 2001). Because of the characteristics of potential for long-range environmental transport, PBDEs can be detected in human tissues of residents from regions far away from PBDE source areas (Chen et al. 2012).

Global emissions of evaporative and fugitive PBDEs in 2016 were measured at 2.43–14.9 tonnes, and the deca-BDE mixture accounted for 86.2–95.3 percent of total emissions (Table 2.1). Landfills are the dominant sources of evaporative and fugitive PBDE emissions (65.4 percent), and production ranks second (32.2 percent). It should be noted that choosing emission sources allows a big difference in the percentage of cumulative emissions and production from multiple sources. Global percentage contribution of PBDE emission depending on their use given in Table 2.1.

Table 2.1. Global percentage contribution of PBDE emissions from production, use, and waste management phases to total PBDE emissions (%) based on year 2016 (Redfern et al. 2017).

	deca-BDE mixture	**octa-BDE mixture**	**penta-BDE mixture**	**Total PBDE mixtures**
tri-BDE	0	0	0.01-0.07	0.01-0.07
tetra-BDE	0	0	0.4-2.4	0.4-2.4
penta-BDE	0	0	0.7-4.0	0.7-4.0
hexa-BDE	0	0.6-0.9	0.09-0.6	0.7-1.5
hepta-BDE	0	1.3.0	0	1.6-3.0
octa-BDE	0	1.0-2.2	0	1.0-2.2
nona-BDE	3.7	0.3-0.6	0	3.9-4.3
Deca-BDE	82.5-91.6	0.02-0.06	0	82.6-91.6
Total PBDEs	82.6-95.3	3.6-6.7	1.1-7.0	100

Table 2.2. Physical and chemical properties of PCBs, PBDEs
(Source: Kodavanti and Loganathan 2019)

Property	PCBs	PBDEs
Physical state at room temperature	Oil to viscous liquid	Viscous liquid to powder
Molecular weight (g/mol)	188 to 498	Up to 959.22
Water solubility (μg/L at 25 °C)	0.0027 to 0.59	0.1 to 13.3
Boiling point (°C)	275 to 450	300 to .400
Melting point (°C)	1	2 7 to 306
Vapor pressure at 25°C (mm Hg)	10^{-12} to 10^{-4}	2.2×10^{-7} to 3.47×10^{-8}
Octanol-water partition coefficient (log Kow)	4.7 to 6.8	6.265 to 6.97
Soil organic carbon-water coefficient (Koc)	No data	4.89 to 6.80
Henry's Law Constant ($atm.m^3/mol$)	2.9×10^{-4} to 4.6×10^{-3}	1.2×10^{-5} to 4.4×10^{-8}

2.2.2. PCBs

PCB is an abbreviation commonly used for the group of organochlorine substances classified as polychlorinated biphenyls or polychlorobiphenyls (Rodenburg et al. 2015). These materials, represented by the general structure shown in Figure 2.2 and the formula $C_{12}H_{10-x}Cl_x$, are based structurally on a biphenyl ring system to which 1–10 chlorine atoms may be attached.

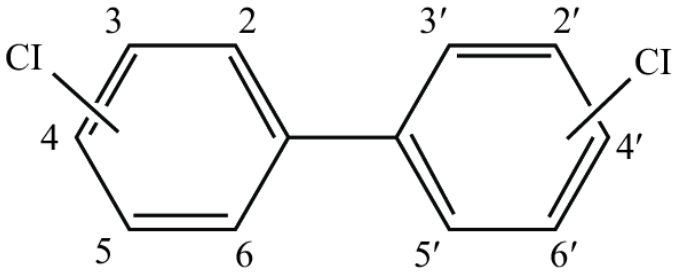

Figure 2.2. The general structure of a polychlorinated biphenyl.

The various chlorine atom compositions give rise to 209 potential PCB congeners, numbered 1–209 depending on the number and locations of chlorine atoms as per the IUPAC convention. Congeners with identical chlorine atoms belong to the same category of homologues and have common physicochemical properties. Under the Stockholm Convection PCBs are specified in Annex A with various exemptions and in Annex C with

no exemptions. PCBs are pollutants that are anthropogenic and have no established natural origin. It was widely used in a variety of commercial applications in the past (Raffetti et al. 2020). In the US, about 99% of all intentional PCB production was carried out by Monsanto, the products sold under the trade name Aroclor. In Europe, PCBs were produced under trade names such as Phenoclor (Raffetti et al. 2020), Fenclor (Italy), Askarel (United Kingdom), and Clophen (Germany) (Ballschmiter and Zell 1980, Rodenburg et al. 2015). Breivik et al. (2007) estimated that 1,325,810 tons of PCBs was produced intentionally via these legacy sources, with 80 % of this occurring in just four countries (the United States, West Germany, the USSR, and France). Breivik et al. (2007), also reported that intentionally produced PCBs were produced between 1930 and 1993, while major emissions of this production were in the USA, Germany, USSR, France, and UK by 48.4%, 12%, 10.7%, 10.2%, 5.0%, respectively. The rate of the remaining 11 countries in emissions of 1,325,810 tons is <5% (Breivik et al. 2007). Further information regarding production can be found in Table 2.3.

Table 2.3. Total PCB production (in tons) reported in literature
(Source:Dai, Min, and Weng 2016)

Manufacturer	**Country**	**Producing time**	**Total (t)**	**Percent (%)**
Monsanto	Unites States	1930-1977	641,246	48.4
Bayer	West Germany	1930-1983	159,062	12
Orgsteklo	Former Soviet Union	1939-1990	141,800	10.7
Prodelec	France	1930-1984	134,654	10.2
Monsanto	United Kingdom	1954-1977	66,542	5
Kanegafuchi	Japan	1954-1972	56,326	4.2
orgsintez	Former Soviet Union	1972-1993	32,000	2,4
Caffaro	Italy	1958-1983	31,092	2.3
S.A.Cross	Spain	1955-1984	29,012	2.2
Chemko	Czecholovakia	1959-1984	21,482	1.6
Xi An	China	1960-1979	8,000	0.6
Mitsubishi	Japan	1969-1972	2,461	0.2
Electrochemical Company	Poland	1966-1970	1000	<0.1
Zaklady Azotowe	Poland	1974-1977	679	<0.1
Geneva Industries	Unites States	1971-1973	454	<0.1
Total	Whole World	1930-1993	1,325,810	100

2.2.3. OCPs

OCPs were extensively used in agriculture from 1950s to 1970s. Early measurements detected OCPs in a wide range of environmental compartments in remote areas, confirming large-scale dispersion and deposition to areas far from the original site of application. The atmosphere plays an important role in their transport over long distances. Due to their resistance to environmental degradation, OCPs have remained major global pollutants, with numerous investigations reporting the continued and ubiquitous presence of OCPs in the global atmosphere (Shen et al. 2005). Chemical structure of γ-hexachlorocyclohexane is shown in Figure 2.3 as an example.

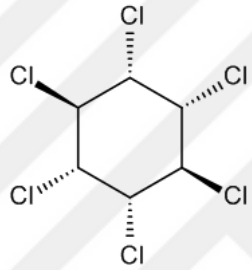

Figure 2.3. Chemical structure of γ-hexachlorocyclohexane as an example

Pesticides are a class of chemicals used to kill insects, plants, fungi, bacteria, and etc. These are generally referred to as insecticides, fungicides, bactericides, herbicides, and rodenticides depending on the target organisms. Some pesticides are capable of killing a wide range of pests or weeds, but some work only against particular pests or pathogens. The desired characteristics of pesticides, such as high lipophilicity, bioaccumulation, long half- and long- transport capacity, have increased the chances of air, water, and soil pollution, even after several years of application (Jayaraj, Megha, and Sreedev 2016). For certain OCP compounds, the constant values of solubility, octanol-water and Henry are specified in Table 2.4.

Table 2.4. Physiochemical properties of some OCPs
(Source:Kengara et al. 2010)

Compound	MW	Solubility mg/L	Log Kow	Henry Values ($Pa.m^3/mol$)
Alpha-HCH (α-HCH)	290.85	10 (28°C)	3.80	0.695 (20°C)
beta-HCH (β-HCH)	290.85	5 (20°C)	3.78	0.046 (20°C)
Gamma-HCH (γ-HCH)	290.85	17 (20°C)	3.71	0.355 (20°C)
delta-HCH (δ-HCH	290.85	10 (20°C)	4.14	0.021 (20°C)
epsilon-HCH (ε-HCH)	290.85	0.68 (@ 25°C)	-	
Pentachlorobenzene (PCB)	250.34	0.2 (@ 20°C)	5.19	72.00 (@ 25°C)
Hexachlorobenzene (HCB)	284.8	0.006 (@ 25°C)	5.14	58.77 (@ 25°C)
p,p′-DDT	354.48	0.003 (@ 25°C)	6.50	0.841 (@ 25°C)
o,p′-DDT	354.48	0.085 (@ 25°C)	6.79	0.060 (@ 25°C)
p,p′-DDD	320.1	0.05 (@ 25°C)	6.02	2.128 (@ 25°C)
o,p′-DDD	320.1	0.10 (@25°C)	5.87	1.824 (@ 25°C)
p,p′-DDE	318.1	0.065 (@ 24°C)	5.50	0.405 (@ 25°C)
o,p′-DDE	318.1	0.0013 (@ 20°C)	6.00	0.828 (@25°C)
trans-Chlordane (trans-CHL)	409.8	0.0014 (@ 25°C)	6.07	8.420 (@ 25°C)
cis-Chlordane (cis-CHL)	409.8	0.042 (@2 0°C)	6.11	12.92 (@ 25°C)
Oxy-Chlordane (OC)	423.8	0.023 (@ 20°C)	4.95	7.48 (@ 25°C)
Heptachlor (HC)	373.3	0.05 (@ 25°C)	6.10	29.79 (@ 25°C)
cis-Hexachloroepoxide (cis-HCE)	389.4	0.275 (@ 25°C)	5.00	1.665 (@ 25°C)
trans-Hexachloroepoxide (trans-HCE)	389.4	0.275 (@ 25°C)	5.40	3.242 (@ 25°C)
Aldrin	364.9	0.011 (@ 20°C)		4.965 (@ 25°C)
Dieldrin	380.9	0.14 (@ 20°C)		0.527 (@ 25°C)
Endosulfan-I	406.9	0.32 (@ 22°C)		1.013 (@ 25°C)
Endosulfan-II	406.9	0.33 (@ 20°C)		1.935 (@ 25°C)
Methoxychlor	345.69	0.10 (@ 25°C)		1.621 (@ 25°C)
Mirex	545.59	5×10^{-7}(@ 22°C)		52.284 (@ 25°C)

2.3. POPs Sampling

Air sampling for POPs has been performed limited number of sites using active, high-volume air samplers. These are costly, require electricity and a qualified operator. Under the SC, signatory countries must perform inventories of sources, classify ongoing sources and provide proof of decreasing ambient rates of POPs for environmental monitoring. In particular, under-developed countries need cost-based approaches that can

work in the absence of resources. Active sampling using traditional high-volume air samplers includes pumps, heads for sampling, and a source of power. Passive air sampler-(PAS) provides the ability to overcome a variety of such problems. They are simple to use, cost-effective, versatile, and capable of being implemented concurrently in several locations. Consequently, this method of sampling can also be very costly and not always feasible, particularly when large number of multiple concurrent samples at different locations (Shoeib and Harner 2002b, Bogdal et al. 2013, Harner, Pozo, et al. 2006, Shoeib and Harner 2002a). In certain cases, the only alternative may be passive samplers. The phases of sorption of airborne chemicals by passive air samplers can be seen in Figure 2.4. In the initial so-called 'linear uptake phase', the amount of airborne chemical sequestered by the sorbent increases linearly with time and under the assumptions of a constant volumetric sampling rate of air and a constant chemical concentration in air is proportional to the sampled air. During exposure period, the absorption rate decreases before equilibrium is reached between sorbent and ambient air. PASs are deployed for a duration no longer than the linear sorption process, the amount of chemical sequestered in the sorbent makes it possible to calculate the pollutant concentration in ambient air, based on the measured volume of air polyurethane foam (PUF) disks, which has proven to be an acceptable sorbent in PAS (Bogdal et al. 2013). Low acquisition costs, minimal maintenance needs, easy handling, and no need for power supply are benefits that PASs provide, especially in countries with limited financial capital or remote areas. The concentration of POPs in air (pg/m^3) is calculated only after dividing the amount of chemicals (pg) by the corresponding air-sampling volume (m^3). POP sorption levels (e.g., PCB) may vary from 2–8 m^3/day, and usually range from 3–4 m^3/day. The deployment time must be long enough to achieve the necessary amount of air-sampling, but it should not be too long to prevent the PUF reaching ambient air equilibrium (Bogdal et al. 2013).

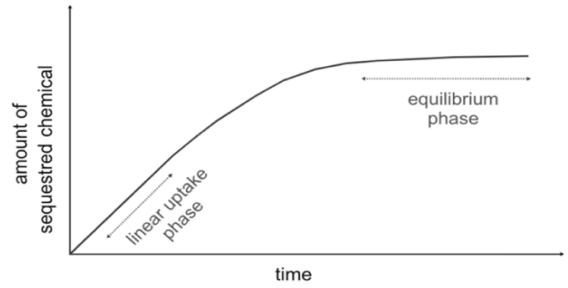

Figure 2.4. Uptake phases of airborne chemicals by passive air samplers
(Source:Bogdal et al. 2013)

Air samplers, consisting of polyurethane foam (PUF) disks housed in stainless steel domed chambers shown in Figure 2.5 (Motelay-Massei et al. 2005).

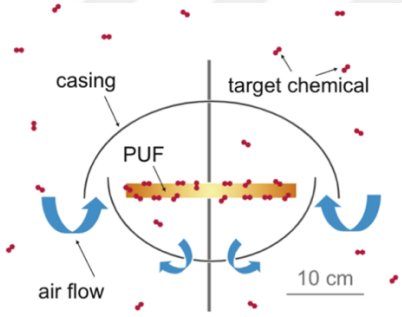

Figure 2.5. Polyurethane foam based passive air sampler
(Source: Bogdal et al. 2013)

2.4. Active Sampling

The sampled air is passed through a filter to collect the POPs in particulate phase and a polyurethane foam (PUF) plug to collect those in gas phase. An illustration is provided as an example of commercially available systems in Figure 2.6 (Tish Environmental Samplers)

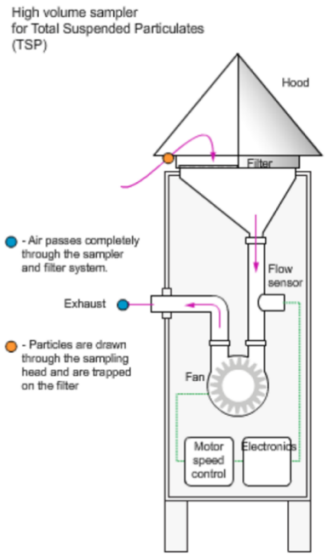

Figure 2.6. Active air sampler
(Source: tisch-env.com)

2.5. Environmental Sources

PCBs were first synthesized in the late 1920s and have been used in many tens of open and closed applications. It has been estimated that the global production since that time is of the order of 10^6 tones but information on the breakdown of usage is very limited, making it very difficult to derive estimates for the historical and contemporary source term (Jones and De Voogt 1999). Historically, PCBs were commonly used as insulating materials in electrical devices, hydraulic oils and heat transfer systems, with lesser amounts being used for many industrial applications. Their strong persistence, though historically a technological asset, ensures they are extremely persistent in the climate, and are thus known as POPs (Rodenburg et al. 2015). For agrochemical POPs the source is clear as the deliberate application to crops and soils. However, despite their deliberate manufacture, data on the total amount entering the environment and regional/global usage patterns of agrochemical POPs is highly uncertain and often poorly known (Mandal et al. 2020). Other POPs have been deliberately manufactured but have multiple diverse and uses. POPs are extremely stable, water-insoluble compounds that have contributed much to modern living and have become economically vital as products (plastics, pesticides, solvents, adhesives, etc.). The more stable the molecules, the longer lived the material and this is considered advantageous in many applications. Unwanted by-products

(dioxins and furans) are economically important in reverse: costly to capture and control. Unfortunately, once in the environment, persistent and fat-soluble molecules tend to accumulate in biological tissue (Godduhn and Duffy 2003). Table 2.5 presents types and sources of POPs.

Table 2.5. Environmental Sources

Type	Environmental sources	Reference
PBDEs	PBDEs are used in transportation in conveyor belts; rubber pipes for insulation; and the textile coatings of seating in automotive, aircraft, and trains. PBDEs are impregnated into polyamide polymers using as pipes and plastic foil.	(Siddiqi et al. 2003)
PBDE	e-Wastes	(Cai et al. 2018, Park et al. 2014)
PCBs	"Fire-resistant" synthetic products (made before 1977), old electrical equipment, leaky containers in PCB disposal sites.	(Abelsohn et al. 2002)
PCBs	Plastics, lubricants and dielectric fluids.	(Macgregor et al. 2010)
Aldrin	Against insects to protect crops such as corn and potatoes.	(Abelsohn et al. 2002)
Chlordane	The insecticide used on vegetables, grains, maize, oilseed, potatoes, sugar cane, beets, fruits, nuts, cotton, and jute.	(Abelsohn et al. 2002)
DDT	The pesticide used during World War II to protect soldiers and civilians against diseases spread by insects.	(Abelsohn et al. 2002)
Dieldrin	The insecticide used to control insects in the soil.	(Abelsohn et al. 2002)
Endrin	Foliar (leaf) insecticide used on field crops such as cotton	(Abelsohn et al. 2002)
HCB	Fungicide used for seed treatment.	(Abelsohn et al. 2002)
Heptachlor	No systemic stomach and contact insecticide used to control insects in soil.	(Abelsohn et al. 2002)
Mirex	Stomach insecticide used to control ants, termites, and mealy bugs.	(Abelsohn et al. 2002)
α-HCH	Insecticide	(Venier et al. 2019)
γ-HCH	Insecticide	(Venier et al. 2019)

2.6. Health Effects of POPs

POPs are highly toxic and give rise to various health and environmental problems. Bioaccumulation and persistence of POPs have made them hazardous materials for life (Thakur and Pathania 2020)**.** According to the World Health Organization, outdoor air pollution is a major environmental health problem affecting everyone in developed and developing countries alike. In the course of the years, many scientific evidences demonstrated a relationship between ambient pollution and several adverse effects on human health (Zacharia 2019). Exposure to air pollution, which ubiquitously contain POPs, can affect the respiratory system, and has been linked to negative outcomes during intrauterine development, and other heterogeneous dysfunctions and diseases, such as type 2 diabetes, neurological diseases and neuropathology, reproductive dysfunctions, endocrine disruption within the reproductive system, the central nervous system, or the immune system, cardiovascular problem (Vitali et al. 2019). Table 2.6 lists the health problems related to POPs reported in the literature.

Virtanen et al. (2005), Roveda et al. (2006), Arrebola et al. (2014), Cabaravdić (2006) and Hardell et al. (2004) reported that exposure to PCBs is related to the cancer. Dirinck et al. (2011) associated PCBs (congeners 138, 153, 170, 180) and OCPs (DDE and β-HCH) with diabetogenic obesogenic effects. Many researchers have reported that occurrence of Type 2 diabetes is related with exposure to POPs (Arrebola et al. 2013, Kim et al. 2014, Lee, Steffes, et al. 2011, Uemura 2012, Zeliger 2013)

Table 2.6. Various diseases and health problems associated with POPs

Compound	Health problems	Reference
Dioxins, furans, PCBs, PBBEs, PBDEs, or OCPs	Type 2 diabetes	(Zeliger 2013)
Organochlorine and PCBs	Type 2 diabetes, insulin resistance	(Kim et al. 2014)
OCPs, PCBs, PBB.	Obesity, dyslipidemia, insulin resistance, common precursors of type 2 diabetes, cardiovascular diseases.	(Lee, Steffes, et al. 2011, Lee, Lind, et al. 2011)
OCPs.	Breast cancer	(Cabaravdić 2006)
p,p′-DDE	Type 2 diabetes	(Arrebola et al. 2013)
PCB congeners (105,118), (DDE), (HCB) and TNC	Obesity	(Roos et al. 2013)
PCB congeners 153, 138, 180, and 170, OCPs, DDE, βHCH	Diabetogenic obesogenic effects	(Dirinck et al. 2011)
PCB (99, 118, 105, 138, 153, and 180)	Ventricular systolic and diastolic dysfunction	(Lind et al. 2013)
PCBs and 10 OCPs	Increased blood pressure	(Henríquez-Hernández et al. 2014)
PCBs, hexachlorobenzene, trans-chlordane	Prostate cancer	(Hardell, Andersson, et al. 2006)
PCB, OCPs, PBDE, 1 dioxin	Abdominal obesity	(Lee et al. 2012)
PCBs	Breast, prostate, testicular, ovarian and uterine cancers	(Roveda et al. 2006)
PCBs	Increase in total cholesterol, HDL, LDL, total serum lipids	(Arrebola et al. 2014)
PCBs	Diabetes and hypertension	(Everett, Frithsen, and Player 2011)
PCBs, OCPs	Type 2 diabetes	(Lee, Steffes, et al. 2011, Lee, Lind, et al. 2011)
PCBs and three OCPs	Change in cholesterol levels	(Ljunggren et al. 2014)
PCBs, DDE, HCB and chlordane's	Testicular cancer	(Hardell et al. 2004)
PCBs, DDE, HCB, PBDEs and chlordane's	Testicular cancer	(Hardell, van Bavel, et al. 2006)
PCBs, DDE, HCB, and chlordane's	Kidney cancer, anorexia-cachexia syndrome	(Hardell, Lindstrom, et al. 2006)
PCBs, OCDD and (PBDE-47)	Cardiovascular Problems (increase in cholesterol levels)	(Penell et al. 2014)
PCBs, OCPs and PCBs	Obesity, insulin resistance, high triglyceride, and low high-density lipoprotein (HDL) cholesterol.	(Lee et al. 2012)
PCBs, PBDE, DDT	Weight gain, advance puberty, and induce changes in gene expression associated with steroid hormones and obesity in female zebrafish.	(Lyche et al. 2010)
PCBs, PCDDs, PCDFs DDT, DDE and HCB	Type 2 diabetes	(Uemura 2012)
PCBs, pesticides, phthalates	Testicular cancer	(Virtanen et al. 2005)
PCBs, DDTs	Embryo defect in zebrafish	(Lyche et al. 2013)

2.7. Ambient Air POP Concentrations Around The World

A review of atmospheric PBDE, PCB, and OCP concentrations measured in different parts of the world is provided in this section under two sampling type categories: active and passive. Table 2.7 shows PBDE, PCB, and OCP concentrations measured by using passive sampling reported between 2017 and 2020. There are a vast number of studies in the literature, thus, a limited selection considering geographical variation is included: China, India, Italy, Jamaica, Thailand, Vietnam, West Antarctica. Because China has been swiftly industrializing, a lot of work has been done. China has a long production history of OCPs and PCBs and was ranked the world's second producer of HCHs and DDTs between 1945 and 1983 (Li et al. 2018). Another remarkable location is the West Antarctic, because there was no production and emissions. Therefore, reported concentrations in West Antarctica have been considered to be a result of LRAT.

Estellano et al. (2017), conducted a study in the urban and rural areas of Italy. They carried out studies in two different periods by passive sampling. The first period was between April and July, which was called spring. The second season is called autumn between August and November. The mean concentrations of the sum of DDX (*p,p′*-DDT, *o,p′*-DDT, *p,p′*-DDE, *o,p′*-DDE, *p,p′*-DDD, and *o,p′*-DDD) in the air ranged from 2.87 pg/m^3 to 50.8 pg/m^3. The average concentrations of the sum of HCHs (α-HCH, γ-HCH, β-HCH) in the air varied from 4.9 pg/m^3 to 10.67 pg/m^3 in all samples. The $\sum_7$PCB revealed a clear spatial variation between urban and rural sites. This is mostly due to the impact of pollution sources, since they were found at higher levels in urban areas than in rural areas. The concentrations ranged between 4 pg/m^3 and 37.46 pg/m^3. The highest mean concentration of $\sum_3$HCH reported in urban area sampling date between August and November 2008 as 10.67 pg/m^3. The highest mean concentration of $\sum_6$DDX reported again in urban area but at sampling time from April to July. For $\sum_7$PCB that is the same and the concentration was 37.46 pg/m^3. Pozo et al. (2017), collected samples in India at two different sites (Urban and Wetland) between December and March 2014 by passive sampling. One PBDE congener, 8 DDX compounds, and 7 PCB congeners were reported. $\sum_8$DDX concentrations ranged between 127 pg/m^3 and 216 pg/m^3 for urban areas. Just one sample collected in the wetland region had a concentration of 108 pg/m^3. The concentration of PBDE-209 ranged from 0.3 pg/m^3 to 23 pg/m^3 and the concentration of PCBs varied between 53 pg/m^3 and 213 pg/m^3 in urban area. PBDE-209 and PCB

concentrations in wetland were reported to be 0.6 pg/m^3 and 9 pg/m^3, respectively. Wang et al. (2017 and 2018), performed studies to measure POPs in western Antarctica by active sampler. POPs can be prone to LRAT to remote areas, especially the Polar Regions. As a consequence, a series of congener concentrations have been reported in areas without pollution sources. Wang et al. (2017) measured 20 congener PCBs between 2011 and 2014. The average of three years ranged from $\sum_{20}$PCB 5.87 pg/m^3 to 12.2 pg/m^3. The highest mean concentration reported in 2011 was $\sum_{20}$PCB=35.7±12.2 pg/m^3. Wang et al. (2018) reported $\sum_{23}$OCP concentration between 5.87 pg/m^3 and 27.9 pg/m^3. The highest mean OCP concentration reported in 2011 as $\sum_{23}$OCP=16.2±4.80 pg/m^3. Trinh et al. (2018) collected active samples at different locations around Vietnam. Samples were collected during dry and rainy seasons. Due to waste incineration, the highest concentration was reported in dry season and industrial area. The PCB concentration for 12 PCBs in Vietnam was $\sum_{12}$ PCB= 8.30 pg/m^3. Later, Anh et al. (2020), collected samples near a recycling area in Vietnam by passive sampler, and a total of 209 PCBs congeners reported. Concentrations ranged from 110 pg/m^3 to 1100 pg/m^3. In addition, PBDE concentrations ranged from 5.3 pg/m^3 to 86 pg/m^3. Khuman & Chakraborty (2019) and Chakraborty et al. (2019), collected passive and active samples, respectively. India was not only the highest producer but also the largest DDT consumer. India accounted for 84% of global vector control use of DDT over the period 2001 to 2014. Khuman & Chakraborty (2019) reported average concentration of heptachlor-epoxide 1186±371 pg/m^3 of urban and suburban Ganga, India. The highest concentration reported by Chakraborty et al. (2019) was $\sum_{3}$DDTs=1645±332 pg/m^3 Parangibettai, India. Rice is a major agricultural product of Thailand. Tipayrom et al. (2020), measured OCPs in two agricultural areas of Thailand. Samples were collected during dry and rainy season. Results indicated that in the wet season there were usually higher concentrations and a larger number of species of OCPs than in the dry season. The concentrations of OCPs reported in the samples for most of the detected compounds were usually below 0.2 ng/m^3. The maximum $\sum_{16}$OCPs concentration was measured as 1.4±2.1 ng/m^3 in the dry season, while it was 2.3±2.5 ng/m^3 in the wet season.

Studies reported POP levels in industrial zones, waste recycling areas, city centers, forest, rural, and remote areas. Concentrations of PCB and PBDE were reported to be higher in samples taken from recycling facilities and urban areas, while concentrations of OCPs were reported to be higher in agricultural land. In addition, POPs

were detected in forests of India and Antarctica, showing the effect of LRAT despite being restricted/prohibited by Stockholm Convection.

Table 2.7. PBDE, PCB, and OCP, concentrations reported from selected locations of the world

Sampling Site	Area	Sampling Type	Sampling Period	#of Samples	Congeners	Concentration	Reference
Tuscany, Italy	Urban	Passive	April to July 2008 (spring summer)	n=6	α–HCH, γ HCH, β HCH	$\sum_3$HCH=8.6 pg/m^3	(Estellano et al. 2017)
					o,p′ -DDD ,*p,p′*-DDD *o,p′*-DDE p,p′ -DDE *o,p′*-DDT *p,p′*-DDT	$\sum_6$DDT=22 pg/m^3	
					PCB#28,52,101,118,153,138,180	$\sum_7$PCBs=16.36 pg/m^3	
	Urban	Passive	August to November 2008 (autumn)	n=6	αHCH,γ HCH,β HCH	$\sum_3$HCH =10.67 pg/m^3	
					o,p′-DDD, *p,p′*-DDD, *o,p′*-DDE,*p,p′*-DDE,*o,p′*-DDT *p,p′*-DDT	$\sum_6$DDT=46 pg/m^3	
					PCB#28,52,101,118,153,138,180	$\sum_7$PCBs=19.89 pg/m^3	
	Urban		November 2008 to April 2009 (winter)	n=6	αHCH, γ HCH, β HCH	$\sum_3$HCH =7.67 pg/m^3	
					o,p′-DDD, *p,p′*DDD, *o,p′*-DDE, *p,p′*-DDE, *o,p′*-DDT, *p,p′*-DDT	$\sum_6$DDT=13 pg/m^3	
					PCB#28,52,101,118,153,138,180	$\sum_7$PCBs=13.13 pg/m^3	

(Cont. on next page)

Table 2.7. (Cont.)

Sampling Site	Area	Sampling Type	Sampling Period	#of Samples	Congeners	Concentration	Reference
Tuscany, Italy	Urban	Passive	April to July 2009 (spring summer)	n=4	α–HCH, γ-HCH, β–HCH	$\sum_3$HCH=10.8 pg/m^3	(Estellano et al. 2017)
					o,p´-DDD, *p,p´*-DDD, *o,p´*-DDE, *p,p´*-DDE,o,p' -DDT, *p,p´*-DDT	$\sum_6$DDT=50.8 pg/m^3	
					PCB#28,52,101,118,153,138,180	$\sum_7$PCBs=37.46 pg/m^3	
	Rural	Passive	April to July 2008 (spring summer)	n=4	α–HCH,γ -HCH,β– HCH	$\sum_3$HCH =6.87 pg/m^3	
					o,p´-DDD, *p,p´*-DDD,*o,p´*-DDE, *p,p´*-DDE, *o,p´*-DDT, *p,p´*-DDT	$\sum_6$DDT=6.1 pg/m^3	
					PCB#28,52,101,118,153,138,180	$\sum_7$PCBs=4.4 pg/m^3	
	Rural		November 2008 to April 2009 (winter)	n=4	α–HCH, γ-HCH, β-HCH	$\sum_3$HCH =4.9 pg/m^3	
					o,p´-DDD, *p,p´*-DDD, *o,p´*-DDE, *p,p´*-DDE, *o,p´*-DDT, *p,p´*-DDT	$\sum_6$DDT=2.87 pg/m^3	
					PCB#28,52,101,118,153,138,180	$\sum_7$PCBs=4 pg/m^3	
	Rural	Passive	April to July 2009 (spring summer)	n=4	α–HCH,γ-HCH,β-HCH	$\sum_3$HCH =8.35 pg/m^3	
					o,p´-DDD, *p,p´*-DDD, *o,p´*-DDE, *p,p´*-DDE, *o,p´*-DDT, *p,p´*-DDT	$\sum_6$DDT=4.98 pg/m^3	
					PCB#28,52,101,118,153,138,180	$\sum_7$PCBs=6.35 pg/m^3	

(Cont. on next page)

Table 2.7. (Cont.)

Sampling Site	Area	Sampling Type	Sampling Period	#of Samples	Congeners	Concentration	Reference
India	Urban	Passive	December 28 to March 27, 2014	n=5	PBDE-209	PBDE-209 =11 ± 9[a] pg/m^3	(Pozo et al. 2017)
						PBDE-209=0.3-23[b] pg/m^3	
					α-HCH, γ-HCH, *o,p´*-DDD, *p,p´*-DDD *o,p´*-DDE, *p,p´*-DDE, *o,p´*-DDT, *p,p´*-DDT	$\sum_8$DDT=161 ± 36.46 [a] pg/m^3	
						$\sum_8$DDT=127-216[b] pg/m^3	
					PCB# 28,52,101, 110,153,138,180	$\sum_7$PCBs=140.6 ± 64.5[a] pg/m^3	
						$\sum_7$PCBs=53-213[b] pg/m^3	
	Wetlands			n=1	PBDE-209	PBDE-209 =0.6 pg/m^3	
						PBDE-209 =10[c] pg/m^3	
					α-HCH, γ-HCH, *o,p´*-DDD, *p,p´*-DDD *o,p´*	$\sum_8$DDT= 108 pg/m^3	
					-DDE *p,p´*-DDE, *o,p´*-DDT, *p,p´*-DDT	$\sum_8$DDT=158[c] pg/m^3	
					PCB#28,52,101,110, 153,138,180	$\sum_7$PCBs=9 pg/m^3	
						$\sum_7$PCBs=164[c] pg/m^3	
West Antarctica		Active	2011	n=10	PCB#11,28,52,101,138,153,180,77,81,105 ,114,118,123,126,157,167,169,189,209	$\sum_{20}$PCBs=35.7±12.2[a] pg/m^3	(Wang et al. 2017)
						$\sum_{20}$PCBs=21.9-72.6[b] pg/m^3	
			2012	n=10		$\sum_{20}$PCBs=19.3±6.7 [a] pg/m^3	
						$\sum_{20}$PCBs=8.5-30.7[b] pg/m^3	
			2013	n=12		$\sum_{20}$PCBs=26±13.6 [a] pg/m^3	
						$\sum_{20}$PCBs=6.9-59[b] pg/m^3	

(Cont. on next page)

Table 2.7. (Cont.)

Sampling Site	Area	Sampling Type	Sampling Period	#of Samples	Congeners	Concentration	Reference
West Antarctica		Active	2011	n=10	PCB#11,28,52,101,138,153,180, 77,81,105,114,118,123,126,157, 167,169,189,209	$\sum_{20}$PCBs=35.7±12.2[a] pg/m^3	(Wang et al. 2017)
						$\sum_{20}$PCBs=21.9-72.6[b] pg/m^3	
			2012	n=10		$\sum_{20}$PCBs=19.3±6.7 [a] pg/m^3	
						$\sum_{20}$PCBs=8.5-30.7[b] pg/m^3	
			2013	n=12		$\sum_{20}$PCBs=26±13.6 [a] pg/m^3	
						$\sum_{20}$PCBs=6.9-59[b] pg/m^3	
			2014	n=1		$\sum_{20}$PCBs=19.7 [a] pg/m^3	
						$\sum_{20}$PCBs=14.2-25.2[b] pg/m^3	
			2011-2014	n=33		$\sum_{20}$PCBs=5.87-12.2 pg/m^3	
			2011	n=10	PBDE#3,7,15,17,28,47,49,66,71 ,77,85,99,100,119,126,138,153, 154,156,183,184,191,196,197,2 06,207,209	$\sum_{27}$PBDEs=3.58±4.22 pg/m^3	
						$\sum_{27}$PBDEs=0.57-16.5[b] pg/m^3	
			2012	n=10		$\sum_{27}$PBDEs=3.10±3.87 pg/m^3	
						$\sum_{27}$PBDEs=0.60-16.1[b] pg/m^3	
			2013	n=12		$\sum_{27}$PBDEs=2.91±4.45[a] pg/m^3	
						$\sum_{27}$PBDEs=0.28-18.3[b] pg/m^3	
			2014	n=1		$\sum_{27}$PBDEs=6.48± pg/m^3	
						$\sum_{27}$PBDEs=9.9-2.99[b] pg/m^3	
			2011 -2014	n=33		$\sum_{27}$PBDEs=0.60-16.1 pg/m^3	

(Cont. on next page)

Table 2.7. (Cont.)

Sampling Site	Area	Sampling Type	Sampling Period	#of Samples	Congeners	Concentration			Reference
China Shanghai	Urban	Active	November 2015 to April 2016	n=8	PBDE#17,28,47 ,99,100,85,154, 153,183	Gas Phase $\sum_7$PBDE=75.7 pg/m^3	Particulate Phase $\sum_7$PBDE=86.4 pg/m^3	Total $\sum_7$PBDE=16 2.1 pg/m^3	(Su et al. 2018)
Vietnam Hochiminh	Urban	Active	July 25 to August15, 2016		PCB#77,126,16 9,181,105,114,1 18,123,156,157, 167,189	$\sum_{12}$PCB=4.86 pg/m^3			(Trinh et al. 2018)
						$\sum_{12}$PCB=5.43 pg/m^3			
						$\sum_{12}$PCB=6.30 pg/m^3			
			January 13 to February 6 2017			$\sum_{12}$PCB=6.21 pg/m^3			
						$\sum_{12}$PCB =5.58 pg/m^3			
	Industrial		July 25 to August15, 2016			$\sum_{12}$PCB=7.80 pg/m^3			
						$\sum_{12}$PCB =7.79pg/m^3			
						$\sum_{12}$PCB =7.55pg/m^3			
			January 13 to February 6 2017			$\sum_{12}$PCB=6.83 pg/m^3			
						$\sum_{12}$PCB =8.16 pg/m^3			
						$\sum_{12}$PCB =8.30 pg/m^3			
	Rural		July 25 to August15, 2016			No sampling			
			January 13 to February 6 2017			$\sum_{12}$PCB=1.76 pg/m^3			
						$\sum_{12}$PCB=2.51 pg/m^3			
						$\sum_{12}$PCB 1.57 pg/m^3			

(Cont. on next page)

Table 2.7. (Cont.)

Sampling Site	Area	Sampling Type	Sampling Period	#of Samples	Congeners	Concentration	Reference
West Antarctica		Active	2011	n=10	HCB, α-HCH, β–HCH γ–HCH, δ–HCH ,*o,p′*-DDE, *p,p′*-DDE, *o,p′*-DDD, *p,p′*-DDD, *o,p′*-DDT and *p,p′*-DDT,HEPT,CHE, THE, CC,TC, CN, TN, Aldrin, Endrin, Dieldrin, Mirex	$\sum_{23}$OCP=16.2±4.80 [a] pg/m^3 $\sum_{23}$OCP=9.23-27.9 [b] pg/m^3	(Wang et al. 2018)
			2012	n=10		$\sum_{23}$OCP=13.9-6.35 [a] pg/m^3 $\sum_{23}$OCP=5.87-25 [b] pg/m^3	
			2013	n=12		$\sum_{23}$OCP=13.7±4.90 [a] pg/m^3 $\sum_{23}$OCP=6.73-25.2 [b] pg/m^3	
			2014	n=1		$\sum_{23}$OCP=9.37 pg/m^3 $\sum_{23}$OCP=9.14-9.61 [b] pg/m^3	
			2011-2014	n=33		$\sum_{23}$OCP=14.3±5.4[a] pg/m^3 $\sum_{23}$OCP=5.87-27.9 [b] pg/m^3	
India-Ganga	Urban/Sub urban	Passive	15th March-25th April 2015	n=7		*p,p′*-DDE =610±427 [a] pg/m^3 *p,p′*-DDT=1079±841 [a] pg/m^3 ΣDDTs=261±3755 [a] pg/m^3 α-HCH=381±149 [a] pg/m^3 β-HCH=183± 110 [a] pg/m^3 γ-HCH=233±112 [a] pg/m^3 δ-HCH=90±46 [a] pg/m^3 ΣHCHs=888±397 [a] pg/m^3 α -Endosulfan=197±105 [a] pg/m^3 β -Endosulfan=110±36 [a] pg/m^3 Endosulfan sulfate=121±82[a] pg/m^3 Aldrin=179±106 [a] pg/m^3 Heptachlor=392±221 [a] pg/m^3 Heptachlor epoxide=1186±371[a] pg/m^3	(Khuman and Chakraborty 2019)

(Cont. on next page)

Table 2.7. (Cont.)

Sampling Site	Area	Sampling Type	Sampling Period	#of Samples	Congeners	Concentration	Reference
India (Parangipettai)	Forest	Active	May to November Summer	n=78	α-HCH β-HCH γ-HCH δ-HCH	$\sum_4$HCH=542±62[a] pg/m^3 $\sum_4$HCH=480-603[b] pg/m^3	(Chakraborty et al. 2019)
			Pre-Monsoon			$\sum_4$HCH=587±282[a] pg/m^3 $\sum_4$HCH=260-1135[b] pg/m^3	
			Monsoon			$\sum_4$HCH=428±147[a] pg/m^3 $\sum_4$HCH=279-636[b] pg/m^3	
			May to November Summer		*p,p′*-DDE, *o,p′*-DDT, *p,p′*-DDT	$\sum_3$DDTs=1645±332[a] pg/m^3 $\sum_3$DDTs=1313-1976 pg/m^3	
			Pre-Monsoon			$\sum_3$DDTs=671±196[a] pg/m^3 $\sum_3$DDTs=352-1024[b] pg/m^3	
			Monsoon			$\sum_3$DDTs=332±177[a] pg/m^3 $\sum_3$DDTs=136-651[b] pg/m^3	
			May to November Summer		α-ENDO, Endosulfan sulfate, β-ENDO	$\sum_3$ENDO=270±81[a] pg/m^3 $\sum_3$ENDO=188-351[b] pg/m^3	
			Pre-Monsoon			$\sum_3$ENDO=166±69[a] pg/m^3 $\sum_3$ENDO=68-290[b] pg/m^3	
			Monsoon			$\sum_3$ENDO=298±336[a] pg/m^3 $\sum_3$ENDO=66-1013[b] pg/m^3	
			May to November Summer		PBDE#28,35,47,100,99,154	$\sum_6$PBDE=119±50[a] pg/m^3 $\sum_6$PBDE=83-155[b] pg/m^3	
			Pre-Monsoon			$\sum_6$PBDE=55±17[a] pg/m^3 $\sum_6$PBDE=32-71[b] pg/m^3	
			Monsoon			$\sum_6$PBDE=48±9[a] pg/m^3 $\sum_6$PBDE=24-47[b] pg/m^3	
Jamaica	Forest/Clearing	Passive	November - February	n=1	PBDE#28,47,99,100,153,154,183,209	$\sum_8$PBDE=13±3.61[a] pg/m^3 $\sum_8$PBDE=19.46±8.42[a] pg/m^3	(Mao et al. 2020)

(Cont. on next page)

Table 2.7. (Cont.)

Sampling Site	Area	Sampling Type	Sampling Period	#of Samples	Congeners	Concentration	Reference
Vietnam	Urban/ELV recycling are/waste recycling area	Passive	January-March 2013 September-November 2015	n=15	All PCB congener from 1 to 209 PBDE#7,10,1515,17,28,3047,49,66,77,85,99,100,119,126,138,139,140,153,154,156,171,180,183,184,191,196,197,201,203,204,205,206,207,208,209	$\sum_{209}$PCB=110-1100[b] pg/m^3 $\sum_{36}$PBDE=5.3-86[b] pg/m^3	(Anh et al. 2020)
China-Zhejiang Province	Urban	Active (G)	August2012-August 2015	n=74	PCB#5+4,18,28,31,44,52,73,56+60,61+74,66+80,77,81,82,89+90+101,126,128,132+168,138+163+164,129+149,153,156,157,158+160,166,167,169,170+190,179,180,182+187,183,189,194,199	$\sum_{40}$PCB=9-341[b] pg/m^3 $\sum_{40}$PCB=145±80[a] pg/m^3	(Mao et al. 2020)
Thailand	**Site I** Agricultural	Active (G+P)	Dry n=17 Wet n=9		α -HCH, b-HCH, g-HCH, γ-HCH, heptachlor, aldrin, heptachlorepoxide, endosulfan I, *o,p´*–DDE, dieldrin, endrin, endosulfan II, DDD, endrin aldehyde, DDT and endosulfan sulfate	$\sum_{16}$OCP=1.4±2.1[a] ng/m^3 $\sum_{16}$OCP=1.2±1.0[a] ng/m^3	(Tipayarom and Oanh 2020)
	Site II Agricultural		Dry n=8 Wet n= 9			$\sum_{16}$OCP=2.0±1.8[a] ng/m^3 $\sum_{16}$OCP=2.3±2.5[a] ng/m^3	
Dalian Northeast China	Urban	Active (G) (P)	November 2016 to November 2017	n=26	PBDE#47,99,100,153,154,183	$\sum_{7}$PBDE=4.40±2.93[a] pg/m^3 $\sum_{7}$PBDE=0.28-11.6[b] pg/m^3 $\sum_{7}$PBDE=42.68±1.64[a] pg/m^3 $\sum_{7}$PBDE=0.86-10.4[b] pg/m^3	(Wang et al. 2020)

a: Average
b: Range
c: Median
(G): Gas Phase Concentration
(P): Particulate Phase Concentration

2.8. Ambient Air POP Concentrations in Turkey

Sampling campaigns have been performed in Turkey's various regions using both active and passive sampling methods. Studies reported levels for locations that can be grouped as urban, suburban, industrial, coastal areas, and agricultural. Many of the studies conducted at industrial sites were attributed to high emission potential. Aydın et al. (2014), Cetin et al. (2007), Kaya et al. (2012), reported PCB concentrations in Aliaga industrial area of Izmir and Birgül et al. (2017) reported PCB concentrations in industrial site of Bursa, Cetin et al. (2018) reported PCB concentrations measured in Dilovası industrial area of Kocaeli. The studied urban places included cities of Aksaray, Antalya, Cankırı, Elazıg, Istanbul, Izmir, Kars, Kastamonu, Kayseri, Kirikkale, Konya, Malatya, Mersin, Usak, and Van. Kurt-Karakus et al. (2018) conducted the only country-wide study by passive sampling at urban and rural locations. PCB studies in Turkey are presented below in chronological order. In addition, the studies conducted with passive and active sampling are separately listed in Table 2.8 and 2.9, respectively.

Cetin et al. (2007) collected samples with active samplers in Izmir at both industrial and urban sites. Samples were collected between March 2004 and April 2005. The highest concentration reported at the industrial site in both seasons. Average (G+P) of Σ_{36}PCB concentration reported as 1371±642 pg/m^3 for winter and 3137±824 pg/m^3 for summer at the industrial site. At the urban site these values reported as 847±610 pg/m^3 and 314±129 pg/m^3, respectively. Additionally, PCB-18 had the highest concentration in winter, PCB-18 in summer for industrial and PCB-33 and PCB-18 at the urban site. Concentrations reported for these congeners were 212.3±105.9 pg/m^3, 520.1±200.3 pg/m^3, 101.6±78.8, 31.0±12.9 pg/m^3 in order. Ozcan and Aydın (2009) studied urban Konya with active sampling. Traffic in the region was claimed to be the only possible source of pollution, where no industrial or other sources except LRAT. Concentrations of total PCBs in the urban air of Konya varied between 3 pg/m^3 and 48 pg/m^3, while the mean concentration of total PCBs was 106 pg/m^3. PCB-28 and PCB-52 accounted for 46% and 35% of total PCBs, respectively. Table 2.9 reveals that low-chlorinated PCBs were mainly in the gas phase, whereas high-chlorinated PCBs were largely measured in the particulate phase. Concentrations of PCBs decreased with an increasing number of Cl in Konya urban air.

Kaya et al. (2012) collected passive samples between July 2009 and May 2010 and analyzed 41 PCB congeners. The PCB levels were ranged from 134 pg/m^3 to 230958 pg/m^3, average of Σ_{41}PCB concentration reported as 8727 pg/m^3. Aydın et al. (2014) collected passive samples at industrial and nonindustrial sites of Izmir. PCB concentrations were higher at industrial sites than non-industrial sites over all seasons, indicating the continuing position of plants in Aliaga as sources of PCBs. At the sampling sites near the iron–steel plants and ship-breaking facilities, higher concentrations of PCBs were measured. The highest concentrations of atmospheric PCBs were reported during summer as 29051 pg/m^3. Lammel et al. (2015), collected samples by passive sampling method in Gulbahce, Urla, Izmir (rural, the sampling site in this study) and Nilufer, Bursa (suburban-rural) in 2012. Seven PCB congeners were measured. For PCB-28, which is the highest concentration congener, was estimated at 22.3 pg/m^3 for Izmir. The average total concentration of the seven PCB congeners was 55.3 pg/m^3. PCB-28 was the highest concentration congener measured for Bursa with a mean value of 13.6 pg/m^3. The total concentration of the seven congeners was reported to be 25.6 pg/m^3, lower than Izmir. Kuzu (2016) collected three active samples at the Yildiz Technical University Campus area and Klanova et al. (2006) during the dust transport from the Sahara Desert to Istanbul. Average concentration of Σ_8PCBs was reported as 279 pg/m^3. Ugranlı et al. (2016), collected air samples at Dokuz Eylul University's Kaynaklar Campus, which is situated in the suburban area of Izmir. Samples were collected once every six days from May 2003 to April 2004. Sampling Campaign divided in two seasons of heating and non-heating. A total of 51 samples were collected, 30 in the non-heating period (April to September) and 21 in the heating period (October to March). The mean gas-phase of $\sum_{32}$PCB concentrations in the non-heating period were as 377 pg/m^3 whereas lower concentrations were reported in the heating period. Particulate-phase concentrations in the non-heating period was not different from the heating period. Birgul et al. (2017) collected at rural, semi urban, urban, agricultural, and industrial sites of Bursa between February 2014 and December 2014. The average industrial Σ_{43}PCB concentrations was reported as 170±150 pg/m^3 with a range of 21 to 340 pg/m^3. Contrary to anticipations, the highest concentration was recorded in the semi-urban area, not the industrial area. Average of Σ_{43}PCB concentration in semi urban area was reported as 180±210 pg/m^3. Dumanoglu et al. (2017), collected samples of ambient air (n = 82) at 22 industrial/urban and 19 rural locations during the summer and winter periods, totally at 41 locations of Kutahya in winter and summer. Concentrations were extremely variable ranging from

19.6 to 675.1 pg/m^3 in winter to 31.6–230.2 pg/m^3 in summer. On average, concentrations of ambient PCBs were 1.5 times higher in winter than those reported in summer. This indicates that increased burning of coal due to residential heating could have added to the PCB levels in wintertime. While the average Σ_{41}PCB concentration was 187.9±132 pg/m^3 in winter, this concentration was 125.3±33.5 pg/m^3 in summer. Air samples (n=16) were taken from Guzelyali Port during two sampling schedules on February 9–March 4 and July 6–13, 2005. Guzelyali Port is an urban location in southern Izmir Bay. Gas phase Σ_{29}PCB concentrations for the winter and summer periods were 1642 ± 817 pg/m^3 and 2078 ± 1026 pg/m^3 while they were 74 ± 75 and 41 ± 40 pg/m^3 for particulate phase. Kurt-Karakus et al. (2018) conducted a country-wide passive sampling campaign from May 2014 to April 2015. The sampling program was conducted with three-month sampling periods at sites around the country on east-west and north-south transects. In addition to Turkey's three corner sites, sixteen provinces were chosen to collect samples at urban and rural sites. Seasonal average concentration for 16 urban and rural sites listed in Table 2.10. The overall average concentration of Σ_{43}PCBs was 108±132 pg/m^3. The top congener was PCB-118 (26.3±44.6 pg/m^3) and the highest contribution was made by penta-CBs with 54.3 percent. The lowest mean concentration was measured in Kayseri (14.5±14.3 pg/m^3) while the maximum was measured in Izmir (403±428 pg/m^3). At rural sites, Aksaray's mean concentration was the lowest reported at 19.0±22.7 pg/m^3, whereas Kastamonu's mean concentration was the highest at 217±353 pg/m^3. Sari et al. (2020) collected samples in summer and autumn in urban Bursa. They put forward that higher concentrations measured in summer may be due to volatilization from soil at higher temperatures. Concentration of average Σ_{40}PCB was reported as 303±183 pg/m^3 and 42±23 pg/m^3 in summer and autumn respectively, which are higher than those reported by Birgül et al. (2017) for Bursa.

Table 2.8. Passive sampling PCBs concentration reported in Turkey Ambient air

Sampling Site/ Sampling Type/ #of samples	**Area**	**Sampling Period**	**Congeners**	**Concentration**						**Reference**
Izmir Aliaga Passive n=159	Industrial	July–August 2009 (summer), October– November 2009 January– February 2010 (winter), April– May 2010 (spring).	PCB#18,17,31,28,33, 5,49,44,74,70,95,101, 99,8,110,82,151,149, 118,153.	**Congener**	**Median**	**Average**	**Congener**	**Median**	**Average**	(Kaya et al. 2012)
				PCB 18	228	1123	PCB 132	24	75	
				PCB 17	99	516	PCB 105	26	90	
				PCB 31	152	825	PCB 138	51	209	
				PCB 28	250	1195	PCB 158	10	28	
				PCB 33	152	750	PCB 187	12	41	
				PCB 52	114	588	PCB 183	7	24	
				PCB 49	79	362	PCB 128	17	52	
				PCB 44	96	419	PCB 177	7	24	
				PCB 74	43	196	PCB 171	5	14	
				PCB 70	91	433	PCB 156	12	32	
				PCB 95	62	238	PCB 180	18	77	
				PCB 101	85	335	PCB 191	6	9	
				PCB 99	26	107	PCB 169	ND	ND	
				PCB 87	34	133	PCB 170	12	44	
				PCB 110	56	242	PCB 199	9	22	
				PCB 82	21	71	PCB 208	5	6	
				PCB 151	13	45	PCB 195	13	17	
				PCB 149	40	163	PCB 194	16	27	
				PCB 118	50	202	PCB 205	ND	nd	
				PCB 153	42	174	PCB 206	12	16	
							PCB 209	5	8	
							$\sum_{41}$PCB	2085	8727	

(Cont. on next page)

Table 2.8. (Cont.)

Sampling Site/ Sampling Type/ #of samples	Area	Sampling Period	Congeners	Concentration		Reference
Izmir Passive n=160	Industrial (n=17) (Aliaga)	July-August 2009 (Summer) October-November2009 January-February 2010 (Winter) April-May 2010 (May)	PCB#18, 17, 31, 28, 33, 52, 49, 44, 74, 70, 95, 101, 99, 87, 110, 82, 151, 149, 118, 153, 132, 105, 138, 158, 187, 183, 128, 177, 171, 156, 180, 170, 199, 194, 206.	$\sum_{35}$PCB=29051.11 pg/m^3 $\sum_{35}$PCB=16933.33 pg/m^3 $\sum_{35}$PCB=6519.44 pg/m^3 $\sum_{35}$PCB=12040.0 pg/m^3		(Aydin et al. 2014)
	Nonindustrial (n=23)	July-August 2009 (Summer) October-November 2009 (Fallahzadeh et al.) January-February 2010 (Winter) April-May 2010 (May)		$\sum_{35}$PCB=2214.29 pg/m^3 $\sum_{35}$PCB=1787.14 pg/m^3 $\sum_{35}$PCB=987.14 pg/m^3 $\sum_{35}$PCB=1587.86 pg/m^3		
Izmir-Gulbahce Passive n=2	Rural	2-31 July 2012	PCB#28,52,101,118,153, 138,180	Compound PCB-28 PCB-52 PCB-101 PCB-118 PCB-153 PCB-138 PCB-180 $\sum_{7}$PCB	Concentration(pg/m^3) 22.3 8.6 4.4 3.5 4.9 7.1 4.5 55.3	(Lammel et al. 2015)

(Cont. on next page)

Table 2.8. (Cont.)

Sampling Site/ Sampling Type/ #of samples	Area	Sampling Period	Congeners	Concentration		Reference
Bursa Nilufer Passive n=1	Suburban-Rural	2 July- 13 August 2012	PCB#28,52,101,118,153,138,180	PCB-28	13.6	(Lammel et al. 2015)
				PCB-52	4.7	
				PCB-101	1.8	
				PCB-118	1.2	
				PCB-153	1.5	
				PCB-138	2.2	
				PCB-180	<1.2	
				$\sum_7$PCB	25.6	
Bursa Passive n=5	Rural	February 2014- December 2014	PCB#18,22,28,31,41/64,44,49,52,54,5,60,70,74,87,90/101,95,99,104,110,11,118,123,132,138,141,149,151,153,15,157,158,167,170,174,180,183,187,18,18,199,203.	$\sum_{43}$PCB= 24.1± 8.20[a] pg/m^3		(Birgül et al. 2017)
	Semiurban			$\sum_{43}$PCB= 43.8± 24.4[a] pg/m^3		
	Semiurban			$\sum_{43}$PCB= 180± 210[a] pg/m^3		
	Urban			$\sum_{43}$PCB= 42.9± 24.60[a] pg/m^3		
	Urban			$\sum_{43}$PCB= 160± 280[a] pg/m^3		
	Agricultural			$\sum_{43}$PCB= 84.2± 105[a] pg/m^3		
	Industrial			$\sum_{43}$PCB= 21± 340[a] pg/m^3		

(Cont. on next page)

Table 2.8. (Cont.)

Sampling Site/ Sampling Type/ #of samples	Area	Sampling Period	Congeners	Concentration	Reference
Kütahya Passive n=82	Industrial/Rural	January 2014-March 2014	PCB#18,17,31,28,33,52,49,44,74,70,95,101,99,87,110,82,151,149,118,153,132,105,138,158,187,183,128,177,171,156,180,191,169,170,199,208,195,194,205,206,209	$\sum_{41}$PCB= 187.9± 132.9[a] pg/m^3	(Dumanoglu et al. 2017)
		June 2014- August 2014		$\sum_{41}$PCB= 125.3± 33.5[a] pg/m^3	
Turkey Passive n=128 Aksaray, Antalya, Cankırı, Elazıg, Istanbul, Izmir, Kars, Kastamonu, Kayseri, Kirikkale, Konya, Malatya, Mersin, Uşak, Van	Urban (n=16)	May-July 2014	PCB#18, 22, 28, 31, 41/64, 44, 49, 52, 54, -56, 60, -70, -74, 87, 90/101, -95, 99, 104, 105, 110, -114, 118, 123, 32, 138, 141, 149, 151, 153, 156, -157, 58, 167, 70, -174, -180, 183, 187, 188, 189, -194, 199, 203	$\sum_{43}$PCB=118.53 pg/m^3	(Kurt-Karakus et al. 2018)
		August-October 2014		$\sum_{43}$PCB=117 pg/m^3	
		November-January 2015		$\sum_{43}$PCB=164 pg/m^3	
		February-April 2015		$\sum_{43}$PCB=100pg/m^3	
	Rural (n=16)	May-July 2014		$\sum_{43}$PCB=64.3 pg/m^3	
		August-October 2014		$\sum_{43}$PCB=98.2 pg/m^3	
		November-January 2015		$\sum_{43}$PCB=187 pg/m^3	
		February-April 2015		$\sum_{43}$PCB=93.1 pg/m^3	

(Cont. on next page)

Table 2.8. (Cont.)

Sampling Site/ Sampling Type/ #of samples	Area	Sampling Period	Congeners	Concentration	Reference
Bursa Gemlik Passive n=12	Urban	January 2016 -December 2016	PCB#4/10, 9/7, 6, 8/5, 12, 13, 18, 9, 15/17, 16/32, 26, 31, 28, 21/53, 22, 45, 52, 47, 49/48, 44, 37/42,71/41/64, 100, 74, 70/61, 66/95, 91, 92, 89/101, 119, 92, 89/101, 119, 83, 81/87, 86, 85, 77/110, 135/144, 14/149, 118, 123, 131,153, 132/105, 163/138, 126, 128, 167,174, 202/171/156, 172, 180, 200, 170/190, 169, 199, 207, 94, 205, 206	$\sum_{81}$PCBs=118± 74[a] pg/m^3	(Cindoruk, Sakin, and Tasdemir 2020)
Bursa Passive	Urban	July-2014-September 2014 Summer October 2014-December 2014 Autumn	PCB#4/10,16/32, 26, 28, 21/53, 22, 45, 52, 49/48, 41/64/71, 74, 66/95, 56/60, 92, 89/101, 119, 81/87, 85, 86, 77/110, 118, 114/149, 123, 153, 138/163, 126,180.	$\sum_{40}$PCB = 303 ±183[a] pg/m^3 $\sum_{40}$PCB= 41± 23[a] pg/m^3	(Sari et al. 2020)

[a]:Average± SD
[b]:Range
[c]:Single Value

Table 2.9. Active sampling PCBs concentration reported in Turkey Ambient air

Sampling Site/ Sampling Site/ # of Samples	Area	Sampling Period	Concentration					Reference
				Industrial		Urban		
				Winter (n = 6)	Summer (n = 7)	Winter (n = 6)	Summer (n = 7)	
İzmir Active n=26 (G+P)	Industrial /Urban	March 28–April 8, 2005	PCB-18	212.3 ± 105.9	520.1 ± 200.3	92.7 ± 107.4	31.0 ± 12.9	(Cetin et al. 2007)
			PCB-17	106.3 ± 49.6	285.5 ± 91.5	65.9 ± 79.0	17.9 ± 9.3	
			PCB-31	125.3 ± 55.3	284.2 ± 97.4	76.0 ± 74.9	22.2 ± 9.2	
			PCB-28	135.0 ± 64.2	330.8 ± 113.9	79.8 ± 71.6	27.4 ± 11.4	
			PCB-33	116.5 ± 55.4	237.0 ± 70.0	101.6 ± 78.8	28.7 ± 9.9	
			PCB-52	96.2 ± 44.5	222.2 ± 53.2	63.3 ± 44.7	20.9 ± 9.4	
			PCB-49	66.8 ± 27.3	141.5 ± 38.4	49.5 ± 31.3	18.2 ± 4.7	
			PCB-44	64.8 ± 26.6	137.3 ± 27.4	38.3 ± 29.7	13.4 ± 5.5	
			PCB-74	25.5 ± 8.5	59.8 ± 10.9	11.4 ± 15.4	4.8 ± 3.1	
			PCB-70	51.4 ± 22.9	111.5 ± 20.8	27.6 ± 25.4	8.3 ± 3.4	
			PCB-95	44.4 ± 21.3	102.0 ± 23.0	26.4 ± 12.2	10.7 ± 4.5	
			PCB-101	44.3 ± 22.8	97.6 ± 22.5	26.3 ± 11.9	11.0 ± 4.5	
			PCB-99	16.4 ± 8.2	34.2 ± 7.1	10.6 ± 6.7	3.9 ± 1.7	
			PCB-87	21.6 ± 12.6	45.9 ± 9.3	12.9 ± 7.0	5.8 ± 1.5	
			PCB-110	39.1 ± 22.3	79.8 ± 15.9	22.6 ± 10.5	9.4 ± 3.9	
			PCB-82	6.7 ± 4.3	12.8 ± 4.3	3.9 ± 2.0	0.7 ± 1.2	
			PCB-151	9.5 ± 5.5	22.2 ± 9.1	5.7 ± 0.6	3.8 ± 1.8	
			PCB-149	30.2 ± 15.8	67.2 ± 22.5	19.3 ± 2.4	10.6 ± 4.6	
			PCB-118	27.4 ± 14.0	55.6 ± 13.0	17.8 ± 7.8	7.6 ± 2.8	
			PCB-153	29.5 ± 16.8	67.3 ± 22.5	19.9 ± 2.2	11.9 ± 4.8	
			PCB-132	11.8 ± 6.7	24.6 ± 7.4	7.3 ± 1.3	3.7 ± 1.4	
			PCB-105	11.1 ± 6.5	24.9 ± 6.2	7.1 ± 3.5	3.3 ± 0.8	
			PCB-138	35.9 ± 20.8	77.7 ± 23.2	23.9 ± 4.3	12.9 ± 4.6	
			PCB-158	4.1 ± 3.0	8.2 ± 2.5	2.9 ± 0.7	1.7 ± 0.8	
			PCB-187	6.5 ± 3.8	13.7 ± 5.4	5.1 ± 1.5	4.3 ± 3.4	

(Cont. on next page)

Table 2.9. (Cont.)

Sampling Site/ Sampling Site/ # of Samples	Area	Sampling Period	Concentration					Reference
				Industrial		Urban		
				Winter (n = 6)	Summer (n = 7)	Winter (n = 6)	Summer (n = 7)	
İzmir Active n=26 (G+P)	Industrial /Urban	March 28–April 8, 2005	PCB-183	4.1 ± 2.8	7.3 ± 3.3	2.9 ± 0.6	2.3 ± 1.6	(Cetin et al. 2007)
			PCB-128	4.1 ± 4.5	11.4 ± 3.9	0.9 ± 2.3	0.5 ± 1.3	
			PCB-177	3.0 ± 3.3	7.2 ± 3.3	2.5 ± 0.6	2.0 ± 1.4	
			PCB-171	1.6 ± 1.9	3.6 ± 1.4	1.4 ± 0.4	1.0 ± 0.6	
			PCB-156	1.7 ± 2.0	5.2 ± 1.8	1.0 ± 1.1	0.6 ± 1.1	
			PCB-180	11.8 ± 5.9	22.0 ± 9.1	8.6 ± 1.4	6.7 ± 4.4	
			PCB-170	5.2 ± 5.0	12.4 ± 6.0	4.6 ± 1.7	2.7 ± 2.1	
			PCB-199	0.4 ± 1.0	2.5 ± 2.8	2.7 ± 4.2	1.9 ± 3.5	
			PCB-208	ND	ND	0.5 ± 1.1	0.2 ± 0.6	
			PCB-194	ND	1.5 ± 2.7	1.1 ± 2.7	0.9 ± 2.3	
			PCB-206	ND	ND	2.9 ± 5.2	0.7 ± 1.9	
			Σ_{36}PCBs	1371 ± 642	3137 ± 824	847 ± 610	314 ± 129	
				Gas Phase (pg/m^3)		Particulate Phase (pg/m^3)		
			PCBs	Winter	Summer	Winter	Summer	
Izmir Güzelyalı Active n=16	Urban	July and February–March 2005	PCB 18	129 ± 62	286 ± 142	11 ± 4	8 ± 7	(Odabasi et al. 2008)
			PCB 17	103 ± 58	135 ± 60	8 ± 2	5 ± 4	
			PCB 31	205 ± 97	221 ± 105	6 ± 5	4 ± 3	
			PCB 28	173 ± 97	210 ± 108	8 ± 6	5 ± 5	
			PCB 33	453 ± 246	212 ± 98	10 ± 7	5 ± 4	
			PCB 52	132 ± 61	169 ± 70	12 ± 20	5 ± 6	
			PCB 49	125 ± 65	134 ± 52	16 ± 20	6 ± 6	
			PCB 44	92 ± 45	118 ± 62	ND	ND	
			PCB 74	47 ± 5	59 ± 27	ND	ND	
			PCB 70	64 ± 34	86 ± 51	ND	ND	

(Cont. on next page)

Table 2.9. (Cont.)

Sampling Site/ Sampling Site/ # of Samples	Area	Sampling Period	Concentration					Reference
				Gas Phase (pg/m^3)		Particulate Phase (pg/m^3)		
			PCBs	Winter	Summer	Winter	Summer	
			PCB 95	27 ± 17	61 ± 34	ND	2	
			PCB 101	21 ± 16	60 ± 36	3 ± 0.1	3 ± 3	
			PCB 99	11 ± 7	29 ± 18	ND	ND	
			PCB 87	12 ± 11	34 ± 19	ND	ND	
			PCB 110	19 ± 12	57 ± 34	ND	2 ± 0.4	
			PCB 82	0.8 ± 0	13 ± 9	ND	ND	
			PCB 151	6 ± 2	9 ± 5	ND	2	
			PCB 149	10 ± 6	31 ± 18	ND	2 ± 0.9	
Izmir Güzelyalı Active n=16	Urban	July and February–March 2005	PCB 118	13 ± 8	41 ± 24	ND	3	(Odabasi et al. 2008)
			PCB 153	9 ± 5	31 ± 18	18 ± 21	2 ± 1.1	
			PCB 132	6 ± 4	14 ± 8	ND	ND	
			PCB 105	9 ± 3	16 ± 9	ND	ND	
			PCB 138	11 ± 9	39 ± 23	4	ND	
			PCB 158	ND	8 ± 3	ND	ND	
			PCB 187	5 ± 4	6 ± 2	7	ND	
			PCB 183	0.8	4 ± 2	ND	ND	
			PCB 128	ND	11 ± 6	ND	ND	
			PCB 177	ND	5 ± 1	1	ND	
			PCB 180	0.8	9 ± 3	ND	ND	
			Σ $_{29}$ PCBs	**Σ $_{29}$=1642 ± 817**	**Σ $_{29}$=2078 ± 1026**	**Σ$_{29}$=74 ± 75**	**Σ $_{29}$=41 ± 40**	

(Cont. on next page)

Table 2.9. (Cont.)

Sampling Site/ Sampling Site/ # of Samples	Area	Sampling Period	Concentration			Reference
Konya-Meram Active n=10	Urban	June 2006 to May 2007.		Gas Phase (pg/m^3)	Particulate Phase (pg/m^3)	
			PCB 28	42	6	
			PCB 52	25	15	(Odabasi et al. 2008)
			PCB 101	4	2	
			PCB138	3	1	
			PCB153	3	3	
			PCB 180	<dl	3	
Istanbul Active n=3	Urban	February-2015		Σ_{84}=279 pg/m^3		(Kuzu 2016)
Kaynaklar Buca Campus) n=51 (30 nonheating/21 heating) Active	Suburban site	2003-2004 Heating Season		Σ_7 PCB=49.7 pg/m^3		(Ugranli et al. 2016)
		Nonheating season		Σ_7 PCB=107 pg/m^3		

OCP studies conducted in Turkey listed for the passive sampling method in Table 2.10 and listed for active sampling in Table 2.11 This is a review of the literature in chronological order for both methods of sampling. Odabasi et al. (2008), collected active samples in urban area of İzmir Guzelyalı. Total gas-phase individual OCP concentrations ranged from 0.2±0.3 (cis-nonachlor) to 1154±502 pg/m^3 (chlorpyrifos) in winter and 0.2±0.1 (transnonachlor) to 4474±1937 pg/m^3 (endosulfan I) in summer. Particulate phase OCPs ranged from 0.1±0.1 (cis-nonachlor) to 10±5 pg/m^3 (chlorpyrifos) and 0.1±0.1 (cis-nonachlor) to 157±115 pg/m^3 (chlorpyrifos) respectively. Pesticides in use, chlorpyrifos and endosulfan I and II had relatively higher concentrations among OCPs, followed by α, γ-HCHs, and endosulfan sulfate. Ozcan and Aydın (2009), conducted sampling campaign in urban area in the Konya region of Meram with active sampling from June 2006 to May 2007. The main source of pollution is transport in the region only. Mean concentrations of OCPs in the gas phase ranged from BDL to 0.36 ng/m^3 while they ranged from BDL to 0.49 ng/m^3 in the particulate phase. Heptachlor epoxide and p,p′-DDT were not detected in the urban air of Konya while the other investigated OCPs were detected. The mean total HCH concentration (α-HCH, β-HCH, γ-HCH, δ-HCH) in the gas and particulate phase were determined as 1.2 ng/m^3 and 0.66 ng/m^3, respectively. This group was dominantly determined in the investigated OCPs as 30% of total OCPs. HCHs are one of the most widely used and most readily detected organochlorine pesticides in environmental samples. Bozlaker et al. (2009), collected active samples in industrial area of Horozgedigi village that is under the direct effect of Aliaga industrial area. Total (gas+particulate phases) average concentrations ranged from 0.2±0.05 pg/m^3 (cis-nonachlor) to 2152±2974 pg/m^3 (endosulfan-I) in summer, and from BDL (δ-HCH, cisnonachlor) to 121±160 pg/m^3 (chlorpyrifos) in winter. It was elaborated that measured high and largely variable levels of endosulfan and chlorpyrifos can be attributed to their usage in the study area. Cindoruk (2011) collected passive samples in Bursa in different environmental media between January and December 2016. At four different sites coastal (Mudanya), urban/traffic (Butal), semi-rural (UUC) and urban/residential (YS), air concentrations of OCPs were calculated to evaluate the present levels. The sites were selected for their characteristics, such as. The concentrations of OCPs in particulate phase ranged from 3.7 pg/m^3 to 874.9 pg/m^3 for Mudanya, from 26.5 pg/m^3 to 828.8 pg/m^3 for Butal, from 1.9 pg/m^3 to 852.2 pg/m^3 for UUC, and 19.9 pg/m^3 to 786.7 pg/m^3 for YS. The gas-phase concentrations of OCPs for Mudanya were 79.6–910.3 pg/m^3, for Butal 75.6-1614.4 pg/m^3, for UUC 28.8–1091.4 pg/m^3, and for YS 84.3–1463.2 pg/m^3. Most

abundant OCP compound was β-HCH, while Endrin aldehyde had the lowest concentrations across all sites. Other OCP compounds, with the exception of HCH isomers, were typically found in the particulate phase at Mudanya and UUC, where agricultural activities were common. Lammel et al. (2015) conducted passive sampling at various points surrounding the Aegean Sea. Measurements in Turkey were made at two points, Bursa and Gulbahçe, Urla, Izmir. $\sum_9$OCP concentration was reported as 43 pg/m^3 in the samples taken in Izmir. The highest congener concentrations were reported for HCB and *α*-HCH, with 12.3 pg/m^3 and 11.2 pg/m^3. In Bursa, $\sum_9$OCP concentration was reported as 25.7 pg/m^3. The highest congener concentration was reported for *p,p′*-DDE as 6.9 pg/m^3. Kuzu et al. (2016), collected active samples at Yildiz Technical University, Davutpasa Campus in Istanbul. Particulate phase OCP concentrations varied between 57.4 pg/m^3 and 160.6 pg/m^3, while gas phase concentrations were between 321.6 pg/m^3 and 571.4 pg/m^3. Particulate fractions of OCPs ranged from 9% to 22%. The largest proportion was β-HCH and heptachlor. The lowest concentrations were reported during the incursion of dust. During dust transport, only β-endosulfan concentration was higher. The authors concluded that LRAT did not seem to have an effect on the distribution of ambient concentrations of OCPs. They used the diagnostic ratio of α-HCH/γ-HCH to infer on the effect of LRAT on the measured concentrations. When the value of ratio is >1, LRAT has an impact on the atmospheric HCH isomer concentrations. Only one sample (February 1st) had detectable particulate concentrations of the two isomers with the ratio being slightly above 1. Eker and Tasdemir (2018), collected active samples between June 2008 and 2009 at Uludag University Campus located in a semi-rural area of Bursa. $\sum_9$OCP concentrations ranged from 63 to 799 pg/m^3 in the particulate phase, while those in the gas phase ranged from 126 to 798 pg/m^3. The average total (gas+particulate) $\sum_9$OCP concentration was measured as 598.6±194.2 pg/m^3 and 35% of the total concentration of $\sum_9$OCP was found in the particulate phase.

OCPs studies in our country were mainly conducted during the summer season in both urban and rural areas. Deposition of OCPs in soil, are possibly due to the use of OCPs as pesticides and the prevalence of agricultural lands in our region The reported concentration values have increased during the summer months due to rising temperatures, increased volatilization and increased agricultural activity.

Table 2.10. OCP concentrations measured by passive sampling in Turkey

Sampling Site	Area	Sampling Period	Congeners	Concentration		Reference
Izmir-Gulbahce Passive n=2	Rural	2-31 July	PeCB, HCB α-HCH, γ-HCH, β-HCH, δ-HCH, o,p'-DDT, o,p'-DDE, p,p'-DDE	Compounds	Concentration (pg/m^3)	(Lammel et al. 2015)
				PeCB	1.4	
				HCB	12.3	
				α-HCH	11.2	
				γ-HCH	2.6	
				β-HCH	1.4	
				δ-HCH	1.2	
				o,p'-DDT	2.9	
				o,p'-DDE	0.55	
				p,p'-DDE	9.4	
				$\sum_9$OCP	43.0	
Bursa Nilufer Passive n=1	Suburban-Rural	2 July- 13 August	PeCB, HCB α-HCH, γ-HCH, β-HCH, δ-HCH, o,p'-DDT, o,p'-DDE, p,p'-DDE	Compounds	Concentration (pg/m^3)	(Lammel et al. 2015)
				PeCB	<0.8	
				HCB	5.5	
				α-HCH	5.1	
				γ-HCH	<1.2	
				β-HCH	1.0	
				δ-HCH	5.2	
				o,p'-DDT	0.79	
				o,p'-DDE	0.24	
				p,p'-DDE	6.9	
				$\sum_9$OCP	25.7	

(Cont. on next page)

Table 2.10. (Cont.)

Sampling Site	Area	Sampling Period	Congeners	Concentration	Reference
Turkey n=128 Aksaray, Antalya, Cankırı, Elazıg, Istanbul, Izmir, Kars, Kastamonu, Kayseri, Kırıkkale, Konya, Malatya, Mersin, Uşak, Van	Urban Rural	May-July 2014 August-October 2014 November-January 2015 February-April 2015

Table 2.11. OCP concentrations measured by active sampling in Turkey

Sampling Site	Area	Sampling Period	Concentration					Reference
Izmir Güzelyalı Active	Urban	February 9–March 4 and July 6–13, 2005		Gas Phase (pg/m^3)		Particulate phase (pg/m^3)		(Odabasi et al. 2008)
				winter	summer	winter	summer	
n=16			α-HCH	43 ± 22	62 ± 19	1.4 ± 0.5	0.8 ± 0.4	
			γ-HCH	88 ± 53	28 ± 8	3 ± 1.1	2 ± 1.3	
			CHLPYR	1154 ± 502	864 ± 255	10 ± 5	157 ± 115	
			Hep epox	91 ± 147	9 ± 3	5 ± 4	1 ± 0.3	
			γ-CHL	9 ± 4	0.8 ± 0.3	0.2 ± 0.2	0.2 ± 0	
			ESLF I	80 ± 26	4474 ± 1937	4 ± 3	13 ± 8	
			α-CHL	6 ± 3	2 ± 0.6	0.3 ± 0.2	0.2 ± 0.3	
			t-NONA	1.4 ± 1	0.2 ± 0.1	0.3 ± 0.1	0.1 ± 0.1	
			ESLF II	11 ± 4	879 ± 464	2 ± 0.9	77 ± 47	
			c-NONA	0.2 ± 0.3	0.4 ± 0.2	0.1 ± 0.1	0.1 ± 0.1	
			ESULFATE	3 ± 1.4	28 ± 19	1.1 ± 0.7	22 ± 11	
			p,p′-DDT	8 ± 8	5 ± 2	2 ± 0.9	2 ± 0.8	
Konya-Meram Active	Urban	June 2006 to May 2007.		Gas Phase (ng/m^3)	Particulate Phase (ng/m^3)	Total (ng/m^3)		(Ozcan and Aydin 2009)
n=10			α-HCH	0.36	0.13	0.49		
			β-HCH	0.34	0.19	0.53		
			γ-HCH	0.16	0.22	0.38		
			δ-HCH	0.34	0.12	0.46		
			Hepchlor	0.02	0.09	0.11		
			Aldrin	0.01	0.06	0.07		
			Hep epox	<dl	<dl	0		
			Dieldrin	0.01	0.05	0.06		
			p,p′-DDE	0.01	0.05	0.06		
			End	0.006	0.02	0.026		
			End al	0.01	0.07	0.08		
			End ket	0.03	0.46	0.49		
			ESLF I	0.008	0.37	0.378		
			ESLF II	<dl	0.09	0.09		

(Cont. on next page)

Table 2.11. (Cont.)

Sampling Site	Area	Sampling Period		Concentration						Reference
				Gas Phase (ng/m^3)			Particulate (ng/m^3)		Total (ng/m^3)	
Konya-Meram Active n=10	Urban	June 2006 to May 2007	*p,p′*-DDD	0.12			0.3		0.42	Ozcan and Aydin 2009)
			Eslf sul	0.05			0.49		0.54	
			p,p′-DDT	0.12			0.3		0.42	
			Meocl	0.003			0.48		0.483	
Izmir Horozgediği Active n=28	Industrial	August 2004-April 2005		Gas (pg/m^3)	Particulate (pg/m^3)	Total (pg/m^3)	Gas (pg/m^3)	Particulate (pg/m^3)	Total (pg/m^3)	(Bozlaker et al. 2009)
			α-HCH	4.0 ± 2.0	102±43	106±43	0.5±0.3	41±32	41±32	
			β-HCH	6.2 ± 6.0	12± 6.0	14±9.1	ND	9.4±5.2	9.4±5.2	
			γ-HCH	4.2 ± 2.1	44±16	49±16	1.0±0.8	12±6.3	13±6.4	
			δ-HCH	1.8 ± 1.3	2.6±0.8	2.8±1.9	ND	ND	ND	
			CHLPYR	7.1 ± 3.7	135±178	143±181	86±137	42±54	121±160	
			HEP EPOX	1.3 ± 1.1	5±2.3	6.0±3.0	1.1±1.4	1.6±1.3	2.2±2.2	
			α-CHL	0.2 ± 0.1	2.9±1.3	3.0±1.4	0.07±0.03	0.6±0.2	0.6±0.2	
			γ-CHL	0.1 ± 0.07	1.6±0.5	1.7±0.6	0.06±0.04	0.5±0.02	0.6±0.3	
			c-Nona	ND	0.2±0.05	0.2±0.05	ND	ND	ND	
			t-Nona	0.05 ± 0.04	1.3±0.4	1.3±0.4	ND	0.4±0.2	0.4±0.2	
			ESLF-I	9.9 ± 5.8	2142±2970	2152±2974	4.0±4.0	19±9.3	21±11	
			ESLF-II	9.9 ± 5.8	271±338	300±351	4.30±3.6	2.2±2.1	5.6±3.9	
			ESLF SUL	4.2 ± 3.1	13±14	17±16	1.1±0.8	0.2±0.2	1.3±0.9	
			p,p′-DDT	12 ± 8.5	46±17	58±16	5.1±3.0	6.2±4.1	11±4.6	
			p,p′-DDD	2.8 ± 1.1	17±5.3	19±4.7	0.9±0.3	2.4±1.4	3.3±1.5	

(Cont. on next page)

Table 2.11. (Cont.)

Sampling Site	Area	Sampling Period	Concentration			Reference
Bursa Active n=35	Coastal	June 2008 to June 2009		Gas Phase(pg/m^3)	Particulate Phase(pg/m^3)	(Cindoruk 2011)
			α-HCH	1.94 ± 3.0	74.38 ± 52.9	
			β-HCH	36.60 ± 42.3	670.82 ± 255.5	
			γ-HCH	12.13 ± 23.6	119.22 ± 75.5	
			δ-HCH	6.57 ± 7.6	14.07 ± 16.5	
			Heptachlor epoxide	29.96 ± 38.5	40.89 ± 55.0	
			Endrin	19.73 ± 28.4	18.58 ± 11.3	
			Eslf II	54.27 ± 75.1	87.06 ± 66.8	
			Endrin aldehyde	32.24 ± 45.7	10.62 ± 11.0	
			p,p′-DDT	28.01 ± 41.2	15.05 ± 12.9	
			Methoxychlor	68.49 ± 68.2	58.62 ± 49.0	
			α-HCH	1.94 ± 3.0	74.38 ± 52.9	
	Urban traffic		β-HCH	36.60 ± 42.3	670.82 ± 255.5	
			γ-HCH	12.13 ± 23.6	119.22 ± 75.5	
			δ-HCH	6.57 ± 7.6	14.07 ± 16.5	
			Heptachlor epoxide	29.96 ± 38.5	40.89 ± 55.0	
			Endrin	19.73 ± 28.4	18.58 ± 11.3	
			Eslf II	54.27 ± 75.1	87.06 ± 66.8	
			Endrin aldehyde	32.24 ± 45.7	10.62 ± 11.0	
			p,p′-DDT	28.01 ± 41.2	15.05 ± 12.9	
			Methoxychlor	68.49 ± 68.2	58.62 ± 49.0	
	Semi-rural		α-HCH	3.35 ± 4.8	43.82 ± 41.2	
			β-HCH	27.86 ± 37.4	212.82 ± 161.4	
			γ-HCH	8.16 ± 13.0	34.01 ± 40.5	
			δ-HCH	6.62 ± 6.2	50.05 ± 76.5	
			Heptachlor epoxide	9.18 ± 22.9	13.53 ± 21.6	
			Endrin	9.03 ± 17.9	6.03 ± 8.5	
			Eslf II	58.14 ± 87.3	31.37 ± 66.2	
			Endrin aldehyde	14.53 ± 44.2	1.92 ± 6.3	
			p,p′-DDT	6.51 ± 17.4	5.96 ± 10.3	
			Methoxychlor	34.69 ± 48.8	21.98 ± 26.3	

(Cont. on next page)

Table 2.11. (Cont.)

Sampling Site	Area	Sampling Period	Concentration				Reference
	Residential urban			Gas Phase (pg/m^3)		Particulate Phase (pg/m^3)	(Cindoruk 2011)
			α-HCH	2.10 ± 2.9		37.26 ± 21.5	
			β-HCH	40.98 ± 55.1		488.21 ± 265.5	
			γ-HCH	11.71 ± 18.8		126.52 ± 122.5	
			δ-HCH	8.29 ± 12.3		30.34 ± 43.3	
			Heptachlor epoxide	11.36 ± 19.6		15.18 ± 26.1	
			Endrin	27.04 ± 40.9		15.78 ± 12.7	
			Endosulfan beta	73.01 ± 93.4		102.08 ± 93.8	
			Endrin aldehyde	34.29 ± 50.1		12.67 ± 18.1	
			p,p′-DDT	22.98 ± 45.8		24.50 ± 46.1	
			Methoxychlor	47.59 ± 68.2		89.28 ± 115.6	
Izmir Horozgedigi Active n=13	Industrial	March-April 2005 (Winter, n=6) June 2005 (Summer n=7)		Gas phase (pg/m^3)		Particulate Phase (pg/m^3)	(Odabasi and Cetin 2012)
				Winter n=6	Summer n=7	Winter n=6	Summer 7
			α-HCH	17.1 ± 10.7	71.9±9.8	0.16±0.04	0.61±0.52
			β-HCH	5.4 ± 4.5	29.8±14.6	0.28±0.07	0.65±0.40
			γ-HCH	57.6 ± 66.6	117±79	7.3±3.8	4.8±1.5
			δ-HCH	1.5±1.9	4.5±3.8	0.51±0.38	0.26±0.13
			γ-chlordane	0.62±0.52	0.73±0.30	0.05±0.02	0.14±0.05
			ESLF-I	14.2±8.7	168±118	1.1±0.7	2.1±1.2
			α-CHL	0.46±0.25	0.79±0.15	0.07±0.05	0.14±0.03
			t-NONA	0.28±0.15	0.28±0.13	0.05±0.02	0.10±0.03
			ESLF-II	2.3±3.1	24.8±16.9	1.9±1.3	3.4±1.3
			p,p′-DDD	0.90±0.37	0.95±0.42	1.2±0.6	0.44±0.21
			c-NONA	0.07±0.03	0.21±0.10	0.06±0.03	0.13±0.04
			ESULFATE	0.28±0.27	3.1±2.7	0.71±0.18	2.4±0.8
			p,p′-DDT	3.4±2.0	3.9±1.6	1.9±0.8	1.2±0.5

(Cont. on next page)

Table 2.11. (Cont.)

Sampling Site	Area	Sampling Period	Concentration			Reference
Istanbul Active n=3	Yıldız Technical University	1 February 2015 2 February 2015 3 February 2015	Sample Sample 1 Sample 2 Sample 3	Particulate (pg/m^3) $\sum_{18}$OCP=69.3 $\sum_{18}$OCP=57.4 $\sum_{18}$OCP=160.6	Gas (pg/m^3) $\sum_{18}$OCP=321.6 $\sum_{18}$OCP=568.6 $\sum_{18}$OCP=571.4	(Kuzu 2016)
Izmır Kaynaklar Buca Campus n=51 (30 nonheating / 21 heating)	Suburban	Heating Season Nonheating Season	∑HCHs=17.1 pg/m^3 ∑HCHs=43.7 pg/m^3 ∑DDTs=33.9 pg/m^3 ∑DDTs=55.3 pg/m^3			(Ugranli et al. 2016)
Bursa Active Urban n=60	Uludag University Campus area	June 2008-June 2009 (alpha-, beta-, and gammahexachlorocyclohexane; heptachlor epoxide; endrin; endosulfan beta; endrin aldehyde; and methoxychlor)	Particulate Phase (pg/m^3) 63-799[b]	Gas Phase (pg/m^3) 126-798[b]	Total Phase (pg/m^3) 598.6±194.2[a]	(Eker and Tasdemir 2018)

[a]:Average± SD
[b]:Range
[c]:Single Value

Lammel et al. (2015), collected passive samples from Bursa and Izmir. Five PBDE congeners were analyzed. The average $\sum_5$PBDE concentration measured in Izmir (8.5 pg/m^3) was much higher than that for Bursa (0.7 pg/m^3). The highest congener concentration was reported as 7.5 pg/m^3 for PBDE 28. Kurt-Karakuş et al. (2017), collected passive ambient air samples in different sites in Istanbul. Concentrations of $\sum_{12}$PBDEs in ambient air ranged from 110 to 620 pg/m^3. Concentrations were ranked as urban > suburban > rural areas. Most prevalent congeners were PBDE-138 (290 pg/m^3), PBDE-153 (210 pg/m^3), PBDE-28 (36 pg/m^3), and pBDE-85 (30 pg/m^3) in urban area. Cetin et al. (2019), investigated PBDE concentration in Dilovası industrial area of Koaceli. Active 264 samples collected through 1 year. Average $\sum_8$PBDE concentration in summer (118.5±98.7 pg/m^3) season were higher than in winter (79.7±69.1 pg/m^3). $\sum_8$PBDE concentrations ranged between 5.73 and 520 pg/m^3 (94.7±78.9). The main congener was PBDE-209, followed by the PBDE-47 and PBDE-99. Besis et al. (2017) collected 22 samples in Gulbahçe, Urla, Izmir, using active sampling during day and night. Except for PBDE-209, the average $\sum_8$PBDE concentration was 10.8 pg/m^3 for the gas phase, 3.57 pg/m^3 for the particulate phase, and 14.37 pg/m^3 for the total concentration. However, the average gas phase BDE-209 concentration was 90 pg/m^3, the particulate phase 93 pg/m^3, and the total 183 pg/m^3 was higher than the sum of other congeners. Detail of other congener listed in Table 2.12. Cetin et al. (2019), conduct studies in Turkey's highly industrialized area, where is Kocaeli-Dilovası. PUF disk passive samplers were placed in 23 different sites. Total 264 samples have been collected to investigate concentrations of 8 congener of PBDEs. Individual level and concentration range reported in Table 2.13. Highest level concentration reported for PBDE-209, PBDE-47, PBDE-99, respectively. PBDE 209 concentration was slightly higher, 69.1±56.58 pg/m^3. The PBDE-47 and PBDE-99 concentrations were recorded at 8.09±8.74 pg/m^3 and 8.07±10.48 pg/m^3, respectively. Moreover, Cetin et al (2019), the average concentration of PBDE collected in the summer season 118.5±98.7 pg/m^3 was higher than that reported in the winter period 79.7±59.1 pg/m^3 and this seasonal variation in industrial/urban sites became clearer and more significant ($p<0.05$). Average concentrations were reported in summer as 233±99.0 pg/m^3, whereas the average concentration in industrial/urban sites decreased in winter to 133±25.9 pg/m^3.

Table 2.12. PBDE concentrations measured by passive sampling in Turkey

Sampling Site	Area	Sampling Period	Congeners	Concentration		Reference
Izmir-Gulbahce Passive n=2	Rural	2-31 July	PBDE#28,47,66,100, 99	Compound PBDE-28 PBDE-47 PBDE-66 PBDE-100 PBDE-99 $\sum_5$PBDE	Concentration(pg/m^3) 7.5 0.76 0.044 <0.05 <0.38 8.5	(Lammel et al. 2015)
Bursa Nilufer Passive n=1	Suburban-Rural	2 July- 13 August	PBDE#28,47,66,100, 99	Compound PBDE-28 PBDE-47 PBDE-66 PBDE-100 PBDE-99 $\sum_5$PBDE	Concentration(pg/m^3) 0.021 <0.41 0.009 <0.12 <0.90 0.7	(Lammel et al. 2015)
Istanbul Passive n=3	Urban Sub-Urban Rural	February- March 2012	PBDE#17,28,47,66,85,99, 100,138,154,183,209	$\sum_{12}$PBDE= 620 pg/m^3 $\sum_{12}$PBDE= 280 pg/m^3 $\sum_{12}$PBDE= 110 pg/m^3		(Kurt-Karakus et al. 2017)
Turkey n=128 Aksaray, Antalya, Cankırı, Elazıg, Istanbul, Izmir, Kars, Kastamonu, Kayseri, Kırıkkale, Konya,Malatya, Mersin, Uşak, Van	Urban	May-July 2014 August-October 2014 November-January 2015 February-April 2015	PBDE#17,28,47, 66, 71,85, 99, 100, 138, 153, 154,183,190 ,209	$\sum_{14}$PBDE=99.3 pg/m^3 $\sum_{14}$PBDE=162 pg/m^3 $\sum_{14}$PBDE=566 pg/m^3 $\sum_{14}$PBDE=5.29 pg/m^3		(Kurt-Karakus et al. 2018)

Table 2.13. PBDE concentrations measured by active sampling in Turkey

Sampling Site	**Area**	**Sampling Period**	**Congeners**	**Concentration(pg/m^3)**				**Reference**
Izmir-Urla Active n=22	Urla	July 2, 2012–July 13, 2012	PBDE#28, 47, 66, BDE,100, 99, 154,153, 209	Congener	Gas phase	Particulate phase	G+P	(Besis et al. 2017)
				PBDE-28	0.816	0.635	1.45	
				PBDE-47	4.93	0.822	5.75	
				PBDE-66	ND	ND	ND	
				PBDE-100	0.848	0.422	1.27	
				PBDE-99	3	0.967	3.92	
				PBDE-154	0.593	0.345	0.939	
				PBDE-153	0.568	0.375	0.943	
				$\sum_8$PBDE	10.8	3.57	14.37	
				PBDE-209	90	93	183	

[a]:Average± SD
[b]:Range
[c]:Single Value

2.9. LRAT of POPs

POPs are transported long distances even across continents and oceans with air masses. They degrade slowly, thus remain in the environment, accumulating in environmental media and organisms including plants, animals, and humans (Porta and Zumeta 2002). Depending on the weather conditions, air contaminants emitted to the atmosphere at a location that circulate across the Globe within a few days to a few weeks (Kallenborn, Hung, and Brorström-Lundén 2015). Air emissions are detected thousands of kilometers away from their sources in several situations. With the help of advanced measurement and modeling technologies, there has been more and more evidence of emissions generated in one region which has adverse effects in other areas of the world.

The environment, for example, is known to be the primary pathway for anthropogenic toxins, including organochlorines and certain heavy metals present in Arctic animal tissues. For example, dust from the Saharan desert in North Africa caused a series of high PM air pollution events in the neighboring regions of Greece, Iraq, Kuwait, Saudi Arabia, and Spain (Pongkiatkul and Oanh 2007) including our country (Kabatas et al. 2018). Many anthropogenic pollutants, like hydrophobic organic compounds (HOCs), are prone to LRAT in vapor and particle-bound phases.

POPs are typically hydrophobic and lipophilic. Based on their semi-volatile character, these compounds can be found in the gas phase, in association with atmospheric particles or distributed between these two phases. The mechanism by which semi-volatile chemicals such as POPs volatilize from warm source areas, LRAT and subsequently condense on surfaces such as soil, vegetation or snow at low temperatures, effectively accumulating in the polar regions, is represented by global distillation and cold condensation. In a series of relatively short jumps, this migration of POPs to higher latitudes is typically referred to as the "grasshopper effect," as seen in Figure 2.7. The compounds migrate, rest and migrate again in harmony with changes in seasonal temperatures at mid latitudes (O'Sullivan and Megson 2014).

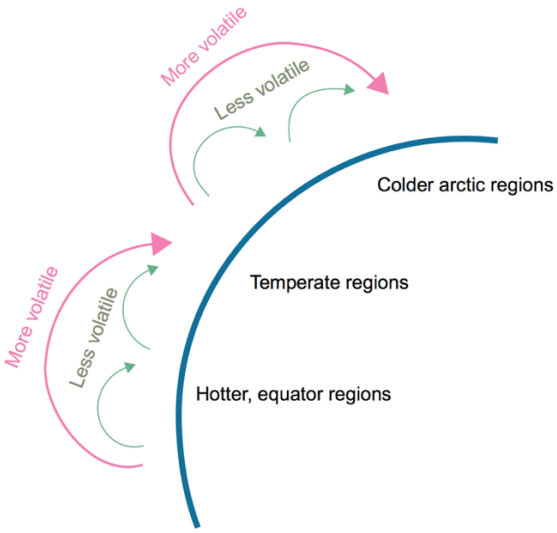

Figure 2.7. Multiple cycles of evaporation, transport by air, and condensation of POPs (Grasshopper effect)

In high latitude areas, colder air temperatures foster precipitation, cold rain and snow efficiently scavenging HOCs such as hexachlorobenzene (HCB), polychlorinated biphenyls (PCBs), and polychlorinated dibenzo-p-dioxins/polychlorinated dibenzofurans (PCDD/Fs) from the environment (Bergknut et al. 2010). Similarly, PBDEs can be transported over long distances (Wania and Dugani 2003). Backward air trajectories are used to infer on the source regions through modeling of air mass movement (Pozo et al. 2017).

2.10. Back-Trajectory Analysis

The National Oceanic and Atmospheric Administration (NOAA) Air Resources Laboratory's (ARL) Hybrid Single-Particle Lagrangian Integrated Trajectory model (HYSPLIT) (Draxler and Hess 1998) is a complete system for computing simple air parcel trajectories as well as complex transport, dispersion, chemical transformation, and deposition simulations. HYSPLIT is extensively used for atmospheric transport and dispersion modeling with back-trajectory analysis to determine the origin of air masses and establish source–receptor relationships.

HYSPLIT has also been used in a variety of simulations describing the atmospheric transport, dispersion, and deposition of pollutants and hazardous materials

(Stein et al., 2015). It is possible to distinguish the contaminated trajectories with high measurement concentration from a large number of trajectories, and then the pollutant route could be roughly calculated (Wang et al. 2009)

2.11. Motivation and Objectives

Results of a previous project conducted by our group indicated LRAT source areas for POPs in south of our country's border where conflict and war zones reside, triggered a hypothesis that the war activity with the machinery – artillery and disrupted soils containing deposited POPs may be a significant source of LRAT for Turkey. To investigate this hypothesis, passive sampling has been conducted at ten sites located on a transect from the southern border area to west (Izmir) and northwest (Bursa) of the country. In addition, active sampling has been conducted in Izmir. The goal was to investigate if there is a relationship between ambient air POP concentrations and proximity to the war zone, and to conduct back-trajectory analysis with a new, independent data set to verify the previous finding because Izmir has been shown to be under the effect of local source areas that include both primary and secondary sources of POP emissions, and LRAT from areas in the North, i.e. Europe, Russia and former Soviet countries.

CHAPTER 3

MATERIAL AND METHODS

3.1. Sampling Sites

Passive samplers have been placed on a transect from south to west, in the provinces near our southern border, Adana, Gaziantep, Osmaniye, Karaman, and Malatya, in Denizli, Isparta, Mugla conforming the Middle-Distance Group, and in Izmir and Bursa as the Far Group (Figure 3.1). In provinces located at close sampling points, samplers were placed on campuses of universities outside the city centers. Samplers were placed on the roofs of buildings to avoid emission sources. Samplers that cannot be placed on roofs are mounted on poles or trees away from the road. Adana is a major city in southern Turkey. The city is situated on the Seyhan River, 35 km inland from the north-eastern coast of the Mediterranean Sea. Adana has agricultural lands and industrial facilities. It has a population of 2,258,718 million (TUIK, 2020). The sampler was placed on the roof of a building located on the campus of Adana Science and Technology University. Osmaniye is a city in the Cukurova region of Turkey, at an elevation of 125 meters. Osmaniye has a population 548,556 (TUIK, 2020). Sampler was placed on the roof of a building in Osmaniye Korkut Ata University campus area.

Gaziantep has a population 2,101,157 (TUIK, 2020). The area of the province is 6.803 km^2. There are 309 people per km^2 in the province. Gaziantep is well developed in industry and trade. Turkey's largest industrial site located in Gaziantep. In Gaziantep, the sampler was placed in the Oguzeli Vocational High School, a closer location to the border. Karaman is located in the south of the Central Anatolia Region. Its height above sea level is 1,033 meters. The general area of the province is 8,869 km^2. It has a population 254,919 end of 2020 (TUIK, 2020). Kazim Karabekir Vocational High School campus of Karamanoglu Mehmet Bey University was used as the sampling point in Karaman. It was placed on a tree 2 m above the ground in the garden of the building. Malatya is located in the western part of the Eastern Anatolia region with a population 806,156. In the province of Malatya, the garden of a private property was used. Sampling was carried out in the garden of a building far from the city center, at a height of 2 m from the ground and away from emission sources. Sampler was placed in middle distances cities can be seen in

Figure 3.1. In provinces located in the middle distance, sampling was also carried out on campus areas. In provinces located in middle distance, samplers were placed on trees. Sampling was carried out in Isparta, at the Suleyman Demirel University campus, at the Acıpayam Vocational School in Denizli, at the Ali Kocman Vocational School in Mugla, Mugla Sıtkı Kocman University. Isparta is located in western Turkey. The city's population was 440,304 in 2020 (TUIK, 2020) and its elevation is 1035 m. Isparta is located in the transition zone between the Mediterranean climate and the continental climate prevailing in Central Anatolia. For this reason, both climatic characteristics are observed within the provincial borders. Mugla is a city in south-western Turkey. Mediterranean climate prevails in Mugla. Summers are hot and dry; winters are warm and rainy. The city's population was 1,000,773 in 2020 (TUIK, 2020). Denizli is an industrial city in the southwestern part of Turkey. It is located in the country's Aegean Region. The city has a population of about 1,040,915. In the far distance, samplings were made in Izmir Institute of Technology and Bursa Technical University campuses, respectively. Izmir is geographically located in the west of Turkey and the entire province is located in the Aegean Region. Its population was 4,394,694 as of 2020 (TUIK, 2020). Bursa is a city in northwestern Turkey. It in under a Mediterranean climate winters are cold and damp, also containing the most rainfall. It has a population 3,101,833 according to Turkey Statistical Institute (TUIK, 2020).

Figure 3.1. Samplings sites

3.2. Sampler Preparation and Deployment

All laboratory analysis equipment was properly cleaned with solvent before to use to ensure that any possible organic traces were entirely removed. Alconox detergent was used to brush and clean the equipment. After brushing with detergent, the equipment was rinsed with tap water. Glassware was rinsed with chromic acid, tap water, and then distilled water. Their openings were covered with aluminum foil and dried in an oven at 100 °C.

Prior to use in air sampling, PUF disks (14 cm in diameter; 1.35 cm in thickness; 365 cm in surface area; 4.40 g in mass; 207 cm^3 in volume; 0.0213 g/cm^3 in density Tisch Environmental, Ohio, USA) were cleaned 24 h with 1:1 acetone: hexane mixture. Then, they were dried under vacuum and wrapped in aluminum foil, preserved in sealed plastic bags, and kept in the freezer (-20 °C) until deployment for sampling. Quartz filters were wrapped loosely with aluminum foil and baked in a muffle furnace at 450 °C for 6 h to remove any organic residue. Then, they were allowed to cool to room temperature in a desiccator. PUF disks have been spiked with a depuration mixture which are listed in Table 3.1 at least for three days prior to deployment. Spiked PUFs were wrapped in aluminum foil, packaged in solvent-cleaned tin cans with Teflon-lined lips, and stored in a refrigerator. Cleaned and prepared PUFs, cartridges, and quartz filters were transported to the sampling fields from the labs in air-tight containers to prevent any exposure to air before sampling.

Table 3.1. Depuration compounds spiked on passive PUFs

Compounds	
$^{13}C_{12}$ PCB-15	d_6-ɣHCH
$^{13}C_{12}$ PCB-32	
PCB-30	
PCB-107	
PCB-198	

3.3. Calculation of Air Volume Passed Through PAS

The estimation of equivalent air volume can potentially be improved with the addition of depuration compounds to the sampling medium prior to deployment. These are isotopically labeled chemicals or unlabeled chemicals that do not exist in the atmosphere (Harner et al. 2004). Sample volumes were calculated based on the fraction of depuration chemicals (Table 3.1) retained by the PUF disk to compute air concentrations. Calculations are based on PCB-30, PCB-107, PCB-198 and d_6-γHCH. Accumulation of compounds of interest depends on the PUF-air partition coefficient ($K_{PUF\text{-}air}$) at equilibrium defined in Equation (3.1) where $K_{PUF\text{-}air}$ is a function of K_{OA} (Pozo et al. 2004). The sampling rate remains linear over the first 100 days for compounds with K_{OA} values greater than $10^{8.5}$, at 3-4 m^3d^{-1}, and is mostly defined by the airside air-side mass transfer coefficient (k_A) (Calculated based on Equation 3.7) (Harner et al. 2004). The PUF disk becomes saturated with respect to the air in less than 100 days for compounds with lower K_{OA}. $K_{PUF\text{-}A}$ is inversely related to the time it takes for a chemical to reach saturation (or its maximal equivalent air volume) (or K_{OA}). Equation (3.2) can be used to estimate sample air volume based on calibration findings.

$$K'_{PUF\text{-}air} = (V_{air}/V_{puf}) = (C_{puf,equilibrium}/ C_{air,equilibrium}) \quad (3.1)$$

where $C_{puf,equilibrium}$ and $C_{air,equilibrium}$ stand for concentration of pollutants in PUF disk and in air (mol/volume).Total sampling profile of passive sampling material is calculated as in Equation (3.2) (Pozo et al. 2004).

$$C_{PUF,equilibrium} =$$

$$K'_{PUF\text{-}air} \times C_{air\text{-}equilibrium} \{1- \exp[(A_{PUF}/V_{PUF}) \times (k_A/K'_{PUF\text{-}air})] \times t\} \quad (3.2)$$

where A_{PUF} is the surface area of PUF disk (m^2), V_{PUF} is the volume of PUF disc, k_A is the transmission rate of POPs from air at the sampling location to PUF (m/day), K'_{PUF}-air is a unitless parameter of the sampling material, and t (days) is the exposure time. In the above equation, $K'_{PUF\text{-}air}$, calculated by using Equation (3.3) given below (Shoeib and Harner 2002), and $\log K_{OA}$ values used in Equation (3.4) available in literature.

$$K'_{PUF\text{-}air} = K'_{PUF\text{-}air} \times d_{PUF} \quad (3.3)$$

$$\log K'_{PUF\text{-}air} = 0.6366 \times \log K_{OA} - 3.1774 \quad (3.4)$$

$$(C_0 \times A \times k_A) / K'_{PUF\text{-}air} = -V(dc/dt) \quad (3.5)$$

$$dc/dt = -(C_0 \times k_A)/ (D_{film} \times K'_{PUF\text{-}air}) = -C_0 \times k_{d.} \quad (3.6)$$

$$C_t = C_0 \times \exp(-k_d \times t) \quad (3.7)$$

$$k_A = (\ln(C/C_0) \times D_{film} \times K'_{PUF\text{-}air})/t \quad (3.8)$$

$$R = k_A \times \text{Surface area of PUF} \quad (3.9)$$

V_{air} can be calculated after calculation of all parameters required for Equation (3.10) (Harner et al 2004).

$$V_{air} = K'_{PUF\text{-}air} \times V_{PUF} \{1 - \exp [-(A_{PUF}/V_{PUF}) \times (k_A / K'_{PUF\text{-}air})] \times t\} \quad (3.10)$$

The calculated air volumes were divided into total sampling date for each of the periods and the uptake rate of air was determined. Calculated effective air volume for each sampling are given in Table 3.2.

3.4. Sample Collection

Passive samplers were deployed for a month for 7 months, while active sampling was conducted weekly for 24 hours for a year. However, in some weeks, samples could not be taken due to excessive rainfall and also sample losses were experienced due to unexpected went off the power. Passive sampling points are grouped according to proximity to the war zone. Five provinces (Adana, Gaziantep, Osmaniye, Karaman, and Malatya) near our southern border are brought together as the close-proximity group. Isparta, Mugla, and Denizli formed the middle-proximity group. There were also two locations that made up the far-away group: Bursa and Izmir. Duplicate sampling was performed every 2 months in each group at one sampling location. The sampling points

were selected to be outside the city centers for minimization of urban effect. Figure 3.2 shows photographs of some sampling points as examples. Detailed information regarding passive and active sampling can be found in Table 3.2 and 3.3, respectively. In Izmir, both passive and active samples were collected.

Modified GPS-11 (Thermo-Andersen Inc.) high volume samplers were used for the collection of gaseous and particulate samples. The diameter of quartz filter was 101 mm. Sandwich-type (density 0.222 g/cm^3) plugs and XAD-2 resin (10 g) sampling media were, fully fitted in the glass holder to eliminate breakthrough. Samples were collected from December 2018 to May 2019 at a frequency of 1 in 7 days for 24 h. The average sampled air volume of active sampling was collected mean 279 m^3 per sample. Samples were wrapped with aluminum foil, sealed in glass jar and kept at -20 °C until the extraction process.

Figure 3.2. Photographs of sampling points (from top-left to bottom-right: Isparta, Mugla, Denizli, Izmir) as examples.

Table 3.2. Passive sampling information

Province	Distance to War Zone	Latitude/ Longitude	Mean Temp. (°C)	Deployment	Harvest	Sampling Days	Effective Air volume (m^3/day)
Malatya	Close	38°18'02.4"N/ 38°14'38.3"E	3.5	06/12/2018	08/01/2019	33	7.02
			6.5	08/01/2019	11/02/2019	34	7.94
			1.8	11/02/2019	09/03/2019	26	6.71
			6.25	09/03/2019	19/04/2019	41	5.21
			10.8	19/04/2019	16/05/2019	27	6.84
			31.06	16/05/2019	20/06/2019	36	6.74
			32.24	20/06/2019	01/08/2019	41	6.74
Gaziantep	Close	36°57'26.8"N/ 37°31'02.0"E	6.7	06/12/2018	09/01/2019	34	6.11
			4	09/01/2019	12/02/2019	34	6.41
			6	12/02/2019	08/03/2019	24	6.17
			14	08/03/2019	10/04/2019	33	5.74
			17	10/04/2019	15/05/2019	35	5.98
			32.86	15/05/2019	19/06/2019	35	6.06
			33.56	19/06/2019	23/07/2019	34	6.06
Osmaniye	Close	37°02'18.3"N/ 36°13'27.0"E	14.5	05/12/2018	04/01/2019	30	4.9
			9	04/01/2019	11/02/2019	38	5.58
			9.2	11/02/2019	06/03/2019	23	7.01
			14.6	06/03/2019	10/04/2019	35	4.19
			17	10/04/2019	15/05/2019	35	6.38
			29.47	15/05/2019	19/06/2019	36	5.22
			30.7	19/06/2019	22/07/2019	33	5.16
Adana	Close	37°02'35.7"N/ 35°24'21.2"E	11.24	05/12/2018	07/01/2019	33	9.53
			10.50	07/01/2019	08/02/2019	32	10.58
			11.6	08/02/2019	09/03/2019	27	7.13
			15	09/03/2019	17/04/2019	39	6.28
			20	17/04/2019	14/05/2019	27	7.91
			32.27	14/05/2019	20/06/2019	37	8.80
			33.56	20/06/2019	22/07/2019	32	8.79
Karaman	Close	37°13'57.9"N/ 32°57'28.0"E	2.5	04/12/2018	07/01/2019	34	6.58
			0.1	07/01/2019	11/02/2019	35	6.67
			3.7	11/02/2019	14/03/2019	31	4.68
			5.5	14/03/2019	11/04/2019	28	7.39
			17	11/04/2019	17/05/2019	36	6.19
			27.8	17/05/2019	20/06/2019	34	6.58
			28.6	20/06/2019	17/07/2019	34	6.58
Isparta	Middle	37°49'58.3"N/ 30°30'56.6"E	4	04/12/2018	04/01/2019	31	6.16
			6	04/01/2019	07/02/2019	34	4.71
			5	07/02/2019	05/03/2019	26	7.05
			8	05/03/2019	08/04/2019	34	3.69
			13	08/04/2019	15/05/2019	36	6.54
			35	15/05/2019	17/06/2019	31.2	4.98
			30.8	17/06/2019	17/07/2019	30	5.15
			30.8	17/06/2019	17/07/2019	30	5.15
Denizli	Middle	37°25'00.1"N/ 29°21'31.5"E	3.9	03/12/2018	07/01/2019	35	5.24
			2	07/01/2019	13/02/2019	37	5.22
			4.7	13/02/2019	06/03/2019	21	8.67
			7.2	06/03/2019	10/04/2019	35	6.37
			12.5	10/04/2019	16/05/2019	34	4.88
			27.94	16/05/2019	20/06/2019	35	4.88
			30	20/06/2019	19/07/2019	29	4.88
Mugla	Middle	37°06'24.1"N/ 28°26'04.2"E	6.06	03/12/2018	05/01/2019	33	6.03
			6	05/01/2019	11/02/2019	37	5.96
			6.3	11/02/2019	06/03/2019	23	6.32
			9	06/03/2019	08/04/2019	33	5.47
			14.8	08/04/2019	14/05/2019	36	4.01
			27.9	14/05/2019	17/06/2019	35	5.75
			30	17/06/2019	25/07/2019	39	4.01

(Cont. on next page)

Table 3.2. (Cont.)

Province	Distance to War Zone	Latitude/ Longitude	Mean Temp. (°C)	Deployment	Harvest	Sampling Days	Effective Air volume (m^3/day)
Bursa	Far	40°10'33.34"N/29°45'1.5"E	5.75	03/12/2018	02/01/2019	30	6.54
			6	02/01/2019	05/02/2019	34	6.68
			5.6	05/02/2019	04/03/2019	27	5.77
			7	04/03/2019	04/04/2019	31	5.3
			14.5	04/04/2019	09/05/2019	35	4.46
			27.86	09/05/2019	21/06/2019	43	5.2
			27.86	09/05/2019	21/06/2019	43	5.2
			29.14	21/06/2019	18/07/2019	28	5.77
			29.14	21/06/2019	18/07/2019	28	5.77
İzmir	Far	38°19'04.9"N/ 26°38'18.1"E	6.72	05/12/2018	04/01/2019	30	6.06
			8	04/01/2019	08/02/2019	35	7.60
			8	08/02/2019	11/03/2019	31	7.3
			10	11/03/2019	11/04/2019	31	5.02
			12	11/04/2019	14/05/2019	33	5.27
			30.6	14/05/2019	21/06/2019	38	5.91
			34.3	21/06/2019	24/07/2019	33	5.27

Table 3.3. Active sampling information

Date	Temperature	Wind (km/h)	Humidity (%)	Precipitation (mm)
6/12/2018	10	18 (N)	67	0
17/12/2018	10	3 (S)	70	2
28/12/2018	11	27 (NW)	72	0
03/01/2019	7	25(NW)	69	10
11/01/2019	11	35 (S)	70	1.9
17/01/2019	10	10 (SE)	8	0
25/01/2019	13	33 (SE)	94	2.5
31/01/2019	10	8 (S)	90	8
5/02/2019	12	0 (E)	80	0
18/02/2019	12	4 (SW)	55	0
22/02/2019	16	3 (NW)	39	0
2/03/2019	13	15 (SE)	54	0
6/03/2019	16	19 (S)	70	0
15/03/2019	12	2 (NW)	69	0
20/03/2019	12	10 (N)	52	0
28/03/2019	17	10 (NW)	49	0
02/04/2019	16	31 (N)	46	0
12/04/2019	20	11 (S)	42	0
21/04/2019	14	14 (NE)	50	0
27/04/2019	19	5 (N)	72	0
30/04/2019	24	23 (S)	49	0

(Cont. on next page)

Table 3.3. (Cont.)

Date	Temperature	Wind (km/h)	Humidity (%)	Precipitation (mm)
07/05/2019	20	10 (S)	60	0
11/05/2019	21	13 (S)	64	0
15/05/2019	27	14 (SE)	68	0
19/05/2019	21	2 (S)	72	0
24/05/2019	24	5 (NW)	59	0
30/05/2019	27	10 (SW)	50	0
3/06/2019	26	10 (SE)	58	0
12/06/2019	28	12 (NW)	47	0
18/06/2019	30	23 (NE)	47	0
26/06/2019	31	11 (NW)	54	0
17/07/2019	29	10 (N)	45	0
21/07/2019	33	5 (N)	45	0
27/07/2019	32	11 (NW)	36	0
9/08/2019	31	18 (N)	46	0
15/08/2019	31	20 (NW)	52	0
21/08/2019	31	23 (N)	43	0
29/08/2019	28	18 (NW)	41	0
19/09/2019	28	8 (S)	50	0
15/10/2019	24	13 (N)	63	0
5/10/2019	17	12 (S)	59	0
15/11/2019	15	5 (SE)	54	0

3.5. Sample Extraction and Analysis

3.5.1. PUF Extraction

PUF (Passive and Active) disks and plugs, and quartz filters were spiked with recovery surrogate chemicals (50 ng PCB-14, -65, -166 and 25 ng PBDE-77, -181) prior to extraction. While the PUF disks extracted using 300 mL acetone: hexane mixture with Soxhlet extractor for 24 h, active PUF-XAD-2 sandwich were extracted using 600 mL solvent with same principles as in passive samples. Extracts were concentrated to approximately about 1 mL using rotary evaporator and solvent was exchanged to isooctane phase. Samples were dried using sodium sulfate column and kept at -20 ºC until analysis.

3.5.2. Quartz Filter Extraction

Filter papers were spiked with surrogate compounds, 100 mL of 1:1 acetone: hexane mixture was added, soaked overnight, and extracted in an ultrasonic bath (Elma 300) for 10 min. After extraction, volume was reduced to 1 mL in a rotary evaporator and it was concentrated to 0.5 mL. One mL of isooctane was added, and volume was again concentrated to 0.5 mL. This process was repeated 2 times, and in the third step final volume was concentrated to 1 mL in isooctane. Then samples were passed through a Na_2SO_4-glasswool column to remove any water present. Finally, all extracts were spiked with an internal standard (12 ng $^{13}C_{12}$PCB105) before instrumental analysis and kept at -20 ºC. Sampling to instrumental analysis process is depicted in Figure 3.3.

3.5.3. Instrumental Analysis

The congeners of the POPs groups targeted in this study are listed in Table 3.4, and the operating parameters used for the analysis of the groups are listed in Table 3.5. PCB congeners were analyzed in GC (Agilent 7890B) equipped with an MSD (Agilent 5977 MSD). GC-MS operated on EI (electron impact)-selective ion monitoring (SIM) mode. Separation of PCB congeners was performed on a DB5-MS capillary column (60 m, 0.25 mm i.d., 0.25 μm film thickness, J&W Scientific). Co-eluted congeners (PCB-41/64 and PCB-90/101) were quantified together. OCPs and PBDEs were analyzed with the same instrument operated on NCI (negative chemical ionization) SIM mode. Separation of OCPs and PBDEs were performed together on a DB-5-MS capillary column (15 m, 0.25 mm i.d., 0.1 μm film thickness).

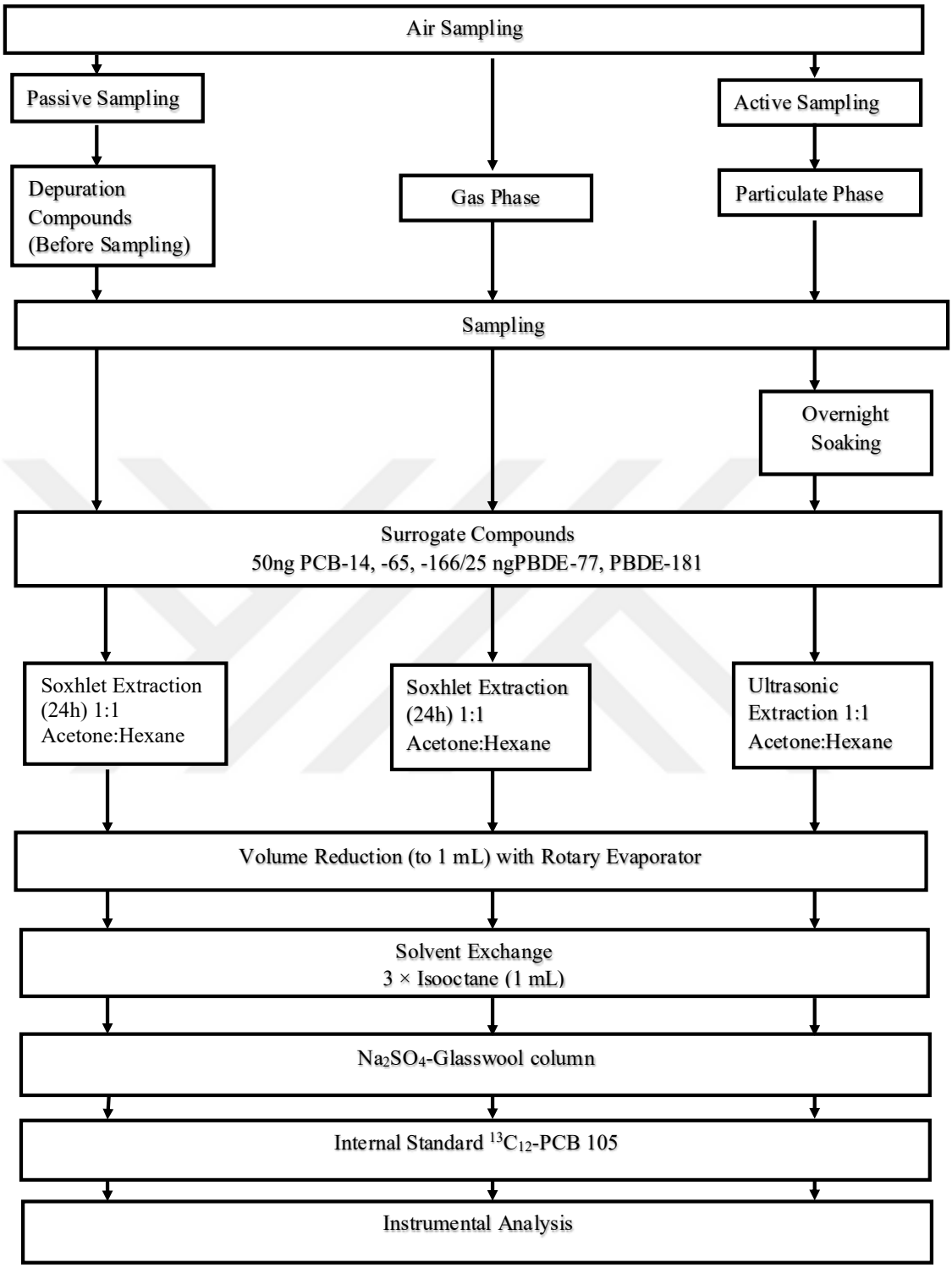

Figure 3.3. Schematic illustration of procedures from sampling to instrumental analysis

Table 3.4. Target Analytes

PBDEs		PCBs			OCPs
PBDE-17	PCB-18	PCB-104	PCB-180	ALD	Aldrin
PBDE-28	PCB-22	PCB-105	PCB-183	α-HCH	α-hexachlorocyclohexane
PBDE-47	PCB-28	PCB-110	PCB-187	β-HCH	β- hexachlorocyclohexane
PBDE-66	PCB-31	PCB-114	PCB-188	γ-HCH	γ-hexachlorocyclohexane (Lindane)
PBDE-71	PCB-41	PCB-118	PCB-189	δ-HCH	δ- hexachlorocyclohexane
PBDE-85	PCB-44	PCB-123	PCB-194		
PBDE-99	PCB-49	PCB-132	PCB-199	*o,p′*-DDT	ortho-para dichloro diphenyl trichloroethane
PBDE-100	PCB-52	PCB-138	PCB-203	*p,p′*-DDT	para-para dichloro diphenyl trichloroethane
PBDE-138	PCB-54	PCB-141		*o,p′*-DDD	ortho-para dichloro diphenyl dichloroethane
PBDE-153	PCB-56	PCB-149		*p,p′*-DDD	para-para dichloro diphenyl dichloroethane
PBDE-154	PCB-60	PCB-151		*o,p′*-DDE	ortho-para dichloro diphenyl dichloroethylene
PBDE-183	PCB-64	PCB-153		*p,p′*-DDE	para-para dichloro diphenyl dichloroethylene
PBDE-190	PCB-70	PCB-155		PCNB	Pentchlornitrobenzene
PBDE-209	PCB-74	PCB-156		DIELD	Dieldrin
	PCB-87	PCB-157		HCB	Hexachlorobenzene
	PCB-90	PCB-158		HEPT	Heptachlor
	PCB-95	PCB-167		HEPX	Heptachlorepoksit
	PCB-99	PCB-170		TC	*Trans* (alfa)- chlordan
	PCB101	PCB174		CC	*Cis* (gamma)-chlordan
				ENDO-I	α-Endosulfan
				ENDO-II	β-Endosulfan
				ENDOSULP	Endosulfan Sulfate
					Endrin Aldehyde
				ENDR	Endrin
					Endrin ketone
					Mirex

Table 3.5. Operating conditions of GC-MS

Operating Conditions	**PBDE Analysis**	**PCB Analysis**	**OCP Analysis**
Column	DB5-MS (J&W Scientific) 15m 0.25mm 0.10 µm	DB5-MS (J&W Scientific) 60m 0.25mm 0.25 µm	DB5-MS (J&W Scientific) 15m 0.25mm 0.10 µm
Ionization Mode	Negative Chemical Ionization (NCI)	Electron Ionization (EI)	Negative Chemical Ionization (NCI)
Reagent Gas	Methane (1.8 mL-%40)	-	Methane (1.1 mL-%40)
Carrier Gas	Helium	Helium	Helium
Carrier Gas Flowrate	1.1 mL/min	1.1 mL/min	1.1 mL/min
Injection Mode	Pulsed- Splitless (NCI)	Splitless (NCI)	Splitless (NCI)
Injection Temperature	320° C	200 ° C	200 ° C
Injection Volume	2 µL	2 µL	1 µL
Ion source Temperature (70ev)	150 ° C	230° C	150 ° C
Quadrupole Temperature	150 ° C	150° C	150° C
Auxilary temperature	320 ° C	300° C	300° C
Tempereture program	Initial Oven Temperature 90° C for 1 min Raised to: 315°C at 20°C /min, (holding for 5 min).	Initial Oven Temperature 90° C for 1 min. Raised to: 160°C at 15°C/min, 210°C at 3°C/min, 310°C at 10°C/min (holding for 7 min).	Initial Oven Temperature 80° C for 2 min. Raised to: 285°C at 10°C/min, (holding 5 min) 315°C at 25°C /min, (holding 5 min).

3.6. Quality Assurance Quality Control

3.6.1. Field Blanks

During the analysis, in order to test whether there is any contamination, 5 field blanks were taken for passive samples, and 3 field blanks for active samples. The blanks were obtained by moving the sampling media to the sampler in the same way as the samples, by placing them on to the sampler and removing it. The control samples were added with the recovery efficiency performance compounds and passed through all the phases of the sample processing. In blank except only three congeners were detected. PBDE 28, PBDE 85, and HCB. Mean±SD concentrations of HCB in the active (1.0±0.35 pg/m^3) and passive (1.2±0.4 pg/m^3) sampling were calculated by using mean air volume. PBDE-28 (0.21±0.07 pg/m^3) and PBDE-85 (0.43±0.07 pg/m^3) were only detected in passive sampling.

3.6.2. Calibration Linearity

For PCB, PBDE, and OCPs, various calibration points were used, i.e. for OCPs 8, for PCBs and PBDEs 10. The lowest calibration R^2 value among all PCB congeners was 0.991 for PCB-141, 0.994 for $EndoSO_4$ among OCPs, and 0.992 for PBDE-183 among PBDE congeners.

3.6.3. Procedural Recovery

To determine the recovery efficiencies, each sample was spiked with surrogate standards, 50 ng (PCB-14, -65, -166; 25 ng PBDE-77, -181) before extraction. The efficiency of procedural recovery was calculated by using Equation (3.11).

$$\text{Recovery Efficiency (\%)} = 100 \times (Cf / Ci) \tag{3.11}$$

where *Cf* is the concentration of the spiked sample processed as a real sample and *Ci* is the initial concentration in the spike solution. The mean ± SD recovery values are summarized in Table 3.6.

Table 3.6. Recovery of Surrogate Compounds

Surrogate Standard	Passive Sampling	Active Sampling (Gas and Particulate Phase)
	Mean ± SD	**Mean ± SD**
PCB-14	91 ± 13	83 ± 9
PCB-65	86 ± 15	82 ± 4
PCB-166	84 ± 16	84 ± 10
PBDE-77	84 ± 14	95 ± 6
PBDE-181	84 ± 13	94 ± 5

3.6.4. Detection Limits

The instrumental detection limit, the IDL of the measuring device used, e.g., the detector, was the lowest concentration (the smallest amount) of an analyte that can be detected, but not quantified, by means of a measuring instrument (Konieczka 2012). Analytical techniques LOD and LOQ apply to absolute and relative values, based on the type of technique and attribute. Detection Limits (LODs) were defined as the lowest analyte concentration that can be reliably detected. LOQs were defined as the lowest analyte concentration that can be reliably quantified (Holst-Jensen 2007). Instrumental detection of PBDE compounds varied between 0.01 and 0.06 pg/ul. Method detection values for these results were calculated between 0.06 and 0.32 pg/m^3 for passive sampling and from 0.04 to 0.22 pg/m^3 for active sampling. For PCB compounds instrumental detection values varied between 0.01 and 0.6 pg/ul. Method detection values for these results were calculated between 0.05 and 2.15 pg/m^3 for passive sampling and from 0.05 pg/m^3 to 3.03 pg/m^3 for active sampling. For OCP compounds instrumental detection values varied from 0.05 pg/ul to 0.1 pg/ul. Method detection values for these results were calculated between 0.253 pg/m^3 and 0.505 pg/m^3 for passive sampling and from 0.18 pg/m^3 to 0.36 pg/m^3 for active sampling. Instrumental and method detection results of each group and each congener are given in the appendix between A4 and A6.

3.7. Trajectory Analysis

In this study, three trajectories were used in order to understand the origin of air masses. Backward air trajectories were created for active sampling days. Monthly clusters and Monthly frequency were used for passive samples to see the percentage and origin of air masses.

Back trajectory analysis was performed by using HYSPLIT4 for Izmir (38°19'04.9"N,26°38'18.1"E) where active samples were collected. The back-trajectory time was chosen for 120 hours (5 days). Backward analyses were made for 3 different heights (300 m, 450m, 600 m, 750 m) also the top of model assumed to be 10,000 m. Meteorological datasets archived on the ARL server were used to drive the HYSPLIT4 model. GDAS data with a horizontal resolution of 1° which corresponds to 100 km x 100 km and 23 vertical layers were used in order to determine back-trajectories.

Monthly cluster analyses arriving at our sampling sites were calculated using the HYSPLIT4 model. Meteorological data in order to run the model are available in the reanalysis part. In this study monthly global reanalysis (.gbl) meteorological data sets were used. Monthly data were run for 6 h (one trajectory) during the sampling period and 8 trajectories were created one cluster.

The trajectory frequency option starts a trajectory from a single location and height every 6 hours and then sums the frequency that the trajectory passed over a grid cell and then normalizes by either the total number of trajectories or endpoints. A trajectory may intersect a grid cell once or multiple times. Computational methods of trajectory cluster and frequency analysis are given in the next sections.

3.7.1. Back Trajectory Computational Calculation

Sum of three-dimensional velocity original position P(t) and the first position P'(t+Δt) are used in order to determine the particle or puff advection. Time and space both interpolate the velocity linearly.

The location of the first guess is

$$P'(t+\Delta t) = P(t) + V(P,t)\ \Delta t. \quad (3.12)$$

the final position is

$$P(t+\Delta t) = P(t) + 0.5\ [\ V(P,t) + V(P',t+\Delta t)\ ]\ \Delta t. \quad (3.13)$$

The integration time phase (Δt) can differ during the simulation. It is determined on the basis of the condition that the distance of advection each time-step be less than the grid spacing. The maximum transport speed shall be calculated from the average transport speed during the preceding hour. The time phases will range from 1 minute to 1 hour and are determined from the relation.

$$U_{max}\ (\text{grid-units min}^{-1})\ \Delta t\ (\text{min}) < 0.75\ (\text{grid-units}) \quad (3.14)$$

The integration approach is very popular and has been used for some time in the trajectory research. Higher-level integration methods do not produce greater accuracy since data measurements are linearly interpolated from the grid to the integration point. Trajectories are terminated when the meteorological data grid exits, but advection continues along the surface if the trajectories intersect.

$$\sigma = (Z_{top} - Z_{msl}) / (Z_{top} - Z_{gl}) \quad (3.15)$$

where Zmsl is the height at the mean sea level to also be transformed to sigma, gl is the height at the ground level, and the top describes the scale height at the top of the model, the level at which the internal sigma surfaces go flat relative to the terrain. The default height of the internal scale is 25 km.

3.7.2. Computational Calculation of Trajectory Cluster Analysis

In the clustering process the spatial variance (SV) is computed between each endpoint (k) along trajectory (j) within its cluster (i):

$$SV_{i,j} = \Sigma k\ (P_{j,k} - M_{i,k})^2 \quad (3.16)$$

Where the sum is taken over the number of endpoints along the trajectory and P is the position vector for the individual trajectory and M is the position vector for the cluster analysis.

CSV stands for cluster spatial variance, which is the sum of all trajectories spatial variance.

$$CSV_i = \Sigma_j SV_{i,j} \tag{3.17}$$

$$TSV = \Sigma_i CSV_{j,k} \tag{3.18}$$

Clustering starts with each trajectory being assigned to its own cluster, resulting in I clusters with j=1 trajectory by each cluster. While two clusters are combined, the cluster numbers are reduced by one in each iteration. As a result of the second iteration, there would be i-1 clusters, with one cluster having two trajectories and the others having only one.

For each iteration, the TSV is calculated for each cluster merge combination, i.e., the trajectories in cluster 1 are added to those in cluster 2, cluster 3, and so on, until the TSV is computed for all remaining cluster combinations, resulting in (i2-i)/2 computations per iteration. The combination with the minimum TSV is transferred to the next iteration.

Originally, the TSV increases significantly, but levels out with the remaining iterations until near the end of the process, at which stage separate clusters continue to converge and the TSV increases again. The ideal final number of clusters would be before the point of increase.

3.7.3. Computational Calculation of Cluster Frequency

The first step is to count how many ways there are in each grid cell that covers the entire area. The dimension of the base grid is 1.0 degrees. The trajectory frequency (F) is the number of trajectories (T) that have passed through each ij grid cell divided by the total number of trajectories (N) that have been evaluated:

$$F_{i,j} = 100 \Sigma T_{i,j} / N \quad (3.19)$$

Consider that all trajectories are counted once in the source grid cell position and each trajectory is counted once per intersection grid cell when the residence time radio button is set to No:

$$\Sigma Ti,j \leq 1.0 \quad (3.20)$$

The residence time alternative counts multiple intersections where they exist, up to the number of endpoints (P) in any one path:

$$\Sigma Ti,j \leq P \quad (3.21)$$

3.8. Statistical Analyses

In this study, normal distribution tests of congeners were performed using Origin Pro 2016. Shapiro Wilk test used (α:0.05 level) for normality determination which was the most powerful test used in literature (Razali et al. 2011). To evaluate the distance-concentration relationship, the Pearson test was applied to the normally distributed congeners using Excel-16.40, while the spearman rank was applied to the congeners that were not normally distributed. Kruskal Wallis and ANOVA tests were performed with IBM SPSS-23.

CHAPTER 4

RESULTS AND DISCUSSION

4.1. Central Tendency of Proximity Groups

Median and geometric mean values can be used to determine central tendency statistics, especially for non-normally distributed data. The mean better represents the central tendency in cases where the average data distribution is normal, whereas the median and geometric mean are used in cases where the distribution is not normal. The distance between the mean and the median gives information about the skewness of the distribution. Therefore, in order to summarize the concentrations measured in this study, all three statistics were calculated for the distance dependent groups and their values for Σ_{25}OCPs, Σ_{14}PBDEs, Σ_{45}PCBs are presented in Table 4.1. The statistics were produced for the Close group with and without Karaman and Malatya because they are relatively farther from the border compared to Adana, Osmaniye, and Gaziantep. The statistics were also produced for İzmir and Bursa separately considering their locations.

Table 4.1. Central Tendency of Concentration (pg/m^3)

		Σ_{14}PBDE	**Σ_{45}PCB**	**Σ_{25}OCP**
CLOSE-1[a]	Mean	236.63	385.08	220.40
	Median	183.07	229.22	184.77
	Geo. Mean	103.42	229.84	184.77
CLOSE-2[b]	Mean	249.01	412.60	261.71
	Median	185.23	237.63	201.79
	Geo. Mean	110.87	256.35	223.49
MIDDLE DISTANCE	Mean	150.66	249.91	186.40
	Median	106.34	163.35	111.08
	Geo. Mean	51.56	144.11	118.09
FAR[c]	Mean	233.45	618.53	131.20
	Median	254.36	466.16	110.64
	Geo. Mean	164.89	147.11	86.67
IZMIR	Mean	172.97	588.42	128.55
	Median	93.35	384.50	101.17
	Geo. Mean	97.73	492.10	116.43
BURSA	Mean	271.94	639.33	132.89
	Median	315.27	547.82	120.12
	Geo. Mean	230.01	375.46	71.83

[a]Karaman ve Malatya included, [b]Karaman ve Malatya not included, [c]Izmir - Bursa together

The range of the central tendency statistics for Σ_{14}PBDEs from 51.56 pg/m^3 to 315.27 pg/m^3. The mean Σ_{14}PBDEs concentrations were 236.63 pg/m^3, 249.01 pg/m^3, 233.45 pg/m^3 in close middle and far groups, respectively. Measured Σ_{14}PBDE concentrations were greater than 191 pg/m^3 which was the general countrywide average concentration (Kurt-Karakus et al. 2018) (urban and rural area averages of 183 pg/m^3 and 200 pg/m^3, respectively).

The mean Σ_{45}PCB concentration in close (385.08 pg/m^3), middle (249.01 pg/m^3), and far regions (618.53 pg/m$^{3)}$ were higher than previous study of Kurt-Karakus et al. (2018). Higher levels were measured in general, but relatively higher values were obtained for Bursa (639.33 pg/m^3) and Izmir (588.42 pg/m^3) in comparison with the average levels measured by others in different cities such as Konya, Kutahya, Istanbul, Bursa while lower values were measured than the levels reported for industrial areas (Aliaga, Dilovası) (Birgül et al. 2017, Cetin et al. 2017, Dumanoglu et al. 2017, Kuzu 2016, Ozcan and Aydin 2009).

Concentrations measured in the close and middle zone were greater than those measured in the far-distance group over 7 months of sampling duration. This can be attributed to the proximity of these cities to industrial zones and emission sources. Birgul et al. (2017) reported the average industrial Σ_{43}PCB concentrations ranged 21 pg/m^3 to 340 pg/m^3 in Kestel, Bursa with an average of 170±150 pg/m^3. In this study, Σ_{45}PCB 639 pg/m^3 measured in Bursa was even higher than the highest value previously measured in Birgul et al (2017). The mean concentrations of Izmir (588.42 pg/m^3) and Bursa (639.33 pg/m^3) were very close. On the other hand, the average concentration of Izmir was lower than previous concentration reported by Aydin et. al., (2014) at different sites. Moreover, higher PCB concentrations were reported than previous study of Kurt-Karakus et al. (2018). Reported country-wide overall average concentration of Σ_{43}PCBs was 108±132 pg/m^3.

OCP values measured in this study are higher in the close (220.40 pg/m^3) region (middle=186.40 pg/m^3, far=131.20 pg/m^3). The reason for this may be the abundance of agricultural areas in this region. As seen in Table 4.2, the total average concentrations in the close region increased during the transition season. In addition, varying rates of air flow were observed in the clusters belonging to the provinces of the close region between Figure 4.20 and Figure 4.24. Between 20% and 79% of the flow coming to the close area came from the war zone at varying rates. These air currents took place between December and April. Lower concentration measured in samples which were collected after April.

This result may be explained there was a transport from war zone to our southern border. But in the far region results of cluster analysis and descriptive statistics was not compatible. In the far region especially in Izmir cluster of each month can be seen in Figure 4.29, all of the air coming from the north. Bursa was only affected by the air flow coming from the south in the first month sampling. However, this rate was limited to 21% as shown in Figure 4.28.

Table 4.2. Seasonal central tendency statistics for total PBDE, PCB and OCP concentrations (pg/m^3)

		Σ_{14}PBDE		Σ_{45}PCB		Σ_{25}OCP	
		Winter	**Transition**	**Winter**	**Transition**	**Winter**	**Transition**
CLOSE-1[a]	Mean	237.24	234.32	302.49	448.0	176.07	256.30
	Median	219.03	132.70	191.90	241.89	172.26	196.42
	Geo.	197.52	61.25	186.72	270.37	155.26	290.09
CLOSE-2[b]	Mean	220.45	325.34	366.13	451.92	197.67	315.89
	Median	219.03	185.23	206.96	397.07	186.25	286.58
	Geo.	182.04	122.63	223.87	287.47	187.16	271.67
MIDDLE DISTANCE	Mean	225.48	91.87	277.78	228.01	176.22	194.39
	Median	226.04	17.72	163.35	166.12	91.80	138.02
	Geo.	207.61	17.26	147.21	141.72	107.84	126.83
FAR[c]	Mean	297.08	201.64	917.94	470.33	145.90	124.49
	Median	335.10	145.00	1010.31	326.44	123.32	90.68
	Geo.	263.49	130.44	775.48	305.91	135.24	69.39
IZMIR	Mean	241.79	121.36	578.93	595.55	145.90	115.53
	Median	293.60	57.61	371.45	507.10	96.37	118.86
	Geo.	197.73	78.91	493.68	490.91	129.98	107.21
BURSA	Mean	352.37	241.78	1256.65	407.72	143.33	128.97
	Median	354.92	184.01	1100.09	252.86	126.51	71.78
	Geo.	351.14	196.27	1218.13	241.48	140.72	55.82

[a]Karaman and Malatya included, [b]except Karaman and Malatya, [c]İzmir and Bursa included

Figure 4.1 shows the average Σ_{14}PBDE Σ_{45}PCB and Σ_{25}OCP concentration for all three regions. In addition, the percentage of each congener in the area is shown. There was no decreasing trend in concentration from close to far distance for PBDEs. Concentration of PBDE-209 (325.23 pg/m^3) in the close region were higher than in other regions. On the other hand, concentrations of PBDE-47, PBDE-99, PBDE-100 were similar in the close and far group and higher than middle group, which may be interpreted as far and close groups had higher levels than middle group because Izmir and Bursa have strong urban and industrial pollution and receive LRAT from polluted regions in Europe, Russia, and former Soviet Union while the close group urban and industrial effects are

less pronounced but they receive also air masses from the war zone (see Sections 4.3 and 4.4). PCB-44 (310.48 pg/m^3, 45.18 pg/m^3, 39.08 pg/m^3) and PCB-74 (34.98 pg/m^3, 25.37 pg/m^3, 22.47 pg/m^3) concentration values tend to decrease as they move away from the war zone. Concentrations of PCB-18 (131.34 pg/m^3, 11.69 pg/m^3, 84.94 pg/m^3), PCB-180 (31.92 pg/m^3, 23.82 pg/m^3, 29.18 pg/m^3) and PCB-123 (605.52 pg/m^3, 53.94 pg/m^3, 441.11 pg/m^3) value were higher in the close group, the measured value in the middle-distance group was lower than far distance group, which agree with the argument made for PBDEs. The majority of OCP congeners were higher in the close and middle regions.

Concentrations were often higher in the close and middle regions, although there was a certain decrease from the close to the far region. The far-group concentrations were higher for a limited number of congeners. This finding can be interpreted as contribution of both the south of the border and agriculture in the region results in higher levels compared to the middle and far groups where agriculture is also considerable but not as much as the close group.

Our country is under the influence of southern winds especially in transition seasons (Spring and Autumn) and desert dust is transported (Doğan, Yeşilnacar, and Cullu 2018). Therefore, the concentrations measured in this study are divided into two seasonal groups as Winter (December-January-February) and Spring (March-August) to explore whether a clearer proximity relation could be observed in the transition season. However, frequency of southerly winds was the highest to the close-group in winter, while the far-group mainly received northerly air masses originating from Europe and Russia. Congeners have high concentration can be seen in Figure 4.1, Figure 4.2, and Figure 4.3 in order of the whole, winter, and transition sampling campaign. The congeners with higher concentrations were measured for PBE-209 (136.89 pg/m^3, 35.03 pg/m^3, 52.45 pg/m^3), PBDE-28 (32.55 pg/m^3, 7.47 pg/m^3, 5.12 pg/m^3), PBDE-47 (62.63 pg/m^3, 52.42 pg/m^3, 63.90 pg/m^3), PBDE-99 (3.12 pg/m^3, 0.83 pg/m^3, 1.94 pg/m^3), PBDE-100 (52.53 pg/m^3, 59.89 pg m^3, 52.09 pg/m^3), PBDE-138 (2.39 pg/m^3,1.41 pg/m^3,1.62 pg/m^3). Similar to the overall case, the middle-group concentration values were lower than the close and far groups. Back trajectory analysis of active sampling results supports this situation. Figure 4.7 and Figure 4.8 pointed out sources resulted from Europe and Russia.

When the PCB congers were examined, for the following congeners were the highest in the close-group: PCB-41/64 (19.04 pg/m^3, 9.71 pg/m^3, 14.13 pg/m^3), PCB-44 (46.19 pg/m^3, 45.18 pg/m^3, 39.08 pg/m^3), PCB-180 (51.16 pg/m^3, 41.21 pg/m^3, 42.43 pg/m^3), PCB-187 (54.25 pg/m^3, 34.51 pg/m^3, 43.07 pg/m^3). Far-group concentrations for other

congeners were higher. The OCP congeners, which showed a decreasing trend from close to far region in winter, were Heptachlor (41.75 pg/m^3, 27.98 pg/m^3, 23.08 pg/m^3) and *p,p'*-DDE (63.91 pg/m^3, 40.03 pg/m^3, 29.50 pg/m^3). Group average values were >0 for γ-HCH (20.74 pg/m^3), heptachlor epoxide (6.73 pg/m^3), EndoSO4 (0.33 pg/m^3) only for close region, and mirex (3.59 pg/m^3) only for far region. Concentrations for the winter season and percent contribution of the congeners are given in Figure 4.2.

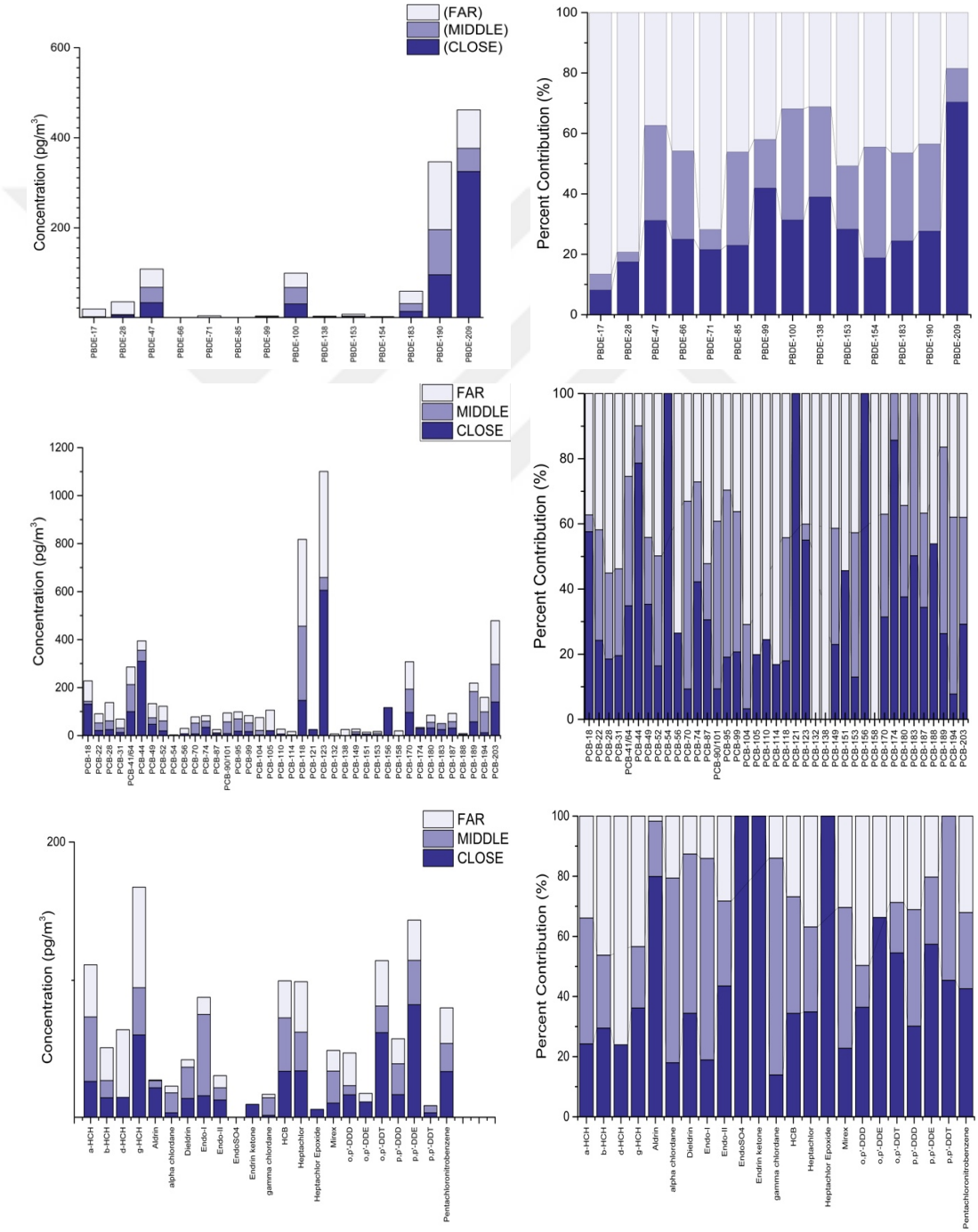

Figure 4.1. The mean POPs concentrations (pg/m^3) and percent contribution

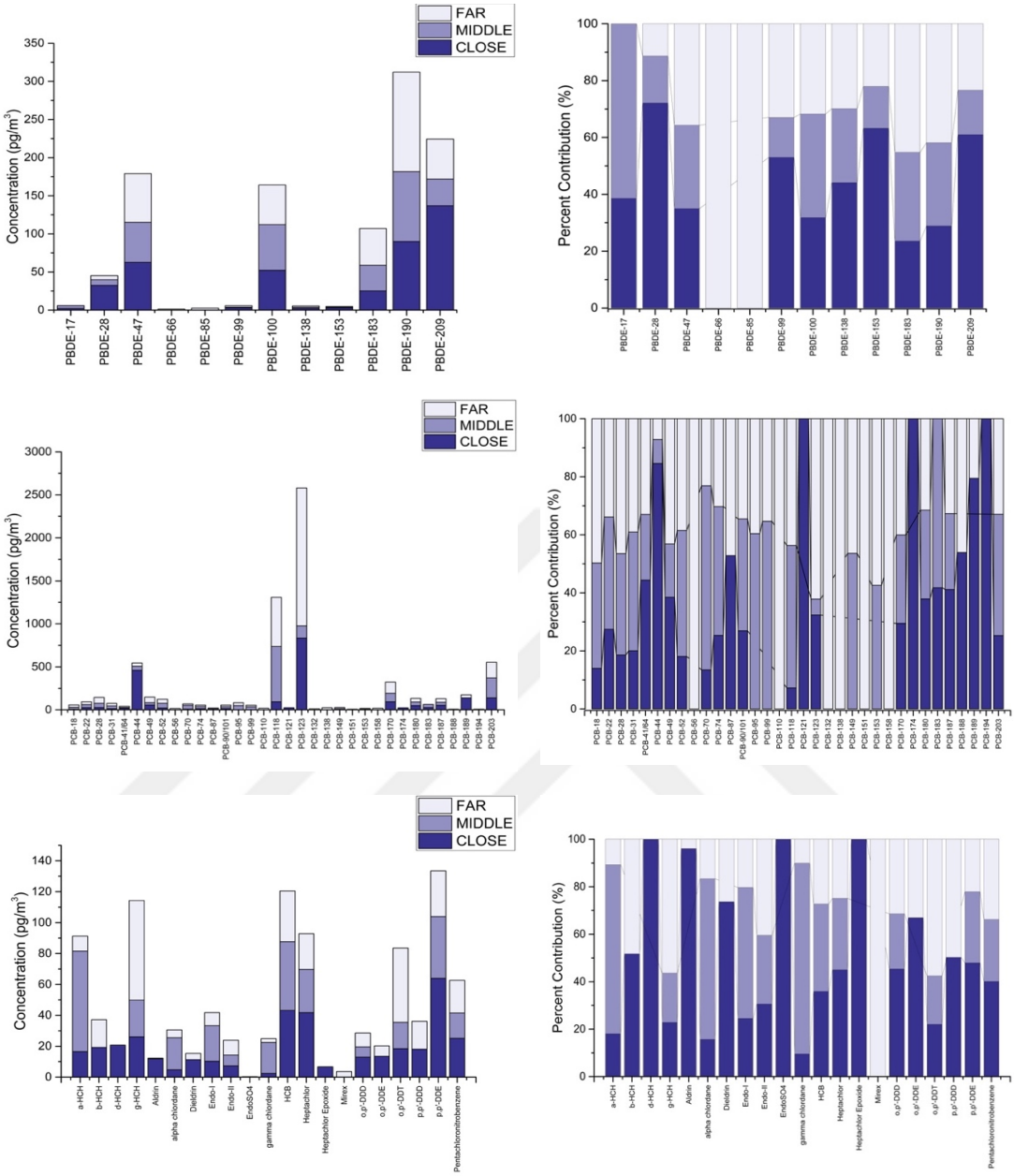

Figure 4.2. The winter period mean POPs concentrations (pg/m^3) and percent Contribution

In the transition season, only PBDE 209 (388.01 pg/m^3, 62.35 pg/m^3, 107.30 pg/m^3) the highest in close-group, whereas the other congeners were at higher levels in the far-group. In the dataset we grouped as transition season, although PCB-18 congeners were higher in the close group, the middle-distance group concentration was not more than the long-distance group. However, the situation was different for PCB 41/64 congener, although the close distance concentration value was higher than the distance

group, the highest concentration value was measured in the middle-distance group. Among OCP congeners, the *o, p'*-DDT (91.49 pg/m^3, 20.27 pg/m^3, 17.56 pg/m^3) concentration value was higher in the close and middle groups, while pentachloronitrobenzene (PCNB) (41.59 pg/m^3, 26.20 pg/m^3, 34.86 pg/m^3) was higher in the close as in the previous cases. Figure 4.3 presents concentration of each congener and each group.

Percent contribution plots indicate that PBDE concentrations being higher in the close group tend to increase with increasing congener MW, whereas lighter congeners tend to be at higher levels in the far group for the whole (Figure 4.1) and winter (Figure 4.2) periods. A trend is not visible in the transition period. Although not as clear as PBDEs, PCBs also depict a similar trend in winter. Considering, the effect of the south of the border was relatively higher in winter compared to the transition period on the close-group along with the increasing contribution with increasing molecular weight may indicate that the source areas are probably close compared to the far-group where increasing contribution with decreasing MW may indicate that the source areas are probably not close. This argument supports the finding of the back-trajectory analysis that the war zone impacts southeast of Turkey while west – northwest of the country is impacted by long-range transport from areas in Europe, Russia, and former Soviet Union countries. Such train of thought would not be appropriate for OCPs because of the dependence on where the individual compounds were used.

Σ_{14}PBDE, Σ_{45}PCB, and Σ_{25}OCP concentration graphs and percent contribution of active samples are shown in Figure 4.4, Figure 4.5, and Figure 4.6, respectively. These figures also provide congener contribution to the total concentration for each sample. Additionally, total concentration of gas and particulate phase for each sample listed in Table 4.6, Table 4.7, and Table 4.8. Concentrations measured in this study are comparable to those of previous studies. In a study by Lammel et al. (2015), which was conducted with passive sampling in July in Izmir at the site of this study, reported Σ_5PBDE= 8.5 pg/m^3 concentration. Besis et al. (2017) conducted active sampling at the same location and reported a PBDE-209 concentration close to that of this study. PBDE-209 was the highest contributing congener to the total concentration. The highest contributing congeners to Σ_{14}PBDE in this study was PBDE-190, PBDE-209, PBDE-100, with average concentrations of 131.5 pg/m^3, 79.42 pg/m^3, 45.84 pg/m^3, respectively. The gas phase Σ_{29}PCB concentrations reported in urban Izmir was = 1642 ± 817 pg/m^3 and 2078 ± 1026 pg/m^3 in winter and summer, respectively. The highest PCB concentration (G-P)

congener was PCB-33 (453±246 – 10±7 pg/m^3), while it was PCB-18 (286±142 – 8±7 pg/m^3) in winter. Total PCB concentration values are higher than the (G+P) values measured in this study probably due to proximity of sampling sites to emission sources. In this study, the average (G + P) concentration value measured in winter and transition months was 213.36 pg/m^3 and 1330.14 pg/$m^{3,}$ respectively. The highest PCB congener concentration was measured in sample collected in May for PCB-22 (1012.20 pg/m^3), PCB-28 (1295.70 pg/m^3), PCB-52 (1348.50 pg/m^3). In the study conducted by Aydin et al. (2014) in the non-nonindustrial area of Izmir, the highest concentrations were reported in July-August (Σ_{35}PCB=2214.29 pg/m^3), April-May (Σ_{35}PCB=1587.86 pg/m^3), and January-February (Σ_{35}PCB=987.14 pg/m^3), respectively. Σ_{45}PCB concentration trend observed by Aydin et al. (2014) is similar to that of in this study. In this study average Σ_{25}OCP concentration was 139 pg/m^3. HCB, heptachlor, HCHs (α-HCH, β-HCH, γ-HCH, δ-HCH) were mostly detected and contributed to total concentration. In a previous study conducted Lammel et al. (2015) with passive sampling at the same sampling site$\sum_9$OCP concentration was reported as 43 pg/m^3 which is lower than our mean value.

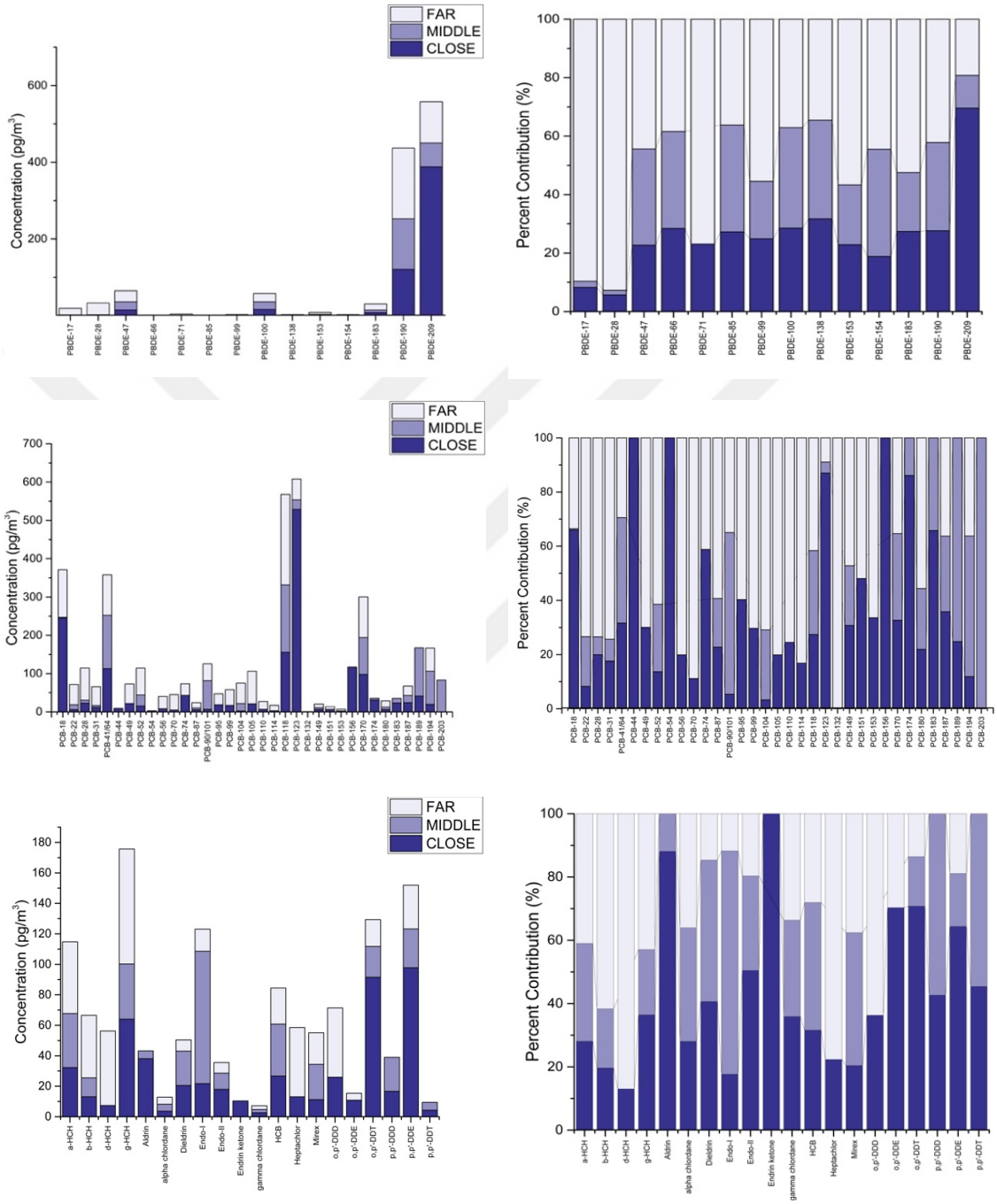

Figure 4.3. The transition period mean POPs concentrations (pg/m^3) and percent contribution

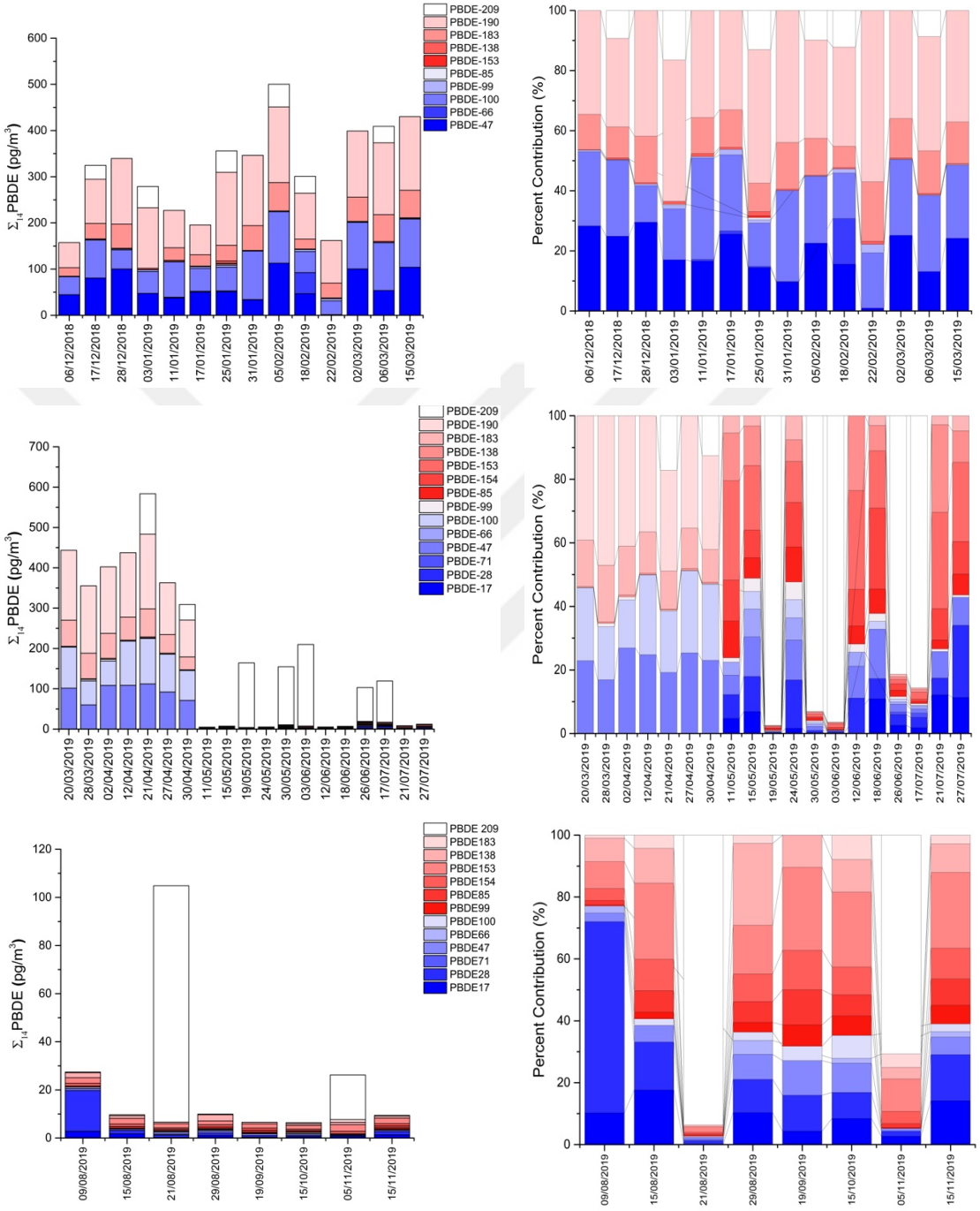

Figure 4.4. Active sampling Σ_{14}PBDEs concentrations and percent contribution sampling periods Winter-Transition-Other

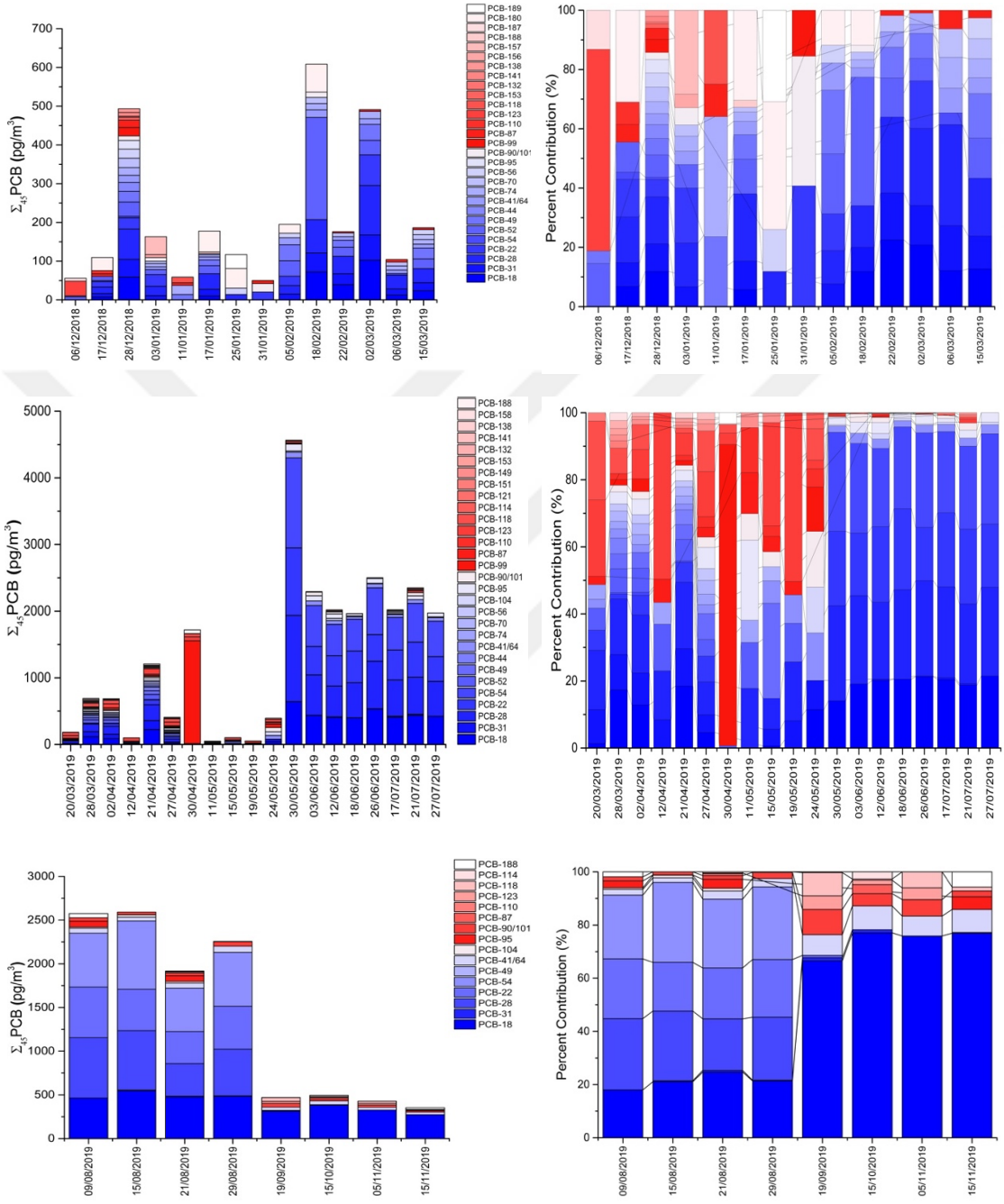

Figure 4.5. Active Sampling Σ_{45}PCBs concentrations percent contribution sampling periods Winter- Transition-Other

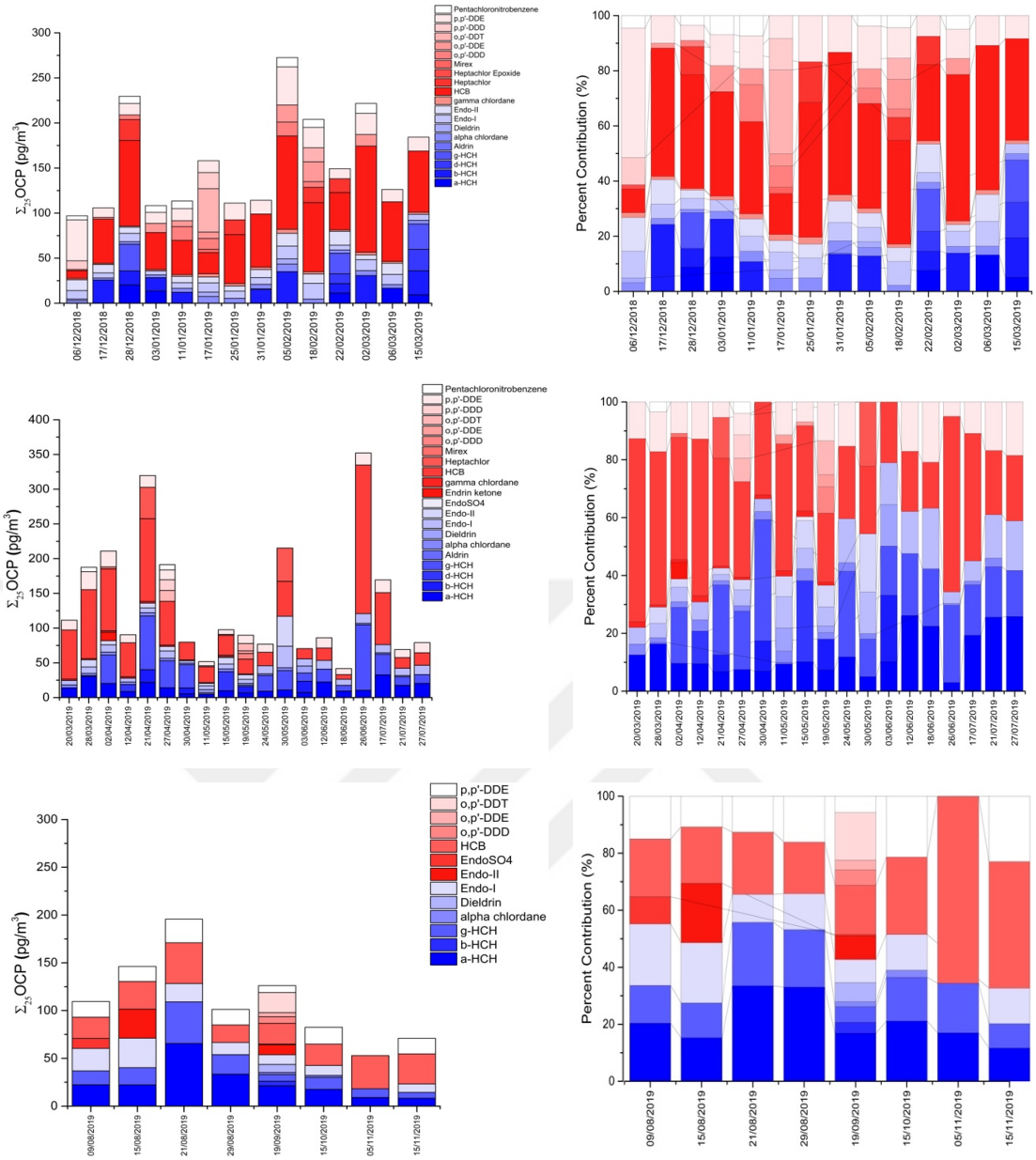

Figure 4.6. Active Sampling Σ_{25}OCPs concentrations and percent contributions sampling periods Winter-Transition-Other

4.2. Proximity Concentration Relation

Our country is under the influence of southern winds especially in transition seasons (Spring and Autumn) and desert dust is transported (Doğan, Yeşilnacar, and Cullu, 2018). Therefore, the concentrations measured in this study are divided into two seasonal groups as Winter (December-January-February) and Spring (March-August) to explore whether a clearer proximity relation could be observed in the transition season.

Seasonal central tendency statistics for passive samples are listed in Table 4.2. Seasonal central tendency statistics for the active samples are presented in Table 4.6, 4.7 and 4.8 for Σ_{45}PCB, Σ_{14}PBDE, and Σ_{25}OCP.

4.2.1. Correlation Analysis

In this study, Pearson and Spearman rank tests were applied to mean, median geometric mean values of the regions grouped as Close, Middle and Far in order to evaluate the relation between regions. Tests were applied to the groups both seasonally and on average concentrations for all months. Moreover, it was applied separately to Bursa and Izmir, which were in the long-distance group. The results obtained with Kruskal Wallis and ANOVA are listed in Tables 4.3, 4.4 and 4.4 up to α=0.10.

4.2.1.1. Winter

Pearson test was applied to compounds which can be assumed to follow normal distribution whereas Spearman rank test was applied to compounds that have non-normal distribution. Tests were applied to the mean, median and geometric mean values calculated for the winter season in which all provinces were included and sampled. Compounds that have r=-1 correlation concentrations were decreasing from close to far regions. Compounds that have strong correlation (r_s=-1) are discussed here while the remaining are listed in the Appendix (A7 and A9).

Among PBDE congeners PBDE 28 have strong correlation (r_s=-1) in the whole sampling period is considered. The mean concentration value measured for the close region (32.55 pg/m^3) was approximately 5.5 times the measured value for the middle (7.47 pg/m^3) distance and 7.7 times the far (5.12 pg/m^3) distance. The correlation value for PBDE-28 did not change when Karaman and Malatya were not included in the close group. Correlation of PBDE-28 was only possible with Bursa in far group sampling points. Measured mean PBDE-28 concentration was 5.12 pg/m^3. Measured mean PBDE-28 concentration in this study was higher than previous measurement in the far sampling points. While the PBDE-28 concentration reported by Lammel et al. (2015) in Urla, Izmir was 7.5 pg/m^3, this concentration value in Nilüfer, Bursa was 0.021 pg/m^3.

Only PCB-44 was highly correlated among all PCB congeners in winter season. Measured mean PCB-44 concentrations were 461.69 pg/m^3, 45.18 pg/m^3, and 39.08 pg/m^3 in close, middle and far groups. The exclusion of Karaman and Malatya did not change the results.

HCB (r_s=-1; median (38.01 pg/m^3, 32.63 pg/m^3, 32.42 pg/m^3) and heptachlor (r_s=-1; median 29.03 pg/m^3, 27.98, 23.08 pg/m^3)), and *p,p'*-DDE (r_s=-1; mean 63.91 pg/m^3, 40.03 pg/m^3, 29.50 pg/m^3) were highly correlated. In addition to this Σ_{25}OCP (197.67 pg/m^3,176.22 pg/m^3,144.62 pg/m^3) was correlated with mean values when Karaman and Malatya were removed from close group.

Alpha chlordane (r_p=-0.61; median values 4.68 pg/m^3, 5.05 pg/m^3, 4.09 pg/m^3), gamma chlordane (r_p=-1; median values 2.34 pg/m^3, 2.25 pg/m^3, 2.14 pg/m^3) and *p,p'*-DDE (r_s=-1; mean values 63.91 pg/m^3, 40.03 pg/m^3, 22.40 pg/m^3) were highly correlated when only Izmir was considered, and *o,p'*-DDD (r_s=-1; mean values 12.95, pg/m^3, 6.62 pg/m^3, 5.95 pg/m^3) was highly correlated when only Bursa was evaluated in the far group.

Results of Kruskal Wallis and ANOVA test are shown in Table 4.3. PBDE-99 (p=0.080), PBDE-183 (p=0.020), PBDE-190 (p=0.072) PBDE 209 (p=0.066) Σ_{45}PCB (p=0.006), Dieldrin (p=0.030), Σ_{25}OCP (p=0.055) have a significant difference in central tendency statistics during the winter season in three regions when all sampling locations were considered. In addition to this, PBDE-183 (p=0.028) and PBDE-190 (p=0.081) have significantly different mean concentrations. Considering only the Izmir far group shows that the PBDE 183 (p=0.089), PBDE-209 (p=0.069), PCB-18 (p=0.049), PCNB (p=0.078), and Σ_{25}OCP (p=0.046) have different median values in groups. Additionally, PCB-18 (p=0.057), Σ_{45}PCB (p=0.037), Dieldrin (p=0.040) Endo I (p=0.034) HCB (p=0.079), Σ_{25}OCP (p=0.046) have meaningful p values with Kruskal Wallis and PBDE 183 (p=0.094) concentration differs regionally as a result ANOVA.

Table 4.3. Winter season Kruskal Wallis and ANOVA results

ALL		**ONLY IZMIR**		**ONLY BURSA**	
ANOVA		**Kruskal Wallis**		**ANOVA**	
Congeners	**p**	**Congeners**	**p**	**Congeners**	**p**
PBDE-183	0.028	PBDE-183	0.089	PBDE-183	0.094
PBDE-190	0.081	PBDE-209	0.069	**Kruskal Wallis**	
Kruskal Wallis		PCB-18	0.049	**Congeners**	**p**
Congeners	p	PCNB	0.078	PCB-18	0.057
PBDE-99	0.080	Σ_{25}OCP	0.079	Σ_{45}PCB	0.037
PBDE-183	0.020			Dieldrin	0.040
PBDE-190	0.072			Endo-I	0.034
PBDE-209	0.066			HCB	0.079
Σ_{45}PCB	0.006			Σ_{25}OCP	0.046
Dieldrin	0.030				
Σ_{25}OCP	0.055				

4.2.1.2. Transition Period

The correlation values of PBDEs with the evaluation of sampling sites in the transition season have a value of r_s=-0.5 and are listed in the Appendix (A7). Considering only Izmir in the far group highly correlate PBDE-100 (r_s=-1; geo. mean 1.35 pg/m^3,1.07 pg/m^3,0.50 pg/m^3) and PBDE-183 (r_s=-1; mean 8.36 pg/m^3, 6.16 pg/m^3, 0.31 pg/m^3) and exclusion of Karaman and Malatya from close group also correlate PBDE-99 (r_s=-1; median 0.57 pg/m^3, 0.45 pg/m^3, 0.39 pg/m^3). When only Bursa was considered in the far group only PBDE-153 (r_s=-1; mean 2 pg/m^3,1.80 pg/m^3,1.35 pg/m^3) was correlated and exclusion of Karaman and Malatya did not change the results.

The correlation values of PCBs with the evaluation of all sampling sites in the transition season have a value of r_s=-0.5 and are listed in the Appendix (A8). Separate evaluation of Izmir and Bursa gives high correlation value in the case of only Izmir in the far group. PCB-123 (r_s=-1; median 696.34 pg/m^3, 26.07 pg/m^3, 9.37 pg/m^3) were correlated. Moreover, without Karaman and Malatya PCB-118 (r_s=-1; median 140.58 pg/m^3, 16.46 pg/m^3, 7.15 pg/m^3) were correlated.

Among OCP compounds gamma chlordane(r_p=-0.97; median 2.71 pg/m^3, 2.05 pg/m^3, 1.80 pg/m^3), Endo I (r_s=-1; median 18.77 pg/m^3,16.74 pg/m^3, 15.93 pg/m^3), Endo II (r_s=-1; median 11.07 pg/m^3, 7.18 pg/m^3, 6.99 pg/m^3), o,*p'*-DDT (r_s=-1; median 21.52 pg/m^3,20.27 pg/m^3, 17.56 pg/m^3), Σ_{25}OCP (r_s=-1; mean 256.30 pg/m^3,194.39 pg/m^3,124.49 pg/m^3) were highly correlated when all sampling sites were considered. In

the case of evaluation of Izmir in the far group gives high spearman rank correlation values for Endo I (r_s=-1, geo. mean 18.83 pg/m^3, 17.83 pg/m^3, 27.68 pg/m^3), γ-HCH (r_s=-1, geo. mean 42.67 pg/m^3, 28.54 pg/m^3, 27.68 pg/m^3), Σ_{25}OCP (r_s=-1; mean 256.30 pg/m^3, 194.39 pg/m^3, 115.53 pg/m^3). Separate evaluation of Bursa gives high correlated number of compounds in the transition season. Gamma chlordane ($r_{p=}$-0.96, median 2.71 pg/m^3, 2.05 pg/m^3,1.83 pg/m^3), Endo I (r_s=-1; median 18.77 pg/m^3, 16.74 pg/m^3, 7.75 pg/m^3), Endo II (r_s=-1; median 11.07 pg/m^3,7.18 pg/m^3, 6.99 pg/m^3), o,*p'*-DDT (r_s=-1; median 21.52 pg/m^3, 20.27 pg/m^3,17.56 pg/m^3), Σ_{25}OCP (r_s=-1; median 196.42 pg/m^3, 138.02 pg/m^3, 71.68 pg/m^3).

Congeners that have a significant difference in central tendency statistics in transition season (α=0.10) are shown in Table 4.5. Congeners with regionally different concentrations are listed in Table 4.5. By evaluating all months, a regional difference was obtained for PBDE-28, PBDE-99, PBDE-154, *p, p'*-DDE, Σ_{14}PBDE, and Σ_{25}OCP.

Consequently, the seasonal evaluation shows that more congeners were correlated in the transition season. Especially, considering only Bursa in the far group establishes more highly correlated congeners that show decreasing concentration from war zone to our west sampling points.

Table 4.4. Transition season Kruskal Wallis and ANOVA results

ALL		**ONLY IZMIR**		**ONLY BURSA**	
ANOVA		**Kruskal Wallis**		**ANOVA**	
Congeners	**p**	**Congeners**	**p**	**Congeners**	**p**
PBDE-85	0.068	PBDE-183	0.057	PBDE-99	0.049
Kruskal Wallis		PBDE-154	0.007	PBDE-85	0.062
Congeners	**p**	PBDE-209	0.074	PBDE-154	0.016
PBDE-28	0.006	PCB-70	0.083	**Kruskal Wallis**	
PBDE-47	0.067	Endo II	0.070	**Congeners**	**p**
PBDE-99	0.046	PCNB	0.046	PBDE-100	0.063
PBDE-154	0.010	*p, p'*-DDE	0.024	PBDE-154	0.007
PBDE-209	0.053	Σ_{45}PCB	0.082	PBDE-209	0.063
PCB-52	0.087	Σ_{25}OCP	0.055	PCB-31	0.087
PCB-95	0.083			Endo II	0.086
Endo II	0.086			*p, p'*-DDE	0.024
PCNB	0.063			PCNB	0.063
p, p'-DDE	0.024			Σ_{14}PBDE	0.034
Σ_{14}PBDE	0.050			Σ_{25}OCP	0.034
Σ_{25}OCP	0.018				

4.2.1.3. The Whole Sampling Period

The correlation coefficients for all months are listed in the Appendix (A7 -A9) since all were at a moderate level. However, high correlation values were obtained by evaluating Izmir and Bursa separately. A correlation was established median values of PBDE-99 (r_s=-1; median 0.60 pg/m^3, 0.41 pg/m^3, 0.40 pg/m^3), PBDE-209 (r_s=-1; median 158.82 pg/m^3, 54.10 pg/m^3, 47.71 pg/m^3), and Σ_{14}PBDE (r_s=-1; median 183.07 pg/m^3, 106.34 pg/m^3, 93.35 pg/m^3) with the evaluation of the Izmir at a far distance. PBDE-47 (r_s=-1; median 33.88 pg/m^3, 12.97 pg/m^3, 5.52 pg/m^3), PBDE-100 (r_s=-1; median 31.16 pg/m^3, 26.47 pg/m^3, 1.65 pg/m^3), PBDE-153 (r_s=-1; median 2.31 pg/m^3,1.51 pg/m^3,1.28 pg/m^3), which were highly correlated with median values by evaluating only the Bursa in the long-distance group. Additionally, PBDE-138 (r_s=-1; mean 1.66 pg/m^3, 1.19 pg/m^3, 1.15 pg/m^3) was highly correlated with mean values. The results obtained by removing Karaman and Malatya from the close group were not different.

Among PCB congeners only PCB-44 (r_s=-1; mean 310.48 pg/m^3, 45.18 pg/m^3, 39.08 pg/m^3), PCB-74 (r_s=-1 mean 34.98 pg/m^3, 25.37 pg/m^3, 22.47 pg/m^3) PCB-123 (r_s=-1; mean 605.52 pg/m^3, 53.94 pg/m^3,9.37 pg/m^3) were highly correlated in the case of only Izmir in far group. In addition to this PCB-118 were highly correlated when Karaman and Malatya removed from the close group.

HCB (r_s=-1; median (29.70 pg/m^3, 28.65 pg/m^3, 18.19 pg/m^3), Aldrin (r_s=-1; median 14.97 pg/m^3, 5.14 pg/m^3,0.48 pg/m^3), gamma chlordane (r_s=-1; median 2.45 pg/m^3, 2.44 pg/m^3,2.14 pg/m^3), *p,p′*-DDE (r_s=-1; median 82.37 pg/m^3, 32.08 pg/m^3, 29.15 pg/m^3) ,and Σ_{25}OCP (r_s=-1; median 184.77 pg/m^3, 111.08 pg/m^3, 101.17 pg/m^3) were highly correlated The removal of Karaman and Malatya from the close group did not affect the results. The highest number of correlations were obtained with the evaluation of Izmir in the long-distance group PCNB (r_p=-0.99), γ–HCH (r_p=-0.94), heptachlor (r_s=-1), Aldrin (r_s=-1), *p,p′*-DDE (r_s=-1), *p,p′*-DDD (r_s=-1), Endo II (r_s=-1), and Σ_{25}OCP (r_s=-1).

Congeners that have significant difference in central tendency statistics are given in Table 4.5. PBDE-28 (p=0.008), PBDE-85 (p=0.046), PBDE-99 (p=0.016), PBDE-154 (p=0.010), PBDE-190 (p=0.021), PCB-31(p=0.064), PCB-52 (p=0.013), PCB-90/101 (p=0.093), PCB-95 (0.090), Dieldrin (p=0.085), *p,p′*-DDE (p=0.003), Σ_{45}PCB (p=0.008), Σ_{25}OCP (p=0.005) have at least a region with different concentration when all sampling

sites were considered (α=0.10). The concentration values of the measured mean OCP compounds were higher in Bursa than in Izmir. In turn, the correlation coefficient values with the evaluation of only Izmir were higher in the far group.

Table 4.5. All sampling months Kruskal Wallis and ANOVA results

ALL		**ONLY IZMIR**		**ONLY BURSA**	
ANOVA		**ANOVA**		**ANOVA**	
Congeners	**p**	**Congeners**	**p**	**Congeners**	**p**
PCNB	0.063	PCB-22	0.093	PCNB	0.048
Kruskal Wallis		**Kruskal Wallis**		**Kruskal Wallis**	
Congeners	**p**	**Congeners**	**p**	**Congeners**	**p**
PBDE-28	0.008	PBDE-154	0.007	PBDE-28	0.002
PBDE-99	0.016	PBDE-209	0.013	PBDE-85	0.057
PBDE-85	0.046	PCB-90/101	0.041	PBDE-99	0.006
PBDE-154	0.010	Σ_{45}PCB	0.021	PBDE-154	0.011
PBDE-190	0.021	PCNB	0.016	PBDE-190	0.062
PCB-31	0.064	*p,p′*-DDE	0.003	PBDE-209	0.021
PCB-52	0.013	Σ_{25}OCP	0.009	PCB-52	0.032
PCB-90/101	0.093			γ-HCH	0.053
PCB-95	0.090			*p,p′*-DDE	0.005
Σ_{45}PCB	0.008			PCNB	0.025
Dieldrin	0.085			HCB	0.025
p,p′-DDE	0.003			Σ_{25}OCP	0.009
Σ_{25}OCP	0.005				

Statistical tests and group concentrations indicated that highly brominated and highly chlorinated compounds were higher in the close group. These compounds were less volatile and the LRAT of these compounds was difficult because of their lower vapor pressure, high MW. Transport of lower-chlorinated and brominated chemicals is easier. These compounds are so volatile that they should be almost entirely sorbed to suspended particles in the environment. As a result, the long-range transport behavior of the particles with which they are connected controls their LRAT (Wania and Dugani 2003). LRAT potential of lower-brominated and chlorinated compounds may be relatively high because they tend to be in the gas phase. Especially, the presence of highly brominated and chlorinated compounds in the close group reveals that there was emission from the war zone but limited transport behavior of these compounds from close sampling sites to middle and far groups. In contrast to close region, especially low chlorinated and low brominated substances have a higher concentration in far groups transported from the north, northeast, and Europe as seen in cluster and trajectories in section 4.3. As can be seen from Tables 4.4, 4.5, and 4.6, compounds with lower vapor pressure (highly

brominated or highly chlorinated) differ between groups because they tend to be bound to the organic material. However, lower-volatility OCP compounds were higher in the close region.

4.3. Back-Trajectory

In Izmir, active sampling was conducted concurrently with the passive sampling time. Sampling period divided in two like groups winter and transition. Additionally, sample collection was continued until November but none of the samples matched air flow coming over the southern border during seven-month period. Back trajectory analysis using HYSPLIT-4 for various heights (300m, 450m, 600m, 750m). Four (every six hours) back trajectories corresponding to each sample were calculated for all sampling days, and when these trajectories were examined, it was seen that they could be grouped from Africa, Europe and Russia / Former USSR countries.

In the winter season group, the highest Σ_{14}PBDE (500.17 pg/m^3) and Σ_{25}OCP (273.60 pg/m^3) concentrations were measured in the air flow coming through Libya in the sample collected on February 5. During transition sampling, the highest Σ_{14}PBDE (583.54 pg/m^3) and Σ_{45}PCB (608.48 pg/m^3) concentrations were measured on 21 April which air flows from Europe and the highest Σ_{25}OCP (319.67 pg/m^3) concentration was measured when air flows came to Russia/USSR. The sampling period, which is named other, samples were mostly taken in summer all air flows came over Russia. The highest Σ_{14}PBDE Σ_{45}PCB and Σ_{25}OCP concentrations were measured as 104.85 pg/m^3, 2575.67 pg/m^3, 195.67 pg/m^3.

The mean concentrations were measured on days European masses Σ_{14}PBDE =229.12 pg/m^3, Σ_{45}PCB pg/m^3 =786.92, Σ_{25}OCP pg/m^3 =138.08 pg/m^3, on days air flows comes Russia/USSR. The mean concentrations were Σ_{14}PBDE =133.89 pg/m^3, Σ_{45}PCB=1690.84 pg/m^3, Σ_{25}OCP =147.10 pg/m^3 and on days airflows come from Africa means concentrations were Σ_{14}PBDE=257.79 pg/m^3, Σ_{45}PCB=202.53 pg/m^3, Σ_{25}OCP=135.12 pg/m^3.

It is observed that the total OCP and PCB concentrations were significantly higher on the days when the air masses originating from Russia / former USSR countries reached our sampling point compared to the days originating from Africa and Europe. This

situation is especially prominent when PCB averages are compared. The fact that high concentrations were measured in the days originating from Africa, similar to the days originating in Europe, may be due to the fact that some of these air masses also spent time over Europe and/or Greece. It is in line with the results of our previous project, numbered 112Y315, where POPs pollution was transported to our country on days originating from Russia.

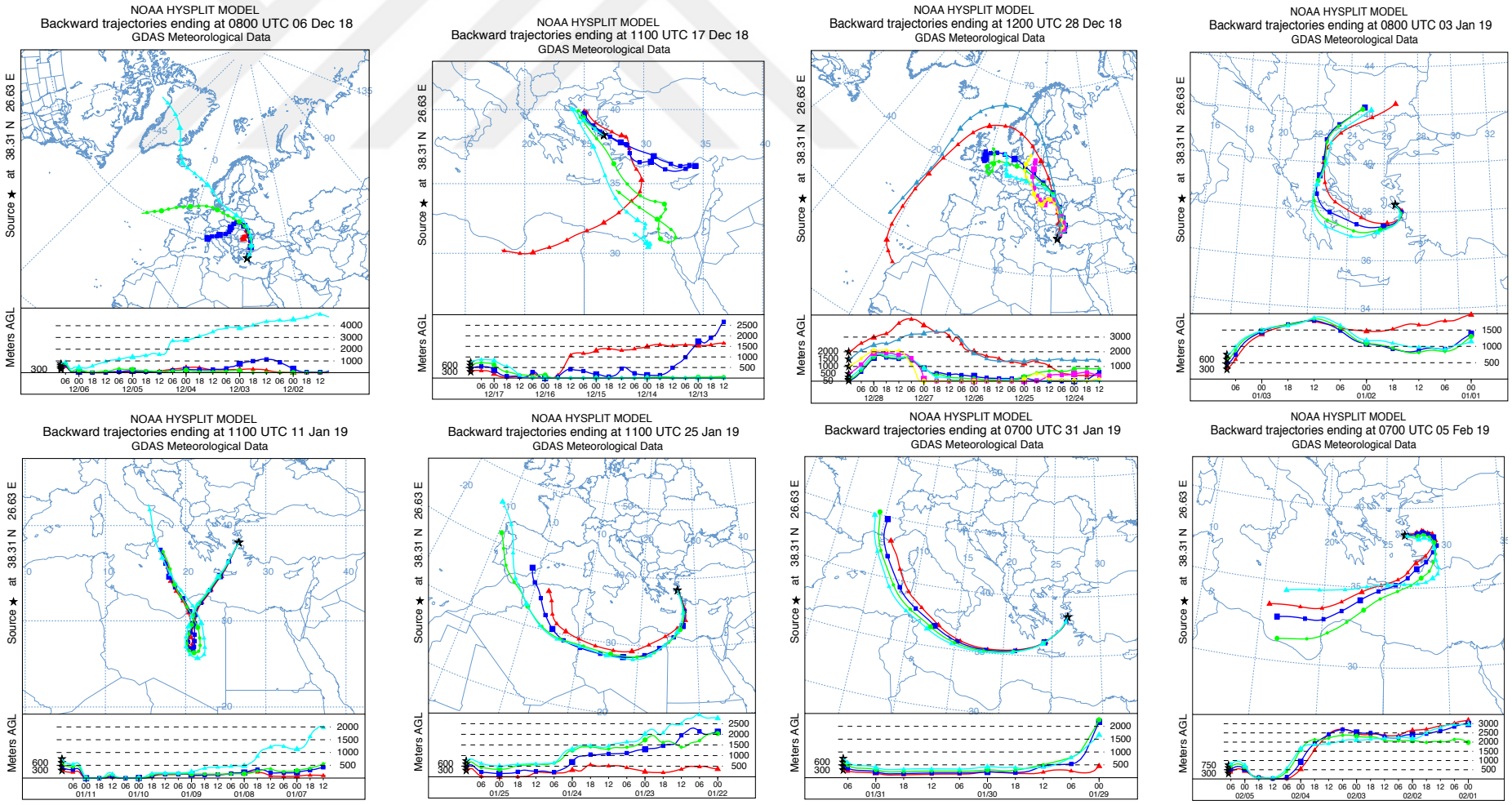

Figure 4.7. Back trajectory analysis of winter period

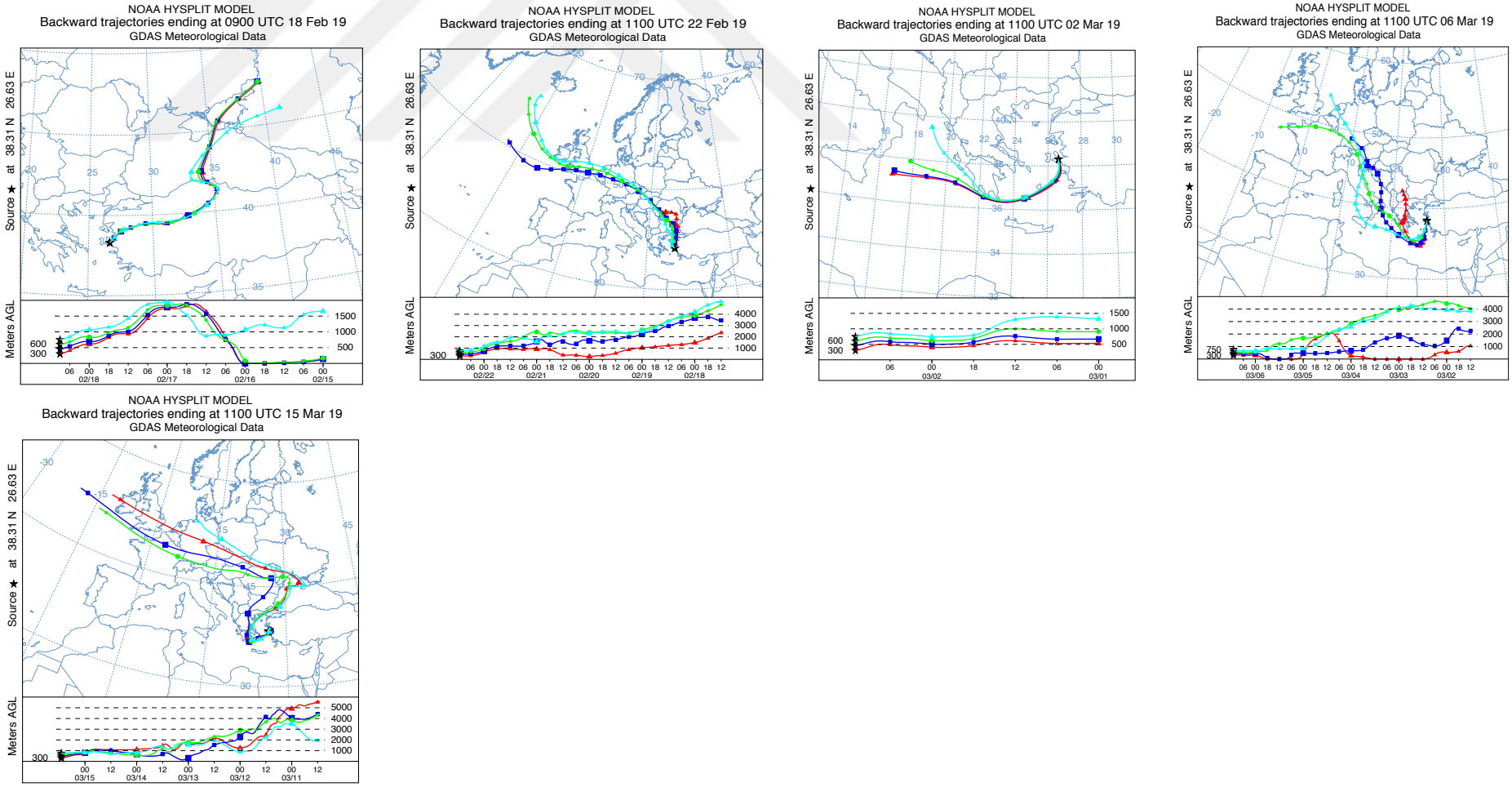

Figure 4.7. (Cont.)

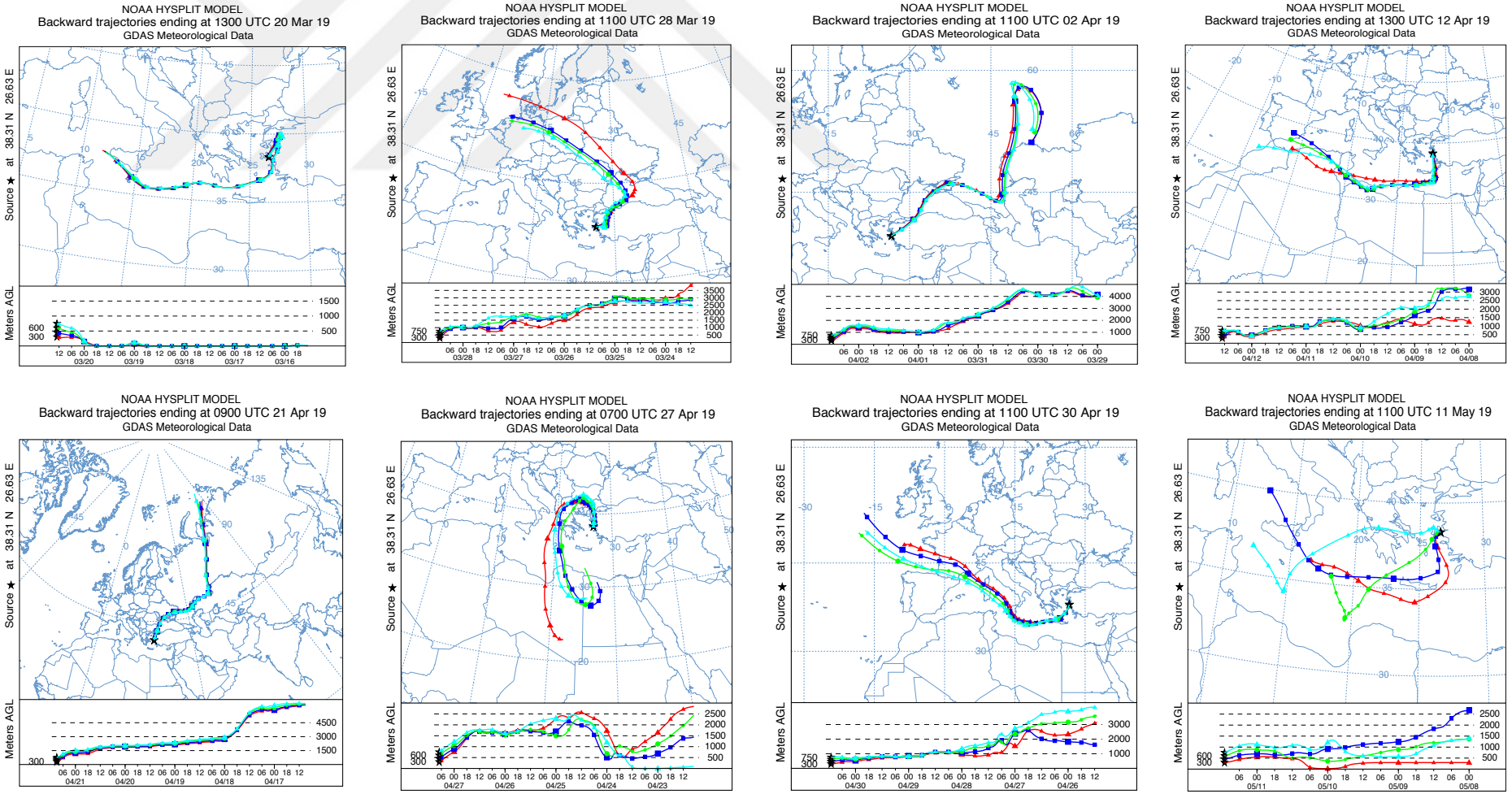

Figure 4.8. Back trajectory analysis of transition period

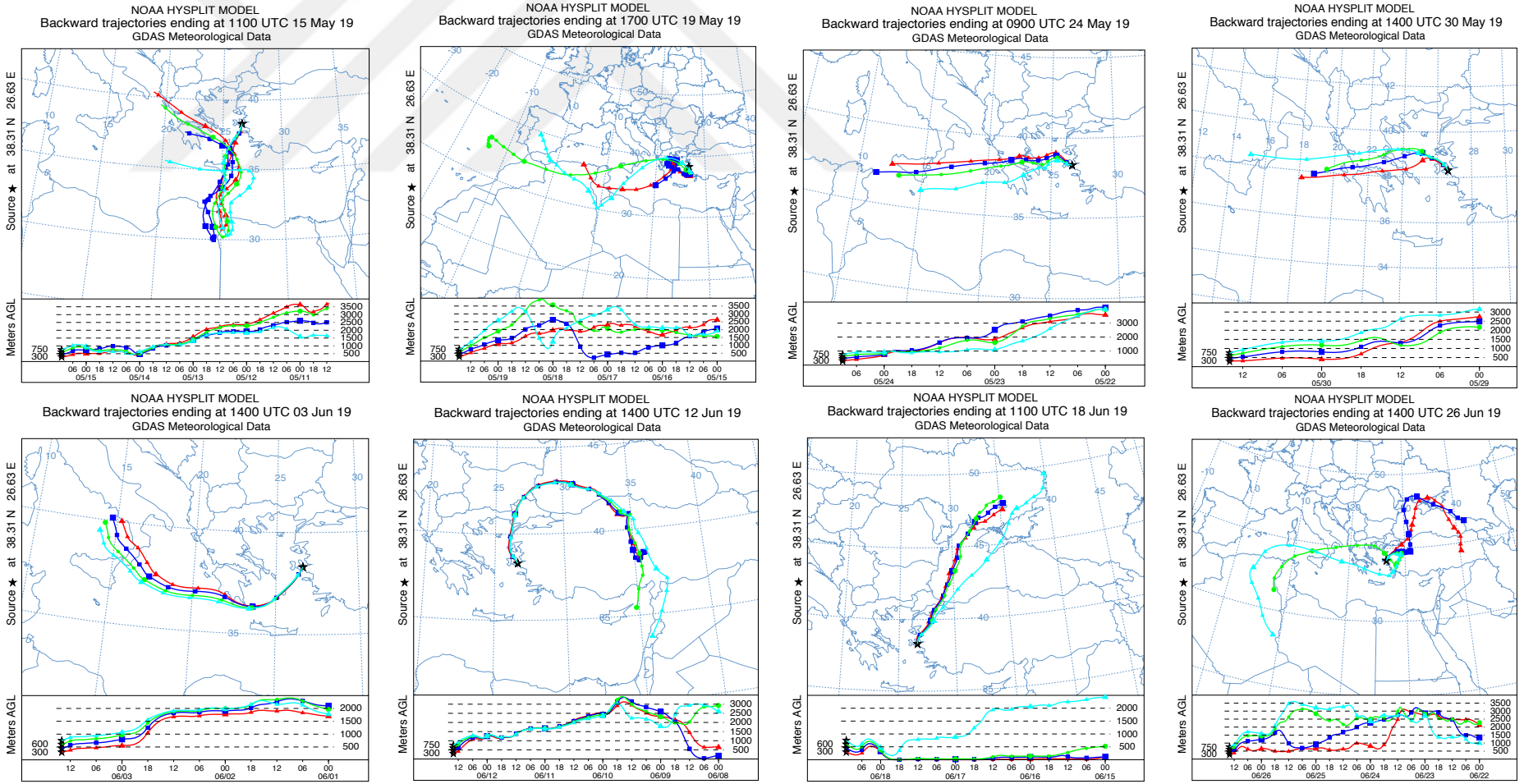

Figure 4.8. (Cont.)

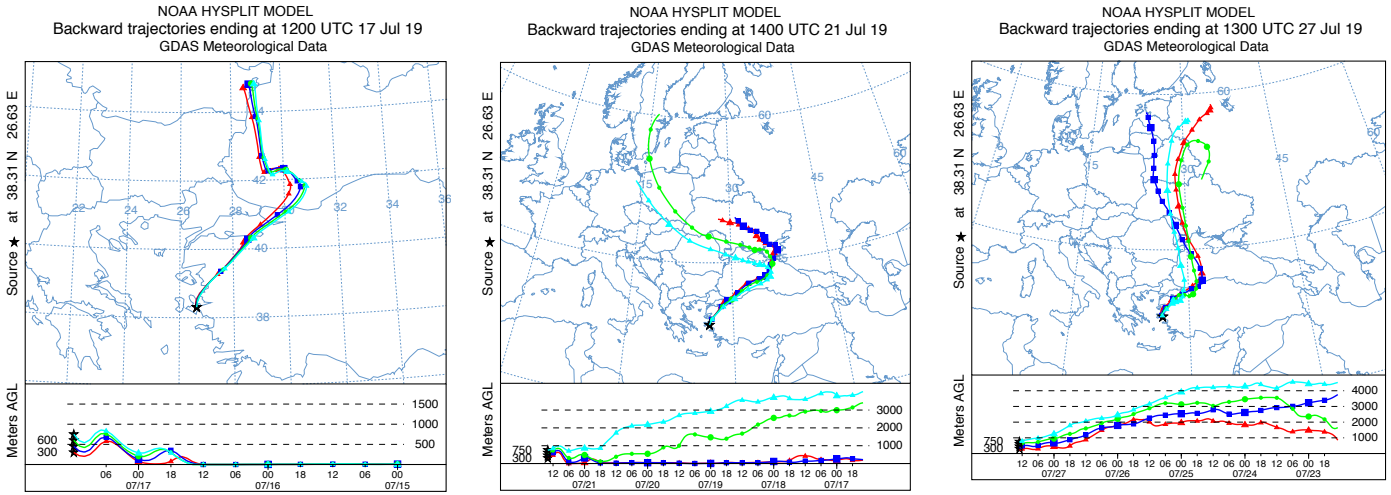

Figure 4.8. (Cont.)

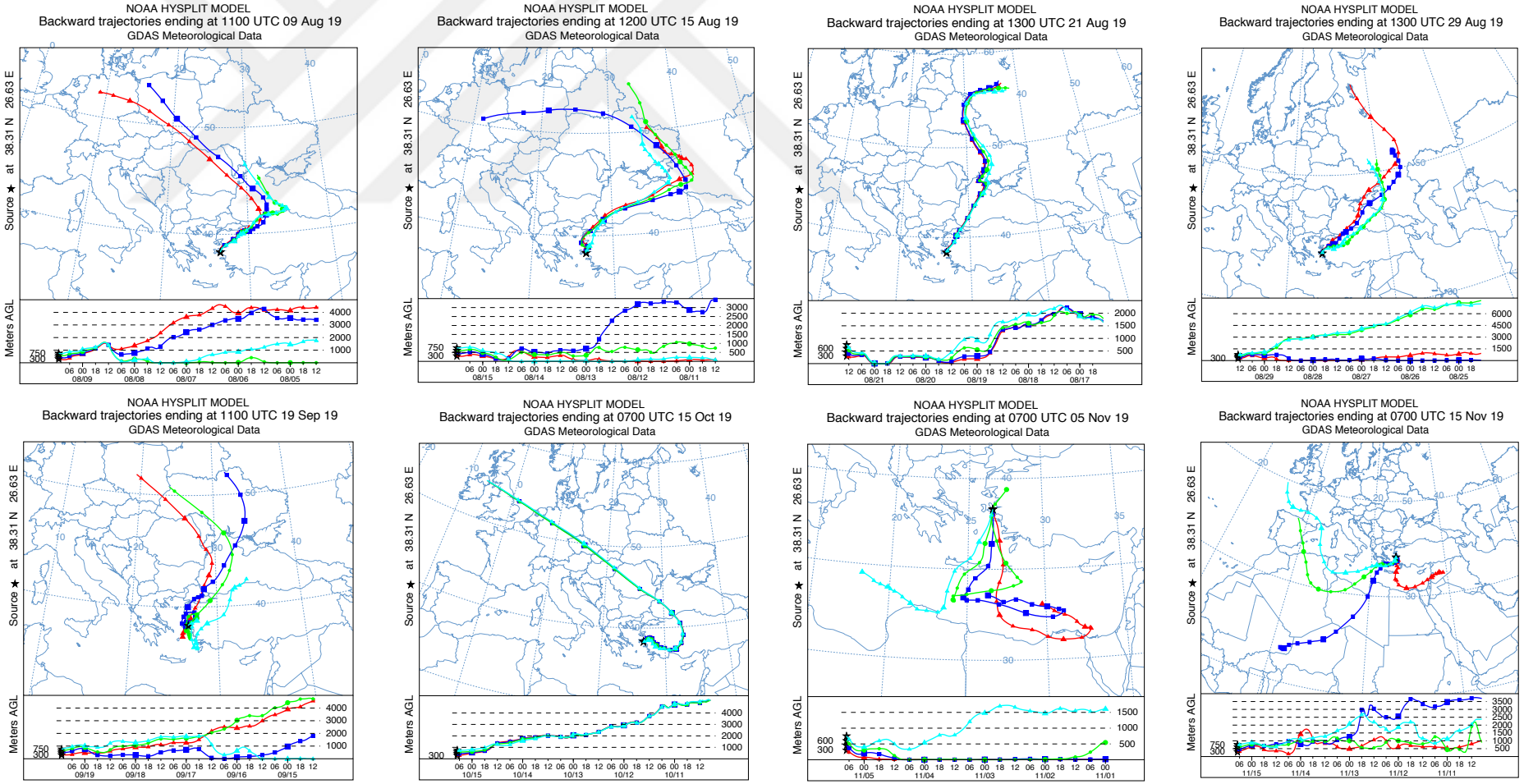

Figure 4.9. Other back trajectories

Table 4 6. G+P (pg/m^3) concentration of the winter samples.

Sampling Date	Σ_{14}PBDE	Σ_{45}PCB	Σ_{25}OCP	Air Mass Origin
6/12/2018	157.53	55.97	96.72	Europe
17/12/2018	324.64	109.56	105.91	Africa
28/12/2018	339.54	493.08	229.63	Europe
3/01/2019	278.72	163.07	108.33	Europe
11/01/2019	227.29	58.78	113.38	Africa
17/01/2019	195.56	177.68	158.17	Europe
25/01/2019	355.92	116.99	111.12	Africa
31/01/2019	346.40	50.06	114.22	Europe
05/02/2019	500.17	195.12	273.60	Africa
18/02/2019	300.92	608.48	203.99	Russia/USSR
22/02/2019	162.10	175.98	149.34	Europe
2/03/2019	399.09	491.23	221.67	Europe
6/03/2019	409.05	104.22	126.22	Europe
15/03/2019	430.11	186.24	184.27	Europe
Mean	316.22	213.36	156.84	

Table 4.7. G+P (pg/m^3) concentration of transition samples

Sampling Date	Σ_{14}PBDE	Σ_{45}PCB	Σ_{25}OCP	Air Mass Origin
20/03/2019	443.44	183.54	111.40	Europe
28/03/2019	355.23	690.23	187.57	Europe
2/04/2019	402.32	686.38	210.97	Russia/USSR
12/04/2019	437.52	99.14	90.46	Europe
21/04/2019	583.54	1207.25	319.67	Russia/USSR
27/04/2019	362.90	406.66	191.33	Africa
30/04/2019	309.18	1719.40	79.76	Europe
11/05/2019	4.97	48.80	52.28	Europe
15/05/2019	7.40	102.19	97.64	Africa
19/05/2019	164.02	52.28	89.95	Europe
24/05/2019	5.41	394.26	76.90	Europe
30/05/2019	154.51	4564.56	215.26	Europe
3/06/2019	209.89	2293.99	70.53	Europe
12/06/2019	5.41	2017.35	86.06	
18/06/2019	7.01	1962.13	41.70	Russia/USSR
26/06/2019	103.20	2501.86	352.16	Europe
17/07/2019	119.23	2019.40	169.39	Europe
21/07/2019	8.49	2350.56	69.13	Russia/USSR
27/07/2019	12.23	1972.66	79.07	Russia/USSR
Mean	194.52	1330.14	136.34	

Table 4.8. G+P (pg/m^3) concentration of other samples

Sampling Date	Σ_{14}PBDE	Σ_{45}PCB	Σ_{25}OCP	Air Mass Origin
9/08/2019	27.44	2575.67	109.43	Russia/USSR
15/08/2019	9.68	2591.92	146.20	Russia/USSR
21/08/2019	104.85	1917.12	195.67	Russia/USSR
29/08/2019	9.68	2257.53	101.22	Russia/USSR
19/09/2019	6.59	469.49	141.03	Russia/USSR
15/10/2019	6.42	494.67	82.58	Europe
5/11/2019	26.20	428.39	52.87	Africa/ Europe
15/11/2019	9.42	352.60	70.92	Europe
Mean	25.07	1385.92	112.49	

4.3.1. Back Trajectory Frequency Analysis of the Passive Sampling Period

Since the back-trajectory analysis performed for active sampling did not have a sampling day for which arriving air masses passed through the war zone, back-trajectory analysis for the entire passive sampling period was performed, and the possibility that the air masses passing through the war zone reflecting in the passive samples was explored. From Figure 4.10 to Figure 4.19, passive sampling back-trajectories are given for the three proximity groups. They are given in order of from Close to Far. According to the results of the back-trajectory frequency analysis performed for passive sampling, it can be seen that there was transport from the war zone to the Provinces of Gaziantep, Osmaniye, and Karaman, included in the Close group, in March, April, and May, which are the transition months. The back-trajectory analysis of these sampling sites are shown in Figures 4.11, 4.12, and 4.13, respectively. However, there was no transport from the war zone to Isparta and Mugla, which are in the Middle-distance group while it varied only between 10 % and 20 % for the Far group.

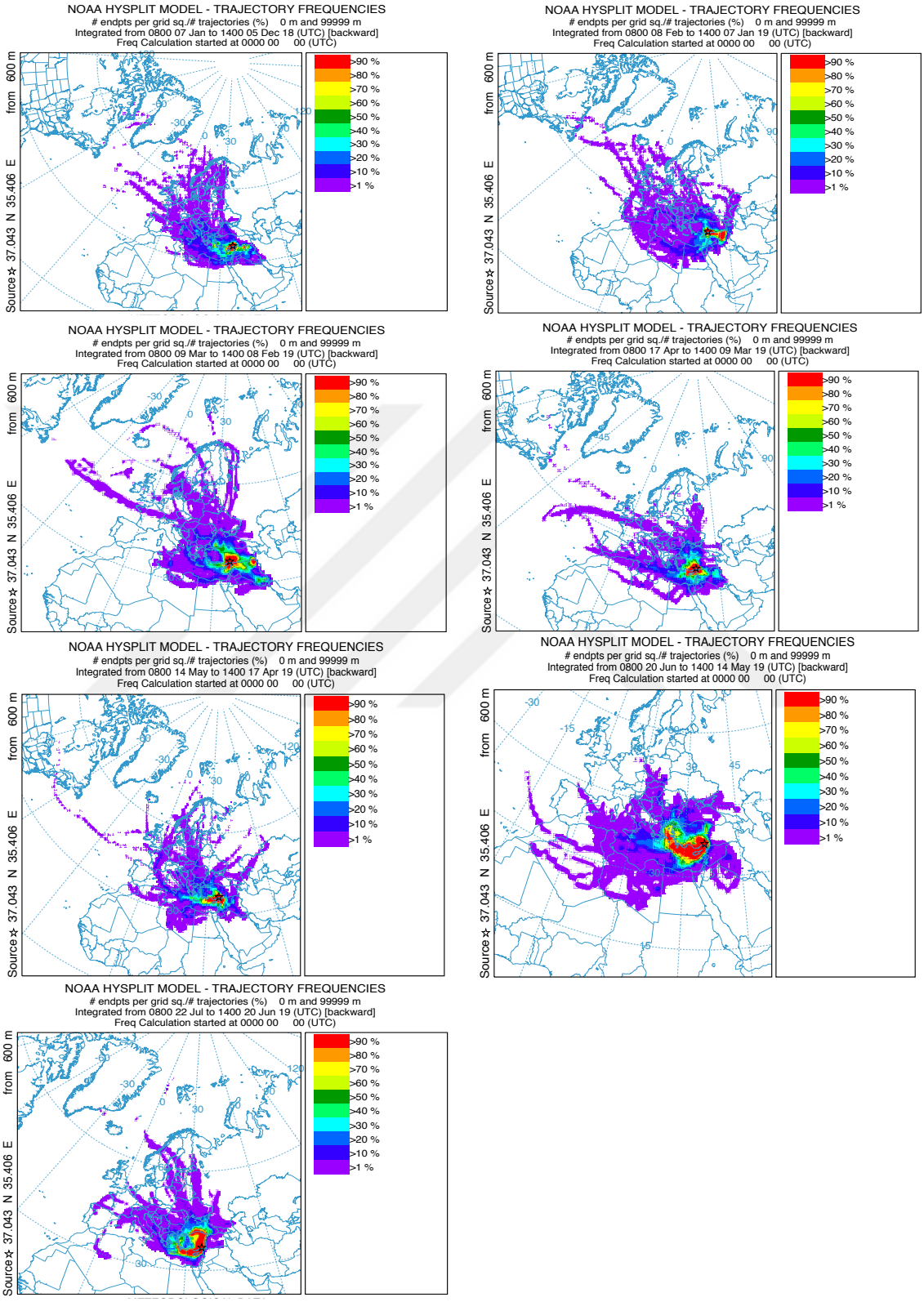

Figure 4.10. Passive sampling period monthly back trajectory frequency analysis-Adana

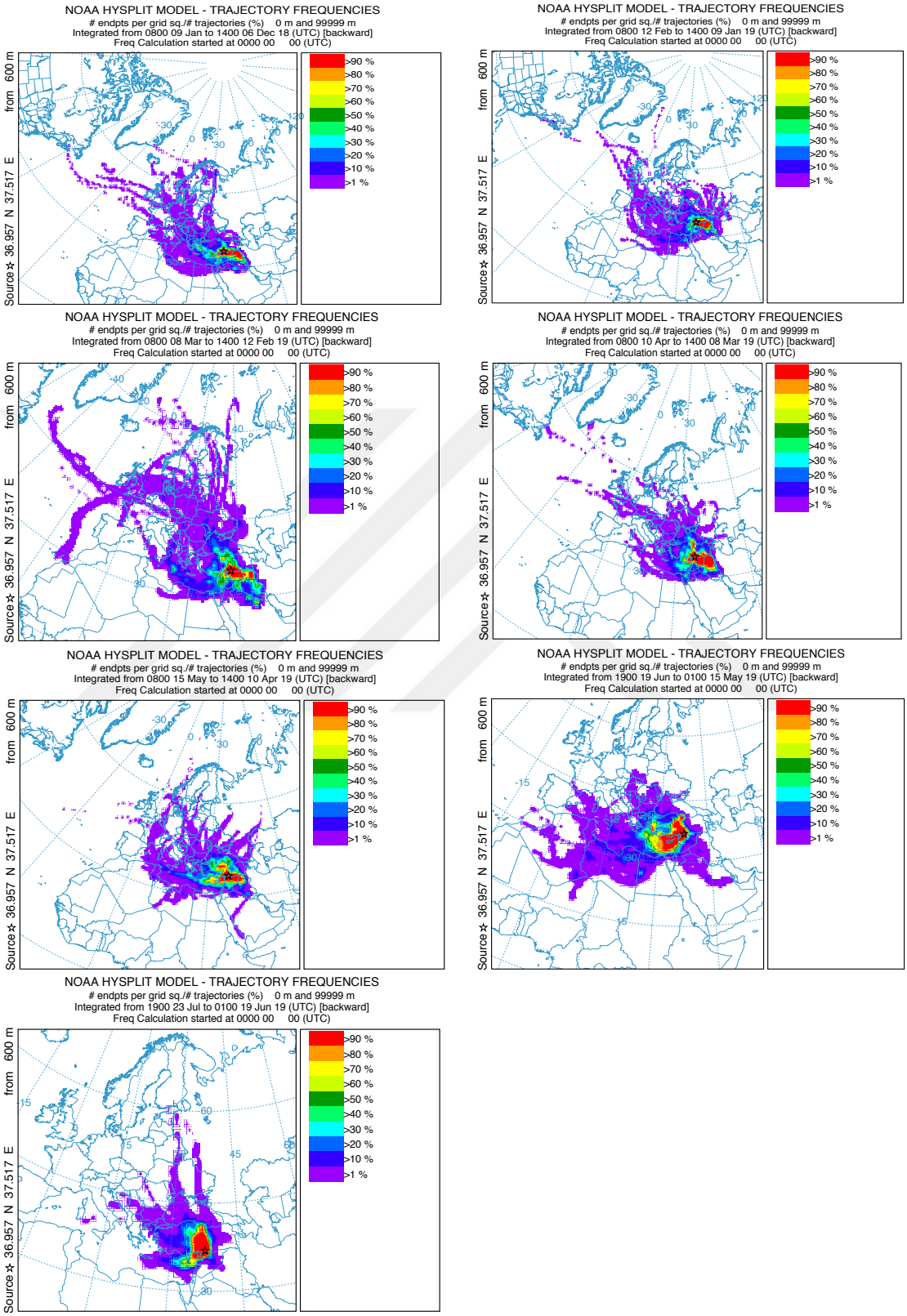

Figure 4.11. Passive sampling period monthly back trajectory frequency analysis-Gaziantep

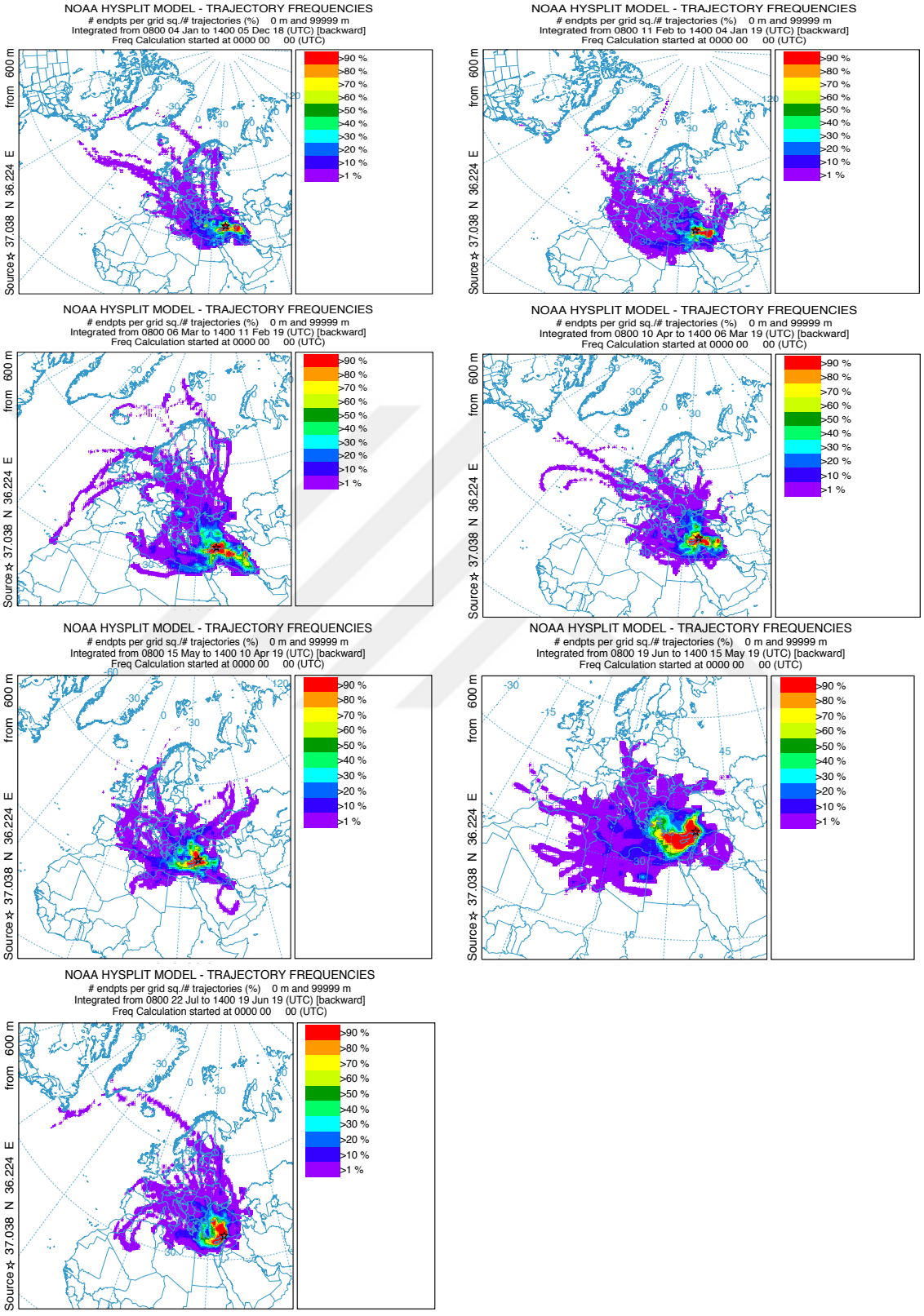

Figure 4.12. Passive sampling period monthly back trajectory frequency analysis-Osmaniye

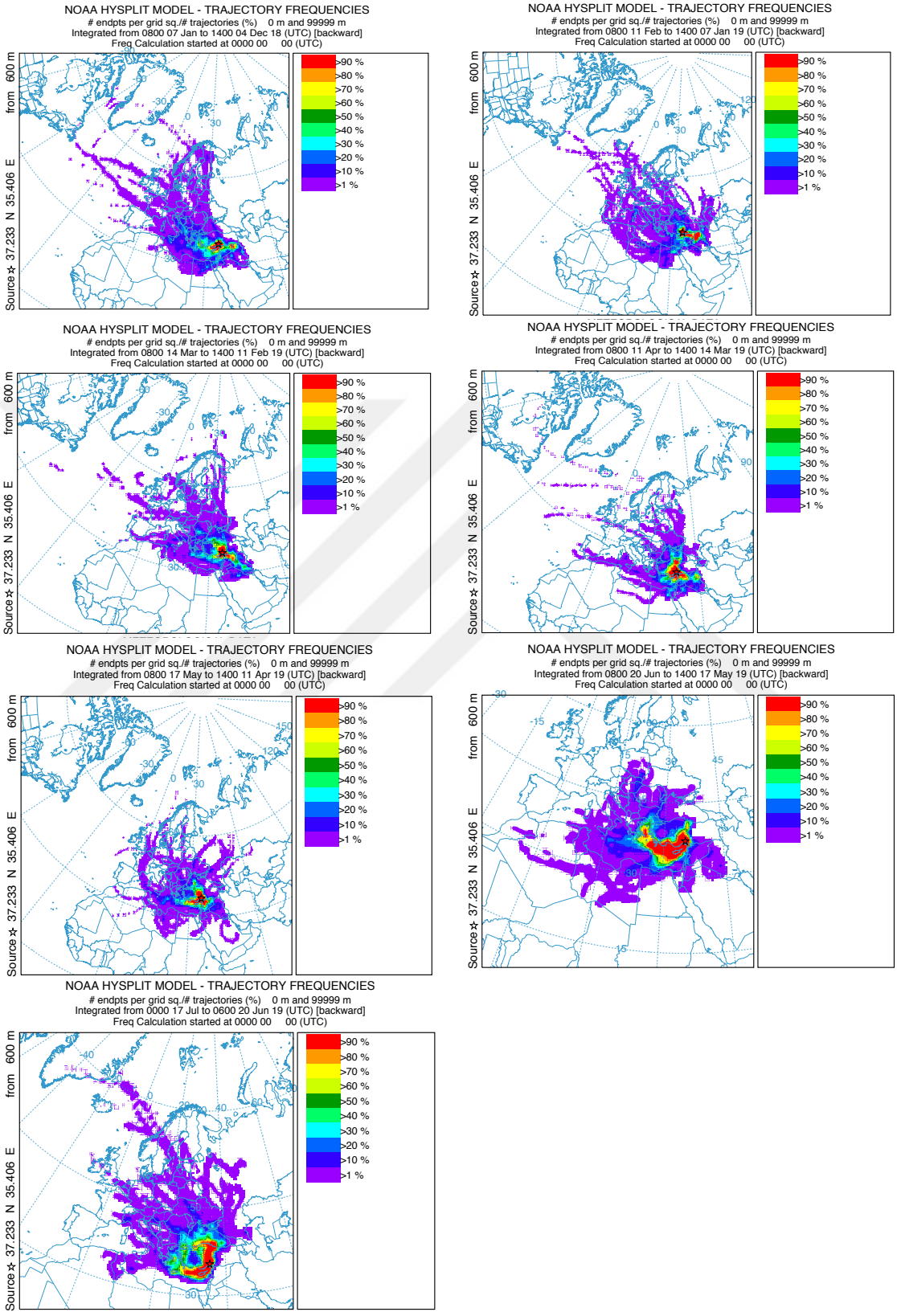

Figure 4.13. Passive sampling period monthly back trajectory frequency analysis-Karaman

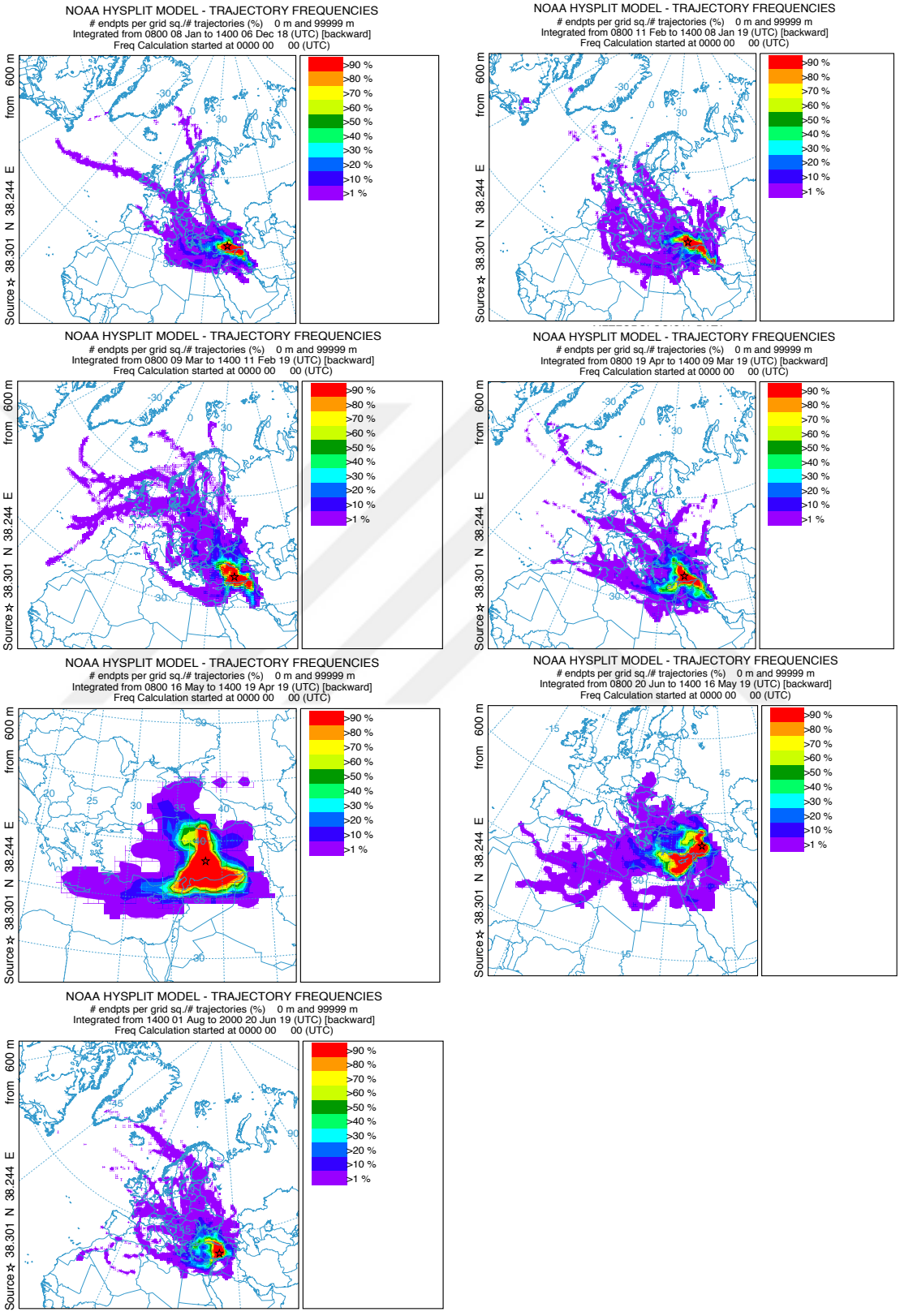

Figure 4.14. Passive sampling period monthly back trajectory frequency analysis-Malatya

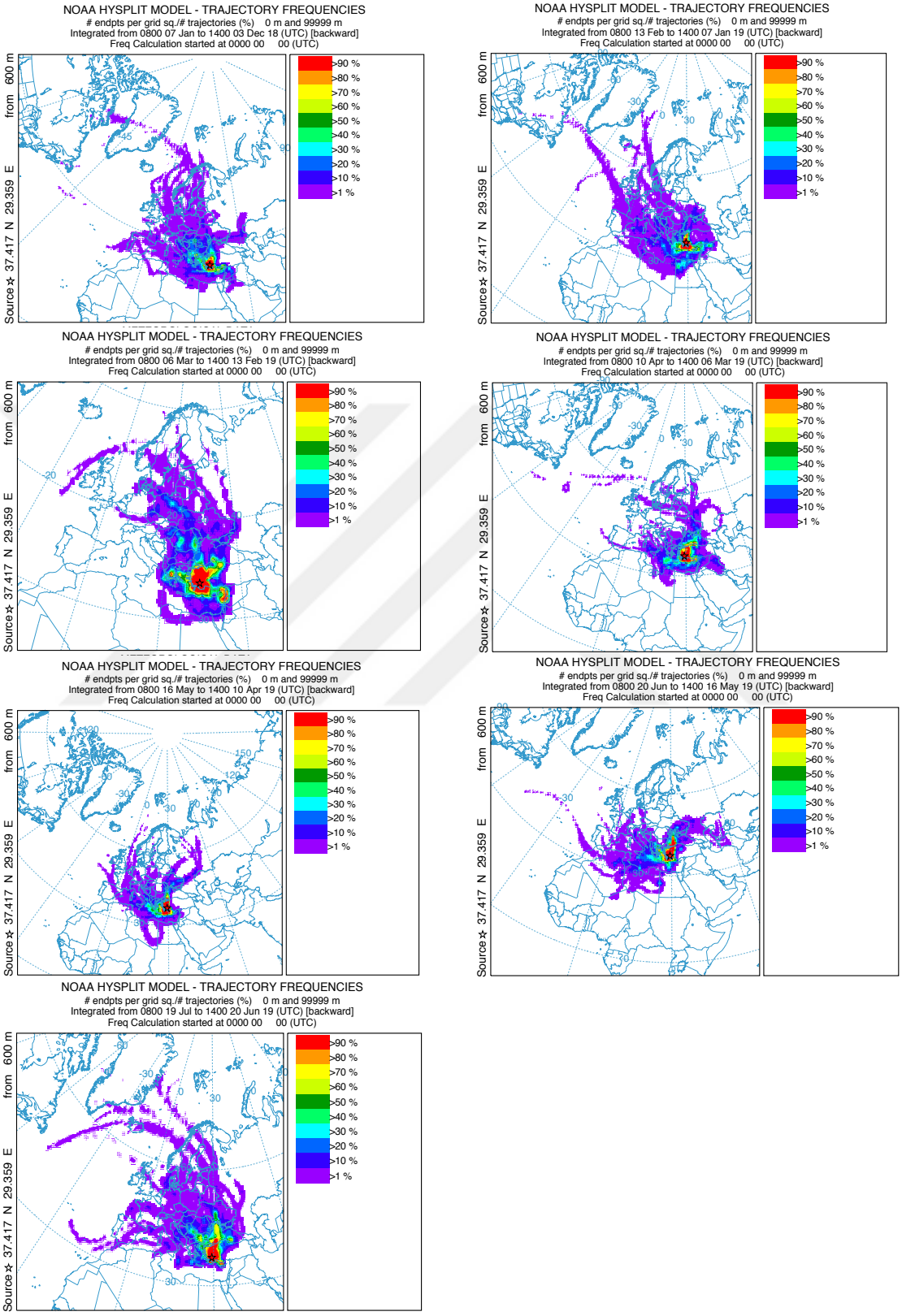

Figure 4.15. Passive sampling period monthly back trajectory frequency analysis-Denizli

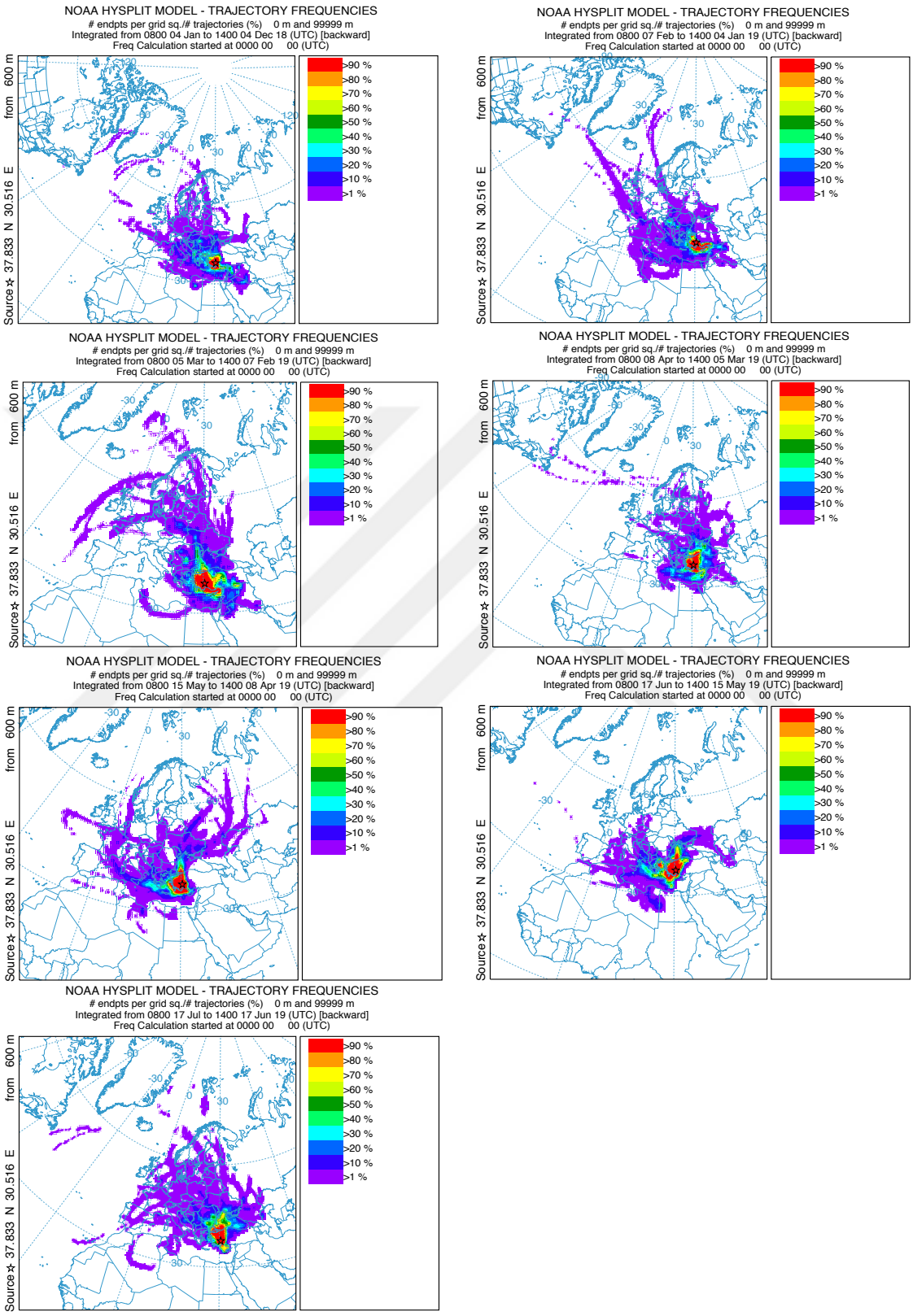

Figure 4.16. Passive sampling period monthly back trajectory frequency analysis-Isparta

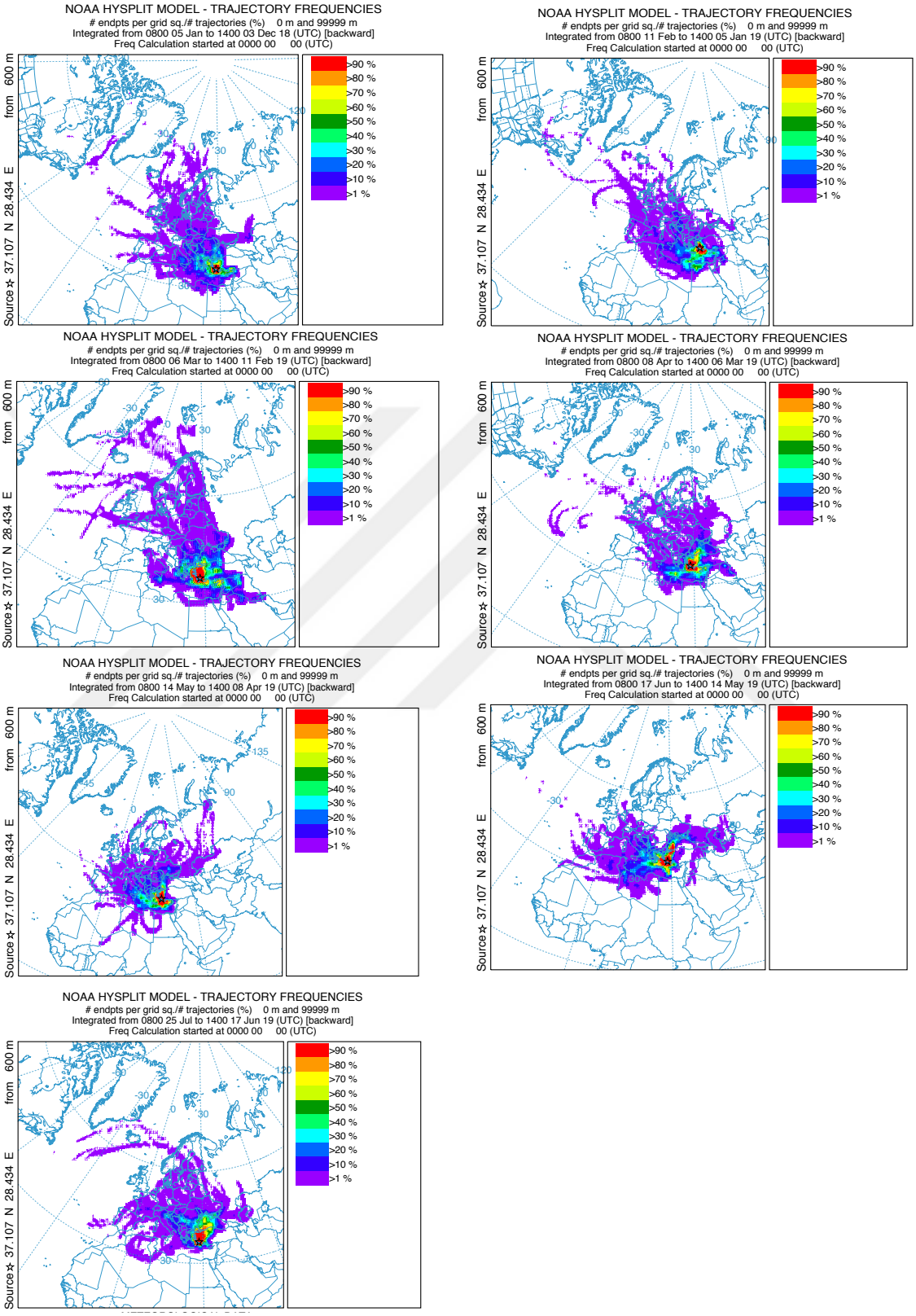

Figure 4.17. Passive sampling period monthly back trajectory frequency analysis-Mugla

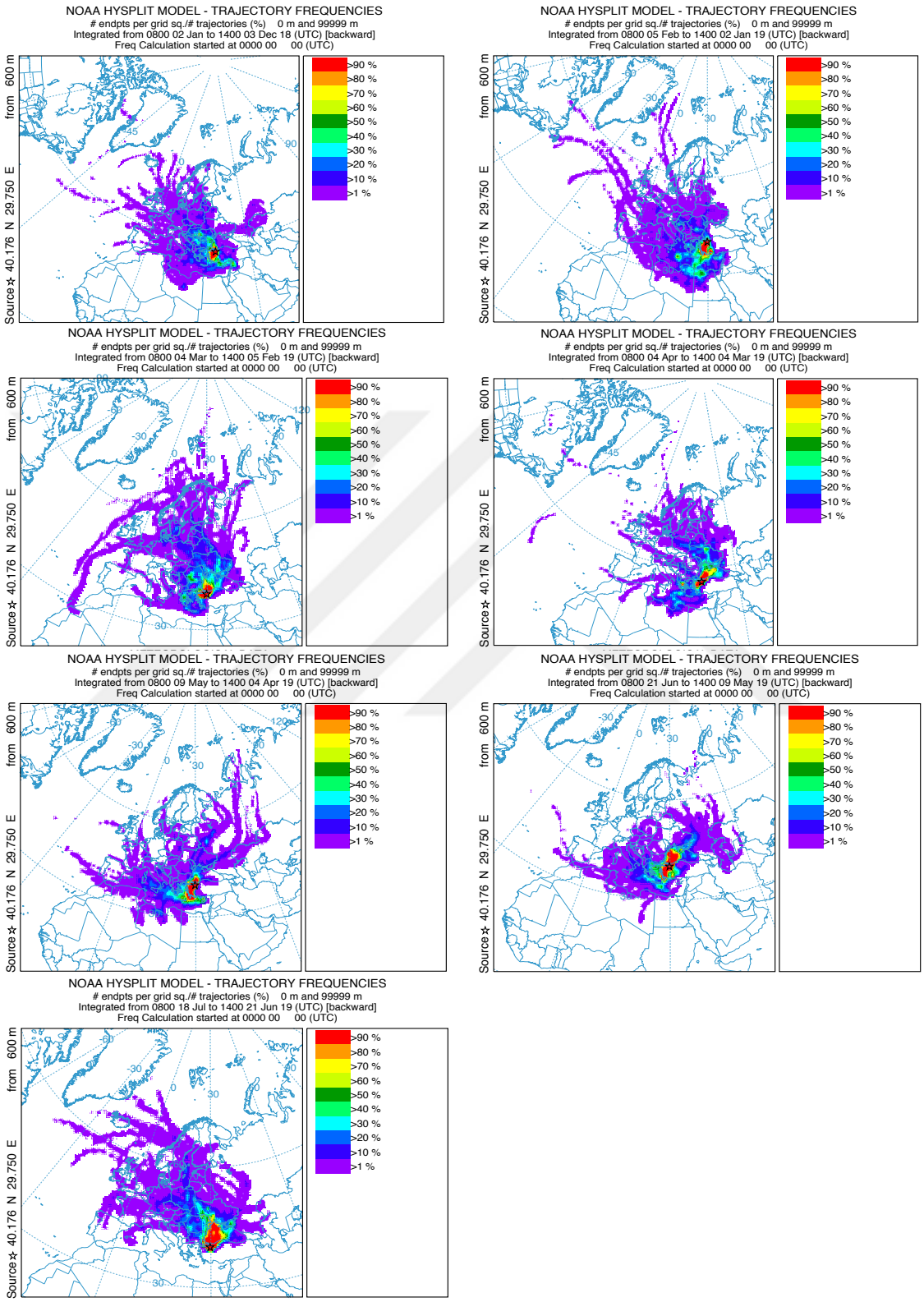

Figure 4.18. Passive sampling period monthly back trajectory frequency analysis-Bursa

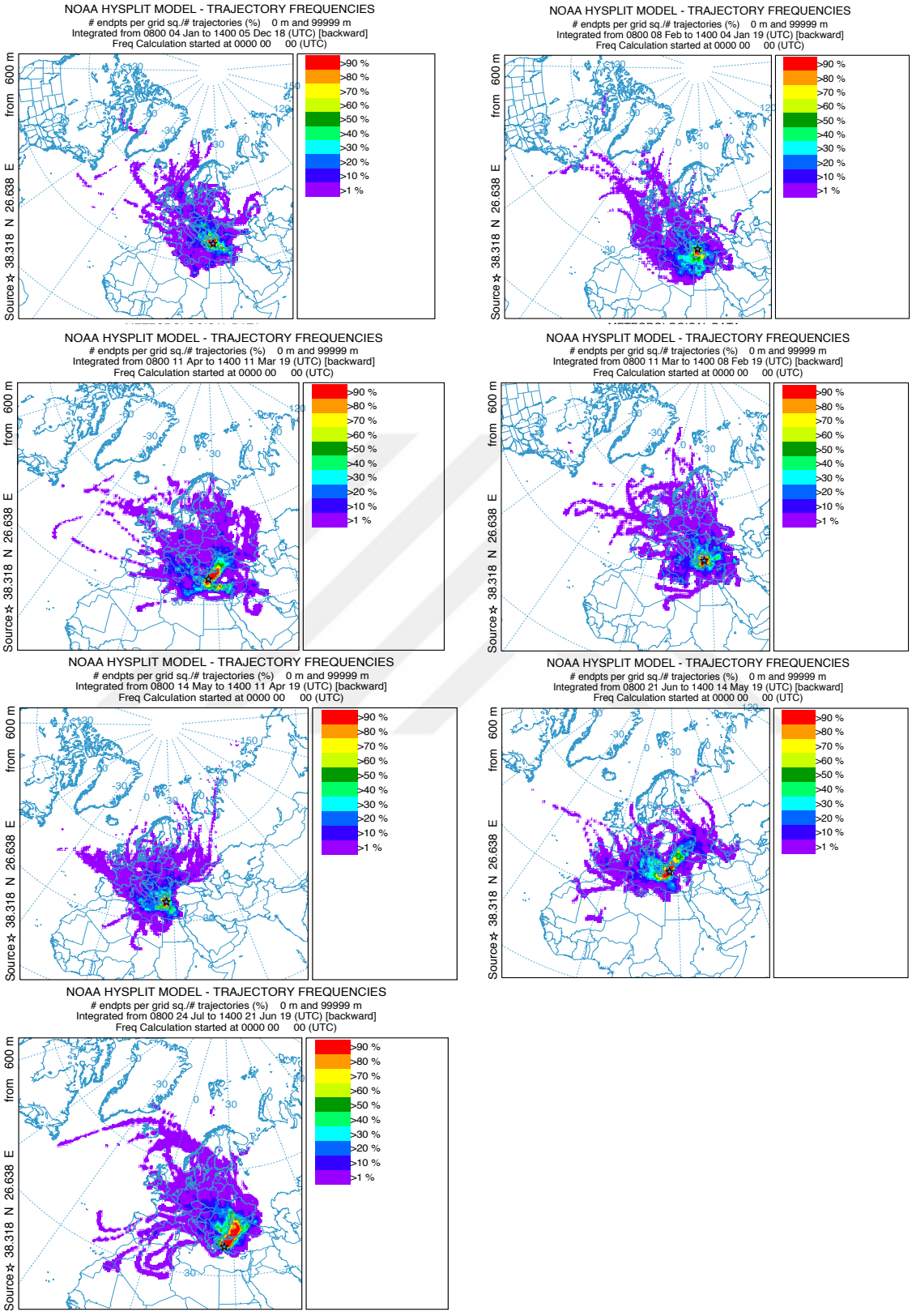

Figure 4.19. Passive sampling period monthly back trajectory frequency analysis-Izmir

4.3.2. Cluster Analysis

Back-trajectory analysis was run 4 times a day, (i.e., at 00, 06, 12, and 18 UTC) for each month and each location. For each day, four 6-hourly trajectories with ending time of 00:00, 06:00, 12:00, and 18:00 were calculated for 600 m. Trajectories were clustered per 48 hours. The number of clusters required was computed by calculating the percent change in total spatial variance (TSV) to the sum of the SPVAR (Spatial Variance). The sum of the squared distances between the endpoints of the cluster's component trajectories and the mean of the trajectories in that cluster constitutes this parameter. Large changes mean the merging of significantly different trajectories into the same cluster. Accordingly, the approximate number of clusters would be found just prior to the large percent change in TSV (Draxler et al. 1999). Cluster numbers were determined based on computational results, but 2 or less clusters were not preferred. At least 3 clusters were preferred for better evaluation of air flows. Cluster analysis of passive samples is given from Figure 4.20 to Figure 4.29 (Each cluster includes sampling month (from 1 to 7) at its bottom left corner.). In contrast to the transition season, the highest air flow over the southern border occurred in the winter season. The number of clusters coming over the southern border was quite low. The contribution of the air flow from this region to the provinces of Adana Gaziantep, Osmaniye, Karaman and Malatya, which were in the close region group, varies between %20-%80. The highest transport occurred in the 4th month to the province of Gaziantep with %79. For the provinces in the close distance group, there was air flow from the southern war zone. However, as we moved away from this area, the air flow decreased, while there was no air flow from this area to Izmir during the sampling period. In all of the provinces in the close region, there was air flow coming over the war zone. However, when we look at the cluster results of the sampling points, these values differed by months. For example, in the first month sampling of Adana province, the average cluster value was %19 the lowest, while the highest 1st month mean cluster value was calculated as % 55 for Osmaniye, the concentration values measured in Osmaniye were lower than Adana. The average cluster value in Denizli, Isparta, and Mugla in the middle-distance group was the highest value in Isparta in the 3rd month. However, during the sampling period, Bursa only received a current from the war zone, with a maximum of % 21 in the first month and 3rd months.

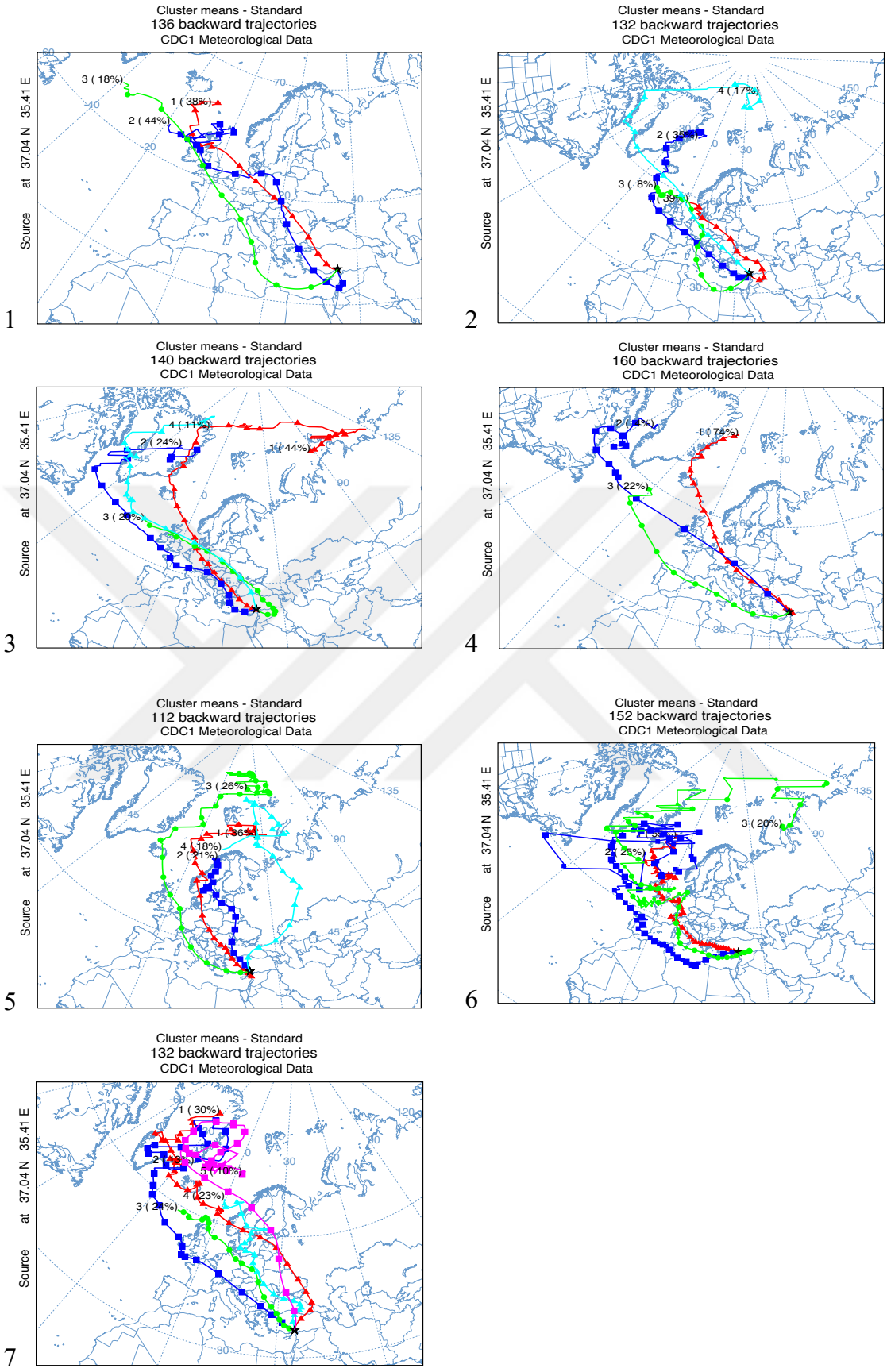

Figure 4.20. Passive sampling period monthly back trajectory cluster analysis - Adana

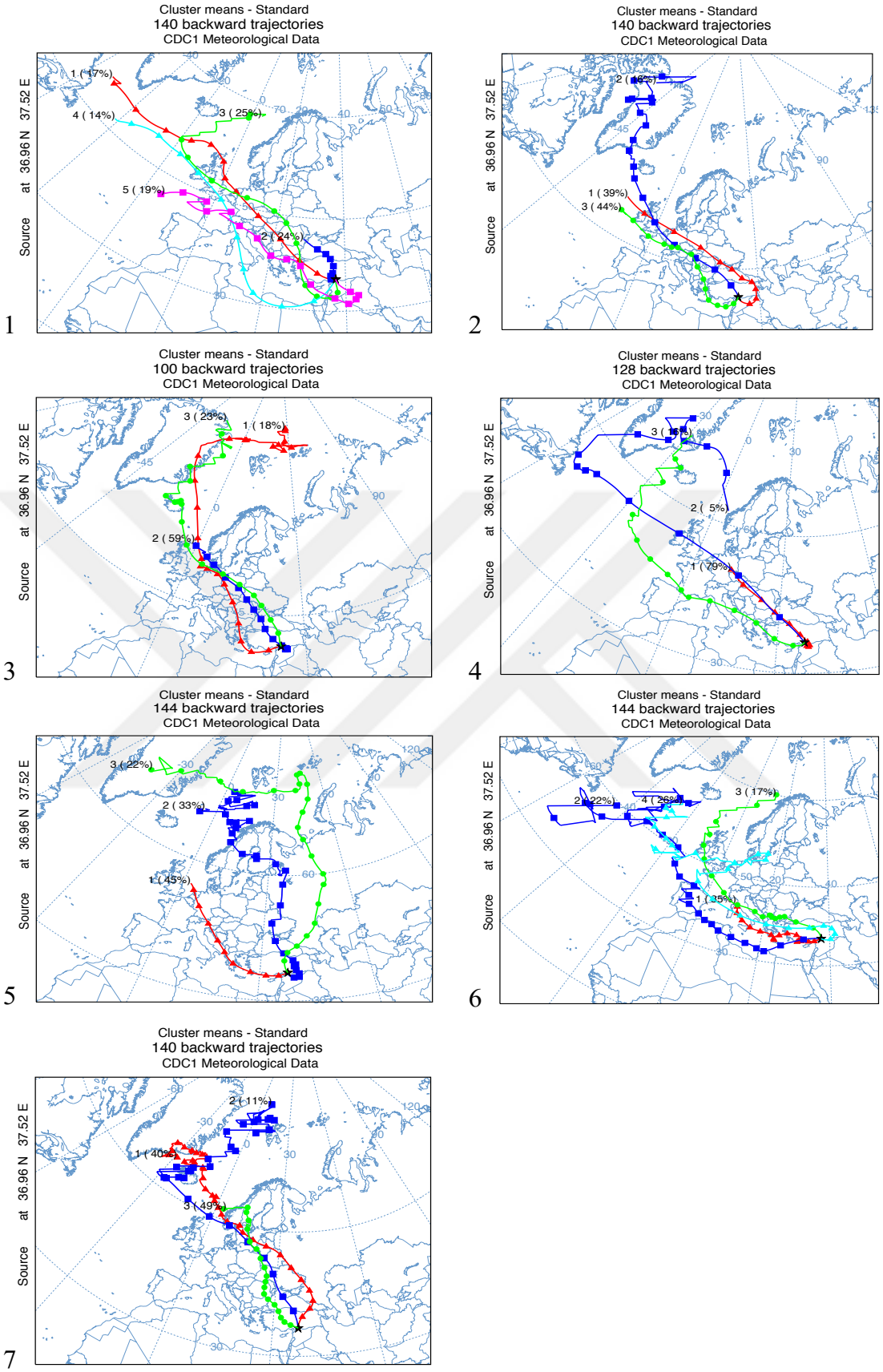

Figure 4.21. Passive sampling period monthly back trajectory cluster analysis - Gaziantep

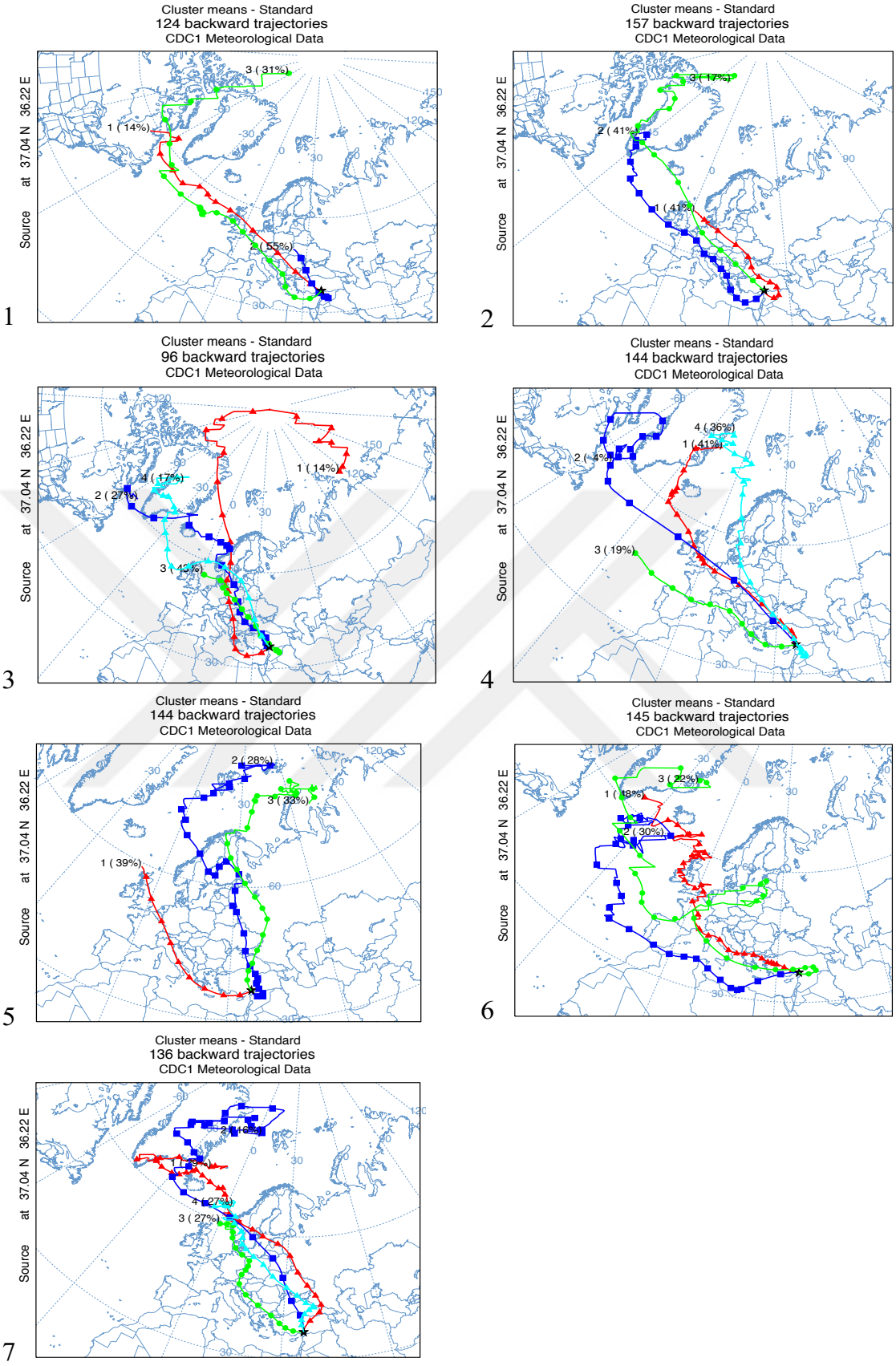

Figure 4.22. Passive sampling period monthly back trajectory cluster analysis-Osmaniye

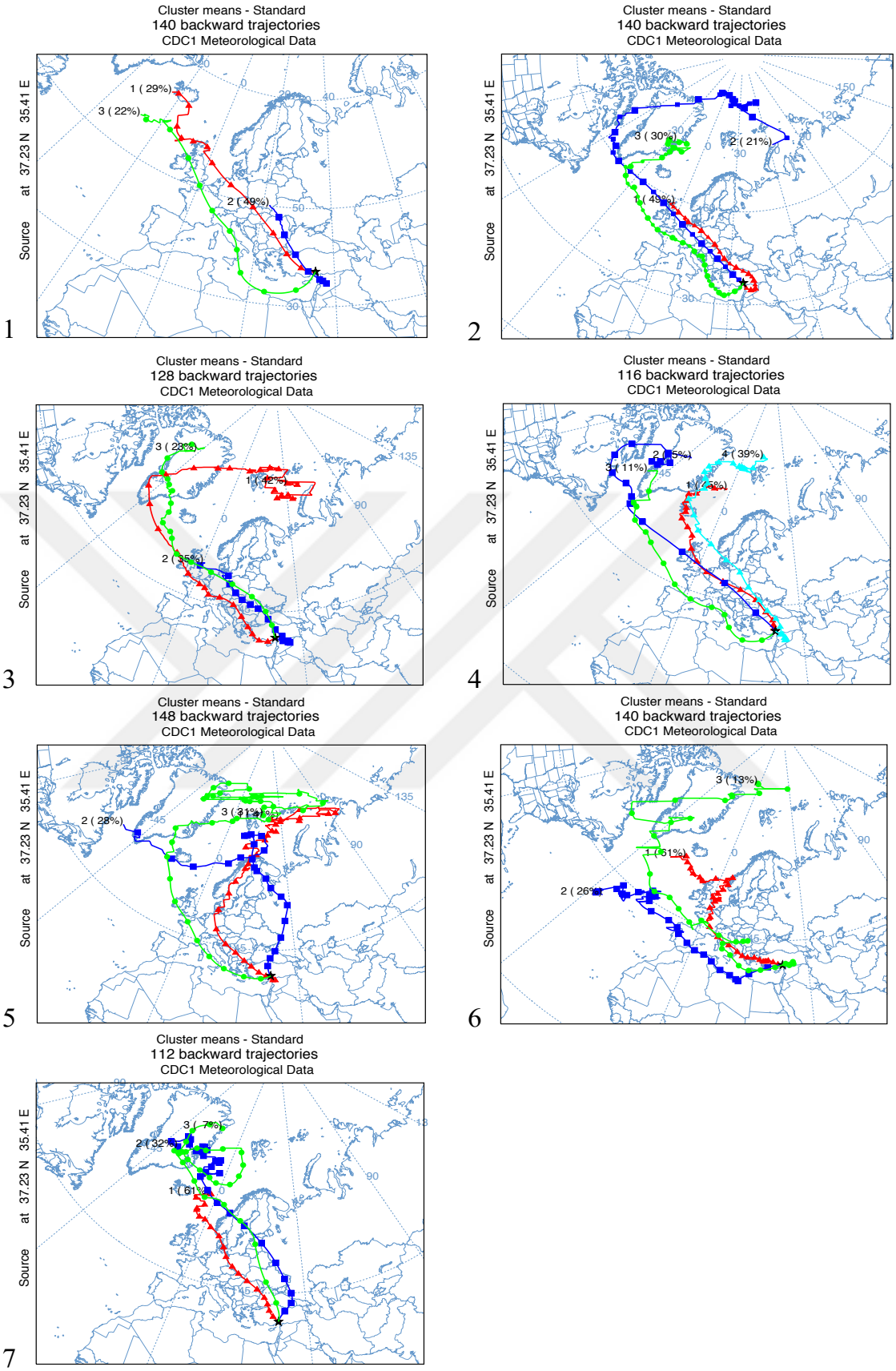

Figure 4.23. Passive sampling period monthly back trajectory cluster analysis-Karaman

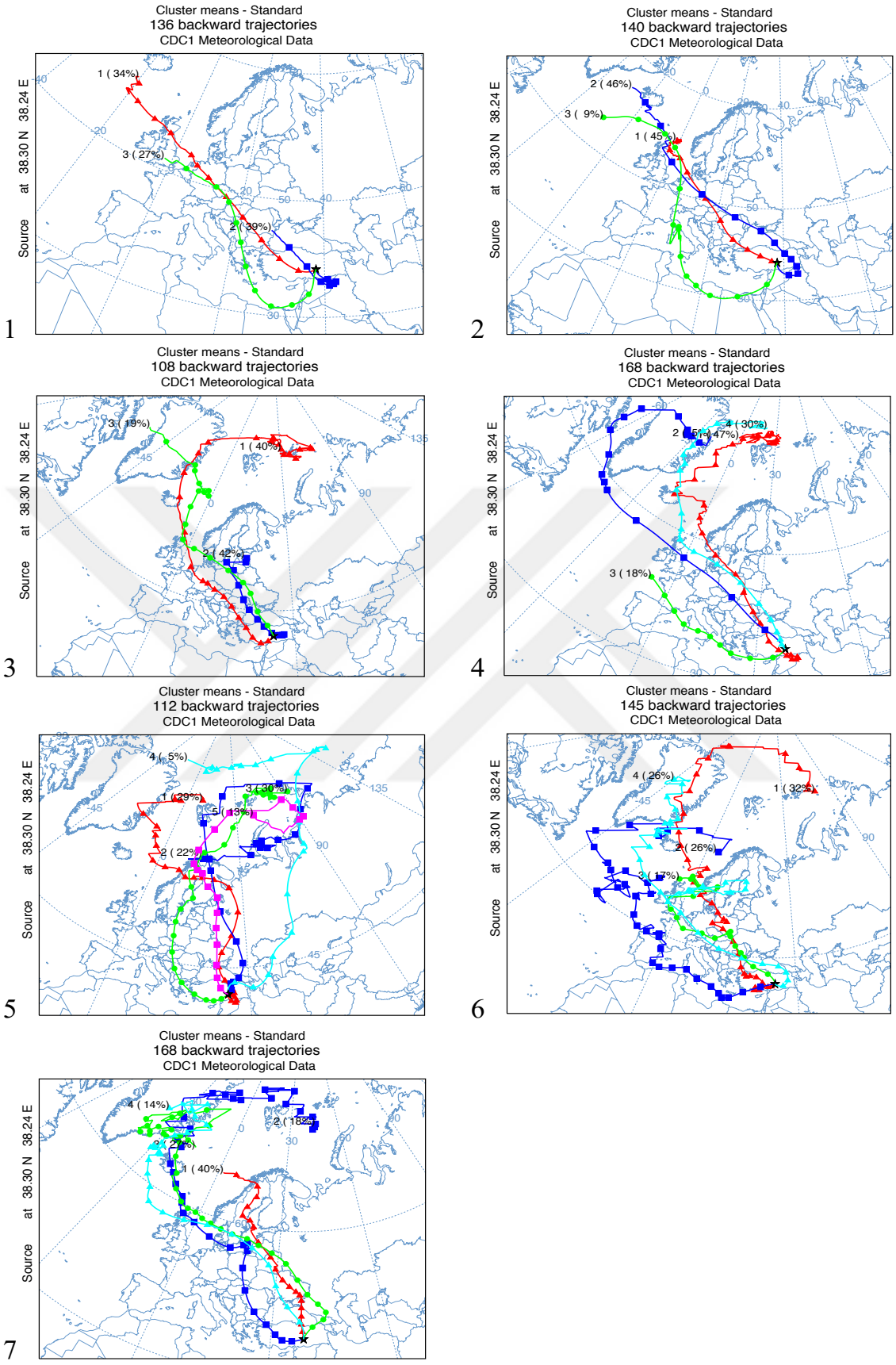

Figure 4.24. Passive sampling period monthly back trajectory cluster analysis-Malatya

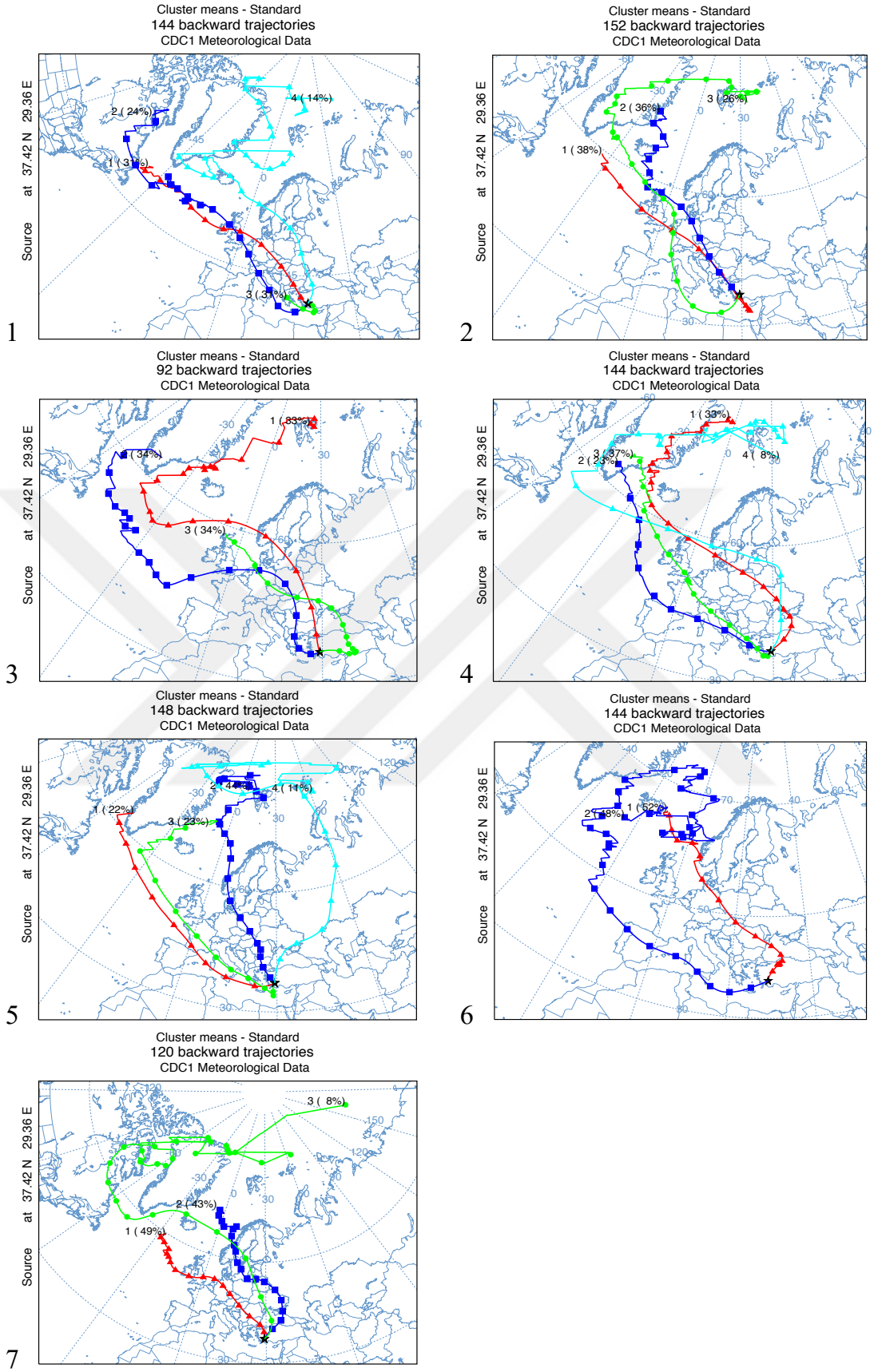

Figure 4.25. Passive sampling period monthly back trajectory cluster analysis-Denizli

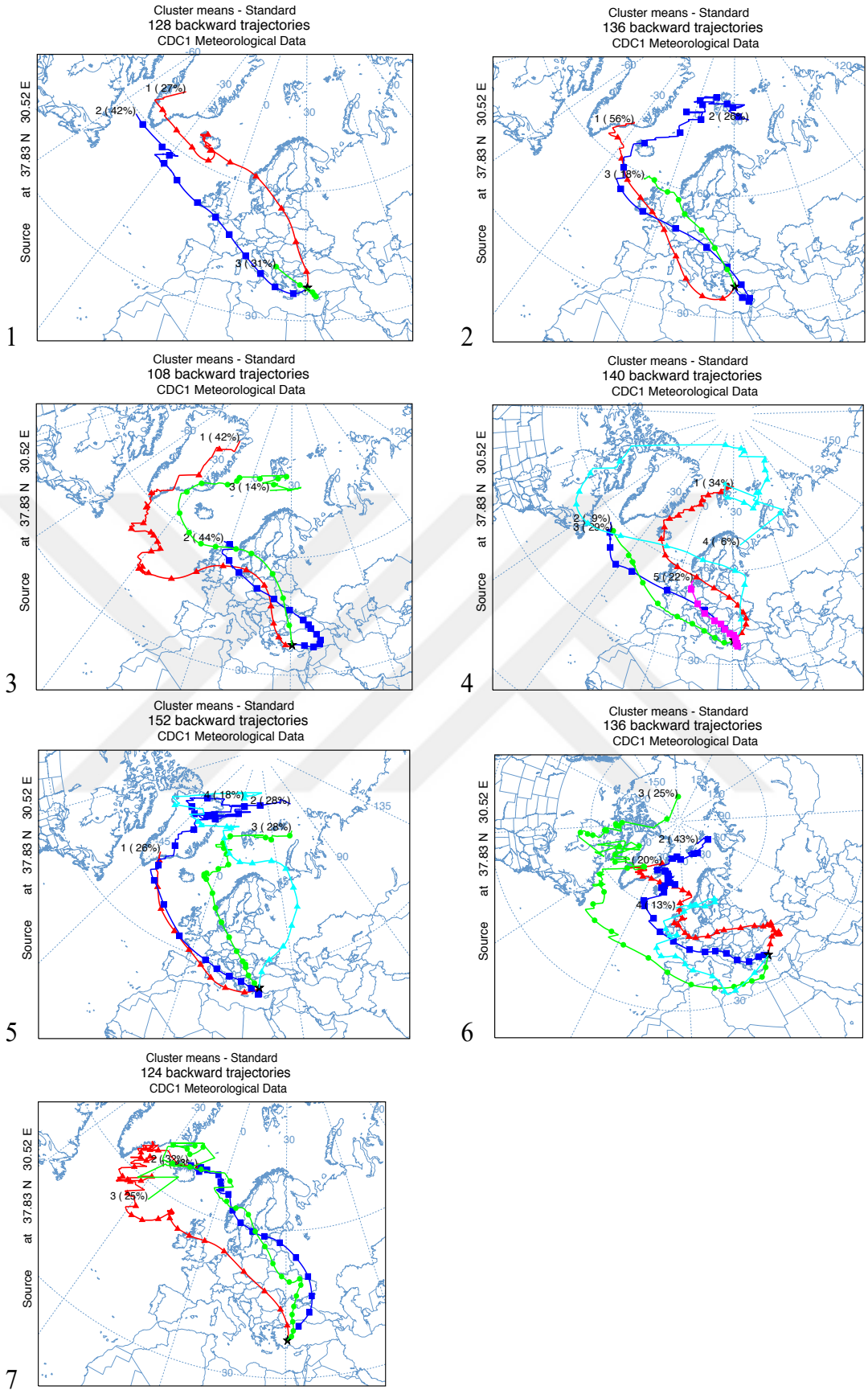

Figure 4.26. Passive sampling period monthly back trajectory cluster analysis - Isparta

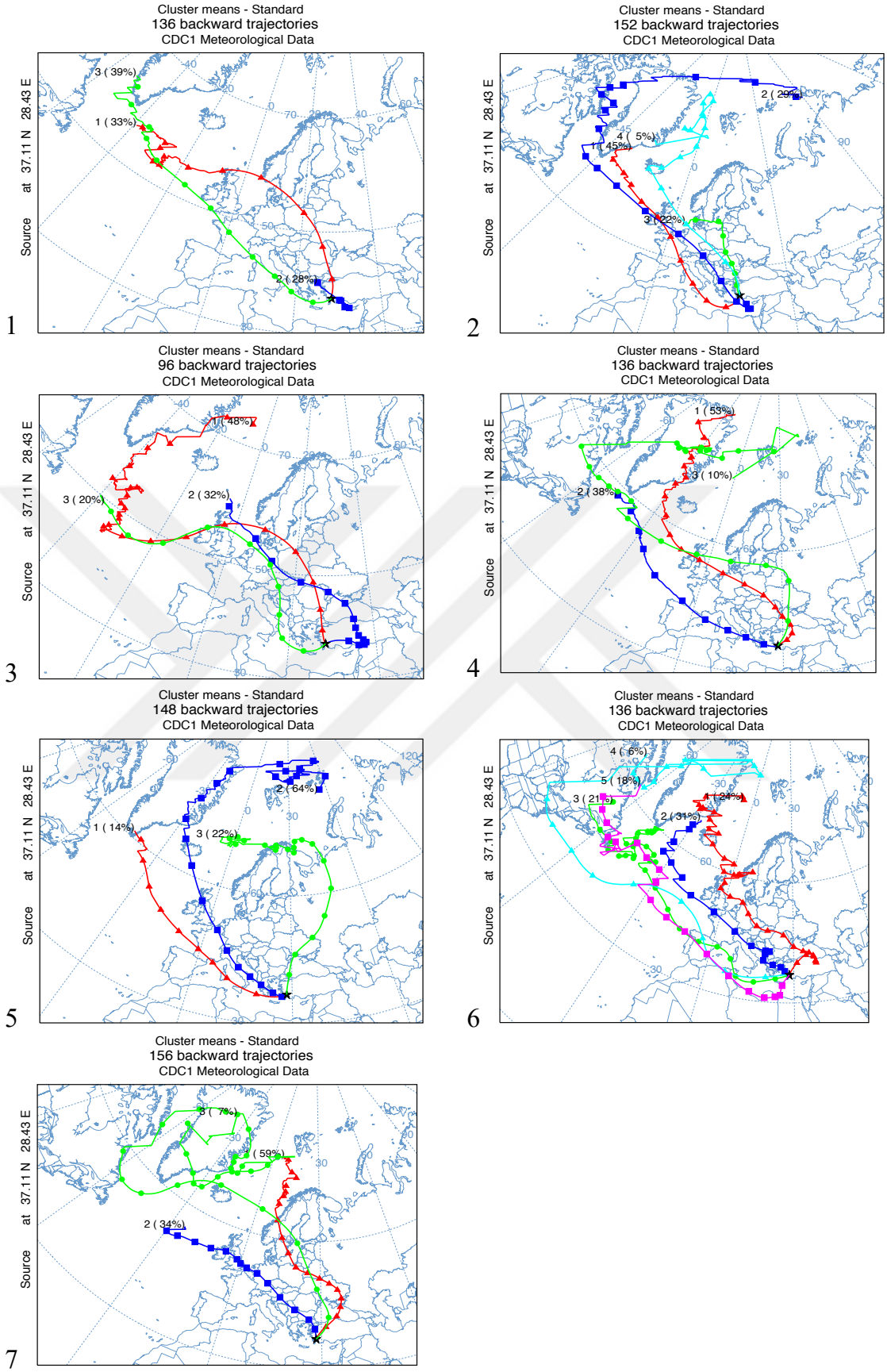

Figure 4.27. Passive sampling period monthly back trajectory cluster analysis-Mugla

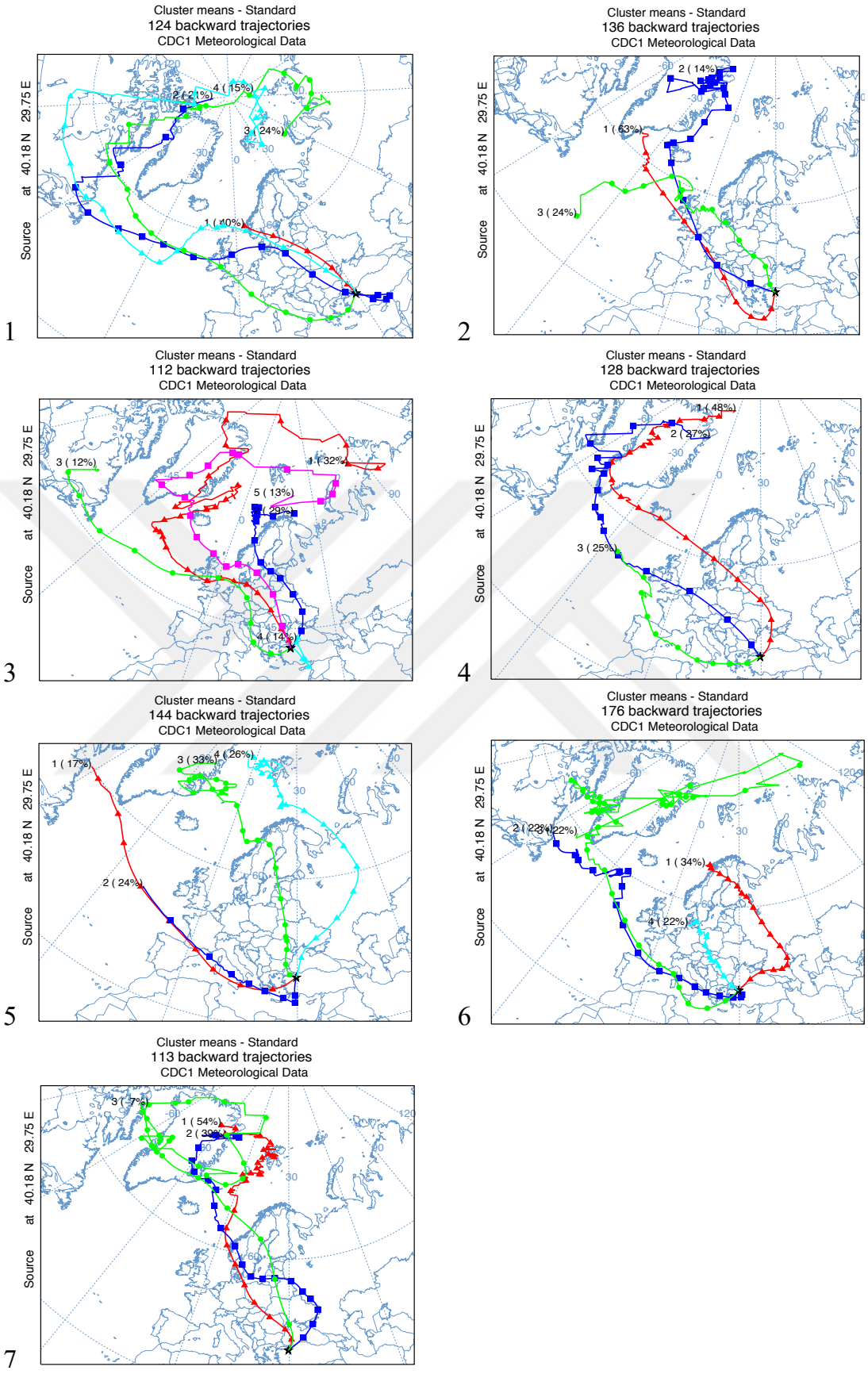

Figure 4.28. Passive sampling period monthly back trajectory cluster analysis - Bursa

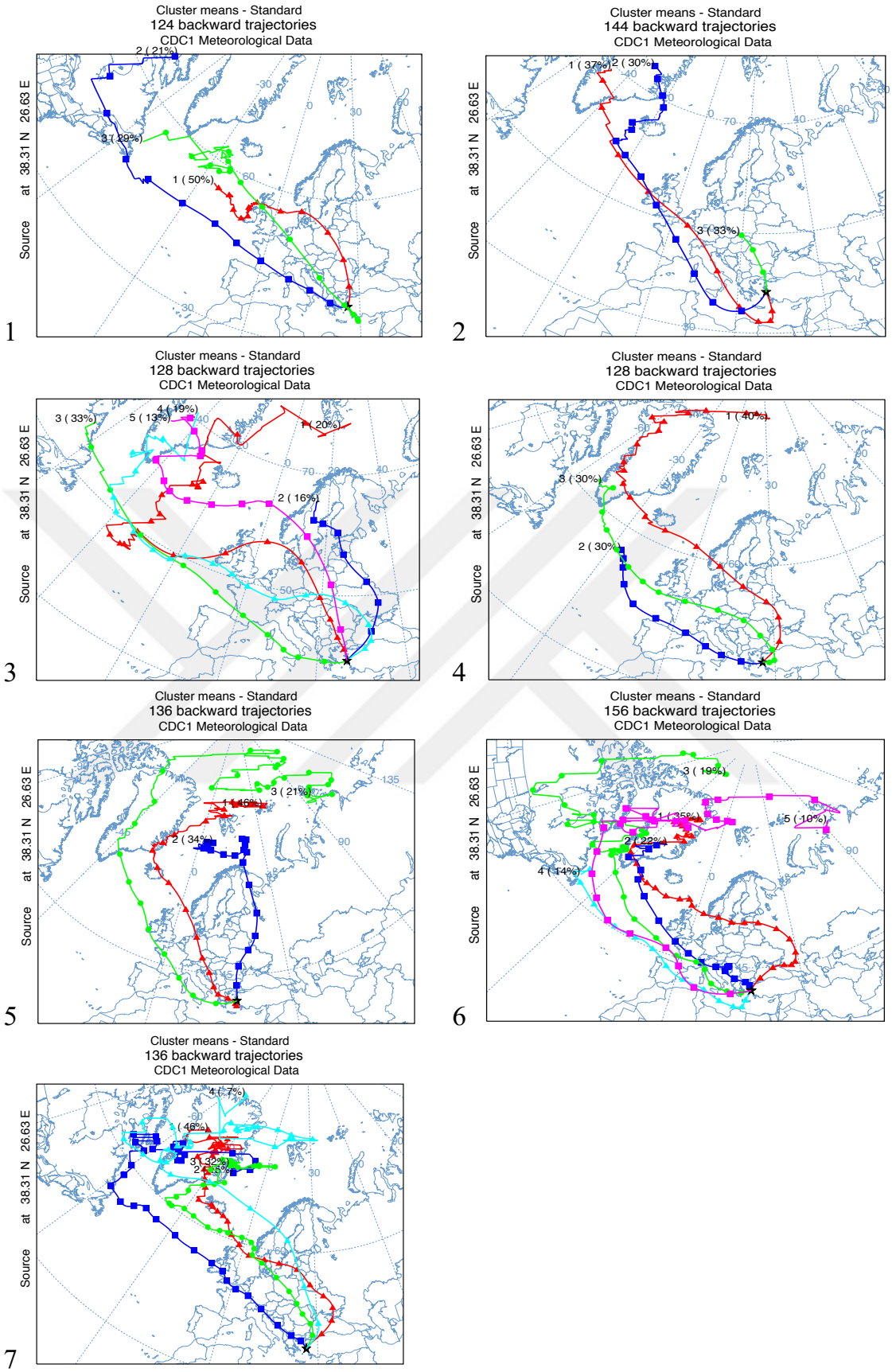

Figure 4.29. Passive sampling period monthly back trajectory cluster analysis-Izmir

CHAPTER 5

CONCLUSION

This thesis utilized measured concentrations obtained from daily high-volume active samples collected once a week at our sampling point at the Izmir Institute of Technology campus in Urla, Izmir, and one-month passive samples collected for seven months at ten different points in the three proximity groups of Close, Middle, and Far to Turkey's southern borders, beyond which war continued. Our hypothesis, based on findings of our previous study and reports of dust transport from the region, was that there may be a considerable contribution from the war zone to the atmospheric POP levels in Turkey. The hypothesis was tested by seeking a concentration – distance relationship using the passive samples and relating them to back-trajectory analysis. When passive sampling data were examined with Pearson correlation, it was seen that various congener central tendency statistic values showed increasing trend with proximity to the war zone. However, support by hypothesis testing with Kruskal-Wallis or ANOVA tests was limited: PBDE-183, Σ_{45}PCB and Dieldrin in winter, PBDE-28, PBDE-99, PBDE-154, *p,p′*-DDE, Σ_{14}PBDE and Σ_{25}OCP in transition period, and for PBDE-28, PBDE-99, PBDE-85, PBDE-154, PBDE-190, PCB-52, Σ_{45}PCB , *p,p′*-DDE and Σ_{25}OCP in the whole sampling period.

Back-trajectory frequency analysis conducted for all provinces for the whole 7-month passive sampling campaign indicated that air masses were transported from the war zone to the close-region. The low-frequency findings observed for the provinces located in the Middle and Far distance groups indicated that transport from the war zone was limited. Back-trajectories for the active sampling data did not produce information to support the findings of passive sampling, because none of the samples matched a transport from the war zone to Izmir where the main route of air masses that resulted in relatively higher POP concentrations were originating from areas in Europe, Russia, and the former Soviet Union countries followed by North Africa.

Concentrations measured by passive air sampling being relatively higher both in the close-group and far-group especially in winter than the middle-group, back-trajectories pointing to the war zone for the close-group and areas in Europe, Russia, and the former Soviet Union countries for the far-group in winter, and increasing contribution

with increasing MW in the close-group while increasing contribution with decreasing MW in the far-group may be interpreted as southeast Turkey was impacted by POP transport from the war zone while west – northwest of the country impacted by POP transport from the areas northwest – north – northeast to the country.

Recommendations for future research

The war zone impacted provinces in the country's eastern and southeastern regions, according to monthly cluster analysis. The northern air affected the country's western regions. For this reason, it would be more appropriate to select the passive sampling points in the east and southeast regions, and two active sampling points in these regions to be able to observe the effect of the transport from the war zone.

REFERENCES

Abelsohn, Alan, Brian L Gibson, Margaret D Sanborn, and Erica Weir. 2002. "Identifying and managing adverse environmental health effects: 5. Persistent organic pollutants." *Cmaj* 166 (12):1549-1554.

Anh, Hoang Quoc, Isao Watanabe, Nguyen Minh Tue, Pham Hung Viet, Ngo Kim Chi, Tu Binh Minh, and Shin Takahashi. 2020. "Polyurethane foam-based passive air sampling for simultaneous determination of POP-and PAH-related compounds: A case study in informal waste processing and urban areas, northern Vietnam." *Chemosphere* 247:125991.

Arrebola, Juan P, Ricardo Ocaña-Riola, Antonio L Arrebola-Moreno, María Fernández-Rodríguez, Piedad Martin-Olmedo, Mariana F Fernández, and Nicolás Olea. 2014. "Associations of accumulated exposure to persistent organic pollutants with serum lipids and obesity in an adult cohort from Southern Spain." *Environmental pollution* 195:9-15.

Arrebola, Juan P, José Pumarega, Magda Gasull, Mariana F Fernandez, Piedad Martin-Olmedo, José M Molina-Molina, María Fernández-Rodríguez, Miquel Porta, and Nicolás Olea. 2013. "Adipose tissue concentrations of persistent organic pollutants and prevalence of type 2 diabetes in adults from Southern Spain." *Environmental research* 122:31-37.

Aydin, Yagmur Meltem, Melik Kara, Yetkin Dumanoglu, Mustafa Odabasi, and Tolga Elbir. 2014. "Source apportionment of polycyclic aromatic hydrocarbons (PAHs) and polychlorinated biphenyls (PCBs) in ambient air of an industrial region in Turkey." *Atmospheric environment* 97:271-285.

Ballschmiter, K., and M. Zell. 1980. Analysis of polychlorinated biphenyls (PCB) by glass capillary gas chromatography. Fresenius' *Zeitschrift für analytische Chemie* 302 (1):20-31.

Baltaci, Hakki. 2017. "Spatial and temporal variation of the extreme Saharan dust event over Turkey in March 2016." *Atmosphere* 8 (2):41.

Bergknut, Magnus, Hjalmar Laudon, and Karin Wiberg. 2010. "Dioxins, PCBs, and HCB in soil and peat profiles from a pristine boreal catchment." *Environmental pollution* 158 (7):2518-2525.

Besis, Athanasios, Gerhard Lammel, Petr Kukučka, Constantini Samara, Aysun Sofuoglu, Yetkin Dumanoglu, Kostas Eleftheriadis, Giorgos Kouvarakis, Sait C Sofuoglu, and Vassiliki Vassilatou. 2017. "Polybrominated diphenyl ethers (PBDEs) in background air around the Aegean: implications for phase partitioning and size distribution." *Environmental Science and Pollution Research* 24 (36):28102-28120.

Birgül, Aşkın, Perihan Binnur Kurt-Karakus, Henry Alegria, Elif Gungormus, Halil Celik, Tugba Cicek, and Emine Can Güven. 2017. "Polyurethane foam (PUF) disk passive samplers derived polychlorinated biphenyls (PCBs) concentrations in the ambient air of Bursa-Turkey: Spatial and temporal variations and health risk assessment." *Chemosphere* 168:1345-1355.

Bogdal, Christian, Martin Scheringer, Esteban Abad, Manoli Abalos, Bert Van Bavel, Jessika Hagberg, and Heidelore Fiedler. 2013. "Worldwide distribution of persistent organic pollutants in air, including results of air monitoring by passive air sampling in five continents." *TrAC Trends in Analytical Chemistry* 46:150-161.

Bozlaker, Ayse, Aysen Muezzinoglu, and Mustafa Odabasi. 2009. "Processes affecting the movement of organochlorine pesticides (OCPs) between soil and air in an industrial site in Turkey." *Chemosphere* 77 (9):1168-1176.

Breivik, Knut, Andy Sweetman, Jozef M Pacyna, and Kevin C Jones. 2007. "Towards a global historical emission inventory for selected PCB congeners—a mass balance approach: 3. An update." *Science of the Total Environment* 377 (2-3):296-307.

Cabaravdić, M. 2006. "Xenoestrogen effects of chemical compounds: influence on the breast cancer." *Medicinski arhiv* 60 (6 Suppl 2):97-100.

Cai, ChuanYang, ShuangYu Yu, Yu Liu, Shu Tao, and WenXin Liu. 2018. "PBDE emission from E-wastes during the pyrolytic process: Emission factor, compositional profile, size distribution, and gas-particle partitioning." *Environmental Pollution* 235:419-428.

Cetin, Banu, Fatma Ozturk, Melek Keles, and Sema Yurdakul. 2017. "PAHs and PCBs in an Eastern Mediterranean megacity, Istanbul: their spatial and temporal distributions, air-soil exchange and toxicological effects." *Environmental Pollution* 220:1322-1332.

Cetin, Banu, Sinan Yatkin, Abdurrahman Bayram, and Mustafa Odabasi. 2007. "Ambient concentrations and source apportionment of PCBs and trace elements around an industrial area in Izmir, Turkey." *Chemosphere* 69 (8):1267-1277.

Cetin, Banu, Sema Yurdakul, and Mustafa Odabasi. 2019. "Spatio-temporal variations of atmospheric and soil polybrominated diphenyl ethers (PBDEs) in highly industrialized region of Dilovasi." *Science of the Total Environment* 646:1164-1171.

Chakraborty, Paromita, Gan Zhang, Jun Li, Pitchai Sampathkumar, Thangavel Balasubramanian, Kandasamy Kathiresan, Shin Takahashi, Annamalai Subramanian, Shinsuke Tanabe, and Kevin C Jones. 2019. "Seasonal variation of atmospheric organochlorine pesticides and polybrominated diphenyl ethers in Parangipettai, Tamil Nadu, India: Implication for atmospheric transport." *Science of the Total Environment* 649:1653-1660.

Chen, Yuan, Jinhui Li, Lili Liu, and Nana Zhao. 2012. "Polybrominated diphenyl ethers fate in China: a review with an emphasis on environmental contamination levels, human exposure and regulation." *Journal of environmental management* 113:22-30.

Cindoruk, S Sıddık. 2011. "Atmospheric organochlorine pesticide (OCP) levels in a metropolitan city in Turkey." *Chemosphere* 82 (1):78-87.

Cindoruk, S Sıddık, A Egemen Sakin, and Yücel Tasdemir. 2020. "Levels of persistent organic pollutants in pine tree components and ambient air." *Environmental Pollution* 256:113418.

Corsolini, Simonetta, and Gianluca Sarà. 2017. "The trophic transfer of persistent pollutants (HCB, DDTs, PCBs) within polar marine food webs." *Chemosphere* 177:189-199.

Dai, Qizhou, Xia Min, and Mili Weng. 2016. "A review of polychlorinated biphenyls (PCBs) pollution in indoor air environment." *Journal of the Air & Waste Management Association* 66 (10):941-950.

Dirinck, Eveline, Philippe G Jorens, Adrian Covaci, Tinne Geens, Laurence Roosens, Hugo Neels, Ilse Mertens, and Luc Van Gaal. 2011. "Obesity and persistent organic pollutants: possible obesogenic effect of organochlorine pesticides and polychlorinated biphenyls." *Obesity* 19 (4):709-714.

Dogan, Tuba Rastgeldi, Nurettin Beşli, Mehmet Azmi Aktacir, Merve Nur Dinç, Mehmet Akif İlkhan, Fatma Öztürk, and Melek Yıldız. 2020. "Seasonal effects of atmospheric particulate matter on performance of different types of photovoltaic modules in sanliurfa, Turkey." *Atmospheric Pollution Research* 11 (12):2173-2181.

Doga, Tuba Rastgeldi, Mehmet İrfan Yeşilnacar, and Mehmet Ali Cullu. 2018. "Seasonal Investigation of Atmospheric Desert Dust Affecting Sanliurfa Using Modis Satellite and Hysplit Model Data." *Sigma J. Eng. Nat. Sci.-Sigma Muhendis. Ve Fen Bilimleri Derg* 36:905-916.

Draxler, Roland R, Barbara Stunder, Glenn Rolph, Ariel Stein, and Albion Taylor. 1999. HYSPLIT4 Users's Guide: US Department of Commerce, National Oceanic and Atmospheric Administration

Dumanoglu, Yetkin, Eftade O Gaga, Elif Gungormus, Sait C Sofuoglu, and Mustafa Odabasi. 2017. "Spatial and seasonal variations, sources, air-soil exchange, and carcinogenic risk assessment for PAHs and PCBs in air and soil of Kutahya, Turkey, the province of thermal power plants." *Science of the Total Environment* 580:920-935.

Eker, Gizem, and Yucel Tasdemir. 2018. "Atmospheric Deposition of Organochlorine Pesticides (OCPs): Species, Levels, Diurnal and Seasonal Fluctuations, Transfer Velocities." *Archives of environmental contamination and toxicology* 75 (4):625-633.

EPA: Unites States Environment Protection Agency (accessed on 27.07.2021 https://www.epa.gov/international-cooperation/persistent-organic-pollutants-global-issue-global-response)

Estellano, Victor H, Karla Pozo, Petra Přibylová, Jana Klánová, Ondřej Audy, and Silvano Focardi. 2017. "Assessment of seasonal variations in persistent organic pollutants across the region of Tuscany using passive air samplers." *Environmental Pollution* 222:609-616.

Everett, Charles Jay, Ivar Frithsen, and Marty Player. 2011. "Relationship of polychlorinated biphenyls with type 2 diabetes and hypertension." *Journal of Environmental Monitoring* 13 (2):241-251.

Fallahzadeh, R. A., M. H. Ehrampoush, A. H. Mahvi, M. T. Ghaneian, A. Dalvand, M. H. Salmani, H. Fallahzadeh, and M. Nabi Meybodi. 2019. Designing and

modeling of a novel electrolysis reactor using porous cathode to produce H2O2 as an oxidant. *MethodsX* 6:1305-1312.

Godduhn, Anna, and Lawrence K Duffy. 2003. "Multi-generation health risks of persistent organic pollution in the far north: use of the precautionary approach in the Stockholm Convention." *Environmental Science & Policy* 6 (4):341-353.

Greig, A., M. A. Palmer, and L. M. Chepulis. 2010. "Hormonal contraceptive practices in young Australian women (<= 25 years) and their possible impact on menstrual frequency and iron requirements." *Sexual & Reproductive Healthcare* 1 (3):99-103.

Griffin, Dale W, Nilgün Kubilay, Mustafa Koçak, Mike A Gray, Timothy C Borden, and Eugene A Shinn. 2007. "Airborne desert dust and aeromicrobiology over the Turkish Mediterranean coastline." *Atmospheric environment* 41 (19):4050-4062.

Hardell, Lennart, Swen-Olof Andersson, Michael Carlberg, Louise Bohr, Bert van Bavel, Gunilla Lindström, Helen Björnfoth, and Claes Ginman. 2006. "Adipose tissue concentrations of persistent organic pollutants and the risk of prostate cancer." *Journal of Occupational and Environmental Medicine* 48 (7):700-707.

Hardell, Lennart, Gunilla Lindstrom, Bert van Bavel, Hans Wedrén, and Birgitte Melgaard. 2006. "High concentrations of organochlorines in a patient with kidney cancer and anorexia-cachexia syndrome." *Medicinal Chemistry* 2 (6):607-610.

Hardell, Lennart, Bert Van Bavel, Gunilla Lindström, Michael Carlberg, Mikael Eriksson, Ann Charlotte Dreifaldt, Hans Wijkström, Hans Starkhammar, Arne Hallquist, and Torgny Kolmert. 2004. "Concentrations of polychlorinated biphenyls in blood and the risk for testicular cancer." *International journal of andrology* 27 (5):282-290.

Hardell, Lennart, Bert van Bavel, Gunilla Lindström, Mikael Eriksson, and Michael Carlberg. 2006. "In utero exposure to persistent organic pollutants in relation to testicular cancer risk." *International journal of andrology* 29 (1):228-234.

Harro, J., K. Aadamsoo, L. Rootslane, O. Laius, A. O'Leary, V. Adomaitiene, B. Kupca, A. Lehtmets, A. Navickas, E. Rancans, M. Taube, E. Terauds, and K. Pops. 2019. Comparison of psychotropic medication use in the Baltic countries. Nordic Journal of Psychiatry.

Harner, Tom, Mahiba Shoeib, Miriam Diamond, Gary Stern, and Bruno Rosenberg. 2004. "Using passive air samplers to assess urban− rural trends for persistent organic pollutants. 1. Polychlorinated biphenyls and organochlorine pesticides." *Environmental science & technology* 38 (17):4474-4483.

Henríquez-Hernández, Luis A, Octavio P Luzardo, Manuel Zumbado, María Camacho, Lluis Serra-Majem, Eva E Álvarez-León, and Luis D Boada. 2014. "Blood pressure in relation to contamination by polychlorobiphenyls and organochlorine pesticides: Results from a population-based study in the Canary Islands (Spain)." *Environmental research* 135:48-54.

Holst-Jensen, Arne. 2007. "Sampling, detection, identification and quantification of genetically modified organisms (GMOs)." *In Food Toxicants Analysis*, 231-268. Elsevier.

Jayaraj, Ravindran, Pankajshan Megha, and Puthur Sreedev. 2016. "Organochlorine pesticides, their toxic effects on living organisms and their fate in the environment." *Interdisciplinary toxicology* 9 (3-4):90-100.

Jones, Kevin C, and P De Voogt. 1999. "Persistent organic pollutants (POPs): state of the science." *Environmental pollution* 100 (1-3):209-221.

Kabatas, B, RB Pierce, A Unal, MJ Rogal, and A Lenzen. 2018. "April 2008 Saharan dust event: Its contribution to PM10 concentrations over the Anatolian Peninsula and relation with synoptic conditions." *Science of the Total Environment* 633:317-328.

Kallenborn, Roland, Hayley Hung, and Eva Brorström-Lundén. 2015. "Atmospheric long-range transport of persistent organic pollutants (POPs) into polar regions." *In Comprehensive Analytical Chemistry*, 411-432. Elsevier.

Kaya, Elife, Yetkin Dumanoglu, Melik Kara, Hasan Altiok, Abdurrahman Bayram, Tolga Elbir, and Mustafa Odabasi. 2012. "Spatial and temporal variation and air–soil exchange of atmospheric PAHs and PCBs in an industrial region." *Atmospheric Pollution Research* 3 (4):435-449.

Kengara, Fredrick Orori, Karl-Werner Schramm, Ulrike Doerfler, Jean Charles Munch, Bernhard Henkelmann, Gerhard Welzl, Silke Bernhoeft, Burkhard Hense, and Reiner Schroll. 2010. "Degradation capacity of a 1, 2, 4-trichlorobenzene mineralizing microbial community for traces of organochlorine pesticides." *Science of the total environment* 408 (16):3359-3366.

Khuman, Sanjenbam Nirmala, and Paromita Chakraborty. 2019. "Air-water exchange of pesticidal persistent organic pollutants in the lower stretch of the transboundary river Ganga, India." *Chemosphere* 233:966-974.

Kim, Ki-Su, Yu-Mi Lee, Sang Geol Kim, In-Kyu Lee, Hyo-Jeong Lee, Ji-Hyun Kim, Jeongkook Kim, Hyo-Bang Moon, David R Jacobs Jr, and Duk-Hee Lee. 2014. "Associations of organochlorine pesticides and polychlorinated biphenyls in visceral vs. subcutaneous adipose tissue with type 2 diabetes and insulin resistance." *Chemosphere* 94:151-157.

Klanova, J., J. Kohoutek, L. Hamplova, P. Urbanova, and I. Holoubek. 2006. Passive air sampler as a tool for long-term air pollution monitoring: Part 1. Performance assessment for seasonal and spatial variations. *Environ Pollut* 144 (2):393-405.

Kodavanti, Prasada Rao S, and Bommanna G Loganathan. 2019. "Polychlorinated biphenyls, polybrominated biphenyls, and brominated flame retardants." *In Biomarkers in Toxicology*, 501-518. Elsevier.

Konieczka, Piotr. 2012. "Validation and Regulatory Issues for Sample Preparation in: Comprehensive Sampling and Sample Preparation."

Kurt-Karakus, Perihan Binnur, Aysun Sofuoglu, Sait C Sofuoglu, Kadir Gedik, Hatice Eser Okten, Kevin Jones,Tugba Ugranlı, Elif Güngörmüş, Kadir Çelik 2015. "Determination of Persistent Organic Pollutants (POPs) in Soil and Air Samples of Selected Urban and Rural Areas in Turkey." Final project report supported by grant number Scientific and Technological Research Council of Turkey 112Y315.

Kurt-Karakus, Perihan Binnur, Henry Alegria, Liisa Jantunen, Askin Birgul, Aslinur Topcu, Kevin C Jones, and Cafer Turgut. 2017. "Polybrominated diphenyl ethers (PBDEs) and alternative flame retardants (NFRs) in indoor and outdoor air and indoor dust from Istanbul-Turkey: levels and an assessment of human exposure." *Atmospheric Pollution Research* 8 (5):801-815.

Kurt-Karakus, Perihan Binnur, Tugba Ugranli-Cicek, Sait C Sofuoglu, Halil Celik, Elif Gungormus, Kadir Gedik, Aysun Sofuoglu, Hatice Eser Okten, Askın Birgul, and Henry Alegria. 2018. "The first countrywide monitoring of selected POPs: Polychlorinated biphenyls (PCBs), polybrominated diphenyl ethers (PBDEs) and selected organochlorine pesticides (OCPs) in the atmosphere of Turkey." *Atmospheric Environment* 177:154-165.

Kuzu, S Levent. 2016. "Compositional variation of PCBs, PAHs, and OCPs at gas phase and size segregated particle phase during dust incursion from the Saharan Desert in the northwestern Anatolian peninsula." *Advances in Meteorology* 2016.

Lammel, Gerhard, Ondřej Audy, Athanasios Besis, Christos Efstathiou, Kostas Eleftheriadis, Jiři Kohoutek, Petr Kukučka, Marie D Mulder, Petra Přibylová, and Roman Prokeš. 2015. "Air and seawater pollution and air–sea gas exchange of persistent toxic substances in the Aegean Sea: spatial trends of PAHs, PCBs, OCPs and PBDEs." *Environmental Science and Pollution Research* 22 (15):11301-11313.

Lee, Duk-Hee, Lars Lind, David R Jacobs Jr, Samira Salihovic, Bert van Bavel, and P Monica Lind. 2012. "Associations of persistent organic pollutants with abdominal obesity in the elderly: The Prospective Investigation of the Vasculature in Uppsala Seniors (PIVUS) study." *Environment international* 40:170-178.

Lee, Duk-Hee, P Monica Lind, David R Jacobs, Samira Salihovic, Bert Van Bavel, and Lars Lind. 2011. "Polychlorinated biphenyls and organochlorine pesticides in plasma predict development of type 2 diabetes in the elderly: the prospective investigation of the vasculature in Uppsala Seniors (PIVUS) study." *Diabetes care* 34 (8):1778-1784.

Lee, Duk-Hee, Michael W Steffes, Andreas Sjödin, Richard S Jones, Larry L Needham, and David R Jacobs Jr. 2011. "Low dose organochlorine pesticides and polychlorinated biphenyls predict obesity, dyslipidemia, and insulin resistance among people free of diabetes." *PloS one* 6 (1).

Li, Qifeng, Yonglong Lu, Pei Wang, Tieyu Wang, Sarvajayakesavalu Suriyanarayanan, Ruoyu Liang, Yvette Baninla, and Kifayatullah Khan. 2018. "Distribution, source, and risk of organochlorine pesticides (OCPs) and polychlorinated biphenyls (PCBs) in urban and rural soils around the Yellow and Bohai Seas, China."*Environmental pollution* 239:233-241.

Li, Yuanyuan, Tian Lin, Limin Hu, Jialiang Feng, and Zhigang Guo. 2016. "Time trends of polybrominated diphenyl ethers in East China Seas: response to the booming of PBDE pollution industry in China."*Environment international* 92:507-514.

Lind, Ylva Sjöberg, P Monica Lind, Samira Salihovic, Bert van Bavel, and Lars Lind. 2013. "Circulating levels of persistent organic pollutants (POPs) are associated with left ventricular systolic and diastolic dysfunction in the elderly."*Environmental research* 123:39-45.

Ljunggren, Stefan A, Ingela Helmfrid, Samira Salihovic, Bert van Bavel, Gun Wingren, Mats Lindahl, and Helen Karlsson. 2014. "Persistent organic pollutants distribution in lipoprotein fractions in relation to cardiovascular disease and cancer."*Environment international* 65:93-99.

Lyche, Jan L, Irena M Grześ, Camilla Karlsson, Rasoul Nourizadeh-Lillabadi, Vidar Berg, Anja B Kristoffersen, Janneche U Skåre, Peter Alestrøm, and Erik Ropstad. 2013. "Parental exposure to natural mixtures of POPs reduced embryo production and altered gene transcription in zebrafish embryos."*Aquatic toxicology* 126:424-434.

Lyche, Jan L, Rasoul Nourizadeh-Lillabadi, Camilla Almaas, Benedicte Stavik, Vidar Berg, Janneche Utne Skåre, Peter Alestrøm, and Erik Ropstad. 2010. "Natural mixtures of persistent organic pollutants (POP) increase weight gain, advance puberty, and induce changes in gene expression associated with steroid hormones and obesity in female zebrafish." *Journal of Toxicology and Environmental Health, Part A* 73 (15):1032-1057.

Macgregor, Kenneth, Ian W Oliver, Lynsay Harris, and Ian M Ridgway. 2010. "Persistent organic pollutants (PCB, DDT, HCH, HCB & BDE) in eels (Anguilla anguilla) in Scotland: current levels and temporal trends." *Environmental Pollution* 158 (7):2402-2411.

Mandal, Asit, Binoy Sarkar, Sanchita Mandal, Meththika Vithanage, Ashok K Patra, and Madhab C Manna. 2020. "Impact of agrochemicals on soil health." *In Agrochemicals Detection, Treatment and Remediation*, 161-187. Elsevier.

Mao, Shuduan, Gan Zhang, Jun Li, Xiaofei Geng, Jiaqi Wang, Shizhen Zhao, Zhineng Cheng, Yue Xu, Qilu Li, and Yan Wang. 2020. "Occurrence and sources of PCBs, PCNs, and HCB in the atmosphere at a regional background site in east China: Implications for combustion sources." *Environmental Pollution*:114267.

Motelay-Massei, A., T. Harner, M. Shoeib, M. Diamond, G. Stern, and B. Rosenberg. 2005. Using passive air samplers to assess urban-rural trends for persistent organic pollutants and polycyclic aromatic hydrocarbons. 2. Seasonal trends for PAHs, PCBs, and organochlorine pesticides. *Environ Sci Technol* 39 (15):5763-73.

Mumtaz, Mehvish, Abdul Qadir, Adeel Mahmood, Andleeb Mehmood, Riffat Naseem Malik, Jun Li, Zubaida Yousaf, Nadia Jamil, Irfan Ahmed Shaikh, and Habib Ali. 2015. "Human health risk assessment, congener specific analysis and spatial distribution pattern of organochlorine pesticides (OCPs) through rice crop from

selected districts of Punjab Province, Pakistan." *Science of the Total Environment* 511:354-361.

Nadal, Martí, Montse Marquès, Montse Mari, and José L Domingo. 2015. "Climate change and environmental concentrations of POPs: A review." *Environmental research* 143:177-185.

O'Sullivan, Gwen, and David Megson. 2014. "Brief overview: discovery, regulation, properties, and fate of POPs." *In Environmental forensics for persistent organic pollutants*, 1-20. Elsevier.

Odabasi, Mustafa, and Banu Cetin. 2012. "Determination of octanol–air partition coefficients of organochlorine pesticides (OCPs) as a function of temperature: Application to air–soil exchange." *Journal of environmental management* 113:432-439.

Odabasi, Mustafa, Banu Cetin, Eylem Demircioglu, and Aysun Sofuoglu. 2008. "Air–water exchange of polychlorinated biphenyls (PCBs) and organochlorine pesticides (OCPs) at a coastal site in Izmir Bay, Turkey." *Marine Chemistry* 109 (1-2):115-129.

Ozcan, Senar, and Mehmet Emin Aydin. 2009. "Polycyclic aromatic hydrocarbons, polychlorinated biphenyls and organochlorine pesticides in urban air of Konya, Turkey." *Atmospheric Research* 93 (4):715-722.

Park, Jong-Eun, Young-Yeul Kang, Woo-Il Kim, Tae-Wan Jeon, Sun-Kyoung Shin, Mi-Jeong Jeong, and Jong-Guk Kim. 2014. "Emission of polybrominated diphenyl ethers (PBDEs) in use of electric/electronic equipment and recycling of e-waste in Korea." *Science of the total environment* 470:1414-1421.

Penell, Johanna, Lars Lind, Samira Salihovic, Bert van Bavel, and P Monica Lind. 2014. "Persistent organic pollutants are related to the change in circulating lipid levels during a 5 year follow-up." *Environmental research* 134:190-197.

Pongkiatkul, Prapat, and Nguyen Thi Kim Oanh. 2007. "Assessment of potential long-range transport of particulate air pollution using trajectory modeling and monitoring data." *Atmospheric Research* 85 (1):3-17.

Porta, Miquel, and Ekhine Zumeta. 2002. Implementing the Stockholm treaty on persistent organic pollutants. BMJ Publishing Group Ltd.

Pozo, K., T. Harner, M. Shoeib, R. Urrutia, R. Barra, O. Parra, and S. Focardi. 2004. "Passive-sampler derived air concentrations of persistent organic pollutants on a north-south transect in Chile." *Environ Sci Technol* 38 (24):6529-37.

Pozo, Karla, Tania Martellini, Simonetta Corsolini, Tom Harner, Victor Estellano, Petr Kukučka, Marie D Mulder, Gerhard Lammel, and Alessandra Cincinelli. 2017. "Persistent organic pollutants (POPs) in the atmosphere of coastal areas of the Ross Sea, Antarctica: indications for long-term downward trends." *Chemosphere* 178:458-465.

Pozo, Karla, Santosh Kumar Sarkar, Victor H Estellano, Soumita Mitra, Ondrej Audi, Petr Kukucka, Petra Přibylová, Jana Klánová, and Simonetta Corsolini. 2017. "Passive air sampling of persistent organic pollutants (POPs) and emerging compounds in Kolkata megacity and rural mangrove wetland Sundarban in India: An approach to regional monitoring." *Chemosphere* 168:1430-1438.

Qiu, Yao-Wen, Dong-Xiao Wang, and Gan Zhang. 2020. "Assessment of persistent organic pollutants (POPs) in sediments of the Eastern Indian Ocean."*Science of The Total Environment* 710:136335.

Radonic, Jelena, Maja Turk Sekulic, Mirjana Vojinovic Miloradov, Pavel Čupr, and Jana Klánová. 2009. "Gas–particle partitioning of persistent organic pollutants in the Western Balkan countries affected by war conflicts." *Environmental Science and Pollution Research* 16 (1):65-72.

Raffetti, Elena, Francesco Donato, Giuseppe De Palma, Lucia Leonardi, Claudio Sileo, and Michele Magoni. 2020. "Polychlorinated biphenyls (PCBs) and risk of hypertension: A population-based cohort study in a North Italian highly polluted area." *Science of The Total Environment*:136660.

Rahman, Frank, Katherine H Langford, Mark D Scrimshaw, and John N Lester. 2001. "Polybrominated diphenyl ether (PBDE) flame retardants."*Science of the Total Environment* 275 (1-3):1-17.

Razali, Nornadiah Mohd, and Yap Bee Wah. 2011. Power comparisons of shapiro-wilk, kolmogorov-smirnov, lilliefors and anderson-darling tests. *Journal of statistical modeling and analytics* 2 (1):21-33.

Redfern, Farran Mack, Wen-Jhy Lee, Ping Yan, John Kennedy Mwangi, Lin-Chi Wang, and Chih-Hsuan Shih. 2017. "Overview and perspectives on emissions of polybrominated diphenyl ethers on a global basis: Evaporative and fugitive

releases from commercial PBDE mixtures and emissions from combustion sources."*Aerosol Air Qual. Res* 17 (5):1117-1131.

Rodenburg, Lisa, Jia Guo, and Robert Christie. 2015. "Polychlorinated biphenyls in pigments: inadvertent production and environmental significance." *Coloration Technology* 131 (5):353-369.

Roos, Vendela, Monika Rönn, Samira Salihovic, Lars Lind, Bert van Bavel, Joel Kullberg, Lars Johansson, Håkan Ahlström, and P Monica Lind. 2013. "Circulating levels of persistent organic pollutants in relation to visceral and subcutaneous adipose tissue by abdominal MRI." *Obesity* 21 (2):413-418.

Roveda, AM, L Veronesi, R Zoni, ME Colucci, and G Sansebastiano. 2006. "Exposure to polychlorinated biphenyls (PCBs) in food and cancer risk: recent advances." *Igiene e sanità pubblica* 62 (6):677-696.

Sari, Mehmet Ferhat, Fatma Esen, Daniel Alejandro Cordova Del Aguila, and Perihan Binnur Kurt Karakus. 2020. "Passive sampler derived polychlorinated biphenyls (PCBs) in indoor and outdoor air in Bursa, Turkey: Levels and an assessment of human exposure via inhalation." *Atmospheric Pollution Research*.

Shen, Li, Frank Wania, Ying D Lei, Camilla Teixeira, Derek CG Muir, and Terry F Bidleman. 2005. "Atmospheric distribution and long-range transport behavior of organochlorine pesticides in North America." *Environmental science & technology* 39 (2):409-420.

Shoeib, M., and T. Harner. 2002. "Characterization and comparison of three passive air samplers for persistent organic pollutants." *Environ Sci Technol* 36 (19):4142-51.

Siddiqi, Muhammad Akmal, Ronald H Laessig, and Kurt D Reed. 2003. "Polybrominated diphenyl ethers (PBDEs): new pollutants–old diseases." *Clinical Medicine & Research* 1 (4):281-290.

Stockholm Convention: Stockholm Convention web page (accessed on 27.07.2021, http://chm.pops.int/TheConvention/Overview/tabid/3351/Default.aspx)

SC,2005: Stockholm Convention Report of the Conference of the Parties of the Stockholm Convention on Persistent Organic Pollutants on the work of its first meeting(accessedon27.07.2021http://chm.pops.int/TheConvention/ConferenceoftheParties/ReportsandDecisions/tabid/208/Default.aspx)

SC,2019: Stockholm Convention 2019 Stockholm Convention on persistent organic pollutions (POPs) (accessed on 27.07.2021).

Su, Peng-hao, Gregg T Tomy, Chun-yan Hou, Fang Yin, Dao-lun Feng, Yong-sheng Ding, and Yi-fan Li. 2018. "Gas/particle partitioning, particle-size distribution of atmospheric polybrominated diphenyl ethers in southeast Shanghai rural area and size-resolved predicting model."*Chemosphere* 197:251-261.

Thakur, Manita, and Deepak Pathania. 2020. "Environmental fate of organic pollutants and effect on human health." *In Abatement of Environmental Pollutants*, 245-262. Elsevier.

Tipayarom, Aungsiri, and Nguyen Thi Kim Oanh. 2020. "Influence of rice straw open burning on levels and profiles of semi-volatile organic compounds in ambient air." *Chemosphere* 243:125379.

Trinh, Minh Man, Ching Lan Tsai, To Thi Hien, Ngo Thi Thuan, Kai Hsien Chi, Chien Guo Lien, and Moo Been Chang. 2018. "Atmospheric concentrations and gas-particle partitioning of PCDD/Fs and dioxin-like PCBs around Hochiminh city." *Chemosphere* 202:246-254.

Turk, Maja, J Jakšić, M Vojinović Miloradov, and Jana Klánová. 2007. "Post-war levels of persistent organic pollutants (POPs) in air from Serbia determined by active and passive sampling methods." *Environmental Chemistry Letters* 5 (3):109-113.

TUIK,2020 Turkey Statistical Institute geographic statistic portal (cip. tuik.gov.tr accessed on 20.05.2021)

TISH Environmental sampler https://tisch-env.com/pesticide-samplers/PUF accessed on 14/06/2021

Uemura, H. 2012. "Associations of exposure to dioxins and polychlorinated biphenyls with diabetes: based on epidemiological findings." Nihon eiseigaku zasshi. *Japanese journal of hygiene* 67 (3):363-374.

Ugranli, Tugba, Elif Gungormus, Pınar Kavcar, Eylem Demircioglu, Mustafa Odabasi, Sait C Sofuoglu, Gerhard Lammel, and Aysun Sofuoglu. 2016. "POPs in a major conurbation in Turkey: ambient air concentrations, seasonal variation, inhalation and dermal exposure, and associated carcinogenic risks." *Environmental Science and Pollution Research* 23 (22):22500-22512.

United Nations Environment Programme UNEP (1999). The Kosovo conflict—consequences for the environment and human settlements. (https://reliefweb.int/sites/reliefweb.int/files/resources/finalreport.pdf accessed on 10.03.2021)

Vecchiato, Marco, Elena Argiriadis, Stefano Zambon, Carlo Barbante, Giuseppa Toscano, Andrea Gambaro, and Rossano Piazza. 2015. "Persistent Organic Pollutants (POPs) in Antarctica: Occurrence in continental and coastal surface snow." *Microchemical Journal* 119:75-82.

Venier, Marta, Amina Salamova, and Ronald A Hites. 2019. "How to distinguish urban vs. agricultural sources of persistent organic pollutants." *Current Opinion in Environmental Science & Health*.

Virtanen, HE, E Rajpert-De Meyts, KM Main, NE Skakkebaek, and J Toppari. 2005. "Testicular dysgenesis syndrome and the development and occurrence of male reproductive disorders." *Toxicology and applied pharmacology* 207 (2):501-505.

Vitali, Matteo, Arianna Antonucci, Malgorzata Owczarek, Maurizio Guidotti, Maria Luisa Astolfi, Maurizio Manigrasso, Pasquale Avino, Badal Bhattacharya, and Carmela Protano. 2019. "Air quality assessment in different environmental scenarios by the determination of typical heavy metals and Persistent Organic Pollutants in native lichen Xanthoria parietina." *Environmental Pollution* 254:113013.

Wang, Pu, Yingming Li, Qinghua Zhang, Qinghua Yang, Lin Zhang, Fubin Liu, Jianjie Fu, Wenying Meng, Dou Wang, and Huizhong Sun. 2017. "Three-year monitoring of atmospheric PCBs and PBDEs at the Chinese Great Wall Station, West Antarctica: levels, chiral signature, environmental behaviors and source implication." *Atmospheric Environment* 150:407-416.

Wang, Pu, Wenying Meng, Yingming Li, Qinghua Zhang, Lin Zhang, Jianjie Fu, Ruiqiang Yang, and Guibin Jiang. 2018. "Temporal variation (2011–2014) of atmospheric OCPs at King George Island, west Antarctica." *Atmospheric Environment* 191:432-439.

Wang, Xiao-ping, Jiu-jiang Sheng, Ping Gong, Yong-gang Xue, Tan-dong Yao, and Kevin C Jones. 2012. "Persistent organic pollutants in the Tibetan surface soil: spatial distribution, air–soil exchange and implications for global cycling." *Environmental pollution* 170:145-151.

Wang, Yan, Yuwei Zhang, Feng Tan, Ya Yang, Zhenping Qu, Jacob Kvasnicka, and Jingwen Chen. 2020. "Characteristics of halogenated flame retardants in the atmosphere of Dalian, China." *Atmospheric Environment* 223:117219.

Wang, YQ, XY Zhang, and Roland R Draxler. 2009. "TrajStat: GIS-based software that uses various trajectory statistical analysis methods to identify potential sources from long-term air pollution measurement data."*Environmental Modelling & Software* 24 (8):938-939.

Wania, Frank, and Chandrasagar B Dugani. 2003. "Assessing the long-range transport potential of polybrominated diphenyl ethers: A comparison of four multimedia models." *Environmental Toxicology and Chemistry: An International Journal* 22 (6):1252-1261.

Wong, Alexander, Ying Duan Lei, Mehran Alaee, and Frank Wania. 2001. "Vapor pressures of the polybrominated diphenyl ethers." *Journal of Chemical & Engineering Data* 46 (2):239-242.

Zacharia, James T. 2019. "Degradation Pathways of Persistent Organic Pollutants (POPs) in the Environment." *In Persistent Organic Pollutants*. IntechOpen.

Zeliger, Harold I. 2013. "Lipophilic chemical exposure as a cause of type 2 diabetes (T2D)." *Reviews on environmental health 28 (1):*9-20.

APPENDIX

A 1. GC / MS instrument detection limit and method detection limit values of PBDEs

PBDE	Instrument Detection Limit (pg/uL)	Passive Sampling Method Detection Limit (pg/m^3)	Active Sampling (Gas and Particulate) Method Detection Limit (pg/m^3)
PBDE77	0.0125	0.06	0.06
PBDE181	0.0125	0.06	0.06
PBDE17	0.0125	0.06	0.06
PBDE28	0.0125	0.06	0.06
PBDE71	0.0125	0.06	0.06
PBDE47	0.0125	0.06	0.06
PBDE66	0.0125	0.06	0.06
PBDE100	0.0125	0.06	0.06
PBDE99	0.0125	0.06	0.06
PBDE85	0.0125	0.06	0.06
PBDE154	0.0125	0.06	0.06
PBDE153	0.0125	0.06	0.06
PBDE138	0.0125	0.06	0.06
PBDE183	0.0125	0.06	0.06
PBDE190	0.0125	0.06	0.06
PBDE209	0.0625	0.32	0.32

A 2. GC / MS instrument detection limit and method detection limit values of PCBs

PCB	Instrument Detection Limit (pg/uL)	Passive Sampling Method Detection Limit (pg/m^3)	Active Sampling (Gas and Particulate) Method Detection Limit (pg/m^3)
$^{13}C_{12}$ PCB9	0.125	0.06	0.04
$^{13}C_{12}$ PCB15	0.125	0.06	0.04
$^{13}C_{12}$ PCB32	0.125	0.03	0.18
PCB14	0.125	0.63	0.45
PCB65	0.25	1.26	0.90
PCB166	0.25	1.26	0.90
PCB30	0.0125	1.26	0.90
PCB18	0.01	0.05	0.04
PCB31	0.01	0.05	0.04
PCB28	0.01	0.05	0.04
PCB22	0.01	0.05	0.04
PCB54	0.01	0.05	0.04
PCB52	0.01	0.05	0.04
PCB49	0.01	0.05	0.04
PCB44	0.01	0.05	0.04
PCB41/64	0.01	0.05	0.04
PCB74	0.01	0.05	0.04
PCB70	0.01	0.05	0.04
PCB60	0.01	0.05	0.04
PCB56	0.01	0.05	0.04
PCB104	0.01	0.05	0.04
PCB95	0.01	0.05	0.04

(Cont. on next page)

A 2. (Cont.)

PCB	Instrument Detection Limit (pg/uL)	Passive Sampling Method Detection Limit (pg/m^3)	Active Sampling (Gas and Particulate) Method Detection Limit (pg/m^3)
PCB95	0.01	0.05	0.04
PCB90/10	0.01	0.05	0.04
PCB99	0.01	0.05	0.04
PCB87	0.01	0.05	0.04
PCB110	0.1	0.51	0.36
PCB123	0.1	0.51	0.36
PCB118	0.1	0.51	0.36
PCB114	0.1	0.51	0.36
PCB105	0.1	0.51	0.36
PCB155	0.01	0.05	0.04
PCB151	0.01	0.05	0.04
PCB149	0.01	0.05	0.04
PCB153	0.01	0.05	0.04
PCB132	0.6	3.03	2.15
PCB141	0.6	3.03	2.15
PCB138	0.6	3.03	2.15
PCB158	0.6	3.03	2.15
PCB167	0.6	3.03	2.15
PCB156	0.6	3.03	2.15
PCB157	0.6	3.03	2.15
PCB188	0.01	0.05	0.04
PCB187	0.01	0.05	0.04
PCB183	0.01	0.05	0.04
PCB174	0.6	3.03	2.15
PCB180	0.01	0.05	0.04
PCB170	0.6	3.03	2.15
PCB189	0.6	3.03	2.15
PCB199	0.6	3.03	2.15
PCB203	0.6	3.03	2.15
PCB194	0.6	3.03	2.15

A 3. GC / MS instrument detection limit and method detection limit values of OCPs

OCP	Instrument Detection Limit (pg/uL)	Passive Sampling Method Detection Limit (pg/m^3)	Active Sampling (Gas and Particulate) Method Detection Limit (pg/m^3)
α–HCH	0.05	0.25	0.18
HCB	0.05	0.25	0.18
β–HCH	0.05	0.25	0.18
PCNB	0.05	0.25	0.18
γ–HCH	0.05	0.25	0.18
Heptachlor	0.05	0.25	0.18
Aldrin	0.1	0.51	0.36
Heptachlor Epoxide	0.1	0.51	0.36
Alpha Chlordane	0.05	0.25	0.18
Gamma Chlordane	0.05	0.25	0.18
ENDO-I	0.05	0.25	0.18
o,p′-DDE	0.05	0.25	0.18
Dieldrin	0.05	0.25	0.18
p,p′-DDE	0.1	0.51	0.36
o,p′-DDD	0.1	0.51	0.36
Endrin	0.1	0.51	0.36
ENDO-II	0.1	0.51	0.36
p,p′-DDD	0.05	0.25	0.18
Endrin Aldehide	0.1	0.51	0.36
o,p′-DDT	0.05	0.25	0.18
$EndoSO_4$	0.1	0.51	0.36
p,p′-DDT	0.1	0.51	0.36
Endrin ketone	0.1	0.51	0.36
Mirex	0.05	0.25	0.18
d_6 γ-HCH	0.1	0.51	0.36

A 4. Descriptive statistics of PBDE (pg/m^3) congener concentrations

PROVINCES		PBDE-17	PBDE-28	PBDE-71	PBDE-47	PBDE-66	PBDE-100	PBDE-99	PBDE-85	PBDE-154	PBDE-153	PBDE-138	PBDE-183	PBDE-190	PBDE-209	$\sum_{14}$PBDE
	MEAN	0.30	0.27	1.43	38.87	0.16	31.60	0.86	0.32	0.78	2.10	1.14	28.49	106.43	58.46	271.21
	MEDIAN	0.30	0.26	0.92	34.05	0.16	17.74	0.56	0.37	0.78	1.72	1.34	33.15	113.67	58.46	263.50
ADANA	GEO.MEAN	0.30	0.24	1.22	9.53	0.15	7.48	0.64	0.31	0.68	1.38	0.76	9.18	96.33	58.09	186.32
	MEAN	1.51	1.23	ND	41.00	0.34	25.72	1.79	0.47	0.50	1.04	1.68	13.57	114.63	130.71	334.19
	MEDIAN	1.51	0.71	ND	44.68	0.34	0.82	0.74	0.40	0.34	0.79	1.63	0.63	99.31	110.55	262.47
GAZIANTEP	GEO.MEAN	0.91	0.94	ND	8.28	0.34	3.51	1.07	0.45	0.45	0.93	1.15	2.36	105.32	119.93	245.64
	MEAN	0.27	0.22	ND	41.26	ND	38.53	4.93	0.26	0.57	1.93	1.71	12.45	100.62	ND	202.76
	MEDIAN	0.27	0.18	ND	22.90	ND	25.13	0.78	0.27	0.59	1.57	0.90	0.58	88.40	ND	141.56
KARAMAN	GEO.MEAN	0.26	0.21	ND	3.16	ND	5.56	0.96	0.26	0.56	1.79	1.00	2.27	86.73	ND	102.76
	MEAN	0.30	0.27	1.43	38.87	0.16	31.60	0.86	0.32	0.78	2.10	1.14	28.49	106.43	58.46	271.21
	MEDIAN	0.30	0.26	0.92	34.05	0.16	17.74	0.56	0.37	0.78	1.72	1.34	33.15	113.67	58.46	263.50
MALATYA	GEO.MEAN	0.30	0.24	1.22	9.53	0.15	7.48	0.64	0.31	0.68	1.38	0.76	9.18	96.33	58.09	186.32
	MEAN	4.19	6.21	0.49	48.31	0.47	55.63	0.85	0.33	0.56	5.48	2.23	0.33	119.63	933.20	1177.92
	MEDIAN	0.76	2.44	0.49	0.89	0.47	41.01	0.86	0.24	0.45	2.52	1.92	0.33	114.74	933.20	1100.30
OSMANIYE	GEO.MEAN	1.12	3.14	0.47	4.12	0.40	9.91	0.63	0.30	0.52	3.42	1.43	0.32	105.66	687.35	818.81
	MEAN	ND	0.36	ND	19.65	0.46	33.11	0.66	0.49	0.73	1.61	0.94	14.96	94.27	44.94	212.17
	MEDIAN	ND	0.24	ND	2.77	0.46	30.11	0.69	0.42	0.78	1.60	0.91	12.19	85.45	44.94	180.57
DENIZLI	GEO.MEAN	ND	0.32	ND	4.12	0.46	6.48	0.58	0.47	0.71	1.46	0.80	4.19	88.94	43.99	152.52
	MEAN	1.36	2.01	ND	39.16	ND	38.72	0.82	0.40	1.47	1.93	1.26	18.38	110.73	66.47	282.70
	MEDIAN	0.25	0.36	ND	11.75	ND	11.72	0.37	0.34	1.17	1.64	0.86	8.69	105.97	66.47	209.59
ISPARTA	GEO.MEAN	0.57	0.73	ND	3.36	ND	4.28	0.45	0.36	1.27	1.67	0.88	4.06	96.69	65.58	179.89
	MEAN	0.59	0.53	ND	37.26	0.28	36.72	0.46	0.44	0.92	1.47	1.34	17.92	89.95	34.28	222.16
	MEDIAN	0.59	0.41	ND	54.77	0.26	53.91	0.35	0.42	1.00	1.46	1.60	16.29	91.85	34.28	257.19
MUGLA	GEO.MEAN	0.50	0.49	ND	5.76	0.27	6.77	0.40	0.44	0.91	1.47	1.17	3.80	89.26	34.28	145.53
	MEAN	2.34	2.28	1.98	43.89	0.48	25.32	1.98	0.39	2.53	11.17	1.39	24.60	168.78	54.53	341.64
	MEDIAN	2.34	0.47	1.98	31.83	0.46	1.00	0.40	0.35	0.98	1.71	1.05	0.44	179.88	38.81	261.69
IZMIR	GEO.MEAN	1.68	0.99	1.98	10.69	0.45	2.48	0.94	0.38	1.52	3.11	1.14	2.51	167.13	50.29	245.29
	MEAN	27.11	38.14	3.81	40.65	0.36	40.10	1.65	0.45	0.77	1.22	1.15	32.33	151.02	97.30	436.07
	MEDIAN	0.72	34.55	4.09	5.52	0.36	1.65	1.52	0.50	0.64	1.28	1.09	39.70	150.38	76.22	318.23
BURSA	GEO.MEAN	2.74	18.19	2.25	7.46	0.31	5.81	1.35	0.44	0.69	0.84	1.01	6.10	147.78	79.49	274.45
	MEAN	2.34	2.28	1.98	43.89	0.48	25.32	1.98	0.39	2.53	11.17	1.39	24.60	168.78	54.53	341.64
	MEDIAN	2.34	0.47	1.98	31.83	0.46	1.00	0.40	0.35	0.98	1.71	1.05	0.44	179.88	38.81	261.69
IZMIR	GEO.MEAN	1.68	0.99	1.98	10.69	0.45	2.48	0.94	0.38	1.52	3.11	1.14	2.51	167.13	50.29	245.29

(Cont. on next page)

A 5. Descriptive statistics of PCB (pg/m^3) congener concentrations

		PCB-18	PCB-31	PCB-28	PCB-22	PCB-54	PCB-52	PCB-49	PCB-44	PCB-41/64	PCB-74	PCB-70	PCB-60	PCB-56	PCB-104	PCB-95	PCB-90/101
	MEAN	35.11	14.17	22.82	26.96	ND	21.42	30.26	27.84	219.26	49.77	6.36	ND	ND	ND	ND	5.27
	MEDIAN	4.35	10.43	20.23	26.96	ND	11.41	29.08	27.84	219.26	49.77	5.92	ND	ND	ND	ND	5.27
ADANA	**GEO.MEAN**	8.76	12.12	18.69	26.96	ND	15.50	29.52	27.84	219.26	22.52	5.73	ND	ND	ND	ND	5.27
	MEAN	1.07	46.01	ND	30.79	ND	ND	ND	ND	122.46	ND	ND	ND	ND	ND	ND	ND
	MEDIAN	1.07	46.01	ND	27.55	ND	ND	ND	ND	30.23	ND	ND	ND	ND	ND	ND	ND
DENIZLI	**GEO.MEAN**	1.05	46.01	ND	26.62	ND	ND	ND	ND	49.01	ND	ND	ND	ND	ND	ND	ND
	MEAN	84.26	10.41	19.31	ND	ND	12.70	141.46	894.54	84.07	41.39	3.55	ND	ND	ND	18.48	6.19
	MEDIAN	5.43	8.81	14.70	ND	ND	12.70	141.46	894.54	53.89	41.39	3.55	ND	ND	ND	18.48	6.19
GAZIANTEP	**GEO.MEAN**	13.13	9.01	17.59	ND	ND	12.56	141.46	894.54	37.83	33.57	3.55	ND	ND	ND	18.48	6.19
	MEAN	460.18	ND	43.32	28.99	ND	12.14	ND	ND	145.60	ND	ND	ND	ND	ND	ND	ND
	MEDIAN	21.40	ND	43.32	28.99	ND	12.14	ND	ND	116.59	ND	ND	ND	ND	ND	ND	ND
KARAMAN	**GEO.MEAN**	67.63	ND	43.32	28.99	ND	12.14	ND	ND	136.66	ND	ND	ND	ND	ND	ND	ND
	MEAN	35.87	4.12	9.00	15.18	ND	9.13	ND	9.04	78.30	26.00	ND	ND	ND	ND	ND	ND
	MEDIAN	35.87	4.12	9.00	15.18	ND	9.13	ND	9.04	78.30	26.00	ND	ND	ND	ND	ND	ND
MALATYA	**GEO.MEAN**	8.40	4.12	9.00	15.18	ND	9.13	ND	9.04	77.61	21.81	ND	ND	ND	ND	ND	ND
	MEAN	46.87	17.96	35.14	19.53	2.94	25.60	32.64	ND	61.67	10.56	10.48	ND	8.04	2.44	19.23	12.01
	MEDIAN	13.45	15.83	37.92	19.53	2.94	14.60	17.21	ND	43.90	10.56	10.48	ND	8.04	2.44	19.23	12.01
OSMANIYE	**GEO.MEAN**	18.38	15.41	31.14	13.99	2.94	19.84	25.61	ND	33.04	10.56	10.26	ND	8.04	2.44	19.23	11.52
	MEAN	22.32	12.75	36.37	ND	ND	41.41	27.37	45.18	77.41	25.37	44.88	ND	ND	19.49	50.66	48.50
	MEDIAN	22.32	7.65	14.61	ND	ND	41.41	27.37	45.18	105.93	25.37	44.88	ND	ND	19.49	50.66	48.50
ISPARTA	**GEO.MEAN**	10.92	7.70	21.28	ND	ND	39.35	25.88	45.18	36.76	25.37	44.88	ND	ND	19.49	50.66	40.65
	MEAN	ND	ND	ND	ND	ND	ND	ND	ND	189.86	ND	ND	ND	ND	ND	ND	ND
	MEDIAN	ND	ND	ND	ND	ND	ND	ND	ND	189.86	ND	ND	ND	ND	ND	ND	ND
MUGLA	**GEO.MEAN**	ND	ND	ND	ND	ND	ND	ND	ND	188.56	ND	ND	ND	ND	ND	ND	ND
	MEAN	45.62	12.42	16.09	19.84	ND	70.16	98.60	ND	88.72	ND	ND	ND	ND	53.31	28.83	58.38
	MEDIAN	9.75	12.42	16.09	19.84	ND	75.20	98.60	ND	59.01	ND	ND	ND	ND	53.31	28.83	53.02
BURSA	**GEO.MEAN**	8.86	12.42	16.09	19.84	ND	45.59	98.60	ND	51.08	ND	ND	ND	ND	53.31	28.82	20.68
	MEAN	113.02	45.21	87.78	45.21	ND	48.37	49.03	39.08	56.67	22.47	25.76	ND	22.36	ND	29.70	20.95
	MEDIAN	35.23	25.82	46.02	35.55	ND	30.11	47.01	39.08	20.50	16.32	18.77	ND	20.51	ND	29.70	19.73
IZMIR	**GEO.MEAN**	54.63	26.94	66.30	40.03	ND	41.38	41.11	39.08	28.86	20.04	16.61	ND	21.12	ND	29.50	20.01

(Cont. on next page)

A 5. (Cont.)

		PCB-99	PCB-87	PCB-110	PCB-123	PCB-118	PCB-114	PCB-121	PCB-105	PCB-155	PCB-151	PCB-149	PCB-153	PCB-132	PCB-141	PCB-138	PCB-158	PCB-167
	MEAN	7.34	12.17	ND	796.90	452.16	ND	25.69	12.23	ND	ND	ND	ND	ND	ND	ND	ND	ND
	MEDIAN	7.34	12.17	ND	834.97	452.16	ND	25.69	12.23	ND	ND	ND	ND	ND	ND	ND	ND	ND
ADANA	**GEO.MEAN**	7.34	12.17	ND	793.53	413.32	ND	25.69	12.23	ND	ND	ND	ND	ND	ND	ND	ND	ND
	MEAN	ND	ND	ND	ND	528.73	ND	ND	ND	ND	ND	4.56	ND	ND	ND	ND	ND	ND
	MEDIAN	ND	ND	ND	ND	480.00	ND	ND	ND	ND	ND	4.56	ND	ND	ND	ND	ND	ND
DENIZLI	**GEO.MEAN**	ND	ND	ND	ND	207.20	ND	ND	ND	ND	ND	4.56	ND	ND	ND	ND	ND	ND
	MEAN	ND	5.08	ND	ND	10.58	ND	ND	ND	ND	ND	4.29	ND	ND	ND	ND	ND	ND
	MEDIAN	ND	5.08	ND	ND	10.58	ND	ND	ND	ND	ND	4.29	ND	ND	ND	ND	ND	ND
GAZIANTEP	**GEO.MEAN**	ND	5.08	ND	ND	10.43	ND	ND	ND	ND	ND	4.29	ND	ND	ND	ND	ND	ND
	MEAN	ND	ND	ND	ND	48.51	ND	ND	29.98	ND	ND	ND	ND	ND	ND	ND	ND	ND
	MEDIAN	ND	ND	ND	ND	48.51	ND	ND	29.98	ND	ND	ND	ND	ND	ND	ND	ND	ND
KARAMAN	**GEO.MEAN**	ND	ND	ND	ND	14.01	ND	ND	29.98	ND	ND	ND	ND	ND	ND	ND	ND	ND
	MEAN	ND	ND	ND	ND	6.47	2.93	ND	ND	ND	ND	ND	ND	ND	ND	ND	ND	ND
	MEDIAN	ND	ND	ND	ND	6.47	2.93	ND	ND	ND	ND	ND	ND	ND	ND	ND	ND	ND
MALATYA	**GEO.MEAN**	ND	ND	ND	ND	6.47	2.93	ND	ND	ND	ND	ND	ND	ND	ND	ND	ND	ND
	MEAN	22.23	5.87	6.64	31.37	ND	ND	ND	ND	ND	6.61	7.38	2.31	ND	ND	ND	ND	ND
	MEDIAN	22.23	5.87	6.64	31.37	ND	ND	ND	ND	ND	6.61	7.38	2.31	ND	ND	ND	ND	ND
OSMANIYE	**GEO.MEAN**	17.49	5.87	6.64	31.37	ND	ND	ND	ND	ND	6.61	7.13	2.31	ND	ND	ND	ND	ND
	MEAN	36.00	4.34	ND	92.11	30.06	ND	ND	ND	ND	ND	15.13	7.90	ND	ND	ND	ND	ND
	MEDIAN	36.00	4.34	ND	92.11	30.06	ND	ND	ND	ND	ND	15.13	7.90	ND	ND	ND	ND	ND
ISPARTA	**GEO.MEAN**	36.00	4.34	ND	77.40	30.06	ND	ND	ND	ND	ND	15.13	7.90	ND	ND	ND	ND	ND
	MEAN	ND	ND	ND	15.76	9.88	ND	ND	ND	ND	ND	ND	ND	ND	ND	ND	ND	ND
	MEDIAN	ND	ND	ND	15.76	9.88	ND	ND	ND	ND	ND	ND	ND	ND	ND	ND	ND	ND
MUGLA	**GEO.MEAN**	ND	ND	ND	11.92	7.37	ND	ND	ND	ND	ND	ND	ND	ND	ND	ND	ND	ND
	MEAN	28.66	5.13	ND	585.02	478.89	14.46	ND	85.00	ND	ND	ND	ND	ND	ND	ND	ND	ND
	MEDIAN	28.66	5.13	ND	99.60	437.03	14.46	ND	85.00	ND	ND	ND	ND	ND	ND	ND	ND	ND
BURSA	**GEO.MEAN**	28.66	5.05	ND	205.09	176.60	14.46	ND	85.00	ND	ND	ND	ND	ND	ND	ND	ND	ND
	MEAN	30.81	17.18	20.45	9.37	10.91	ND	ND	ND	ND	7.88	11.42	7.61	7.10	ND	25.65	20.25	ND
	MEDIAN	31.52	14.93	20.39	9.37	10.91	ND	ND	ND	ND	7.88	11.42	7.61	7.10	ND	25.65	20.25	ND
IZMIR	**GEO.MEAN**	23.51	14.68	19.36	9.37	10.24	ND	ND	ND	ND	7.85	11.30	6.97	3.06	ND	25.65	20.25	ND

(Cont. on next page)

A 5. (Cont.)

		PCB-156	PCB-157	PCB-188	PCB-187	PCB-183	PCB-174	PCB-180	PCB-170	PCB-189	PCB-199	PCB-203	PCB-194	Σ_{45}PCB
	MEAN	159.57	ND	4.87	17.94	ND	4.43	26.86	70.89	37.01	ND	97.46	12.59	533.85
	MEDIAN	159.57	ND	4.87	17.94	ND	4.43	26.86	75.04	37.01	ND	97.46	12.59	318.21
ADANA	**GEORT**	108.54	ND	4.87	17.94	ND	4.43	26.86	54.48	37.01	ND	85.40	10.37	313.15
	MEAN	ND	ND	ND	20.85	ND	ND	ND	94.21	ND	ND	ND	ND	426.07
	MEDIAN	ND	ND	ND	20.85	ND	ND	ND	98.34	ND	ND	ND	ND	199.45
DENIZLI	**GEORT**	ND	ND	ND	20.72	ND	ND	ND	87.07	ND	ND	ND	ND	213.39
	MEAN	ND	ND	ND	34.37	23.21	6.50	31.53	41.92	49.97	ND	ND	11.95	337.23
	MEDIAN	ND	ND	ND	31.39	15.27	6.50	31.53	41.92	49.97	ND	ND	11.95	175.64
GAZIANTEP	**GEORT**	ND	ND	ND	31.13	20.24	6.50	23.10	41.92	49.97	ND	ND	11.95	221.04
	MEAN	ND	ND	ND	ND	ND	55.84	4.37	ND	49.29	ND	286.52	ND	575.78
	MEDIAN	ND	ND	ND	ND	ND	55.84	4.37	ND	49.29	ND	286.52	ND	324.83
KARAMAN	**GEORT**	ND	ND	ND	ND	ND	23.14	4.29	ND	46.47	ND	286.52	ND	348.12
	MEAN	32.61	ND	ND	18.36	27.61	24.92	50.09	59.97	80.59	ND	ND	ND	127.26
	MEDIAN	32.61	ND	ND	18.36	27.61	24.92	50.09	57.65	80.59	ND	ND	ND	100.96
MALATYA	**GEORT**	32.61	ND	ND	18.36	27.61	24.92	50.09	52.73	54.68	ND	ND	ND	110.75
	MEAN	ND	ND	ND	37.99	27.32	ND	74.70	198.07	ND	ND	78.39	ND	314.77
	MEDIAN	ND	ND	ND	43.69	27.32	ND	74.70	239.76	ND	ND	78.39	ND	245.08
OSMANIYE	**GEORT**	ND	ND	ND	33.42	23.81	ND	74.70	133.58	ND	ND	78.39	ND	223.37
	MEAN	ND	ND	ND	22.70	12.13	ND	ND	88.37	ND	ND	ND	86.50	163.62
	MEDIAN	ND	ND	ND	22.70	12.13	ND	ND	87.54	ND	ND	ND	86.50	137.59
ISPARTA	**GEORT**	ND	ND	ND	21.00	12.13	ND	ND	62.12	ND	ND	ND	86.50	96.93
	MEAN	ND	ND	ND	36.39	38.04	4.93	23.82	107.76	125.69	ND	157.09	ND	209.33
	MEDIAN	ND	ND	ND	36.39	38.04	4.93	23.82	93.27	125.69	ND	157.09	ND	210.25
MUGLA	**GEORT**	ND	ND	ND	34.13	38.04	4.93	16.28	79.47	125.69	ND	138.54	ND	181.49
	MEAN	ND	ND	ND	36.39	ND	ND	ND	109.01	ND	ND	ND	60.37	639.33
	MEDIAN	ND	ND	ND	36.39	ND	ND	ND	102.36	ND	ND	ND	60.37	547.82
BURSA	**GEORT**	ND	ND	ND	34.42	ND	ND	ND	106.59	ND	ND	ND	60.37	375.46
	MEAN	ND	ND	4.17	31.14	ND	ND	29.18	118.66	36.10	ND	181.92	ND	588.42
	MEDIAN	ND	ND	4.17	31.14	ND	ND	29.18	140.95	36.10	ND	181.92	ND	384.50
IZMIR	**GEORT**	ND	ND	4.17	30.39	ND	ND	26.00	109.10	36.10	ND	181.92	ND	492.10

A 6. Descriptive statistics of OCP (pg/m^3) congener concentrations

		α-HCH	Aldrin	alpha chlordane	b-HCH	γ-HCH	Dieldrin	Endo-I	Endo-II	EndoSO4	Endrin	Endrin Aldehide	Endrin ketone	gamma chlordane
	MEAN	18.72	15.85	3.77	14.14	20.74	16.54	12.72	7.73	0.32	ND	ND	10.39	2.12
	MEDIAN	15.03	14.97	3.50	14.14	22.88	9.12	11.98	7.34	0.32	ND	ND	10.39	2.31
ADANA	**GEO.MEAN**	17.85	15.70	3.53	13.50	20.01	12.72	10.81	6.98	0.32	ND	ND	10.39	1.93
	MEAN	18.72	5.14	4.46	12.44	ND	22.55	13.55	11.94	ND	ND	ND	ND	2.02
	MEDIAN	17.17	5.14	4.66	12.44	ND	22.55	7.94	6.91	ND	ND	ND	ND	2.24
DENIZLI	**GEO.MEAN**	17.65	5.14	4.42	12.44	ND	22.55	10.70	9.59	ND	ND	ND	ND	2.00
	MEAN	60.22	62.48	4.10	19.21	ND	15.16	15.13	9.65	ND	ND	ND	ND	2.67
	MEDIAN	60.22	62.48	3.51	25.85	ND	5.78	14.30	8.70	ND	ND	ND	ND	2.34
GAZIANTEP	**GEO.MEAN**	60.22	62.48	3.11	13.33	ND	10.16	13.42	8.98	ND	ND	ND	ND	2.43
	MEAN	19.51	ND	5.93	ND	ND	7.92	19.20	13.60	ND	ND	ND	ND	2.61
	MEDIAN	19.51	ND	5.93	ND	ND	7.92	19.20	13.60	ND	ND	ND	ND	2.61
KARAMAN	**GEO.MEAN**	19.51	ND	5.93	ND	ND	7.92	19.20	13.60	ND	ND	ND	ND	2.61
	MEAN	29.40	ND	3.96	ND	8.72	ND	24.76	25.58	ND	ND	ND	ND	2.40
	MEDIAN	25.03	ND	4.95	ND	8.72	ND	12.26	17.65	ND	ND	ND	ND	2.67
MALATYA	**GEO.MEAN**	25.88	ND	2.46	ND	8.72	ND	17.45	16.98	ND	ND	ND	ND	2.29
	MEAN	28.30	1.67	4.26	4.88	5.95	8.60	12.80	15.37	ND	ND	ND	ND	2.68
	MEDIAN	12.65	1.67	4.17	4.88	5.95	8.60	13.41	10.26	ND	ND	ND	ND	2.53
OSMANIYE	**GEO.MEAN**	18.54	1.67	3.32	4.88	5.95	8.60	12.12	12.26	ND	ND	ND	ND	2.52
	MEAN	71.54	ND	26.68	ND	ND	ND	116.45	5.52	ND	ND	ND	ND	27.59
	MEDIAN	36.74	ND	5.25	ND	ND	ND	9.38	5.27	ND	ND	ND	ND	1.48
ISPARTA	**GEO.MEAN**	47.46	ND	6.76	ND	ND	ND	18.10	5.48	ND	ND	ND	ND	3.44
	MEAN	50.90	ND	4.88	ND	ND	ND	13.33	7.88	ND	ND	ND	ND	2.47
	MEDIAN	50.90	ND	5.08	ND	ND	ND	8.94	7.45	ND	ND	ND	ND	2.58
MUGLA	**GEO.MEAN**	50.84	ND	4.73	ND	ND	ND	11.20	7.84	ND	ND	ND	ND	2.39
	MEAN	84.77	ND	4.84	24.64	48.91	5.39	12.21	8.85	ND	ND	ND	ND	2.35
	MEDIAN	84.77	ND	4.51	19.21	48.91	4.87	9.41	8.63	ND	ND	ND	ND	2.29
BURSA	**GEO.MEAN**	84.77	ND	4.73	22.10	45.62	4.91	10.72	8.65	ND	ND	ND	ND	2.30
	MEAN	22.04	0.48	4.89	20.91	ND	5.29	12.58	8.45	ND	ND	ND	ND	2.60
	MEDIAN	23.10	0.48	4.09	20.91	ND	5.29	9.22	8.45	ND	ND	ND	ND	2.14
IZMIR	**GEO.MEAN**	19.59	0.48	4.68	20.91	ND	5.29	10.54	8.45	ND	ND	ND	ND	2.45

Cont. on next page

A 6. (Cont.)

		HCB	Heptachlor	Mirex	*o,p′*DDD	*o,p′*DDE	*o,p′*-DDT	PCNB	*p,p′*-DDD	*p,p′*-DDE	*p,p′*-DDT	Σ_{25}OCP
	MEAN	31.61	41.75	10.92	28.06	8.27	20.67	40.19	25.20	157.00	ND	309.48
	MEDIAN	31.54	29.03	10.92	17.38	7.32	24.45	41.70	25.20	129.59	ND	277.48
ADANA	**GEO.MEAN**	26.05	32.75	10.92	21.25	7.62	19.64	38.27	25.11	115.38	ND	275.68
	MEAN	39.71	27.98	21.48	8.81	ND	19.19	21.87	22.37	26.83	5.15	159.87
	MEDIAN	30.89	27.98	21.48	8.81	ND	18.63	21.81	22.37	24.56	5.15	132.47
DENIZLI	**GEO.MEAN**	31.75	27.98	19.89	8.81	ND	19.09	21.24	22.37	25.66	5.15	145.30
	MEAN	42.83	13.08	2.21	4.02	11.27	136.33	33.14	9.58	42.87	4.28	240.93
	MEDIAN	32.38	13.08	2.21	2.53	8.42	14.98	33.14	9.58	43.33	4.28	173.91
GAZIANTEP	**GEO.MEAN**	27.25	13.08	2.21	3.45	9.06	42.37	33.14	8.89	40.37	4.28	196.12
	MEAN	24.40	ND	15.94	24.98	6.13	ND	27.57	ND	59.69	ND	189.15
	MEDIAN	24.40	ND	15.94	24.98	6.13	ND	27.57	ND	59.69	ND	189.15
KARAMAN	**GEO.MEAN**	24.40	ND	15.94	24.98	6.13	ND	27.57	ND	59.69	ND	189.15
	MEAN	31.07	ND	ND	6.61	7.22	8.28	ND	ND	20.73	ND	110.04
	MEDIAN	26.67	ND	ND	6.61	2.97	8.28	ND	ND	21.84	ND	96.78
MALATYA	**GEO.MEAN**	28.16	ND	ND	6.61	5.15	8.28	ND	ND	19.67	ND	102.14
	MEAN	42.11	ND	ND	17.16	25.57	101.96	30.95	ND	90.59	ND	214.23
	MEDIAN	39.09	ND	ND	13.92	11.15	101.96	30.95	ND	76.70	ND	196.42
OSMANIYE	**GEO.MEAN**	39.74	ND	ND	14.07	15.01	101.96	30.95	ND	72.80	ND	205.20
	MEAN	39.52	ND	28.40	4.42	ND	ND	13.94	ND	44.11	ND	256.21
	MEDIAN	25.81	ND	28.40	4.42	ND	ND	13.94	ND	17.89	ND	91.80
ISPARTA	**GEO.MEAN**	27.16	ND	28.40	4.42	ND	ND	13.94	ND	25.25	ND	120.57
	MEAN	36.16	ND	21.13	ND	ND	ND	ND	ND	20.15	ND	103.20
	MEDIAN	32.37	ND	21.13	ND	ND	ND	ND	ND	18.57	ND	78.06
MUGLA	**GEO.MEAN**	32.85	ND	21.13	ND	ND	ND	ND	ND	18.84	ND	92.89
	MEAN	16.95	41.53	15.17	32.31	4.57	17.56	32.52	ND	40.16	ND	132.89
	MEDIAN	14.65	40.90	15.17	13.97	4.57	17.56	31.50	ND	40.16	ND	120.12
BURSA	**GEO.MEAN**	12.48	39.00	15.17	18.57	4.45	17.56	32.26	ND	34.22	ND	71.83
	MEAN	42.14	16.37	14.92	10.47	10.91	48.10	12.12	17.96	26.00	ND	128.55
	MEDIAN	36.90	16.37	14.92	10.47	10.91	48.10	12.12	17.96	25.62	ND	101.17
IZMIR	**GEO.MEAN**	29.58	16.37	9.71	9.78	10.91	48.10	11.80	17.96	25.24	ND	116.43

A 7. Spearman rank correlation values of PBDEs

WINTER					
MEDIAN		GEO.MEAN		MEAN	
PBDE-28	-1	PBDE-28	-1	PBDE-28	-1
PBDE-138	-0.5	PBDE-100	-0.5	PBDE-99	-0.5
PBDE-209	-0.5	PBDE-138	-0.5	PBDE-100	-0.5
		PBDE-153	-0.5	PBDE-138	-0.5
		PBDE-209	-0.5	PBDE-153	-0.5
				PBDE-209	-0.5
WINTER SEASON EXCEPT KARAMAN AND MALATYA					
MEDIAN		GEO.MEAN		MEAN	
PBDE-28	-1	PBDE-28	-1	PBDE-28	-1
PBDE138	-0.5	PBDE-100	-0.5	PBDE-138	-0.5
PBDE-209	-0.5	PBDE-138	-0.5	PBDE-153	-0.5
		PBDE-153	-0.5	PBDE-209	-0.5
		PBDE-209	-0.5		
WINTER SEAOSN ONLY IZMIR IN THE FAR GROUP					
MEDIAN		GEO.MEAN		MEAN	
PBDE-190	-0.5	PBDE-138	-0.5	PBDE-47	-1
		PBDE-209	-0.5	PBDE-99	-0.5
				PBDE-153	-0.5
				PBDE-138	-0.5
				PBDE-209	-0.5
WINTER SEASON ONLY IZMIR IN THE FAR GROUP EXCEPT FOR KARAMAN AND MALATYA IN THE CLOSE GROUP					
PBDE-138	-0.5	PBDE-138	-0.5	PBDE-47	-1
PBDE-209	-0.5	PBDE-209	-0.5	PBDE-153	-0.5
				PBDE-138	-0.5
				PBDE-209	-0.5
WINTER SEASON ONLY BURSA IN THE FAR GROUP					
MEDİAN		GEOMEAN		MEAN	
PBDE-28	-1	PBDE-28	-1	PBDE-28	-1
PBDE-153	-0.5	PBDE-100	-0.5	PBDE-100	-0.5
PBDE-138	-0.5	PBDE-153	-1	PBDE-99	-0.5
		PBDE-138	-0.5	PBDE-153	-1
		PBDE-209	-0.5	PBDE-138	-0.5
				PBDE-209	-0.5
WINTER SEASON ONLY BURSA IN THE FAR GROUP EXCEPT FOR KARAMAN AND MALATYA IN THE CLOSE GROUP					
MEDIAN		GEO.MEAN		MEAN	
PBDE-28	-1	PBDE-28	-1	PBDE-28	-1
PBDE-138	-0.5	PBDE-153	-0.5	PBDE-138	-0.5
PBDE-209	-1	PBDE-138	-0.79	PBDE-209	-0.5
		PBDE-209	-0.71		
TRANSITION SEASON					
MEDIAN		GEO.MEAN		MEAN	
PBDE-100	-0.5	PBDE-100	-0.5	PBDE-138	-0.5
PBDE-138	-0.5	PBDE-153	-0.5	PBDE-209	-0.5
PBDE-209	-0.5	PBDE-209	-0.78	Σ_{14}PBDE	-0.5
TRANSITION SEASON EXCEPT FOR KARAMAN AND MALATYA IN THE CLOSE GROUP					
MEDIAN		GEO.MEAN		MEAN	
PBDE-183	-0.5	PBDE-17	-0.5	PBDE-209	-0.5
PBDE-209	-0.5	PBDE-28	-0.5	Σ_{14}PBDE	-0.5
Σ_{14}PBDE	-0.5	PBDE-47	-0.5		
		PBDE-100	-0.5		
		PBDE-138	-0.5		
		PBDE-209	-0.5		

(Cont on next page)

A 7. (Cont.)

TRANSITION SEASON ONLY IZMIR IN THE FAR GROUP					
MEDIAN		GEO. MEAN		MEAN	
PBDE-28	-0.5	PBDE-100	-1	PBDE-100	-0.5
PBDE-99	-0.5	PBDE-183	-0.5	PBDE-183	-1
PBDE-100	-0.5	PBDE-209	-0.5	PBDE-209	-0.5
PBDE-183	-0.5	Σ_{14}PBDE	-0.5	Σ_{14}PBDE	-0.5
PBDE-209	-0.5				
Σ_{14}PBDE	-0.5				
TRANSITION ONLY IZMIR IN THE FAR GROUP EXCEPT FOR KARAMAN AND MALATYA IN THE CLOSE GROUP					
MEAN		GEO. MEAN		MEAN	
PBDE-28	-0.5	PBDE-17	-0.5	PBDE-28	-0.5
PBDE-99	-1	PBDE-28	-0.5	PBDE-100	-0.5
PBDE-100	-0.5	PBDE-47	-0.5	PBDE-183	-0.5
PBDE-183	-0.5	PBDE-99	-0.5	PBDE-209	-0.5
PBDE-209	-0.5	PBDE-100	-1	Σ_{14}PBDE	-0.5
Σ_{14}PBDE	-0.5	PBDE-138	-0.5		
		PBDE-183	-1		
		PBDE-209	-0.5		
		Σ_{14}PBDE	-0.5		
TRANSITION SEASON ONLY BURSA IN THE FAR GROUP					
MEDIAN		GEOMEAN		MEAN	
PBDE-209	-0.78	PBDE-153	-0.77	PBDE-153	-1
		PBDE-209	-0.78	PBDE-209	-0.5
TRANSITION SEASON ONLY BURSA IN THE FAR GROUP EXCEPT FOR KARAMAN AND MALATYA IN THE CLOSE GROUP					
PBDE-209	-0.5	PBDE-47	-0.5	PBDE-153	-1
Σ_{14}PBDE	-0.5	PBDE-100	-0.5	PBDE-209	-0.5
		PBDE-138	-0.5	Σ_{14}PBDE	-0.5
		PBDE-153	-0.5		
		PBDE-183	-0.5		
		PBDE-209	-0.5		
WHOLE SAMPLING					
MEDIAN		GEOMEAN		MEAN	
PBDE-100	-0.5	PBDE-100	-0.5	PBDE-138	-0.5
PBDE-138	-0.5	PBDE-153	-0.5	PBDE-209	-0.5
PBDE-209	-0.5	PBDE-209	-0.5	Σ_{14}PBDE	-0.5
EXCEPT KARAMAN AND MALATYA					
PBDE-100	-0.5	PBDE-100	-0.5	PBDE-99	-0.5
PBDE-138	-0.5	PBDE-138	-0.5	PBDE-138	-0.5
PBDE-209	-0.5	PBDE-153	-0.5	PBDE-209	-0.5
		PBDE-209	-0.5	Σ_{14}PBDE	-0.5
WHOLE SAMPLING FAR GROUP ONLY IZMIR IN THE FAR GROUP					
MEDIAN		GEOMEAN		MEAN	
PBDE-28	-0.5	PBDE-28	-0.5	PBDE-28	-0.5
PBDE-99	-1	PBDE-100	-0.5	PBDE-100	-0.5
PBDE-100	-0.5	PBDE-183	-0.5	PBDE-138	-0.5
PBDE-138	-0.5	PBDE-209	-0.5	PBDE-209	-0.5
PBDE-183	-0.5	Σ_{14}PBDE	-0.5	Σ_{14}PBDE	-0.5
PBDE-209	-1				
Σ_{14}PBDE	-1				

(Cont. on next page)

A 7. (Cont.)

WHOLE SAMPLING FAR GROUP ONLY IZMIR IN THE FAR GROUP EXCEPT FOR KARAMAN AND MALATYA IN THE CLOSE GROUP					
PBDE-28	-0.5	PBDE-28	-0.5	PBDE-28	-0.5
PBDE-99	-1	PBDE-100	-0.5	PBDE-100	-0.5
PBDE-100	-0.5	PBDE-209	-0.5	PBDE-38	-0.5
PBDE-138	-0.5	Σ_{14}PBDE	-0.5	PBDE-209	-0.5
PBDE-138	-0.5			Σ_{14}PBDE	-0.5
PBDE-209	-1				
Σ_{14}PBDE	-1				
WHOLE SAMPLING ONLY BURSA IN THE FAR GROUP					
MEDIAN		GEOMEAN		MEAN	
PBDE-17	-0.5	PBDE-153	-0.5	PBDE-99	-0.5
PBDE-47	-1	PBDE-209	-0.5	PBDE-138	-1
PBDE-99	-1			PBDE-153	-1
PBDE-100	-1			PBDE-209	-0.5
PBDE-138	-0.5				
PBDE-153	-1				
PBDE-209	-0.5				
WHOLE SAMPLING ONLY BURSA IN THE FAR GROUP EXCEPT FOR KARAMAN AND MALATYA IN THE CLOSE GROUP					
PBDE-17	-0.5	PBDE-138	-0.5	PBDE-99	-0.5
PBDE-47	-1	PBDE-153	-0.5	PBDE-138	-1
PBDE-99	-0.5	PBDE-209	-0.5	PBDE-153	-1
PBDE-100	-1			PBDE-209	-0.5
PBDE-153	-1				
PBDE-138	-0.5				
PBDE-209	-0.5				

A 8. Spearman rank correlation values of PCBs

WINTER SEASON					
MEDIAN		GEOMEAN		MEAN	
PCB-22	-0.5	PCB-44	-1	PCB-44	-1
PCB-44	-1	PCB-41/64	-0.5	PCB-41/64	-0.5
PCB-41/64	-0.5	PCB-187	-0.5	PCB-187	-0.5
PCB187	-0.5	PCB-180	-0.5	PCB-180	-0.5
PCB-180	-0.5				
EXCEPT KARAMAN AND MALATYA					
MEDIAN		GEOMEAN		MEAN	
PCB-22	-0.5	PCB-22	-0.5	PCB-44	-1
PCB-44	-1	PCB-44	-1	PCB-41/64	-0.5
PCB-41/64	-0.5	PCB-41/64	-0.5	PCB-187	-0.5
PCB-74	-0.5	PCB-187	-0.5	PCB-180	-0.5
PCB-187	-0.5	PCB-180	-0.5		
PCB-180	-0.5				
WINTER SEASON ONLY IZMIR IN THE FAR GROUP					
MEDIAN		GEOMEAN		MEAN	
PCB-44	-1	PCB-44	-1	PCB-44	-1
PCB-41/64	-0.5	PCB-49	-0.5	PCB-49	-0.5
PCB-118	-0.5	PCB-41/64	-0.5	PCB-41/64	-0.5
PCB-187	-0.5	PCB-118	-0.5	PCB-118	-0.5
PCB-180	-0.81	PCB-180	-0.5	PCB-187	-0.5
		PCB-180	-0.5	PCB-180	-0.5
WINTER SEASON ONLY IZMIR IN THE FAR GROUP EXCEPT FOR KARAMAN AND MALATYA IN CLOSE GROUP					
MEDIAN		GEOMEAN		MEAN	
PCB-44	-1	PCB-44	-0.5	PCB-44	-1
PCB-41/64	-0.5	PCB-49	-0.5	PCB-49	-1
PCB-74	-0.5	PCB-41/64	-0.5	PCB-41/64	-0.5
PCB-187	-0.5	PCB-74	-0.5	PCB-187	-0.5
PCB-180	-0.5	PCB-187	-0.5	PCB-180	-0.5
		PCB-180	-0.5		
WINTER SEASON ONLY BURSA IN THE FAR GROUP					
MEDIAN		GEOMEAN		MEAN	
PCB-18	-0.5	PCB-18	-0.5	PCB-18	-0.5
PCB-22	-0.5	PCB-22	-0.5	PCB-31	-0.5
PCB-41/64	-0.5	PCB-41/64	-0.54	PCB-41/64	-0.5
PCB-187	-0.5	PCB-187	-0.5	PCB-187	-0.5
WINTER SEASON ONLY BURSA IN THE FAR GROUP EXCEPT FOR KARAMAN AND MALATYA IN CLOSE GROUP					
PCB-18	-0.5	PCB-18	-0.5	PCB-18	-0.5
PCB-22	-0.5	PCB-22	-0.5	PCB-22	-0.5
PCB-187	-0.5	PCB-31	-0.5	PCB-31	-0.5
		PCB-41/64	-0.5	PCB-41/64	-0.5
		PCB-187	-0.5	PCB-170	-0.5
				PCB-187	-0.5
TRANSITON SEASON					
MEDIAN		GEOMEAN		MEAN	
PCB-18	-0.5	PCB-18	-0.5	PCB-18	-0.5
PCB-41/64	-0.5	PCB-41/64	-0.5	PCB-41/64	-0.5
PCB-123	-0.5	PCB-123	-0.5	PCB-123	-0.5
EXCEPT KARAMAN AND MALATYA					
PCB-123	-0.85	PCB-123	-0.83	PCB-123	-0.83
PCB-18	-0.84	PCB-118	-0.43		
TRANSITON SEASON ONLY IZMIR IN THE FAR GROUP					
MEDIAN		GEOMEAN		MEAN	
PCB-41/64	-0.5	PCB-41/64	-0.5	PCB-18	-0.5
PCB-118	-0.5	PCB-118	-0.5	PCB-41/64	-0.5
PCB-123	-1	PCB-123	-1	PCB-118	-0.5
				PCB-123	-1

(Cont. on next page)

A 9. (Cont.)

TRANSITON SEASON ONLY IZMIR IN THE FAR GROUP EXCEPT FOR KARAMAN AND MALATYA IN CLOSE GROUP					
MEDIAN		**GEO. MEAN**		**MEAN**	
PCB-123	-1	PCB-41/64	-0.5	PCB-41/64	-0.5
PCB-118	-1	PCB-118	-1	PCB-118	-1
		PCB-123	-1	PCB-123	-1
				PCB-187	-0.5
				PCB-170	-0.5
TRANSITON SEASON ONLY BURSA IN THE FAR GROUP					
PCB-18	-0.5	PCB-18	-0.5	PCB-18	-0.5
PCB-28	-0.5	PCB-28	-0.5	PCB-28	-0.5
PCB-41/64	-0.5	PCB-87	-0.5	PCB-87	-0.5
PCB-87	-0.5	PCB-123	-0.5	PCB-123	-0.5
PCB-123	-0.5			Σ_{45}PCB	-0.5
TRANSITON SEASON ONLY BURSA IN THE FAR GROUP EXCEPT FOR KARAMAN AND MALATYA IN CLOSE GROUP					
PCB-18	-0.5	PCB-18	-0.5	PCB-18	-0.5
PCB-28	-0.5	PCB-28	-0.5	PCB-28	-0.5
PCB-41/64	-0.5	PCB-87	-0.5	PCB-87	-0.5
PCB-87	-0.5	PCB-123	-0.5	PCB-123	-0.5
PCB-118	-0.5	Σ_{45}PCB	-0.5	PCB-187	-0.5
PCB-123	-0.5			Σ_{45}PCB	-0.5
Σ_{45}PCB	-0.5				
WHOLE SEASON					
MEDIAN		GEOMEAN		MEAN	
PCB-22	-0.5	PCB-44	-1	PCB-18	-0.5
PCB-41/64	-0.5	PCB-41/64	-1	PCB-44	-1
PCB-74	-0.5	PCB-123	-0.5	PCB-41/64	-0.5
PCB-123	-0.5	PCB-189	-0.5	PCB-74	-1
PCB-189	-0.5			PCB-123	-0.5
				PCB-180	-0.5
				PCB-189	-0.5
EXCEPT KARAMAN AND MALATYA					
PCB-22	-0.5	PCB-44	-1	PCB-44	-1
PCB-44	-1	PCB-41/64	-0.5	PCB-41/64	-0.5
PCB-41/64	-0.5	PCB-74	-0.5	PCB-74	-1
PCB-74	-0.5	PCB-123	-0.5	PCB-123	-0.5
PCB-123	-0.5	PCB-180	-0.5	PCB-170	-0.5
PCB-118	-0.5	PCB-189	-0.5	PCB-180	-0.5
PCB-180	-0.5			PCB-189	-0.5
PCB-187	-0.5				
PCB-189	-0.5				
WHOLE SAMPLING ONLY IZMIR IN FAR GROUP					
PCB-41/64	-0.5	PCB-44	-1	PCB-18	-0.5
PCB-74	-0.5	PCB-41/64	-1	PCB-44	-1
PCB-118	-0.5	PCB-74	-0.5	PCB-41/64	-0.5
PCB-123	-1	PCB-118	-0.5	PCB-74	-1
PCB-189	-0.5	PCB-123	-1	PCB-118	-0.5
		PCB-189	-0.5	PCB-123	-1
				PCB-180	-0.5
				PCB-187	-0.5
				PCB-189	-0.5

(Cont. on next page)

A 9. (Cont.)

WHOLE SAMPLING ONLY IZMIR IN FAR GROUP EXCEPT FOR KARAMAN AND MALATYA IN CLOSE GROUP					
MEDIAN		GEO.MEAN		MEAN	
PCB-44	-1	PCB-44	-1	PCB-44	-1
PCB-41/64	-0.5	PCB-41/64	-0.5	PCB-41/64	-0.5
PCB-74	-0.5	PCB-74	-0.5	PCB-74	-1
PCB-123	-1	PCB-118	-1	PCB-123	-1
PCB-118	-1	PCB-123	-1	PCB-118	-0.5
PCB-180	-0.5	PCB-180	-0.5	PCB-180	-0.5
PCB-187	-0.5	PCB-189	-0.5	PCB-187	-0.5
PCB-189	-0.5				
WHOLE SAMPLING ONLY BURSA IN FAR GROUP					
MEDIAN		GEOMEAN		MEAN	
PCB-28	-0.71	PCB-18	-0.60	PCB-18	-0.70
PCB-22	-0.83	PCB-28	-0.86	PCB-28	-0.46
PCB-41/64	-0.54	PCB-87	-0.72	PCB-87	-0.73
PCB-87	-0.48				
PCB-123	-0.82				
EXCEPT KARAMAN AND MALATYA					
MEDIAN		GEOMEAN		MEAN	
PCB-18	-0.5	PCB-18	-0.5	PCB-18	-0.5
PCB-28	-0.5	PCB-28	-0.5	PCB-22	-0.5
PCB-22	-0.5	PCB-41/64	-1	PCB-28	-0.5
PCB-41/64	-0.5	PCB-87	-0.5	PCB-31	-0.5
PCB-87	-0.5	PCB-123	-0.5	PCB-41/64	-0.5
PCB123	-0.5			PCB-87	-0.5
				PCB-123	-0.5

A 10. Spearman rank correlation values of OCPs

WINTER SEASON					
MEDIAN		**GEOMEAN**		**MEAN**	
α-HCH	-0.5	α-HCH	-0.5	α-HCH	-0.5
HCB	-1	HCB	-1	HCB	-0.5
heptachlor	-1	heptachlor	-1	heptachlor	-1
Endo I	-0.5	Endo I	-0.5	Endo I	-0.5
p,p′-DDE	-0.5	*p,p′*-DDE	-0.5	*p,p′*-DDE	-1
o,p′-DDD	-0.5	*o,p′*-DDD	-0.5	*o,p′*-DDD	-0.5
Σ_{25}OCP	-0.5	Σ_{25}OCP	-0.5	Σ_{25}OCP	-0.5
WINTER SEASON EXCEPT KARAMAN AND MALATYA IN CLOSE GROUP					
α-HCH	-0.5	α-HCH	-0.5	α-HCH	-0.5
HCB	-1	HCB	-1	HCB	-1
heptachlor	-1	heptachlor	-1	heptachlor	-1
PCNB	-0.5	PCNB	-0.5	PCNB	-0.5
heptachlor	-1	heptachlor	-1	Endo I	-0.5
Endo I	-0.5	Endo I	-0.5	*p,p′*-DDE	-1
p,p′-DDE	-0.5	*p,p′*-DDE	-0.5	*o,p′*-DDD	-0.5
o,p′-DDD	-0.5	*o,p′*-DDD	-0.5	Σ_{25}OCP	-1
Σ_{25}OCP	-0.5	Σ_{25}OCP	-0.5		
WINTER SEASON FAR GROUP ONLY IZMIR					
α-HCH	-0.5	α-HCH	-0.5	α-HCH	-0.5
PCNB	-1	PCNB	-1	PCNB	-1
heptachlor	-1	heptachlor	-1	heptachlor	-1
Alpha chlordane	-0.5	Endo I	-0.5	alpha chlordane	-0.5
Gamma chlordane	-1	Alpha chlordane	-0.5	*p,p′*-DDE	-1
Endo I	-0.5	*o,p′*-DDD	-0.5	*o,p′*-DDD	-0.5
p,p′-DDE	-0.5	*p,p′*-DDE	-1	Σ_{25}OCP	-0.5
Σ_{25}OCP	-0.5	Σ_{25}OCP	-0.5		
WINTER SEASON FAR GROUP ONLY IZMIR EXCEPT FOR KARAMAN AND MALATYA IN CLOSE GROUP					
α-HCH	-0.5	α-HCH	-0.5	α-HCH	-0.5
PCNB	-1	PCNB	-1	PCNB	-1
heptachlor	-1	heptachlor	-1	heptachlor	-1
Alpha chlordane	-0.5	Endo I	-0.5	Gamma chlordane	-0.5
Gamma chlordane	-1	*p,p′*-DDE	-1	*p,p′*-DDE	-1
Endo I	-0.5	Σ_{25}OCP	-1	*o,p′*-DDD	-0.5
p,p′-DDE, Σ_{25}OCP	-0.5			Σ_{25}OCP	-1
WINTER SEASON FAR GROUP ONLY BURSA					
HCB	-1	HCB	-1	HCB	-0.5
Endo-I	-0.5	Heptachlor	-0.5	Heptachlor	-0.5
o,p′-DDD	-1	*p,p′*-DDE	-0.5	Endo I	-0.5
Σ_{25}OCP	-0.5	*o,p′*-DDD	-1	*p,p′*-DDE, Σ_{25}OCP	-0.5
		Σ_{25}OCP	-0.5	*o,p′*-DDD	-1
WINTER SEASON FAR GROUP ONLY BURSA EXCEPT FOR KARAMAN AND MALATYA IN CLOSE GROUP					
HCB	-1	HCB	-1	HCB	-0.5
Endo-I	-0.5	Heptachlor	-0.5	Heptachlor	-0.5
p,p′-DDE	-0.5	*p,p′*-DDE	-0.5	*o,p′*-DDD	-1
o,p′-DDD	-0.95	*o,p′*-DDD	-1	Σ_{25}OCP	-0.5
Σ_{25}OCP	-0.63	Σ_{25}OCP	-0.5		
TRANSITION SEASON					
HCB	-0.5	HCB	-0.5	HCB	-0.5
PCNB	-0.5	Endo I	-	PCNB	-0.5
Gamma chlordane	-1	Dieldrin	-0.5	Gamma chlordane	-0.5
Endo I	-1	*p,p′*-DDE	-0.5	Dieldrin	-0.5
Dieldrin	-0.5	Endo II	-1	*p,p′*-DDE	-0.5
Endo II	-1	*o,p′*-DDT	-1	Endo II	-0.5
p,p′-DDE	-0.5	Σ_{25}OCP	-1	*o,p′*-DDT	-1

(Cont. on next page)

A.10. (Cont.)

TRANSITION SEASON					
MEDIAN		**GEOMEAN**		**MEAN**	
o,p′-DDT	-1			Σ_{25}OCP	-1
Σ_{25}OCP	-1				
TRANSITION SEASON EXCEPT FOR KARAMAN AND MALATYA IN CLOSE GROUP					
HCB	-0.5	HCB	-0.5	HCB	-0.5
PCNB	-0.5	PCNB	-0.5	PCNB	-0.5
Gamma chlordane	-0.5	Gamma chlordane	-0.5	Gamma chlordane	-0.5
Dieldrin	-0.5	Endo I	-0.5	Endo I	-0.5
p,p′-DDE	-0.5	Dieldrin	-0.5	Dieldrin	-0.5
Endo II	-1	*p,p′*-DDE	-0.5	*p,p′*-DDE	-0.5
o,p′-DDT	-1	Endo II	-1	Endo II	-1
Σ_{25}OCP	-1	*o,p′*-DDT	-1	*o,p′*-DDT	-1
		Σ_{25}OCP	-1	Σ_{25}OCP	-1
TRANSITION SEASON FAR GROUP ONLY IZMIR					
HCB	-0.5	γ-HCH	-1	α-HCH	-0.5
γ-HCH	-0.5	Endo I	-1	γ-HCH	-1
Endo I	-0.5	*p,p′*-DDE	-0.5	*p,p′*-DDE	-0.5
p,p′-DDE	-0.5	Σ_{25}OCP	-1	Σ_{25}OCP	-1
Σ_{25}OCP	-1				
TRANSITION SEASON FAR GROUP ONLY IZMIR EXCEPT FOR KARAMAN AND MALATYA					
HCB	-0.5	HCB	-0.5	α-HCH	-0.5
γ-HCH	-0.5	Endo I	-0.5	γ-HCH	-1
p,p′-DDE	-0.5	γ-HCH	-1	Endo I	-0.5
Σ_{25}OCP	-1	*p,p′*-DDE	-0.5	*p,p′*-DDE	-0.5
		Σ_{25}OCP	-1	Σ_{25}OCP	-1
TRANSITION SEASON FAR GROUP ONLY BURSA					
HCB	-0.5	HCB	-0.5	HCB	-0.5
PCNB	-0.5	PCNB	-0.5	PCNB	-0.5
Gamma chlordane	-1	Gamma chlordane	-01	Gamma chlordane	-1
Endo-I	-1	Endo I	-1	Dieldrin	-0.5
Dieldrin	-0.5	Dieldrin	-0.5	Endo II	-1
Endo-II	-1	Endo II	-1	*o,p′*-DDT	-1
o,p′-DDT	-1	*o,p′*-DDT	-1	Σ_{25}OCP	-1
Σ_{25}OCP	-1	Σ_{25}OCP	-1		
TRANSITION SEASON FAR GROUP ONLY BURSA EXCEPT FOR KARAMAN AND MALATYA					
HCB	-0.5	HCB	-0.5	HCB	-0.5
PCNB	-0.5	PCNB	-0.5	PCNB	-0.5
Gamma chlordane	-1	Gamma chlordane	-1	Gamma chlordane	-0.5
Endo I	-1	Endo I	-1	Dieldrin	-0.5
Dieldrin	-0.5	Endo II	-1	Endo II	-1
Endo II	-1	Dieldrin	-0.5	*o,p′*-DDT	-1
o,p′-DDT	-1	*o,p′*-DDT	-1	Σ_{25}OCP	-1
Σ_{25}OCP	-1	Σ_{25}OCP	-1		
WHOLE SAMPLING					
Aldrin	-1	Aldrin	-1	HCB	-0.5
HCB	-1	HCB	-0.5	PCNB	-0.5
PCNB	-0.5	PCNB	-0.5	Aldrin	-1
Gamma chlordane	-1	Endo I	-0.5	Dieldrin	-1
Endo I	-0.5	Dieldrin	-0.5	*p,p′-DDE*	-1
Dieldrin	-0.5	*p,p′*-DDE	-0.5	Endo II	-0.5
p,p′-DDE	-0.5	*o,p′*-DDT	-0.5	*o,p′*-DDT	-0.5
p,p′-DDD	-0.5	Endo II	-0.5	Σ_{25}OCP	-1
Σ_{25}OCP	-1	Σ_{25}OCP	-1		
WHOLE SAMPLING EXCEPT FOR KARAMAN AND MALATYA IN CLOSE GRUOP					
heptachlor	-0.5	HCB	-0.5	HCB	-0.5
aldrin	-1	PCNB	-0.5	PCNB	-0.5
Alpha chlordane	-0.5	Aldrin	-1	Aldrin	-1
Gamma chlordane	-1			Dieldrin	-1

(Cont. on next page)

A.10. (Cont.)

WHOLE SAMPLING EXCEPT FOR KARAMAN AND MALATYA IN CLOSE GRUOP					
MEDIAN		**GEO. MEAN**		**MEAN**	
Endo I	-0.5	Endo I	-0.5	Endo I	-0.5
Dieldrin	-0.5	Endo II	-0.5	Endo II	-0.5
p,p′-DDE	-0.5	*p,p′-DDE*	-0.5	*p,p′*-DDE	-1
o,p′-DDD	-0.5	*p,p′-DDD*	-0.5	*o,p′*-DDT	-0.5
Endo II	-0.5	Σ_{25}OCP	-1	Σ_{25}OCP	-1
p,p′-DDD	-0.5				
Σ_{25}OCP	-1				
WHOLE SAMPLING FAR GROUP ONLY IZMIR					
PCNB	-1	α-HCH	-0.5	α-HCH	-0.5
γ-HCH	-0.5	PCNB	-1	PCNB	-1
heptachlor	-0.5	γ-HCH	-1	γ-HCH	-1
aldrin	-1	heptachlor	-0.5	heptachlor	-1
Gamma chlordane	-1	Aldrin	-1	Aldrin	-1
Endo I	-0.5	Endo I	-0.5	Endo I	-0.5
p,p′-DDE	-0.5	*p,p′*-DDE	-0.5	Dieldrin	-0.5
o,p′-DDD	-0.5	*o,p′*-DDD	-0.5	*p,p′*-DDE	-1
p,p′-DDD	-0.5	Endo II	-0.5	*o,p′*-DDD	-0.5
Σ_{25}OCP	-1	Σ_{25}OCP	-1	Endo II	-1
				o,p′-DDT	-0.5
				Σ_{25}OCP	-1
WHOLE SAMPLING FAR GROUP ONLY IZMIR EXCEPT KARAMAN AND MALATYA IN CLOSE GROUP					
PCNB	-1	α-HCH	-0.5	α-HCH	-0.5
gHCH	-0.5	PCNB	-1	PCNB	-1
heptachlor	-0.5	g-HCH	-1	gHCH	-1
Aldrin	-1	heptachlor	-0.5	heptachlor	-1
Gamma chlordane	-1	Aldrin	-1	Aldrin	-1
Dieldirn	-0.5	Endo I	-0.5	Endo I	-0.5
p,p′-DDE	-0.5	Dieldrin	-0.5	Dieldrin	-0.5
o,p′-DDD	-0.5	*p,p′*-DDE	-0.5	*p,p′*-DDE	-1
p,p′-DDD	-0.5	*o,p′*-DDD	-0.5	*o,p′*-DDD	-0.5
Σ_{25}OCP	-1	Endo II	-0.5	Endo II	-1
		Σ_{25}OCP	-1	*o,p′*-DDT	-0.5
				Σ_{25}OCP	-1
WHOLE SAMPLING FAR GROUP ONLY BURSA IN CLOSE GROUP					
HCB	-1	HCB	-0.5	HCB	-0.5
PCNB	-0.5	PCNB	-0.5	PCNB	-0.5
Gamma chlordane	-0.5	Endo I	-0.5	Gamma chlordane	-0.5
Endo I	-0.5	Dieldrin	-0.5	Endo I	-0.5
Dieldrin	-0.5	*p,p′*-DDE	-0.5	Endo II	-0.5
p,p′-DDE	-0.5	Endo II	-0.5	Dieldrin	-0.5
o,p′-DDT	-1	*o,p′*-DDT	-1	*p,p′*-DDE	-0.5
Σ_{25}OCP	-0.5	Σ_{25}OCP	-1	Endo II	-0.5
				o,p′-DDT	-1
				Σ_{25}OCP	-1
WHOLE SAMPLING FAR GROUP ONLY BURSA IN CLOSE GROUP EXCEPT FOR KARAMAN AND MALATYA IN CLOSE GROUP					
HCB	-1	HCB	-0.5	HCB	-0.5
PCNB	-0.5	PCNB	-0.5	PCNB	-0.5
Gamma chlordane	-0.5	Endo I	-1	Gamma chlordane	-0.5
Endo I	-0.5	Dieldrin	-0.5	Endo I	-0.5
Dieldrin	-0.5	*p,p′*-DDE	-0.5	Dieldrin	-0.5
p,p′-DDE	-0.5	*o,p′*-DDT	-1	*p,p′*-DDE	-0.5
o,p′-DDT	-1	Σ_{25}OCP	-1	Endo II	-0.5
Σ_{25}OCP	-0.5			*o,p′*-DDT,	-1
				Σ_{25}OCP	-1